

Imperial College London

Department of Chemical Engineering and Chemical Technology

**Thin Film Composite Membranes by Interfacial  
Polymerization for Organic Solvent Nanofiltration**

By

**María Fernanda Jiménez Sólomon**

Supervisor: Prof. Andrew G. Livingston

A thesis submitted for the degree of Doctor of Philosophy of Imperial College  
London and the Diploma of Imperial College London

2013

I certify that the work in this thesis is my own and that the work of others is  
appropriately acknowledged

“The copyright of this thesis rests with the author and is made available under a Creative Commons Attribution Non-Commercial No Derivatives licence. Researches are free to copy, distribute or transmit the thesis on the condition that they attribute it, that they do not use it for commercial purposes and that they do not alter, transform or build upon it. For any reuse or redistribution, researches must make clear to others the licence terms of this work”

To Ricardo, Lorena, Rodrigo, Jorge, Ana, Memé y el Güero

Coincido...

# Abstract

One of the challenges of current organic solvent nanofiltration (OSN) membranes is to improve permeability in polar and non-polar solvents without compromising selectivity. Here, the development of a new generation of OSN membranes: High flux Thin Film Composite membranes (TFC) via interfacial polymerization (IP), is proposed. This thesis offers a comprehensive study that analyses the relationship of OSN high flux TFC membrane formation and post-formation parameters, morphology, structure and surface polarity, to membrane functional performance in both polar and non polar solvents. The dissertation starts with the development of novel high flux TFC membranes for polar aprotic solvents to address the trade-off between permeability and selectivity. This is accomplished by using two different approaches: (a) incorporation of polyethylene glycol inside the pores of the support prior to the IP reaction, and; (b) post-treatment of the TFC membranes with an “activating solvent”. Subsequently, a detailed analysis of membrane performance and morphology, considering the aforementioned approaches was conducted, resulting in dramatically increased solvent fluxes without compromising rejection. Additionally, a detailed study to manipulate molecular weight cut-off (MWCO) of these TFC membranes was carried out and successfully achieved by using different amines in the IP reaction. Next, novel high flux hydrophobic TFC membranes via IP with tuned MWCO for non-polar solvents were developed, elucidated and studied. The surface properties of hydrophilic TFC OSN membranes were modified by capping the free acyl chloride groups on their surface with different monomers containing hydrophobic groups. A detailed study on surface polarity and membrane performance was undertaken, suggesting that surface chemistry plays an important role in solvent permeation. The membrane performance was compared to commercial OSN integrally skinned asymmetric (ISA) and TFC rubber-coated membranes. In the next stage of this thesis, the effects of different support membranes on TFC membrane formation and functional performance were studied for both polar and non-polar solvents. It was found that support membranes have an effect on TFC membrane formation and solvent permeation. Finally, to increase permeability even further without a requirement for treating the TFC membrane with an activating solvent, highly porous TFC membranes have been developed via IP by controlling the structure of the top layer at a molecular level. This was achieved by incorporating a monomer with a contorted structure during the IP reaction, resulting in a highly porous polymer network. It is believed high flux TFC OSN membranes prepared by interfacial polymerization may offer new degrees of freedom in membrane design, which could lead to the next generation of high performance OSN membranes.

# Acknowledgments

I would like to thank my supervisor Professor Andrew G. Livingston for his encouragement and support throughout the course of my PhD. It has been a privilege working and learning from you.

I am also grateful to all my colleagues in the Livingston's group who were always there to advise me and support me. Special thanks to Dr. Yogesh for working closely with me during many stages of my PhD, to Marta for working with me during the research on TFC-PIMs membranes, and to Iwona, Humera and Asia for their important input in my work, and their support during my PhD.

I would like to thank those who technically contributed to this work, Jeong for conducting GPC analyses, and Joanna and Elin for collaborating with me.

I would like to acknowledge financial support provided by the 7<sup>th</sup> Framework Programme of the European Commission's Marie Curie Initiative (NEMOPUR project, grant No. 214226-2).

Special thanks to my friends Elisa, Armando, David, Iwona, Fabian, Alonso, Ana and Ioscani, who were always there to support me. I am also grateful to all my Friends from Mexico, who despite the distance have always been there for me: Roberto, Jesica, Mariana, Alexandra, Tanya, Maricarmen, Alejandro, Adri, and Andrea.

To the above-mentioned and many other unnamed colleagues and friends, who have also contributed to the completion of this work and gave me their support, I extend my sincere thanks.

Thanks Tom (: for your support and all the good times we had during my write-up period.

Finalmente quiero agradecerle a mi familia, a quien extraño todos los días. Gracias a su amor, su gran apoyo y su amistad tengo la oportunidad de celebrar este éxito, el cual también es suyo.

# Publications

## Parts of this thesis have been published or submitted for publication:

M.F. Jimenez Solomon, Y. Bhole, and A.G. Livingston, High flux membranes for organic solvent nanofiltration (OSN)—Interfacial polymerization with solvent activation. *J. Membr. Sci.* 423–424 (2012) 371-382.

M.F. Jimenez Solomon, Y. Bhole, and A.G. Livingston, High flux hydrophobic membranes for organic solvent nanofiltration (OSN)—Interfacial polymerization, surface modification and solvent activation. *J. Membr. Sci.* 434 (2013) 193-203.

Joanna Stawikowska, M.F. Jimenez Solomon, Y. Bhole, and A.G. Livingston, Nanoprobe contrast agents to elucidate the structure of thin film composite nanofiltration membranes. *J. Membr. Sci.* 442 (2013) 107-118.

György Székely, Patrizia Marchetti, M.F. Jimenez Solomon, and A.G. Livingston, Nanofiltration Membranes in Organic Solvents. *Encyclopedia of Membrane Science and Technology*, Wiley (2013) *Accepted*.

M.F. Jimenez Solomon, Patricia Gorgojo, and A.G. Livingston, Beneath the surface: Influence of supports on thin film composite membranes by interfacial polymerization for organic solvent nanofiltration. *J. Membr. Sci.* (2013) *in Press*.

# Patents

**Parts of this thesis have resulted in patent applications:**

M.F. Jimenez Solomon, Y. Bhole, and A.G. Livingston, UK Patent application No 1117950.4, Membranes for separation (2010).

M.F. Jimenez Solomon, Y. Bhole, and A.G. Livingston, UK Patent application No 1012083.0, Thin Film Composite Membranes for separation (2011).



# List of Figures

<b>Figure 1.</b> Schematic representation of polymeric membranes; (a) integrally skinned asymmetric membrane; (b) thin film composite membrane. ....	5
<b>Figure 2.</b> RO membranes performance. ....	5
<b>Figure 3.</b> Membrane casting. ....	8
<b>Figure 4.</b> Schematic representation of TFC membrane formation. ....	10
<b>Figure 5.</b> Chemical structure of polyamide FT-30 membrane. ....	11
<b>Figure 6.</b> Diagram of typical TFC membrane production process. ....	19
<b>Figure 7.</b> Chemical potential ( $\mu_i$ ), pressure (p), and solvent activity ( $\gamma_i c_i$ ) profiles for pressure-driven permeation through a membrane according to (a) solution-diffusion and (b) pore-flow transport models. ....	38
<b>Figure 8.</b> SEM images of surface of TFC membranes. (a) PESf- TFC-MPD membrane; (b) TFC-MPD membrane prepared on crosslinked polyimide support; (c) TFC-PIP membrane prepared on crosslinked polyimide support. ....	53
<b>Figure 9.</b> ATR-FTIR spectra of crosslinked PI support and TFC-MPD membrane. ....	54
<b>Figure 10.</b> ATR-FTIR spectra of crosslinked P84 UF supports with and without PEG. ....	56
<b>Figure 11.</b> MWCO curves and fluxes of TFC membranes prepared on a crosslinked polyimide support membrane with and without PEG as conditioning agent, and with and without post- treatment with DMF as an activating solvent. Nanofiltration of a feed solution comprising polystyrene oligomers dissolved in methanol has been performed at 30 bar and 30°C. (a) No PEG, no activating solvent treatment; (b) No PEG, with activating solvent treatment; (c) With PEG, no activating solvent treatment; (d) With PEG, with activating solvent treatment. ....	57
<b>Figure 12.</b> MWCO curve and flux of TFC membranes prepared on a crosslinked polyimide support membrane without (a) and with (b) PEG as conditioning agent. Nanofiltration of a feed solution comprising polystyrene oligomers dissolved in DMF has been performed at 30 bar and 30°C. ....	58
<b>Figure 13.</b> Repeatability of MWCO curve and flux of TFC membranes prepared on a crosslinked polyimide support membrane with PEG as conditioning agent. Nanofiltration of a feed solution comprising polystyrene oligomers dissolved in DMF has been performed at 30 bar and 30°C. ....	59

<b>Figure 14.</b> SEM images of TFC OSN membranes. (a) Shows the cross-section of TFC-MPD before DMF treatment; (b) Shows the cross-section of TFC-MPD after treating with DMF; (c) Shows the surface of TFC-MPD membrane before treating with DMF; (d) is the surface of TFC-MPD after treating with DMF. ....	61
<b>Figure 15.</b> MWCO curve and flux of TFC-MPD membranes without (a) and with (b) treatment with DMF as an activating solvent. Nanofiltration of a feed solution comprising polystyrene oligomers dissolved in acetone performed at 30 bar and 30°C. ....	62
<b>Figure 16.</b> MWCO curves and fluxes of TFC-MPD membranes after treatment with DMF as an activating solvent. Nanofiltration of a feed solution comprising polystyrene oligomers dissolved in ethyl acetate or toluene has been performed at 30 bar and 30°C. (a) ethyl acetate as solvent; (b) toluene as solvent. ....	63
<b>Figure 17.</b> MWCO curves and fluxes of membranes after treatment with DMF as an activating solvent. Comparative study between TFC-MPD membranes and commercial integrally skinned asymmetric OSN membranes (DM150). Nanofiltration of a feed solution comprising polystyrene oligomers dissolved in THF or acetone has been performed at 30 bar and 30°C. (a) THF as solvent; (b) acetone as solvent. ....	63
<b>Figure 18.</b> MWCO curves and flux of TFC membranes prepared with different amines after immersion in DMF as an activating solvent. Nanofiltration of a feed solution comprising alkanes dissolved in THF performed at 30 bar and 30°C. ....	65
<b>Figure 19.</b> MWCO curves and flux of TFC membranes prepared with different amines after immersion in DMF as an activating solvent. Nanofiltration of a feed solution comprising polystyrene oligomers dissolved in acetone performed at 30 bar and 30°C. (a) amine is MPD; (b) amine is PIP; (c) amine is HDA. ....	65
<b>Figure S1.</b> Electromicrographs of PA/XP84 TFC membrane (courtesy of J. Stawikowska). (a) TEM cross sectional image of the PA/P84 membrane after filtration from the surface side, (b) and the open side.....	67
<b>Figure S2.</b> High magnification TEM cross-sectional images of the PA composite separation layer. Three images acquired from different regions (courtesy of J. Stawikowska). ....	68
<b>Figure 20.</b> Strategies for Hydrophobic TFC membrane formation. ....	77
<b>Figure 21.</b> MWCO curves and fluxes of TFC membranes after treatment with DMF as an activating solvent. Nanofiltration of a feed solution comprising polystyrene oligomers dissolved in toluene has been performed at 30 bar and 30°C. (a) Comparison study between control TFC membrane and commercial integrally skinned asymmetric OSN membrane (SM 122); (b) TFC membrane capped with fluoro-alkylamine; (c) TFC membrane capped with silicone-alkylamine; (d) TFC membrane capped with fluoro-alkylacylchloride. ....	81
<b>Figure 22.</b> MWCO curves and fluxes of TFC membranes after treatment with DMF as an activating solvent. Nanofiltration of a feed solution comprising polystyrene oligomers dissolved in THF performed at 30 bar and 30°C. (a) Control TFC membrane; (b) TFC membrane capped with fluoro-alkylamine; (c) TFC membrane capped with silicone-alkylamine; (d) TFC membrane capped with fluoro-alkylacylchloride. ....	83

<b>Figure 23.</b> MWCO curves and fluxes of TFC membranes after treatment with DMF as an activating solvent. Nanofiltration of a feed solution comprising polystyrene oligomers dissolved in Toluene has been performed at 30 bar and 30 °C. (a) Control TFC membrane prepared by 3 steps IP; (b) 3-steps IP TFC membrane capped with fluoroalkylacetylchloride; (c) Control TFC membrane; (d) TFC membrane capped with fluoroalkylacetylchloride. ....	84
<b>Figure 24.</b> MWCO curves and fluxes of TFC membranes after treatment with DMF as an activating solvent. Nanofiltration of a feed solution comprising polystyrene oligomers dissolved in Ethyl acetate performed at 30 bar and 30°C. ....	86
<b>Figure 25.</b> MWCO curves and fluxes of TFC membranes after treatment with DMF as an activating solvent. Nanofiltration of a feed solution comprising polystyrene oligomers dissolved in Toluene performed at 30 bar and 30°C. Comparison study between TFC membranes and commercial rubber coated TFC OSN membranes (S380). ....	87
<b>Figure 26.</b> MWCO curves of crosslinked polyimide (XP84 <sub>(DMSO)</sub> ) and poly(ether ether ketone) (PEEK) UF support membranes. Filtration of feed solutions comprising dextran dissolved in water has been performed at 2 bar and 25°C. ....	100
<b>Figure 27.</b> Flux curves of crosslinked polyimide (XP84 <sub>(DMSO)</sub> ) and poly(ether ether ketone) (PEEK) UF support membranes. Filtration of feed solutions comprising dextran dissolved in water has been performed at 2 bar and 25°C. ....	100
<b>Figure 28.</b> AFM topographical images of UF support membranes revealing changes in surface roughness: (a)XP84 <sub>(DMSO)</sub> membrane without PEG , (b) XP84 <sub>(DMSO)</sub> membrane with PEG, (c) PEEK membrane without PEG, (d) PEEK membrane with PEG. ....	101
<b>Figure 29.</b> The data shown here has been reproduced from Figure 11 for convenience of comparison. MWCO curves and fluxes of TFC membranes prepared on a crosslinked polyimide support membrane with and without PEG as conditioning agent, and with and without post-treatment with DMF as an activating solvent. Nanofiltration of a feed solution comprising polystyrene oligomers dissolved in methanol has been performed at 30 bar and 30°C. (a) No PEG, no activating solvent treatment; (b) No PEG, with activating solvent treatment; (c) With PEG, no activating solvent treatment; (d) With PEG, with activating solvent treatment. ....	105
<b>Figure 30.</b> SEM images of TFC membranes revealing changes in surface morphology: (a) TFC membrane prepared on XP84 <sub>(DMSO)</sub> without PEG, (b) TFC membrane prepared on XP84 <sub>(DMSO)</sub> with PEG, (c) TFC membrane prepared on PEEK without PEG, (d) TFC membrane prepared on PEEK with PEG. ....	106
<b>Figure 31.</b> SEM images of TFC membranes revealing changes in surface morphology: (a) TFC membrane prepared on XP84 <sub>(DMSO)</sub> without PEG post-treated with DMF, (b) TFC membrane prepared on XP84 <sub>(DMSO)</sub> with PEG post-treated with DMF, (c) TFC membrane prepared on PEEK without PEG post-treated with DMF, (d) TFC membrane prepared on PEEK with PEG post-treated with DMF. Post-treatment was done by immersion in DMF for 10 min. ....	107

- Figure 32.** MWCO curves and fluxes of TFC membranes prepared on a poly (ether ether ketone) (PEEK) support membrane with and without PEG as conditioning agent, and with and without post-treatment with DMF as an activating solvent. Nanofiltration of a feed solution comprising polystyrene oligomers dissolved in methanol has been performed at 30 bar and 30°C. (a) No PEG, no activating solvent treatment; (b) No PEG, with activating solvent treatment; (c) With PEG, no activating solvent treatment; (d) With PEG, with activating solvent treatment. .... 108
- Figure 33.** Comparison MWCO curves and fluxes of commercial membrane Duramem® 150 and TFC membranes prepared on either a poly (ether ether ketone) (PEEK) or a crosslinked polyimide support membrane impregnated with PEG as conditioning agent, and with post-treatment using DMF as an activating solvent. Nanofiltration of a feed solution comprising polystyrene oligomers dissolved in THF has been performed at 30 bar and 30°C. .... 109
- Figure 34.** Comparison MWCO curves and fluxes of commercial membrane Starmem™ 122 and hydrophobic TFC membranes prepared on either a poly (ether ether ketone) (PEEK) or a crosslinked polyimide support membrane impregnated with PEG as conditioning agent, and with post-treatment using DMF as an activating solvent. Nanofiltration of a feed solution comprising polystyrene oligomers dissolved in toluene has been performed at 30 bar and 30°C. .... 110
- Figure 35.** MWCO curves and flux of TFC-PIMs membranes prepared on a crosslinked polyimide (PI) support membrane with PEG as conditioning agent, and with and without post-treatment in the oven at 85°C for 10 minutes and commercial membrane DM300. Nanofiltration of a feed solution comprising polystyrene oligomers dissolved in acetone has been performed at 30 bar and 30°C. .... 119
- Figure 36.** MWCO curves and flux of TFC-PIMs membranes prepared on a crosslinked polyimide (PI) support membrane with PEG as conditioning agent, and with and without post-treatment in the oven at 85°C for 10 minutes. Nanofiltration of a feed solution comprising polystyrene oligomers dissolved in methanol has been performed at 30 bar and 30°C. .... 120
- Figure 37.** MWCO curves and flux of TFC-PIMs membranes prepared on a crosslinked polyimide (PI) support membrane with PEG as conditioning agent, and with and without post-treatment in the oven at 85°C for 10 minutes. Nanofiltration of a feed solution comprising polystyrene oligomers dissolved in DMF has been performed at 30 bar and 30°C. .... 121
- Figure 38.** MWCO curves and flux of TFC-PIMs membranes prepared on a crosslinked polyimide (PI) support membrane with PEG as conditioning agent, and with and without post-treatment in the oven at 85°C for 10 minutes and commercial membranes DM500 and DM900. Nanofiltration of a feed solution comprising polystyrene oligomers dissolved in THF has been performed at 30 bar and 30°C. .... 121
- Figure 39.** MWCO curves and flux of TFC-PIMs membranes prepared on a crosslinked polyimide (PI) support membrane with PEG as conditioning agent, and with and without post-treatment in the oven at 85°C for 10 minutes. Nanofiltration of a feed solution comprising polystyrene oligomers dissolved in toluene has been performed at 30 bar and 30°C. .... 122

---

<b>Figure 40.</b> MWCO curves and flux of TFC-PIMs membranes prepared on a poly(ether ether ketone) (PEEK) support membrane with PEG as conditioning agent, and with post-treatment in the oven at 85°C for 10 minutes. Nanofiltration of a feed solution comprising polystyrene oligomers dissolved in acetone, THF or toluene performed at 30 bar and 30°C; (a) acetone as a solvent; (b) THF as a solvent; (c) toluene as a solvent. ....	124
<b>Figure 41.</b> Permeate flux of TFC OSN membranes at 30bar and 30°C over 1 week operation. ....	130
<b>Figure 42.</b> Permeate flux of DM200 membranes at 30bar and 30°C over 1 week operation. ....	130
<b>Figure 43.</b> Diafiltration modelling of TFC-OSN membranes based on initial rejection data...	132
<b>Figure 44.</b> Diafiltration modelling of DM200 membranes based on initial rejection data.....	133
<b>Figure 45.</b> Gas separation performance of TFC-PIMs membrane prepared on a PEEK support membrane. (a) shows CO <sub>2</sub> /N <sub>2</sub> selectivity vs. CO <sub>2</sub> permeability; (b) shows CO <sub>2</sub> /CH <sub>4</sub> selectivity vs. CO <sub>2</sub> permeability. ....	149

## List of Tables

<b>Table 1.</b> Polymers used to prepare solvent stable UF support membranes. ....	23
<b>Table 2.</b> Summary on membrane characterization. ....	36
<b>Table 3.</b> Membrane codes for the TFC membranes. ....	47
<b>Table 4.</b> Contact angle of supports with and without PEG. ....	56
<b>Table 5.</b> TFC-MPD membranes flux after post-treatment in different solvents. ....	66
<b>Table 6.</b> Solutions used for the preparation of TFC membranes. ....	74
<b>Table 7.</b> Membrane codes. ....	74
<b>Table 8.</b> Contact angle of TFC membranes. ....	79
<b>Table 9.</b> Surface Elemental Composition. ....	79
<b>Table 10.</b> Membrane codes. ....	94
<b>Table 11.</b> Repeatability analysis. ....	97
<b>Table 12.</b> PEG uptake. ....	99
<b>Table 13.</b> Mercury porosimetry <sup>a</sup> and N <sub>2</sub> adsorption <sup>b</sup> results. ....	99
<b>Table 14.</b> Contact angle of UF supports with and without PEG. ....	99
<b>Table 15.</b> A quantitative summary of surface roughness. ....	101
<b>Table 16.</b> Membrane codes for TFC-PIMs and commercial membranes. ....	117
<b>Table 17.</b> Membranes identification codes. ....	128
<b>Table 18.</b> Rejection of Molecule A at 30bar and ~30°C over 1 week operation. ....	131
<b>Table 19.</b> Rejection of Molecule B at 30bar and ~30°C over 1 week operation. ....	131
<b>Table 20.</b> Process comparison for TFC-OSN and DM200 membranes and 3 stage LLE. ....	133

## List of acronyms and abbreviations

AFM	Atomic force microscopy
APIs	Active Pharmaceutical Ingredients
ATR-IR	Attenuated total reflection IR spectroscopy
BA	3,5-diaminobenzoic acid
CNTs	Carbon nanotubes
CSA	Camphor sulfonic acid
DCM	Dichloromethane
DMAc	Dimethylacetamide
DMDA	dimethylenediamine
DMF	N,N-dimethylformamide
DMSO	Dimethylsulfoxide
EA	Ethyl acetate
FT-IR	Fourier transfer IR spectroscopy
GSK	GlaxoSmithKline
HDA	1,6-hexamethylenediamine
IP	Interfacial polymerization
IPC	Isophthaloyl chloride
ISA	Integrally skinned asymmetric
JS	Joanna Stawikowska
LLE	Liquid-liquid extraction
MBRs	Membrane bioreactors
MEK	Methyl ethyl ketone
MeOH	Methanol
MET	Membrane Extraction Technology
MFJS	Maria F. Jimenez Solomon
MIBK	Methyl isobutyl ketone
MPD	<i>m</i> -phenylenediamine
MSA	Methane sulfonic acid
MWCO	Molecular weight cut-off
NF	Nanofiltration

---

NMDA	1,9-nonamethylenediamine
NMP	N-methyl pyrrolidone
NP	Nanoprobes
OPD	<i>o</i> -phenylenediamine
OSN	Organic Solvent Nanofiltration
PA	Polyamide
PAA	Polyacrylic acid
PAH	Poly(amide hydrazide)
PAI	Poly(amide imide)
PALS	Positron annihilation lifetime spectroscopy
PAN	Polyacrylonitrile
PAS	Positron annihilation spectroscopy
PBI	Polybenzimidazole
PDMS	Polydimethylsiloxane
PEA	Poly(ether amide)
PEBAX	Poly(ether- <i>b</i> -amide)
PEEK	Poly(ether ether ketone)
PEG	Polyethylene glycol
PEI	Polyetherimide
PEI	Polyethyleneimine
PESf	Polyethersulfone
PI	Polyimide
PIMs	Polymers with intrinsic microporosity
PIP	Piperazine
PPD	<i>p</i> -phenylenediamine
PPESK	Poly(phthalazinone ether sulfone ketone)
PPO	Poly(2,6-dimethyl-1,4-phenyleneoxide)
PPz	Polyphosphazene
PS	Styrene oligomers
PTMSP	Poly[1-(trimethylsilyl)-1-propyne]
PU	Polyurethane
PUA	Poly(urea amide)
PVA	Poly(vinyl alcohol)
PVDF	Poly(vinylidene fluoride)
RMS	Root mean-square
RO	Reverse Osmosis
SC	Sebacoyl chloride



SEM	Scanning electron microscopy
SLS	Sodium lauryl sulfate
S-MPD	m-phenylenediamine-5-sulfonic acid
SPPEK	Sulfonated poly(phthalazinone ether sulfone ketone)
TEA	Triethylamine
TEM	Transmission electron microscopy
TFC	Thin film composite
THF	Tetrahydrofuran
TMC	Trimesoyl chloride
TPC	Terephthaloyl chloride
TPC	Terephthaloyl chloride
TTS	5,5',6,6'-tetrahydroxy-3,3,3',3'-tetramethyl-1,1'-spirobisindane
UF	Ultrafiltration

# Contents

<b>Chapter 1. Research motivation and thesis structure.</b> .....	1
<b>Chapter 2. Literature review.</b> .....	4
<b>2.1 Background.</b> .....	4
2.1.1 <i>Membrane development for reverse osmosis.</i> .....	5
2.1.2 <i>Influence of external parameters on membrane performance.</i> .....	6
<b>2.2 Polymeric membranes.</b> .....	7
2.2.1 <i>Integrally skinned asymmetric membranes.</i> .....	7
2.2.2 <i>Thin Film Composite membranes.</i> .....	8
2.2.3 <i>Post-treatment of polymeric membranes.</i> .....	8
2.2.4 <i>Advantages over ISA nanofiltration membranes.</i> .....	9
<b>2.3 TFC membranes prepared by interfacial polymerization.</b> .....	10
2.3.1 <i>Theoretical model of interfacial polymerization.</i> .....	11
2.3.2 <i>Monomers used during IP to prepare TFC membranes.</i> .....	12
2.3.3 <i>Effects of additives, complexing agents and aprotic solvents during the IP     reaction on TFC membrane performance.</i> .....	16
2.3.4 <i>Post-treatment of TFC-IP membranes.</i> .....	18
<b>2.4 TFC membranes prepared by dip-coating.</b> .....	19
<b>2.5 Organic Solvent Nanofiltration.</b> .....	20
2.5.1 <i>OSN membranes.</i> .....	20
2.5.2 <i>Research work on polymeric ISA membranes for OSN.</i> .....	21
2.5.3 <i>Research work on TFC membranes for OSN.</i> .....	22
2.5.4 <i>Novel NF membranes with OSN potential.</i> .....	26
2.5.5 <i>Commercial OSN polymeric membranes.</i> .....	27
<b>2.6 Membrane characterization.</b> .....	29
2.6.1 <i>Functional performance.</i> .....	30
2.6.2 <i>Physical-chemical characterization.</i> .....	30
<b>2.7 Transport models.</b> .....	37

---

<b>Chapter 3. Project objectives.</b> .....	39
Objective 1. Development of high flux TFC OSN membranes for applications in polar solvents via IP. ....	39
Objective 2. Development of high flux TFC OSN membranes for applications in non-polar solvents via IP. ....	40
Objective 3. Study the influence of support membranes on formation and performance of novel TFC OSN membranes by IP. ....	41
Objective 4. Develop new high free volume TFC OSN membranes via IP. ....	41
Objective 5. High flux TFC OSN membranes for the purification of Active Pharmaceutical Ingredients. ....	42
<b>Chapter 4. High Flux Membranes for Organic Solvent Nanofiltration-Interfacial Polymerization with Solvent Activation.</b> .....	43
<b>4.1 Introduction.</b> .....	43
<b>4.2 Experimental.</b> .....	45
4.2.1 <i>Materials.</i> .....	45
4.2.2 <i>Preparation of crosslinked PI UF support membranes.</i> .....	46
4.2.3 <i>Preparation of polyamide thin film composite membranes.</i> .....	47
4.2.4 <i>Treatment of TFC membranes with activating solvent.</i> .....	48
4.2.5 <i>Membrane Characterization.</i> .....	48
4.2.6 <i>Membrane performance.</i> .....	50
<b>4.3 Results and discussion.</b> .....	51
4.3.1 <i>Characterization of TFC OSN membranes.</i> .....	51
4.3.2 <i>Effects of impregnating UF supports with PEG.</i> .....	55
4.3.3 <i>Treatment with activating solvent.</i> .....	57
4.3.4 <i>Controlling permeation pathway dimensions of TFC OSN membranes.</i> .....	64
4.3.5 <i>DMSO as an alternative to DMF as activating solvent.</i> .....	66
<b>4.4 Conclusion.</b> .....	66
<b>4.5 Supplementary information.</b> .....	67
<b>Chapter 5. High Flux Membranes for Organic Solvent Nanofiltration-Interfacial Polymerization, Surface modification and Solvent Activation.</b> .....	69
<b>5.1 Introduction.</b> .....	70
<b>5.2 Experimental.</b> .....	72
5.2.1 <i>Materials.</i> .....	72
5.2.2 <i>Preparation of crosslinked PI UF support membranes.</i> .....	73
5.2.3 <i>Preparation of polyamide thin film composite membranes.</i> .....	73
5.2.4 <i>Treatment of TFC membranes with activating solvent.</i> .....	77

---

5.2.5 Membrane Characterization. ....	78
5.2.6 Membrane performance. ....	78
<b>5.3 Results and discussion. ....</b>	<b>79</b>
5.3.1 TFC OSN membranes characterization. ....	79
5.3.2 Membrane performance. ....	80
<b>5.4 Conclusion. ....</b>	<b>87</b>
<b>Chapter 6. Beneath the surface: Influence of supports on thin film Composite membranes by interfacial polymerization for Organic Solvent Nanofiltration. ....</b>	<b>89</b>
<b>6.1 Introduction. ....</b>	<b>90</b>
<b>6.2 Experimental. ....</b>	<b>92</b>
6.2.1 Materials. ....	92
6.2.2 Preparation of crosslinked PI UF support membranes. ....	93
6.2.3 Preparation of PEEK UF support membranes. ....	93
6.2.4 Preparation of polyamide thin film composite membranes. ....	93
6.2.5 Treatment of TFC membranes with activating solvent. ....	94
6.2.6 Membrane Characterization. ....	95
6.2.7 UF support membranes performance. ....	96
6.2.8 Membrane performance. ....	97
<b>6.3 Results and discussion. ....</b>	<b>98</b>
<b>UF support membranes. ....</b>	<b>98</b>
6.3.1 PEG uptake, mercury porosimetry and BET analyses. ....	98
6.3.2 UF membrane performance. ....	99
6.3.3 AFM-surface roughness analysis. ....	101
<b>TFC membranes. ....</b>	<b>102</b>
6.3.4 Contact angle. ....	102
6.3.5 TFC membranes performance and characterization. ....	102
6.3.6 Impacts of support on permeability for hydrophilic and hydrophobic TFC Membranes. ....	108
<b>6.4 Conclusion. ....</b>	<b>110</b>
<b>Chapter 7. High Flux TFC Membranes with intrinsic microporosity by interfacial polymerization for Organic Solvent Nanofiltration. ....</b>	<b>112</b>
<b>7.1 Introduction. ....</b>	<b>113</b>
<b>7.2 Experimental. ....</b>	<b>115</b>
7.2.1 Materials. ....	115
7.2.2 Preparation of crosslinked PI UF support membranes. ....	115

---

7.2.3 Preparation of PEEK UF support membranes. ....	116
7.2.4 Preparation of network PIMs-like thin film composite membranes by IP. ....	116
7.2.5 Membrane performance. ....	118
<b>7.3 Results and discussion. ....</b>	<b>119</b>
7.3.1 TFC-PIMs-PI membrane performance. ....	119
7.3.2 TFC-PIMs-PEEK membrane performance. ....	123
<b>7.4 Conclusion. ....</b>	<b>125</b>
<b>Chapter 8. High flux TFC OSN membranes for the purification of Active Pharmaceutical Ingredients. ....</b>	<b>127</b>
<b>8.1 Introduction. ....</b>	<b>127</b>
<b>8.2 Experimental. ....</b>	<b>128</b>
8.2.1 Materials. ....	128
8.2.2 TFC membrane preparation. ....	128
8.3.3 Membrane performance. ....	128
<b>8.3 Results and discussion. ....</b>	<b>129</b>
8.3.1 Membrane Flux and Rejection. ....	129
8.3.2 Membrane Stability. ....	131
8.3.3 Separation of API/impurity and process comparison. ....	132
<b>8.4 Conclusion. ....</b>	<b>134</b>
<b>Chapter 9. Final conclusions and future directions. ....</b>	<b>135</b>
<b>9.1 Final conclusions. ....</b>	<b>135</b>
<b>9.2 Future directions. ....</b>	<b>136</b>
<b>Bibliography. ....</b>	<b>139</b>
<b>Appendix. ....</b>	<b>149</b>

# Chapter 1

## Research motivation and thesis structure

A challenge for nanofiltration (NF) and reverse osmosis (RO) is to broaden their application range from aqueous to organic feeds. Industries from oil refining to pharmaceuticals could reap major benefits from reduced energy consumption and simplification of solvent based processes, just as the desalination industry has benefitted from the introduction of reverse osmosis membranes. Meeting this challenge requires solvent stable membranes that preserve their separation characteristics in a wide range of solvents, and which offer defect-free morphology and controlled molecular weight cut-offs (MWCOs). Organic Solvent Nanofiltration (OSN) is an emerging technology for molecular separation and purification processes carried out in organic solvents [1], based on selective solvent stable membranes.

Many of the OSN membranes developed to date are integrally skinned asymmetric membranes prepared by the Loeb-Sourirajan method [1, 2]. These integrally skinned asymmetric membranes suffer from limitations in terms of flux for some organic solvents, and tight membranes (MWCO=150-300 Daltons) have poor fluxes in polar and non-polar solvents. This limitation might be overcome by carefully controlling the formation of the separation layer. Another possibility is to adopt a more sophisticated strategy: develop Thin Film Composite (TFC) membranes via interfacial polymerization (IP) for OSN applications. TFC membranes (first developed by Cadotte [3]) consist of an ultra-thin “separating barrier layer” prepared via IP on top of a chemically different porous support, which gives more freedom to design an effective membrane for a specific application.

Conventional TFC membranes used for aqueous applications cannot be used in strongly swelling solvents because the membrane supports tend to swell or dissolve, affecting the membrane separation performance. Thus, the solvent stability of TFC membranes must be improved. The aim of this thesis is to develop TFC OSN membranes via IP for polar and non-polar solvents. The hypothesis of this work is that TFC OSN membranes have the potential to achieve higher fluxes than integrally skinned asymmetric OSN membranes, without sacrificing selectivity. However, to

date there are no reported TFC OSN membranes prepared via IP which are stable in strongly swelling solvents, such as polar aprotic solvents, including DMF and THF.

Conventional purification technologies in the manufacture of Active Pharmaceutical Ingredients (APIs) include crystallisation, distillation, liquid-liquid extraction, chromatography, and adsorption onto activated carbon or silica. However, they have limitations in cost, scale up and selectivity. During the production of APIs harsh organic solvents of different polarities are used. Thus, stable membranes with controlled polarity are required. In order to make this process viable and versatile, new polymeric and ceramic OSN membranes with high selectivity, improved permeability and tuneable polarity need to be developed.

To date, there is no research evidence in the use of TFC OSN membranes to purify active pharmaceutical ingredients. However, such an OSN process, in principle, could be employed. This work will focus on developing a new generation of OSN membranes: High flux TFC OSN membranes via interfacial polymerization. As a result, a cheaper, more selective and more efficient process for the removal of impurities during the manufacture of APIs could be developed.

It was decided to try different chemistries to make defect-free films by interfacial polymerization as the TFC top layer. These films should be resistant in organic solvents and have good permeance in polar or non-polar solvents. Once these chemistries were selected, the properties of the supports on the overall TFC membrane performance were studied and a real API purification was carried out as a proof of concept.

It is possible to prepare different polymer chemistries by interfacial polymerization. In Chapter 4, polyamide was the selected chemistry to prepare the top layer of hydrophilic OSN TFC membranes for polar solvents as the formed polyamide and the monomers used present several advantages compared to other polymer systems: (a) polyamide network is stable in many organic solvents; (b) the interfacial polymerization reaction to form polyamide is fast, forming a thin film instantly avoiding the formation of defects; (c) the chosen amines (MPD, PIP and HDA) used to make polyamide are soluble in water and can diffuse to the organic phase (hexane) easily; (d) the selected amines and acyl chloride are commercially available. Several attempts to polyethers top layer by interfacial polymerization failed because the reaction was very slow; the film formed after several days. In Chapter 4, novel high flux hydrophilic TFC OSN membranes were developed via interfacial polymerization on crosslinked polyimide support. Different parameters during the TFC membrane formation were studied and controlled, to achieve higher permeability without compromising selectivity. Their MWCOs were controlled by using different amines during the IP reaction. To prove the potential of these TFC membranes for the purification of APIs in polar

solvents, in collaboration with Elin Rundquist (GSK), a purification study is described in Chapter 8. To ensure TFC membranes can be used in non-polar solvents, a detailed analysis on surface modification and incorporation of hydrophobic monomers during the IP reaction was undertaken in Chapter 5 to find an optimum method to render the TFC membranes hydrophobic. In Chapter 6, the effect of the support membrane on the overall TFC membrane performance in polar and non-polar solvents was studied. Two different solvent stable supports were developed for the formation of both hydrophilic and hydrophobic TFC membranes. A detailed study on the morphology, porosity, surface chemistry and polarity of each support was undertaken to understand the influence of these parameters on TFC membrane formation and performance. Finally, in Chapter 7 to further enhance permeability a PIM-like network polyester was formed as the top layer of TFC OSN membranes. A contorted monomer was used during the IP reaction to provide concavity and higher porosity to the top layer. Polyester being more hydrophobic than polyamide would perform well in both polar and non-polar solvents. It is also stable in many organic solvents and the formation of the film is instantaneous, resulting in a defect-free top layer. The effects of curing on TFC membrane performance were studied to find an optimum MWCO without compromising permeability. The performance of these ultra high flux PIM-like membranes was compared with commercial integrally skinned asymmetric membranes and with the TFC OSN membranes prepared in Chapters 5 and 6.



# Chapter 2

## Literature review

This review seeks to provide insight into state-of-the-art research in TFC membranes for both aqueous and organic applications, as well as into how different parameters in the membrane formation and post-formation processes affect overall membrane performance.

### 2.1 Background

Currently, in RO and NF applications, membranes with very thin top layers are used. Membranes displaying this combination of a separating top layer on a more porous support structure are called asymmetric membranes [4]. These membranes will be explained in further detail in *section 2.2*.

Phase inversion, developed by Loeb and Sourirajan [5] in the early sixties, is one of the most adaptable, economical and reproducible techniques for the formation of asymmetric polymeric membranes. These membranes possess a skin-layer on top of a more porous sublayer with the same chemical composition as shown in Figure 1(a), and are often called integrally skinned asymmetric (ISA) membranes. The key for high performance is the thin skin-layer, which makes higher selectivity possible. Another important class of membranes, effective for RO and NF, are TFC membranes developed by Cadotte [6]. They consist of a thin “separating barrier layer” on top of a chemically different porous support as shown in Figure 1(b). The separating layer of TFC membranes is normally prepared via dip-coating or by interfacial polymerization on a support-layer, which is formed by phase inversion. Because of their layered structure, TFC membranes are very flexible and the chemistry and performance of both barrier-layer and porous substrate can be independently optimized to maximize overall membrane performance [3, 8, 7].

In general, attention has been on the development of TFC membranes for aqueous applications, in particular sea water desalination. However, these membranes can also be used for filtrations in certain organic solvents and, with some optimization, in a wider range of solvents.

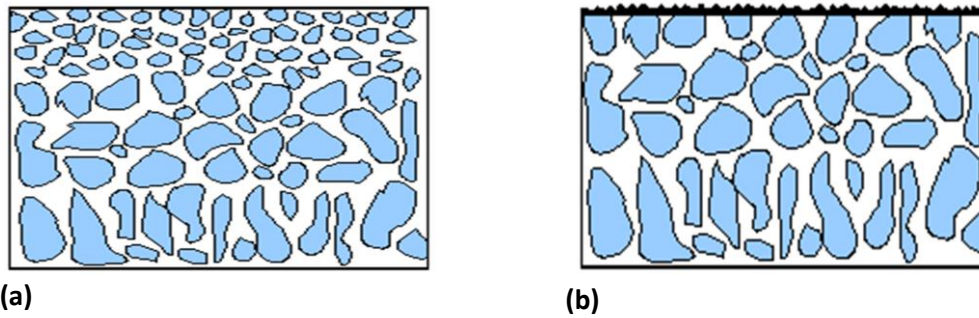


**Figure 1.** Schematic representation of polymeric membranes; (a) integrally skinned asymmetric membrane; (b) thin film composite membrane.

### 2.1.1 Membrane development for reverse osmosis

Figure 2 shows the performance of important RO membranes produced for the desalination market. The dotted line at 99.3 in the plot, divides the figure in two sections. This value is the minimum sodium chloride rejection that can produce potable water from seawater in just one pass [9]. Only Cellulose triacetate, PEC-1000 and some types of cross-linked fully aromatic polyamides can fulfil this requirement. However, cellulose triacetate has lower fluxes and deteriorates in water. Thus, the only types of RO membranes that can efficiently produce potable water in a single pass from sea water are cross-linked polyether and cross-linked fully aromatic polyamide membranes. This is one of the reasons why most development has been focussed on polyamide TFC membranes.

The first asymmetric RO membranes, prepared by Loeb and Sourirajan at the beginning of 1960s, showed a water flux 100 times higher than any symmetric membranes known [5]. This development enabled the successful commercialisation of reverse osmosis membranes. In 1970, cellulose acetate membranes were the first type to be commercially available [4]. One of the main disadvantages of cellulose acetate membranes is their deterioration due to hydrolysis, which is strongly dependent on the pH of the feed. Therefore, careful pH control and adjustment is needed. Another disadvantage of these membranes is that they tend to compact under high pressure, decreasing their flux as well as their overall performance [4].

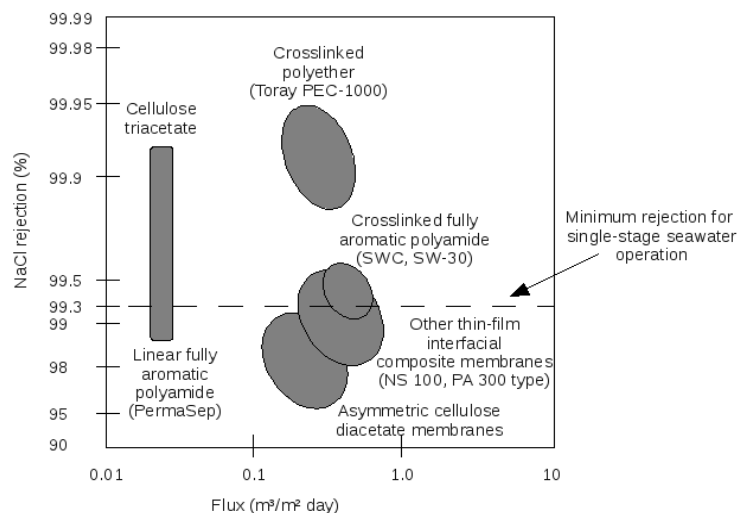


**Figure 2.** RO membranes performance (adapted from [6]).

Cellulose acetate membranes are still commercially available. However, they are being increasingly replaced by TFC membranes (e.g. PEC 1000, and cross-linked polyamide membranes), which have a high physical stability, since the skin layer is chemically bonded to the support.

Thin film composite membranes can be prepared by different methods, which will be explained later in this chapter. The most developed one is interfacial polymerization, a technique invented by Cadotte [10, 11, 12] which allows the production of polymer layers down to 50 nm thick. Since this discovery, this method has become the new industry standard in reverse osmosis [6].

Interfacial TFC membranes have significantly higher salt rejections and fluxes than cellulose acetate membranes, with less than half the salt passage and two times the water flux [6]. TFC membranes are physically and chemically more stable, possess strong bacterial degradation resistance, do not hydrolyse, are less influenced by membrane compaction and are also stable in a wider range of feed pH (3-11). Nevertheless, composite membranes are less hydrophilic and as a consequence, they are more prone to fouling than cellulose acetate membranes in RO applications, and deteriorate in the presence of very small amounts of free chlorine in the feed solution [4].

### 2.1.2 Influence of external parameters on membrane performance

In order to be efficient, membranes should present high flux and high solute rejection. Very thin membrane separation layers are required to achieve high permeability because flux is inversely proportional to the membrane thickness.

Solvent flux is proportional to the applied pressure gradient. Selectivity can be measured in a number of ways, but conventionally, it is measured as the solute rejection coefficient  $R$ .

Solvent flux ( $J$ ) is determined by measuring permeate volume ( $V$ ) per unit area ( $A$ ) per unit time ( $t$ ) according to equation 1. The rejection coefficient ( $R_i$ ) is a measure of the ability of the membrane to separate a solute  $i$  from the feed solution and is calculated from equation 2, where  $C_{P,i}$  and  $C_{F,i}$  correspond to marker concentrations in the permeate and the feed respectively.

$$J = \frac{V}{A \cdot t} \quad (1)$$

$$R_i = \left(1 - \frac{C_{P,i}}{C_{F,i}}\right) \cdot 100\% \quad (2)$$

In membrane separation some general rules apply as follows [13]:

1. when the operating pressure is increased the solvent flux first increases almost linearly, levels off as the pressure is raised further, and finally may even decrease at elevated pressure;
2. flux decreases as the solute concentration is increased;
3. at higher concentrations rejection strongly decreases and overall efficiency goes down.

## 2.2 Polymeric membranes

### 2.2.1 Integrally skinned asymmetric membranes

ISA membranes present a layered structure in which the porosity, pore size, and membrane composition change from the top to the bottom surface of the membrane. They have a thin selective layer supported on a much thicker, highly permeable microporous substrate of the same material. Because the selective membrane is very thin, membrane fluxes are high. The microporous substrate is essential as it offers the strength required for handling the membrane [6]. Depending on the preparation conditions, these membranes can be used for ultrafiltration or nanofiltration applications.

ISA membranes can be prepared in the ultrafiltration range and used as support membranes for TFC membrane formation. They are made by the wet phase inversion technique [14], which involves the precipitation of a casting solution by immersion in a nonsolvent (water) bath. Water adsorption and loss of solvent cause the film to rapidly precipitate from the top surface down. A casting solution consisting of only one phase is precipitated into two phases: a solid, polymer-rich phase that forms the matrix of the membrane and a liquid, polymer-poor phase that forms the membrane pores [6].

In solution casting, a uniform film of an appropriate polymer is spread across a non-woven fabric (see figure 3). The casting knife comprises a steel blade, resting on two runners, arranged to form a precise gap between the blade and the plate onto which the film is cast. After casting, the film is precipitated by immersion in a water bath. Water precipitates the top surface of the cast film rapidly, forming the dense, selective layer. This layer slows the entry of water into the underlying polymer solution, which precipitates much more slowly and forms a more porous substrate. The thickness of the dense skin varies from 0.1 to 1.0  $\mu\text{m}$  and it depends on the casting solution, the polymer, and other parameters. The thermodynamic properties of the system and the kinetics involved in the exchange of solvent and non-solvent have an impact on the membrane morphology, affecting its permeability and solute rejection [15].

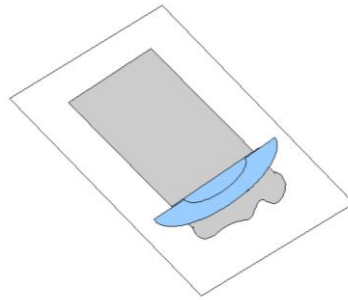


**Figure 3.** Membrane casting.

The dope solution should be sufficiently viscous; usually polymer concentrations are in the range of 15 - 25 (w/w) % [6]. The best solvents for dope solutions are aprotic solvents such as dimethylformamide, which can dissolve a large variety of polymers. Dope solutions based on these solvents precipitate rapidly when immersed in water to give porous ISA membranes.

### 2.2.2 Thin Film Composite membranes

Because of their layered structure, TFC membranes are very flexible and the chemistry and performance of both barrier-layer and porous support can be independently optimized to maximize the overall membrane performance [3,7,8].

The main methods for the formation of the top-layer of TFC membranes are [16]: (a) casting an ultrathin film separately, then laminating it onto a support; (b) interfacial polymerization at the surface of a support; (c) dip-coating/solvent casting a solution of a polymer onto a support; (d) dip-coating a solution of a reactive monomer or pre-polymer onto a support, followed by a post-curing with heat or irradiation; (e) depositing a barrier film directly from a gaseous phase monomer plasma.

TFC membranes for organic solvent applications have been prepared using dip-coating. Currently, mostly all TFC RO membranes are prepared by interfacial polymerization (IP) and a lot of work has been done to understand the effect of different preparation parameters on the membrane's performance.

### 2.2.3 Post-treatment of polymeric membranes

Post-treatment procedures can be applied to both types of polymeric membranes: ISA and TFC membranes. In order to increase the long term stability of ISA membranes and to enhance their separation performance, various conditioning or post-treatment methods can be used, such as crosslinking, wet or dry annealing, drying by solvent exchange, and treatment with conditioning agents [8]. Post-treatment is also crucial for polymeric ultrafiltration (UF) supports used to prepare TFC membranes [17]. It is also possible to further enhance the performance of TFC membranes

by applying an appropriate post-treatment method [1]. Several techniques to enhance membrane performance have been reported in the literature, including curing, grafting, plasma, UV and chemical treatment [1]. More details on the curing and chemical post-treatment methods for TFC membranes can be found elsewhere [18 -24].

#### 2.2.4 Advantages of TFC over ISA nanofiltration membranes

In aqueous applications, interfacial composite membranes have significantly higher salt rejections and fluxes than ISA cellulose acetate membranes. Typical TFC membranes, tested with 3.5 % sodium chloride solutions, have a salt rejection of 99.5 % and a water flux of  $51.0 \text{ Lm}^{-2}\text{h}^{-1}$  at 55 bar ( $0.9 \text{ Lm}^{-2}\text{h}^{-1}\text{bar}^{-1}$ ); this is less than half the salt passage and two times the water flux of cellulose acetate membranes [6].

In the last decades, a significant increase in membrane performance with respect to permeability and salt rejection can be observed. In 1981, Cadotte [11] reported flux values of  $43 \text{ (Lm}^{-2}\text{h}^{-1}\text{)}$  for composite membranes at standard test conditions (3.2 % NaCl, 55 bar,  $25^\circ \text{ C}$ , 8 % recovery), while membranes today reach flux values of as high as  $(201 \text{ Lm}^{-2}\text{h}^{-1})$  [4]. These values are accomplished with brackish water of low salinity, and for seawater membranes classical flux values are significantly lower. From 1996 to 2007, typical seawater membranes increased their rejection from 99.6 % to 99.8 %, whereas flux increased from  $43 \text{ (Lm}^{-2}\text{h}^{-1}\text{)}$  to  $69 \text{ (Lm}^{-2}\text{h}^{-1}\text{)}$  [4].

An advantage of TFC membranes is that the thin barrier layer can be optimized for the desired flux and solute rejection, while the porous support can be optimized for maximum strength and compression resistance, and a minimum resistance to permeate flow. Moreover, the thin barrier layer can be formed from a large variety of chemical compositions, including both linear and crosslinked polymers, whereas the asymmetric membrane formation process is quite limited to linear, soluble polymers. Only a few of such linear polymers have the right combination of flux and solute rejection characteristics to generate commercially attractive membranes [3].

A disadvantage of TFC membranes is that their manufacturing is more expensive compared to ISA membranes. However, the extra cost of manufacturing TFC membranes is more than counterbalanced by the improved performance characteristics of the resulting membrane products [16]. Similarly to water desalination, TFC OSN membranes have the potential to achieve higher fluxes than ISA OSN membranes, without sacrificing selectivity.

Producing an ultrathin layer *in situ* on a microporous substrate also allows the use of a variety of cross-linked polymeric compositions, which can present higher hydrophobicity or hydrophilicity for OSN applications as well as higher chemical resistance compared to linear polymers.

### 2.3 TFC membranes prepared by interfacial polymerization

These membranes are made by interfacially polymerizing a thin layer of polymer at the surface of a porous support membrane. Some general aspects of support membranes for solvent resistant TFC membranes will be discussed later (see *section 2.5.3*).

In IP, an aqueous solution of a reactive monomer, such as amine (hydrophilic monomer), is first deposited in the pores of a porous support membrane, usually a polysulfone ultrafiltration membrane. Then, the polysulfone support loaded with amine is immersed in a water-immiscible solvent solution containing a reactant, such as triacid chloride in hexane (hydrophobic monomer) (see Figure 4). The two monomers react at the interface of the two immiscible solutions, until a thin membrane film presents a diffusion barrier and the reaction is completed to form a highly cross-linked thin membrane layer that remains attached to the substrate. The thin layer can be from several tens of nm to several  $\mu\text{m}$  thick [3, 8, 25].

The dense, cross-linked polymer layer can only form at the interface, and as it is thin on the order of  $0.1\ \mu\text{m}$  or less, the membrane permeability is high. Because the polymer is highly cross-linked, its selectivity is also high. Even though the crosslinked interfacial polymer layer determines membrane selectivity, the nature of the porous UF support membrane affects membrane flux considerably. The film must be finely porous to stand the high pressures applied but should also have a high surface porosity so it is not obstructing solvent flow [6].

A large number of IP TFC membranes have been successfully developed consisting mainly of a polyamide (PA) top-layer, but poly(amide imide) (PAI), poly(ether amide) (PEA), polyurea and poly(urea amide) (PUA) TFC membranes have been developed as well [3].

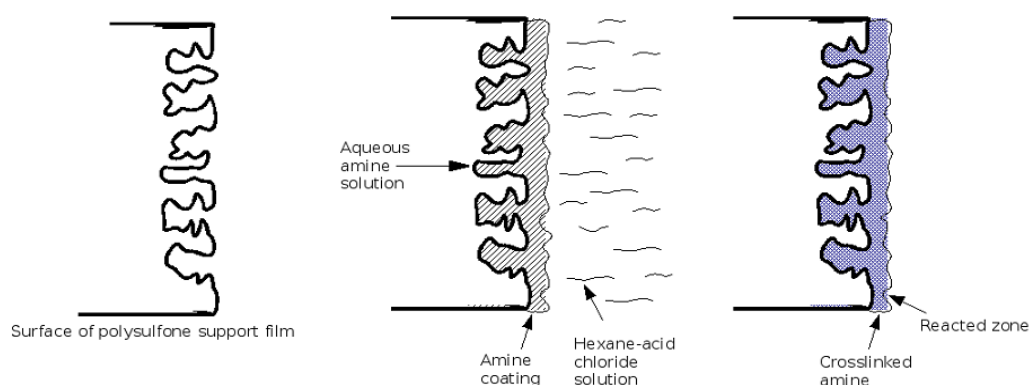


**Figure 4.** Schematic representation of TFC membrane formation.

The development of the FT-30 membrane by Cadotte was very important as it made single-pass seawater desalination with TFC membranes possible, and is the best commercial TFC membrane available for RO [26]. It was produced by the reaction of *m*-phenylenediamine with trimesoyl chloride, shown in Figure 5. This membrane consists of an all-aromatic, highly crosslinked structure giving exceptionally high water flux and consistent salt rejections of 99.5 % from seawater [12].

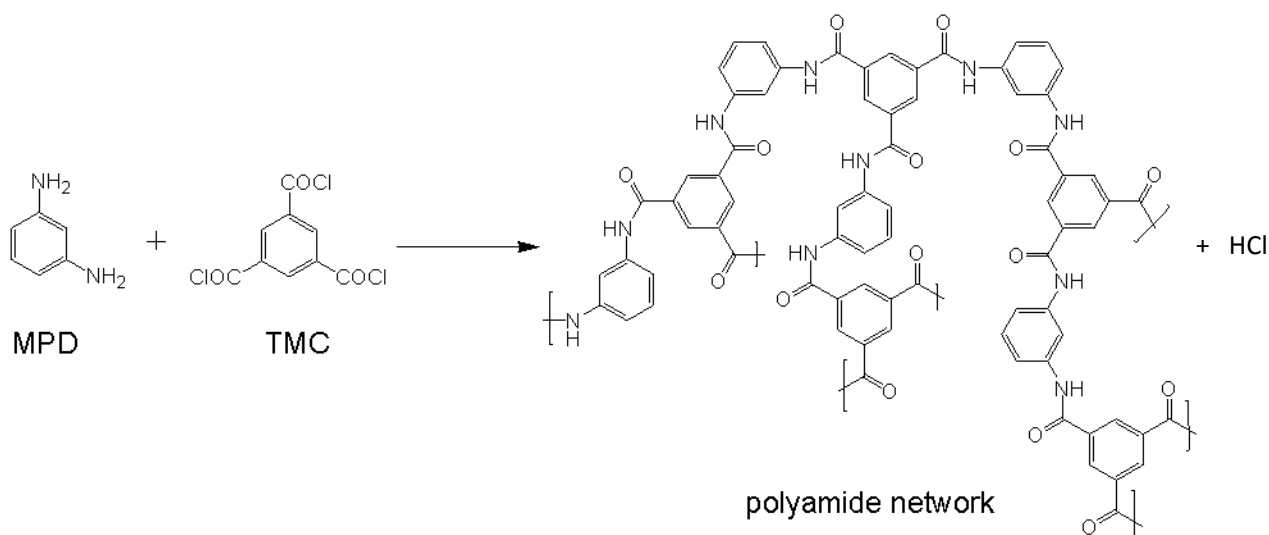


**Figure 5.** Chemical structure of polyamide FT-30 membrane

In sections 2.3.2 to 2.3.4, the effect of different parameters during the IP reaction and membrane post-treatment on overall membrane performance will be explained in detail.

### 2.3.1 Theoretical model of interfacial polymerization

Interfacial polymerization takes place at an interface of two immiscible, low molecular weight fluids, each containing one of the reactants. The dissolved monomers diffuse to the interface, where they undergo the copolymerization reaction. The resulting copolymer is usually incompatible with either of the liquid phases and as a result, a polymer film grows at the interface.

The theoretical description [27,28] of the creation of a thin polymeric layer through interfacial polymerization specifically takes into account the effects of polydispersity on the formation of the polymer film at the liquid-liquid interface. Consequently, models [27,28] can predict both the kinetics of film formation and the molecular weight distribution of the polymer structure of the growing film. Predictions of the film thickness as a function of reaction time have been successfully related to experimental data.



To start the reaction the diamine partitions into the organic phase. It initially meets a high concentration of diacid chloride and is acylated at both ends. The following diamine molecules react with both the diacid chloride and the oligomers with acid functionalities at each end. The growing oligomer chains remain in the solution without precipitation as long as their concentration is less than their respective solubility limit in the organic phase. Phase separation of the oligomeric species starts when the concentration of the growing chains reaches the binodal of the oligomer-solvent phase diagram. Since the chains grow due to a fast reaction, it is assumed that phase separation starts when the concentration of the growing chains becomes equal to the spinodal concentration [27]. Thus, there is some amount of super-saturation allowed before precipitation begins. After the spinodal is crossed, it is assumed that the precipitation of the chains occurs instantly.

The film that initially precipitates has the highest molecular weight. This high molecular weight stays constant for an extended period of time. However, the average molecular weight decreases as more oligomers of lower molecular weight exceed their solubility limit and start to precipitate, increasing the polydispersity of the polymer film. Hence, there is an optimum reaction time to get an adequately thick polymer film with a nearly constant high molecular weight [27].

### 2.3.2 Monomers used during IP to prepare TFC membranes

The thin layer formed via interfacial polymerization mostly consists of a polyamide crosslinked polymer, which is stable in a wide range of solvents including toluene, acetone, dimethylformamide (DMF), hexane and alcohols. Thus, the work reported on aqueous applications for membranes prepared via IP can be carried out in certain organic solvents. The trade-off between permeability and solute rejection in TFC membranes can be partially overcome by carefully choosing the monomers and the polymerization conditions [3, 29, 30].

#### *Amines*

Membranes prepared from aromatic diamines show better rejections, but lower fluxes compared to those prepared using aliphatic diamines. Thus, the former are typically used for RO-membranes, while piperazine or amine-substituted piperidines are preferred for NF applications [3]. One of the main factors affecting rejection is the position of the acyl chloride and the amine groups on the aromatic rings. This has been shown for the reaction of *o*-, *m*- and *p*-phenylenediamine (*OPD*, *MPD*, *PPD*) with isophthaloyl or terephthaloyl chloride (IPC or TPC) [29, 30]. In the polyamide FT-30 membrane the triple functionality of the acyl compound results in a highly crosslinked, mechanically stable and selective network. Hydrolysis of the unreacted acyl groups can also

occur, leading to TFC membranes with fixed charges. This hydrophilization improves water fluxes, and at the same time decreases the density and rejection of the top-layer [29, 30].

In order to prepare loose RO or NF membranes, MPD is often blended with piperazine (PIP). This aliphatic diamine provides higher free volumes and larger pore sizes to the thin active layer [31].

The support is often relatively hydrophobic. However, the wettability of the support can be enhanced by adding *wetting agents* (e.g. polyethylene glycols (PEGs)) to the aqueous diamine solution [31]. Furthermore, the overall membrane performance can be enhanced by adding *swelling agents* (e.g. DMF), improving the interaction between the top-layer being formed and the swollen support [31].

#### *Effect of amine structure*

Previous work [32] studied the permeation performance of TFC membranes obtained from different diamines using TMC as the acyl chloride. All the thin films obtained showed a crosslinked structure. The thin films prepared with aliphatic diamines including 1,6-hexamethylenediamine (HDA), 1,9-nonamethylenediamine (NMDA) and dimethylenediamine (DMDA), had an aliphatic-aromatic network structure. However, the thin-films prepared with aromatic diamines including PPD and MPD had fully aromatic network structures. Network-structure polyamides showed a relatively high salt rejection compared to linear structure polyamides. In the case of the membranes having aliphatic-aromatic network structures, the water flux and the salt rejection decreased with increasing length of the aliphatic methylene chain. On the other hand, thin films with fully aromatic network structures showed high salt rejection and relatively high water flux compared to membranes having aliphatic-aromatic network structures.

Furthermore, the polar component of surface tension was evaluated as a possible measure of the hydrophilicity of the thin active film [32]. The polar force for the thin-films made from aliphatic diamines decreases as the methylene chain of the aliphatic amines increases in length.

#### *Acyl chlorides*

Similar to amines, a broad range of aromatic acyl chlorides have been used to prepare polyamide (PA) based TFC membranes. The number and position of the acyl halide groups on the aromatic ring is a major factor affecting the salt rejection, as they determine the chain structure and the crosslinking degree of the PA network formed [30]. The hydrolysis of acyl chloride groups to carboxylic acid groups has an important effect on the hydrophilicity, surface charge and degree of crosslinking of the membrane [29]. In addition to acyl chloride monomers, polymers with acyl chloride pendant groups can be used. Mixtures of isophthaloyl chloride (IPC) with

poly(isobutylmethacrylate-co-aryloyl chloride) in combination with a tetrafunctional aromatic amine showed good film forming properties [33]. The contact between the phases containing the reactive monomers was improved by replacing the organic phase with benzene or 1,2-dichloroethane, as these are better solvents for the formed PA polymer. By replacing the organic phase, rejections were significantly improved [34].

#### *Effect of acyl chloride structure*

Different properties of linear as well as network structures prepared using di/tri-functional aromatic and aliphatic acyl chloride monomers have been studied using MPD as the diamine. The di-functional acyl chlorides including sebacoyl chloride (SC), isophthaloyl chloride (IPC), and terephthaloyl chloride (TPC) result in a linear structure, whereas the tri-functional acyl chloride, TMC results in a network structure. SC results in an aromatic (amine)-aliphatic (acyl chloride) structure, but the polymers prepared using aromatic acyl chlorides including IPC, TPC, and TMC have a fully aromatic structure. The thin active films that had linear structures (SC, IPC, and TPC) had low salt rejection, whereas network structures (TMC) gave higher salt rejection. Thin active films with the aromatic-aliphatic linear structure (SC) showed high water fluxes, while fully aromatic linear structures (IPC and TPC) resulted in lower water fluxes [32].

The components affecting the polar force are an amide bond, an amine and carboxylic acid end-group, and a free carboxylic acid group in the network structure. The free carboxylic acid groups result in unreacted acyl chloride groups, which can easily be converted to the corresponding carboxylic acids through hydration. The polar forces of the thin polyamide films with fully aromatic linear structure are lower compared to the polyamide having aromatic-aliphatic linear structure [32].

#### *Effects of polymerization parameters*

Monomer concentration has a great influence on the performance of TFC membranes. Lu et al. [35] suggested that the key of the IP method was to select the right partition coefficient of the reactants in the two-phase solution and to set the appropriate diffusion speed of the reactants to achieve the ideal degree of densification of the membrane surface. Moreover, the concentration of the diamine is an important factor, which can affect the performance of the resulting membrane, since it may control the uniformity and thickness of the ultimate polyamide top-layer. Since the IP process is diffusion controlled in the organic phase [36], the effect of organic phase reactant is likely to have a great impact on membrane performance.

Higher monomer concentrations [22, 31, 37], higher reaction rates [29] and longer polymerization times [22, 31, 37] generally improve the efficiency of film formation. These result in thicker and

denser barrier-layers with increased rejections but decreased fluxes. As the concentration of the monomers increases, the thickness of the barrier-layer also increases. The polymerization reaction takes place at the interface between both phases, but the nascent film then gradually grows away from the aqueous phase as the amines diffuse through the interface and the film being formed. As the reaction continues, the film thickness will prevent further amine-diffusion and stop film growth [31].

In previous work [37], the effect of TMC on the membrane properties was studied based on the piperazine/3,5-diaminobenzoic acid (PIP/BA) system. In the case of nanofiltration membranes, it is speculated that the TMC content has a high impact on the rate and degree of reaction, which eventually affects the final performance of the membrane. The relationship between PIP/BA and TMC systems were studied. As the concentration of TMC content is increased, the pore size is reduced. TMC content plays an important role in determining the rate of reaction, while the reaction time will determine the extent of reaction. For short reaction time (5s), the extent of crosslinking is low, and the pore size produced (calculated using the Donnan Steric Pore Flow Model) is larger (0.74nm) [37]. However, when the concentration of TMC is increased, the rate of reaction is increased tremendously. In the case of PIP/BA mixtures, its reduced reactivity produces a more porous structure. It was also found that at higher BA ratio to PIP, the pore size produced is bigger. The increases in rejection at 0.10 % TMC and 0.15 % TMC are due to the decreasing pore size as a result of crosslinking. However, it was observed that the rejection performance dropped at high-TMC content (0.20 %), because pore loosening starts to occur where the reaction rate is so high that excessive 3,5-diaminobenzoic acid is introduced [35]. Skin layers with higher BA content produce membranes with loose structures.

#### *Effects of soaking time on TFC membrane performance*

It is known that with the soaking time being prolonged, the top layer in the TFC membranes thickens, the rejection of the TFC membrane increases, and flux decreases [38]. The polycondensation reaction between amine and acid chloride is exothermic, and so the reaction rate increases with increasing temperature, increasing the extent of crosslinking [38].

#### *Solubility of the monomers*

Prior to the preparation of the TFC membranes, the solubility of the monomers should be determined in order to select appropriate solvents for the acyl chloride solution that do not solubilise the UF support membranes [38].

When the two monomer solutions are brought into contact, both monomers partition across the liquid-liquid interface and react to form a polymer. However, polymerization occurs predominantly

in the organic phase due to the relatively low solubility of most acid chlorides in water. Therefore, it is common to use a large excess of amine over acid chloride (typically about 20:1), which drives partition and diffusion of the amine into the organic phase. Any factors that alter the solubility and diffusivity of the amine monomer in the organic phase affect the reaction rate, and thus, the morphology and structure of the resulting polyamide film, which ultimately define separation performance and interfacial properties [39, 40].

Selecting the organic solvent is crucial since it affects the amine monomer solubility and diffusivity in the reaction zone [18]. It is common in practice to use combinations of additives to influence monomer solubility, diffusivity, hydrolysis, or protonation or to scavenge inhibitory reaction by-products [18] (see additives in *section 2.3.3*).

Generally, in RO membranes, water permeability and salt rejection increase with increasing MPD diffusivity and decreasing MPD solubility. If higher MPD diffusivity is accomplished by changing to an organic solvent also giving higher MPD solubility, films exhibit higher water flux, salt passage, thickness, and roughness, but less crosslinking. If higher MPD diffusivity is accomplished by heating an organic solvent with low MPD solubility, films exhibit higher water flux, salt passage, crosslinking, and roughness [18].

### **2.3.3 Effects of additives, complexing agents and aprotic solvents during the IP reaction on TFC membrane performance**

The use of additives in monomer solutions can influence the rate and extent of interfacial polymerization as well as the extent of crosslinking [41].

The performance of polyamide membranes can be improved with several *aqueous phase additives* (e.g. lower alcohols: n-propanol or i-propanol), which can enhance the contact between both reagent phases. They tend to make the interface between both phases more diffuse, and consequently have a beneficial effect on film formation, thus leading to more selective membranes [34]. However, when the interface gets too diffuse, the path length of the monomers to the reaction site can become excessive, making film formation difficult. This results in rather rough membrane surfaces often showing defects [42].

It has been shown that membrane flux increases when polymeric amines, like poly(aminostyrene), are used in combination with TMC but lower rejections are observed. Furthermore, the addition of small amounts of MPD to the aqueous amine phase enhances rejection rates significantly without affecting water fluxes [29, 30].

Another option to increase water flux is to add 3,5-diamino benzoic acid to the water. Water flux is enhanced because the hydrophilicity is increased by the introduction of non-polymerizable carboxylic groups in the polyamide film [30]. Adding m-phenylenediamine-5-sulfonic acid (S-MPD) also provided hydrophilization and flux improvement effects [43].

As mentioned earlier, addition of small amounts of hydrophilic water-soluble polymers or a polyhydric alcohol to the amine solution can produce membranes with high-flux and good rejection. Aprotic solvents like N,N-dimethylformamide (DMF) have been added to the aqueous aromatic amine solution, inhibiting crosslinking and producing a more negative charge and higher water flux [18]. The use of aprotic solvents such as DMAc and DMF decreased the surface strain between the support surface and the coating solution [38]. This was advantageous for the preparation of TFC membranes with high flux and salt rejection. Dimethylsulfoxide (DMSO) can also be used, however, it is important to choose an *aprotic solvent* in which the support is partly soluble and swells, so that the interaction between the top layer being formed and the swollen support can be increased [38]. Furthermore, adding DMSO to the aqueous amine solution increases miscibility of water and hexane and probably also enhances MPD diffusivity, ultimately, improving water flux by formation of a thinner polyamide film [41, 44]. Increased water-organic miscibility may cause hydrolysis of acid chlorides or de-protonation of amines, thereby reducing their reactivity and the extent of crosslinking.

Sodium hydroxide, sodium tertiary phosphate, dimethyl piperazine, triethylamine (TEA), and other acylation catalysts accelerate the MPD-TMC reaction by removing hydrogen halides formed during amide bond formation [3]. The aqueous solution may further contain a surfactant or organic acids like camphor sulfonic acid (CSA), which improve absorption of the amine solution in the support [45, 46]. Previous work showed that the TFC membranes formed by the addition of TEA-CSA to the aqueous MPD solution present dramatically increased water permeability, salt rejection is unchanged, contact angle is slightly reduced and surface roughness is significantly reduced [18]. Adding salt of TEA and CSA to the aqueous-MPD solution increases MPD-TMC performance by inhibiting amine protonation and acid chloride hydrolysis, and possibly by protecting the support membrane during high temperature curing [18].

The addition of phosphate-containing compounds as a complexing agent into the acyl chloride solution has been patented [47, 48]. This complexing agent removes the halides formed during amide bond formation, which minimises hydrolysis and results in enhanced permeabilities.

### 2.3.4 Post-treatment of TFC-IP membranes

Applying an adequate post-polymerization treatment can further enhance the performance of TFC membranes. Different techniques have been described including curing, grafting, plasma, UV and chemical treatment. Treatment of the active PA layer with ammonia or certain alkylamines at elevated temperatures has been claimed to be flux-enhancing, without altering rejection [49]. Alternatively, NF membranes have been obtained by contacting the PA layer of RO membranes with strong mineral acids (e.g. phosphoric acid), followed by treatment with a rejection-enhancing agent (e.g. tannic acid) [50].

#### *Effect of curing temperature and curing time on membrane performance*

Most studies of the MPD-TMC system indicate that curing is a necessary step to stabilize polyamide thin films [51, 52]. Heat curing is used after film formation to remove residual organic solvent from the film and to promote additional crosslinking through dehydration of amine and carboxylic acid residues. This tends to increase water flux and salt rejection.

However, elevated temperature and curing times promote crosslinking of polymers, producing a dense top layer. High temperatures also produce shrinkage of the substrate membrane surface. Further crosslinking and shrinkage or pore collapsing, result in higher rejection and significant decrease in water flux [38]. With increasing curing time or temperature, the porosity of the polyamide film is reduced by crosslinking and the microporous skin layer of the support membrane can be damaged, resulting in shrinkage or annealing of the support membrane pores. Generally, curing temperatures ranging from 40 to 120°C are used [53].

Membrane surface roughness decreases with increasing curing temperature up to 75°C, but then increases dramatically at 90°C. The rougher surface formed by curing at 90°C temperature could be due to the violence of the rapidly volatilizing solvent [18].

#### *Effects of processing conditions during fabrication of TFC membranes*

Apart from modifying the parameters on the IP reaction, it is also possible to increase flux by modifying the processing conditions used in the fabrication of TFC membranes. A typical TFC production process is shown in figure 6.

After formation of the polyamide layer, the membrane is usually washed thoroughly to remove residual MPD, which, if left behind, can have detrimental effects, such as loss of flux [45]. The washing must be followed by a drying step, if a dry membrane is desired for fabrication of spiral-wound membrane elements. Before drying, it is common practice to dip the membrane in a

solution of glycerol and/or surfactant to prevent loss of porosity in the underlying support layer during drying, and to promote re-wetting. In addition, water flux of TFC membranes can be greatly enhanced by soaking the membrane in an organic salt solution and drying after formation [45].

In previous work [45], after the IP reaction membranes were dried in an oven, they were washed and soaked in solutions containing various organic species, including glycerol, sodium lauryl sulfate (SLS), and the salt of triethylamine with camphorsulfonic acid. Finally, the membranes were dried in an oven for four to six minutes. When the membranes did not contain any flux-preserving species during oven drying, the flux was low, suggesting that the porous structure of the polysulfone support suffered a significant degree of pore collapse during drying. When glycerol was used and a second oven drying was carried out, it preserved the porosity of the support and the surfactant also promoted re-wetting of the membrane. Glycerol did not simply maintain membrane flux during drying; the process of drying the glycerol-treated membranes actively enhanced the membrane flux, without any loss of salt rejection. The best flux was for membranes prepared with 6 % TEA/CSA in the amine solution and dipped in glycerol/SLS and TEA/CSA solution after washing and before the second drying [45]. Thus, the steps of dipping in TEA/CSA and oven drying actually enhanced the membrane flux as well.

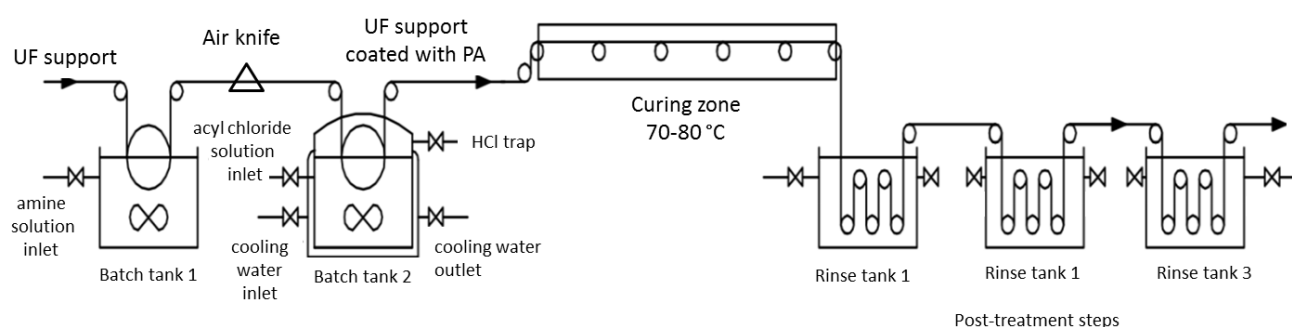


**Figure 6.** Diagram of typical TFC membrane production process.

## 2.4 TFC membranes prepared by dip-coating

A very simple technique of particular interest for the preparation of TFC membranes is the coating of a polymer solution on a support. The coating solution can be cast on the support with a casting knife or spread over the tilted support by pouring, depending on its viscosity [8, 17]. Increased viscosities not only enhance the thickness of the coated film, but also prevent intrusion of the coating solution in the support. Such intrusion should be avoided as it can drastically lower fluxes. The parts of the top-layer present in the pores of the support suffer from steric restrictions, limiting their swelling during filtration [17]. On the other hand, a limited intrusion in the layer might be beneficial for the adhesion of the top-layer. Multiple coatings result in thicker top-layers and thus



lower fluxes, but might be necessary to repair defects. The solvent in which the polymer is dissolved co-determines the adhesion between polymer solution and support. The support characteristics, particularly surface roughness, porosity and hydrophilicity, also influence the adhesion of the top-layer [1].

An example of a composite membrane prepared via dip-coating with very good performance available in the market for RO applications is the Toray PEC-1000. The top layer of PEC-1000 is made out of polyether. This membrane exhibits lower flux than FT-30 but its organic removal efficiency is higher-reported to be 97 % for ethanol [54]. Some examples of composite membranes prepared via the dip-coating technique include membranes that are resistant in organic solvents and will be explained in *section 2.5.3*.

## 2.5 Organic Solvent Nanofiltration

Organic Solvent Nanofiltration (OSN) is a pressure driven membrane process– capable of discriminating between molecules in the range of 200-1000 Dalton – featuring gentle operating conditions and thus providing high-quality products. OSN has significant potential in chemical-related industries employing non-aqueous media, such as organic solvents, including ionic liquids. Application areas can be found in the pharmaceutical, biopharmaceutical, fine chemical, biorefinery and natural product industries. OSN can be applied as a stand-alone operation unit or combined with various separation technologies such as chromatography, adsorbents, distillation and crystallization in a hybrid process. OSN-based technologies have the advantages of: (i) reducing energy consumption, operation time and process complexity, and (ii) improving production sustainability, quality and yield. Designing and preparing membranes with the required nanostructure to allow molecular scale separations is an on-going challenge. Academic and industrial researchers are working on expanding their knowledge of OSN, covering both fundamental and experimental aspects. Most of the OSN membranes developed until now are integrally skinned asymmetric membranes (prepared by phase inversion) [5]. These membranes dominate most of the OSN market due to their low manufacturing costs. However, another possibility is to use a more sophisticated method and prepare TFC membranes.

### 2.5.1. OSN membranes

Polymeric and inorganic materials have been used for the preparation of OSN membranes. These materials must possess film forming properties, chemical and thermal stability and be commercially available. Ceramic membranes are superior considering mechanical, thermal and chemical stability; they do not compact under pressure, do not swell in organic solvents and can be easily cleaned. However, upscaling is difficult; they are more expensive and brittle than

polymeric membranes. For this reason, polymeric membranes are more widespread for OSN applications than ceramic membranes.

### 2.5.2 Research work on polymeric ISA membranes for OSN

Several chemically stable polymeric materials have been used for the preparation of OSN ISA membranes by phase inversion [8, 17, 55]. Materials used to prepare OSN ISA membranes include: polyacrylonitrile (PAN), polyimide (PI) (Matrimid), polyimide (PI) (P84), polyaniline (PANI), polybenzimidazole (PBI), polysulfone/sulfonated poly (ether ether ketone) blends and , poly(ether ether ketone) (PEEK) and Poly(vinylidene fluoride) (PVDF) both as UF support membranes [1].

Many studies have been undertaken studying different factors during and after the membrane formation process and the effect that these have on the membrane performance. The polymer concentration in the dope solution has an effect on the structure of ISA membranes; higher polymer concentrations give membranes with thicker and denser skin layers, resulting in higher selectivities but lower permeabilities [56-61]. Addition of volatile solvents to the dope enhances the selectivities of ISA membranes, resulting in a defect-free ultrathin and dense skin-layer on top of a highly porous sublayer with sponge-like structure [62]. This technique is used to prepare highly selective ISA OSN membranes made from PI [56, 63], poly(ether imide) (PEI) [59] and sulfonated poly(phthalazine ether sulfone ketone) (SPPEK) [61]. It has been previously reported that increasing the evaporation time or the casting temperature induce lower permeabilities but higher selectivities for PI [56, 64, 65], PEI [59], polyamide (PA) [66], and PPEK [67]. Crosslinking is used to enhance chemical stability and rejection properties of ISA membranes. See Toh et al. [68] showed that crosslinking P84 polyimide ISA membranes made them stable in polar aprotic solvents such as DMF. Membranes made from other polymeric materials, such as PAN have been also crosslinked to enhance their chemical stability [69, 70, 71]. Polyaniline (PANI) crosslinked membranes were found to be stable at temperatures up to 70°C and showed solvent stability in various organic solvents including acetone, THF and DMF [72].

The performance, microscale morphology and formation mechanism of OSN ISA membranes made from P84 polyimide has been reported [68, 73, 74, 75, 76]. The rejection of PI OSN membranes was improved by heating for a short period at high temperatures compromising permeability [77]. A drastic flux decline due to gradual loss in microporosity was observed upon heating a P84 PI membrane from 0-150°C [56].

In conventional ISA membranes, the microporosity is extrinsic, arising from the template effects of solvent molecules, and can be lost when the polymer rearranges over time or due to an applied pressure or temperature. An ideal NF polymeric membrane would be one that does not compact

under pressure and does not lose its nanoporosity upon heating.

### 2.5.3 Research work on TFC membranes for OSN

#### *Supports for TFC OSN membranes*

A strong binding between the support and the top-layer is not crucial and can cause problems with the membrane's stability in the long term, creating top-layer peel off, in particular under conditions of excessive top-layer swelling. It is known that the formation of an interpenetrating layer of the active layer inside the pores of the support strengthens the interaction [3]. However, excessive penetration into the support will result in this interface becoming rate-limiting, thus reducing membrane flux considerably [78]. Top-layer intrusion can be reduced using a solvent to fill the pores of the support; further procedures use non-volatile additives (e.g. glycerol, mineral oil and hexadecane) [17]. These additives not only keep the support pores open, but also prevent intrusion of the dip-coating solution into the support and pore collapse.

The support-layer has an important role as it functions as a container for one of the precursors, and co-defines the interface where the interfacial polymerization reaction will occur [1]. The effectiveness of TFC membranes for non-aqueous applications partly depends on the solvent resistance of the support layer in organic solvents.

The permeability of a composite membrane may be further enhanced by decreasing the resistance of the support. Indeed, the thinner the top-layer, the higher the probability that the support will become rate limiting. One important reason for high support resistance could be the collapse of the smallest pores in the top of the support due to capillary forces [1].

For TFC OSN membranes, solvent resistance of the support must be guaranteed. Solvent stability is related to the chemical structure of the polymer and the presence of certain structural elements, such as aromatic groups, imide bonds or F-atoms. In general, copolymerization induces rigid segments which give solvent resistance [1]. Table 1 shows stable polymers appropriate for the formation of OSN support membranes, which can all be crosslinked to further enhance their stability.

PAN supports used in RO TFC membranes could be used as supports for TFC OSN membranes. Interfacial polymerization on PAN support containing carboxylic acid groups at its surface induced ionic bonds between the formed polyamide top-layer and the support. These carboxylic groups were formed via base-induced partial hydrolysis of the nitrile groups in the PAN support. The formation of ionic bonds enhanced the membrane chemical stability [79].

**Table 1.** Polymers used to prepare solvent stable UF support membranes

Polymer	Structure	References
Polyacrylonitrile (PAN)		1, 79
Poly(vinylidene fluoride) (PVDF)		1
Polyimide (Matrimid) (PI)		1
Polyimide (P84) (PI)		69, 70, 71
Polyaniline (PANI)		1, 72
Polybenzimidazole (PBI)		1
Poly(ether ether ketone) (PEEK)		1
Polypropylene (PP)		80, 81, 82

Polypropylene is a very interesting support material for solvent resistant TFC membranes, as it possesses high durability, resistance to pH variations and to a wide range of solvents. Nevertheless, as the polymer is highly hydrophobic, hydrophilization of the support is indispensable to guarantee proper wettability and adhesion between the top-layer and the support when TFC membranes prepared via IP [1]. Hydrophilization has been carried out by low temperature plasma polymerization with hydrophilic monomers such as allylamine [80], or by surface oxidation with chromic acid [81, 82].

Using thermal annealing procedures, asymmetric UF polyimide-based membranes with exceptional solvent resistance and high permeabilities have been obtained [83]. The annealed PI membranes could be used as supports for the development of TFC OSN membranes.

As the performance, composition and morphology of TFC membranes depends on many parameters, they should be carefully selected. These parameters include: concentration of the reactants, their partition coefficients and reactivities; solubility of the emerging polymer in the solvent phase; possible additives (e.g. wetting agents, swelling agents); overall diffusion rates and kinetics of the reactants; presence of by-products; competitive side reactions; cross-linking reactions and post-reaction treatment [1, 3].

#### *TFC OSN membranes*

Although polyamide based TFC membranes prepared by interfacial polymerization have been specifically designed for aqueous applications, the use of PA TFC membranes in organic solvents has been previously reported. TFC membranes comprising a thin film synthesized from piperazine/m-phenylenediamine and trimesoyl chloride on a PAN support membrane performed well in methanol, ethanol and acetone, less well in i-propanol and methyl ethyl ketone (MEK), and gave no flux in hexane [84]. These membranes performed well in water, ethanol and methanol and are clearly not suited for filtrations in more non-polar media. In order to allow hexane-based applications, non-reactive polydimethylsiloxane (PDMS) can be added during the polymerization reaction. The resulting silicone-blended PA membrane showed high hexane permeabilities [85, 86]. A method for the separation of lube oil from organic solvents (e.g. furfural, MEK/toluene, etc.) with a cross-linked PA membrane has been patented, using PEI and a diisocyanate on a solvent-resistant nylon 6,6 support [87]. As an alternative to PA, PAI has been reported to be useful for the synthesis of thermally and chemically stable TFC membranes [88]. As mentioned earlier, polypropylene support membranes have been used as solvent stable supports for polyamide TFC membranes and shown chemical stability in certain organic solvents [81, 82, 89, 90]. Another way to prepare TFC OSN membranes is by dip-coating. The polymer choice for preparing OSN membranes via dip-coating depends on many parameters including the mechanical strength and

chemical stability of the polymer, its film forming properties, solubility in solvents and possibility for crosslinking. As solvent casting mostly leads to non-porous top-layers, affinity of the polymer for the solvent to be permeated is a crucial aspect [4]. PDMS, PEI, poly(2,6-dimethyl-1,4-phenylene oxide) (PPO), poly(vinyl alcohol) (PVA), chitosan and other cellulose derivatives, poly(ether-b-amide) (PEBAX), polyacrylic acid (PAA), polyphosphazene (PPz), poly(aliphatic terpenes), poly[1-(trimethylsilyl)-1-propyne] (PTMSP) and polyurethanes (PUs) have all been studied as coating materials [1]. PDMS is chemically stable in some organic solvents when crosslinked, but it is preferably used in apolar solvents, due to its low polarity. However, like most elastomers, PDMS tends to swell excessively in organic solvents, especially nonpolar solvents. Prior to coating a PDMS solution, the support is often water impregnated to prevent extensive intrusion, and sometimes pre-treated with an adhesion promoter. A zeolite filled PDMS membrane has been developed [91]. Addition of fillers [91] turned elastomers into highly useful OSN membranes that can be used in solvents that induce very high swelling and in temperatures as high as 80°C. The problem of reduced permeability upon filler addition was overcome by using zeolites with porous structure that avoid polymer intrusion. Furthermore, these zeolites improved the membrane selectivity by increasing transport of solvent molecules and rejecting the larger solutes sterically [86].

Novel polymeric materials with ultra-high free volume that retain their nanoporosity upon heating have been developed and are known as polymers with intrinsic microporosity (PIMs) [92]. In these materials, the intrinsic microporosity forms as a direct consequence of the shape and rigidity of the macromolecular chain and is preserved, not allowing the resulting polymers to pack closely [92]. The high free volume leads to high permeability and therefore, these materials show an enormous potential in separation applications. To date, PIM-1 has been selected as the PIM polymer in membrane development mostly focused in gas separation [93] and pervaporation applications [94, 95], resulting in high permeability and selectivity. Recently Fritsch et al. [96] produced TFC membranes using PIM-1 for OSN showing 30 times higher permeance than commercial Starmem 240 and no compaction at high pressure after 300h. Tsarkov et al. [97] used PIM-1 for OSN with different dyes in ethanol showing significant sorption of the dye within the membrane. Another promising novel class of polymeric materials for high permeability membranes are block copolymers, which self-assemble to form different ordered nanostructures. A new class of nanostructured TFC membranes for OSN applications was recently reported [98], where the top layer was formed using blends of a polystyrene-b-poly(ethylene oxide) diblock copolymers and a poly(acrylic acid) homopolymer as template.

#### 2.5.4 Novel NF membranes with OSN potential

Nanotechnology has produced entirely new classes of functional materials whose application to desalination, water purification and OSN need exploration. For example, recent reports on filtration and desalination membranes fabricated from rigid star amphiphiles [99, 100], zeolite films [101, 102] and carbon nanotubes [103, 104, 105] offer exciting new possibilities. Mixed matrix or nanocomposite membranes may exhibit improved mechanical, chemical, and thermal stability as well as improved separation and permeability.

Polymeric membranes based on rigid star amphiphiles have been recently reported [99, 100]. They were prepared by direct percolation of solutions of rigid star amphiphiles in methanol, through ISA polyethersulfone support membranes. The barrier layer in these membranes is 20nm thick. These membranes exhibited very smooth surfaces with an average roughness in the range of 1-2 nm. They were able to control MWCO and obtained a narrower pore size distribution due to the composite multilayer dendrimer structure. According to K.P. Lee et al. [106], polymeric membranes fabricated by rigid star-shaped amphiphilic molecules is one of the first real breakthroughs since the interfacially polymerised RO/NF membrane as it offers the possibility of engineering membrane structure at a nano level. However, to date there is no reported research on the fabrication of RO membranes using this technique [106].

Another breakthrough is the zeolite-polyamide nanocomposite thin film by interfacial polymerization, which can dramatically increase the permeability of an RO membrane [101]. The process involves a thin polyamide film with relatively hydrophobic pores periodically interrupted by NaA zeolite nanoparticles having super-hydrophilic and negatively charged three-dimensional molecular sieve pore network. While water diffuses through the polyamide pores only under high applied pressure, water penetrates through the nanoparticle pores with very little applied pressure. Because the nanoparticle pore walls are even more negatively charged than the membrane surface, ion exclusion is enhanced in concert with increased water permeability. The super-hydrophilic nanoparticles also enhance fouling resistance by making the overall membrane more hydrophilic. These molecular sieve zeolite nanoparticles provide preferential flow paths for water permeation while maintaining high solute rejection through a combination of steric and Donnan exclusion [101, 102]. Pure water permeability was double than that of hand-cast polyamide membranes with equivalent solute rejection [101, 102].

Carbon nanotubes (CNTs) are potential materials for separation due to their fluid transport similarity with water transport channels in biological membranes [107]. Membranes made from CNTs with a uniform pore distribution and a more permeable separation layer can potentially

maintain or improve salt rejection while increasing permeability. Recent research on the transport of water through hydrophobic double-walled carbon nanotubes demonstrated that water flux is three orders of magnitude higher than through polymeric membranes [103, 104]. However, there are technological challenges to incorporating carbon nanotube materials, which include the development of efficient synthesis methods to align arrays of single-walled CNTs with sub-nanometre diameters and the functionalization of the pores to increase selectivity and potentially reduce hydrophobicity at the surface [108]. A novel TFC polyamide membrane with embedded 0.8 nm single walled CNTs in the polyamide barrier has been patented [105]. To blend the CNTs with the trimesoyl chloride organic solution, the CNTs were functionalized to increase their solubility in organic solvents. These novel membranes showed double the water flux and salt rejection coefficients that exceed those of TFC membranes prepared without CNTs [105]. This novel technique to incorporate CNTs into a TFC membrane is promising and scalable but the manufacturing costs of the suggested single walled CNTs for RO membranes can range from US \$1,800 per gram and upwards [106]. Unless savings from improved overall membrane performance are proven, the incorporation of CNTs into membranes for water desalination seems economically unfavourable [106]. Nonetheless, the overall membrane performance can be further enhanced by more dense and ordered packing of CNTs. As suggested by K.P. Lee et al. [106], “instead of blending CNTs with polymer solutions, *in situ* growth of CNTs by ceramic templating could offer a better method of engineering these novel membranes”.

Recently, diamond-like carbon nanosheets were used as ultrathin free-standing amorphous carbon membranes for OSN by Karan et al. [109]. The top layer of their TFC membranes supported on porous alumina supports had 1 nm hydrophobic pores; these membranes were able to separate organic dyes at a rate three orders of magnitude greater than that of commercially available membranes. In their nanofiltration performance experiments, they used a very low concentration of dye [109], however, such a high flux may be a problem in terms of concentration polarization when higher concentrations of solute are used.

### 2.5.5 Commercial OSN polymeric membranes

The actual commercial market for OSN membranes is still very young and even though excellent membranes are available for some applications, they are completely absent still for others. Commercially available OSN membranes are made of both polymeric and inorganic materials. Most of the OSN membranes developed up until now are ISA membranes. Commercial OSN membranes include the Starmem™ and the Koch SelRO® membranes and the recently commercialized SolSep, Duramem® and Puramem® membranes.



Koch SelRO® membranes. Koch Membrane Systems, USA [110] was the first company to enter the OSN market with their OSN flat sheet hydrophobic composite membranes MPF-60 and MPF-50. They comprised polydimethylsiloxane as a top layer over a PAN support, which was crosslinked through reaction and heat treatment [111,112]. However, these products suffered from variable performance and were withdrawn. Only their hydrophilic membrane MPF-44 (MWCO 250 Da) is still available in flat sheet and spiral wound configuration [1]. They also sell a UF membrane (MWCO 20 000 Da) based on crosslinked PAN, available in both spiral-wound elements (MPS-U20S) and flat sheets (MPF-U20S) [1, 110]. According to the manufacturer, their hydrophilic OSN membranes are stable in acetone, methanol, cyclohexane, 2-propanol, MEK, ethanol, pentane, butanol, methyl isobutyl ketone (MIBK), hexane, formaldehyde, dichloroethane, ethylene glycol, trichloroethane, propylene oxide, methylene chloride, nitrobenzene, tetrahydrofuran (THF), diethylether, ethyl acetate, acetonitrile, carbon tetrachloride, xylene, dioxane, and toluene, and have limited stability in DMF, *N*-methyl pyrrolidone (NMP), and dimethylacetamide (DMAc) [110].

The MPF 50 and 60 membranes were tested in many applications, including recovery of organometallic complexes from dichloromethane (DCM), THF, and ethyl acetate, and of phase transfer catalysts from toluene, for solvent exchange in pharmaceutical manufacturing and separation of triglycerides from hexane [1].

Starmem™ membranes (W. R. Grace & Co.). These membranes were distributed by Membrane Extraction Technology (MET) Ltd. but are no longer available in the market. The membrane series consisted of hydrophobic ISA NF membranes manufactured from polyimides by phase inversion [113].

Starmem membranes were tested in many applications, including catalyst recycle and product separations; solvent exchange in pharmaceutical manufacturing; ionic liquid-mediated reactions; membrane bioreactors (MBRs) for biotransformations; and microfluidic purifications [1]. Starmem membranes have been widely used to study solute and solvent transport through OSN membranes and were the first OSN membranes applied at a large scale, in the refining industry for solvent recovery from lube oil dewaxing (MAX-DEWAX™) [2].

SolSep® membranes. These membranes are distributed by the Dutch company SolSep BV [114] and consist of five NF-membranes with different stabilities and nominal MWCO-values (based on 95 % rejection) between 300 and 750 Da, and a UF-membrane with a MWCO around 10,000 Da. They present chemical stability in alcohols, esters and ketones, and some membranes are also stable in aromatics and chlorinated solvents. It is believed that these membranes are of TFC type and some of them have been proven to possess a silicone top layer [115]. There are limited

publications on the performance of these membranes [1, 115, 116, 117, 118]. Recently, Akzo Nobel reported filtration data for SolSep 030306F in ethanol, iso-propanol, hexane, heptane, cyclohexane, toluene, xylene and butyl acetate [118].

Duramem® membranes. These membranes are distributed by Evonik-MET. They are ISA OSN membranes based on crosslinked polyimide [119] prepared by phase inversion. These membranes are available in a wide range of MWCOs (150 to 900 Da) as spiral-wound elements and flat sheets [120]. They possess excellent chemical stability in a range of solvents, including polar aprotic solvents [68], where other commercial membranes fail. They are stable in solvents including, acetone, ethanol, methanol, tetrahydrofuran, dimethylformamide, dimethylsulfoxide, DMAc, iso-propanol, acetonitrile, MEK, and ethyl acetate and are not recommended in the presence of chlorinated solvents and strong amines. Possible re-imidization and loss of crosslinking at elevated temperatures limit their range of applications at high temperatures.

Puramem® membranes. This new membrane series is distributed by Evonik-MET Ltd. According to the supplier, these membranes are available in a wide range of MWCOs (280 to 600 Da) in both configurations; spiral-wound elements and flat sheets [120]. They possess excellent chemical stability in a range of solvents, including apolar hydrocarbon-type solvents. They are stable in solvents including, toluene, heptane, hexane, MEK, MIBK, and ethyl acetate and are not recommended in most polar aprotic solvents, chlorinated solvents and strong amines.

GMT membranes. These membranes are distributed by GMT-GmbH, Germany. They are TFC OSN membranes based on a silicone layer. Their silicone separation layer is coated and then crosslinked by irradiation to avoid swelling in organic solvents; this crosslinking process has been patented [121].

## **2.6 Membrane characterization**

To date, the development of nanofiltration membranes to achieve a specific performance remains a challenge. A better understanding and characterization of their structure at a molecular level would allow predicting their performance. In order to understand and study TFC membranes, different characterization techniques are used for the determination of their structural, morphological, chemical and physical properties (see Table 2). Membrane characterization methods can be divided into two categories: (1) functional and (2) physical-chemical characterization [122].

### 2.6.1 Functional performance

Membrane functional characterization measures their performance in terms of permeability and selectivity. In order to be efficient, membranes should present high permeability and high solute rejection. Very thin membrane separation layers are required to achieve high permeability because permeability is inversely proportional to the membrane thickness. Flux is generally expressed in terms of  $\text{Lm}^{-2}\text{h}^{-1}$  and permeability is expressed in terms of  $\text{Lm}^{-2}\text{h}^{-1}\text{bar}^{-1}$ . Selectivity is conventionally measured in terms of rejection.

Membranes discriminate between dissolved macromolecules of different sizes and are usually characterized by their molecular weight cut-off, which is used to classify membranes in terms of selectivity. It is defined as the molecular weight of the molecule which is 90 % rejected by the membrane. The value is interpolated from a curve of MW vs. rejection. However, the MWCO is a loose definition, as the shape of the molecule to be retained has a major effect on retention and is as important as its molecular weight. Thus, it is important to consider that even though the MWCO of membranes is normally characterized by the solute MW, several other factors affect permeation through the membrane. In OSN membranes different oligomers have been used to estimate MWCO, making it difficult to choose a suitable OSN membrane for a desired application. A simple and reliable method was developed by See Toh et al. [123] to determine MWCO of OSN membranes using a homologous series of polystyrene oligomers spanning the NF range (200-2000  $\text{g mol}^{-1}$ ), which are soluble in a wide range of solvents.

### 2.6.2 Physical-chemical characterization

#### 2.6.2.1 Fourier-Transform Infra-Red (FTIR) spectroscopy

Attenuated total reflection (ATR) Fourier transform infrared (FTIR) spectroscopy is used to determine the functional chemistry of unknown materials. Functional groups in the material absorb energy at specific wavelengths, which results in an attenuated signal at the infrared detector [8]. An interferometer is used to encode the detected signal which is digitally Fourier transformed to produce an FTIR spectrum (absorbed intensity vs. wave number). The resulting absorption spectrum is a unique fingerprint of a compound [8].

*Application of ATR-FTIR to membranes prepared throughout this work*

ATR-FTIR is used in membrane science to characterize new structures after crosslinking and surface modification of existing membranes [124]. In this thesis, ATR-FTIR has been used to determine the presence of polyethylene glycol (PEG) in the UF support membranes, to confirm the crosslinking of the UF support membranes and to determine the chemical composition of the active layer in the TFC membranes. The limitation of the technique is that it penetrates further than the thickness of the top layer, so it is difficult to separate information of the UF support and the top layer in TFC membranes.

**2.6.2.2 XPS**

X-ray photoelectron spectroscopy is used to perform chemical analysis of a sample. The sample surface is irradiated with X-rays, which produce photoelectrons in the sample and the photoelectrons that escape into the vacuum are collected and counted as a function of their kinetic energy [8]. A binding energy can be calculated from the kinetic energy. The binding energy is a characteristic of individual elements, which can be therefore identified. The limitation of the technique is that it can only characterize up to 12nm in depth [8]. However, this results in an advantage for the characterization of the TFC membranes prepared in this work as only the top layer's chemistry is desired. XPS has been used in Chapter 5 to characterize the chemistry of the top layer on different TFC membranes.

**2.6.2.3 Contact angle**

The contact angle technique is used to measure the hydrophobicity of solid materials. It is the angle at which a liquid/vapor interface meets a solid surface [8]. The contact angle of a liquid drop on an ideal solid surface is defined by the mechanical equilibrium of the drop under the action of three interfacial tensions with the Young's equation:

$$\gamma_{lv} \cos \theta = \gamma_{sv} - \gamma_{sl} \quad (3)$$

where  $\gamma_{lv}$ ,  $\gamma_{sv}$ , and  $\gamma_{sl}$  represent the liquid-vapor, solid-vapor, and solid-liquid interfacial tensions, respectively, and  $\theta$  is the contact angle.

In general two methods are used to measure the contact angle: (a) the captive bubble point method; and (b) the sessile drop method [8]. The main difference between these two methods is that the contact angle with the captive bubble method is measured in a wet state, and in the sessile drop method the contact angle is measured with a dry material [8].

*Application of Contact angle to membranes prepared throughout this work*

The surface properties of the membrane play a big role in membrane performance. The contact angle technique is suitable for the characterization of membrane surface properties, estimating differences in hydrophobicity between different membranes [125].

In membrane science, the contact angle is a measure of wettability of the membrane. A contact angle of zero degree (assuming water as the droplet) corresponds to an ideal hydrophilic surface.

In this thesis, contact angle measurements have been carried out using the sessile drop method, where a drop of water is placed on the membrane's dry surface and the angle is determined by constructing a tangent to the profile at the point of contact of the drop with the solid surface. This technique was used to determine whether the surface of the UF support membranes and TFC membranes prepared throughout this thesis are hydrophilic or hydrophobic.

**2.6.2.4 Polymer swelling**

Polymer swelling can have an effect on flux and rejection for OSN membranes [126, 127, 128]. Several methods have been developed to quantify swelling of polymeric membranes. However, results of the swelling experiments could not be correlated with NF performance of membranes in terms of solvent flux and solute rejection.

In membrane science, Hildebrand solubility parameters indicate the ability of solvents to act as swelling agents for polymeric membranes. The Hildebrand solubility parameter is a measure of the intermolecular energy and can be calculated for liquids from the enthalpy of vaporization [8]. The energy of mixing is small for polymeric systems so their solubility is determined by the enthalpy of mixing. Hildebrand defined the solubility parameter as the square root of the cohesive energy density:

$$\delta = [(\Delta H_v - RT) / V_m]^{1/2} \quad (4)$$

where  $\Delta_v$  is the heat of vaporization, and  $V_m$  the molar volume.

Polymers degrade before vaporization and their solubility parameters values are determined indirectly; they are assigned to the parameters of the solvent causing the maximum swelling in a series of polymer swelling experiments [8].

Hildebrand solubility parameters can only be applied to non-polar compounds where the attraction forces are non-specific. Hansen proposed an extension of the Hildebrand parameter method to estimate the relative miscibility of polar and hydrogen bonding systems [8]:

$$\bar{\delta}^2 = \bar{\delta}_d^2 + \bar{\delta}_p^2 + \bar{\delta}_h^2 \quad (5)$$

where  $\bar{\delta}_d$ ,  $\bar{\delta}_p$ , and  $\bar{\delta}_h$  are the dispersion, electrostatic, and hydrogen bond components of  $\bar{\delta}$ , respectively.

### 2.6.2.5 Microscopy

Advances in the study of membrane structure have been made possible thanks to microscopy techniques such as scanning electron microscopy (SEM) [129], transmission electron microscopy (TEM) [130] and atomic force microscopy (AFM) [131]. A long-standing goal of materials microscopy is the imaging of nanoporous polymeric membranes at nanometre resolution. The difficulty lies with the low electron contrast of polymers, which has prevented high magnification images from being acquired [132]. SEM applications are varied and focus on membrane structure characterization [133]. However, the major drawback of this technique is that polymeric membranes are not conductive and need to be coated. The nanostructures of NF membranes have dimensions that lie within the resolution of the microscope, making the interpretation of nanoscale features challenging. Atomic force microscopy (AFM) has been widely employed to characterize NF membranes for more than a decade in order to measure pore size, nodule size, and roughness [134-138]. A recent publication shows that nanometre scale pore size measurements for polymeric membranes using AFM are not very reliable due to lack of resolution [132]; rather phase imaging using AFM offers very interesting information describing the internal polymer packing at the membrane surface. The magnitudes of the phase lag and the dissipation energy have been demonstrated to have a correlation with the membrane functional performance; flux and MWCO [132].

Recently, a technique to measure nanopores with dimensions in the 0.5-2 nm range for NF ISA polymeric membranes has been developed [139]. This nanoprobng imaging technique measures the size of the transport-active pores. Nanopores in an ISA OSN polyimide membrane are filled with high contrast osmium dioxide ( $\text{OsO}_2$ ) nanoparticles, whose spatial arrangement is mapped under TEM. Stawikowska et al. [139] found a correlation between the estimated pore size using their nanoprobng imaging technique and the membrane separation performance, suggesting that the molecular separation mechanism in P84 polyimide ISA membranes is due to size exclusion of the larger nanoparticles.

### ***Atomic force microscopy***

AFM is a high resolution type of scanning probe microscopy used to profile surfaces in 3D. A cantilever with a sharp tip scans the surface of the sample assisted by a piezoelectric system. When the probe tip is brought close to the sample surface, forces between the tip and the sample lead to a minute deflection which can be measured using sensitive laser reflection [8]. The laser beam reflects from the cantilever and travels to the photodiode detection system to register the cantilever deflections to convert them into a 3D image.

The most commonly used modes of operation for AFM are the contact mode and the tapping mode. In the contact mode, the tip is continuously in contact with the surface, scanning is fast and relatively easy to set up [8]. In the tapping mode the cantilever is driven close to its resonance frequency at a constant set-point amplitude, and its response amplitude or phase angle is registered on the detector [8]. This operational mode is suitable for analysis of soft materials such as polymers.

#### *Application of AFM to membranes prepared throughout this work*

AFM has been used in Chapter 6 of this thesis to study the topography of the polymeric UF supports developed throughout this work. Surface roughness is an important structural property of UF support membranes, which require a low surface roughness to allow the formation of a defect-free top layer. Surface roughness can be presented as the average roughness ( $R_a$ ), root-mean-squared (RMS) roughness ( $R_q$ ), or peak-to valley height ( $R_z$ ). It is well known that the average roughness increases with an increase of the scan size; hence, when comparing different support membranes it is recommended to use the same scanning size.

### ***Scanning electron microscopy***

Scanning electron microscopy (SEM) is a technique to obtain an image of the sample by radiation of the sample with an electron beam. SEM measures the low energy secondary electrons emitted from the sample surface due to excitations in the sample itself produced by the electron beam [8]. The resolution is dependent on the applied voltage. With polymeric membranes the material will damage when high voltages are applied and generally the resolution is not larger than 5 nm, which may only give information on the macrostructure of the membrane [8].

#### *Application of SEM to membranes prepared throughout this work*

SEM applications are varied and focus on membrane structure characterization [133]. However, the major drawback of this technique is that polymeric membranes are not conductive and need to

be coated. The nanostructures of NF membranes have dimensions that lie within the resolution of the microscope, making the interpretation of nanoscale features challenging. In this thesis SEM has been used to characterize the surface morphology of the different TFC membranes developed.

### 2.6.2.6 Porosity

Porosity is the fraction of accessible free volume of the membrane (defined as the volume of the pores divided by the total volume of the membrane). Two techniques are commonly used to determine membrane porosity: (a) gas adsorption-desorption; and (b) mercury porosimetry [8].

#### Gas adsorption-desorption

Gas adsorption-desorption is used to determine the specific area, pore volume and pore size distribution of porous materials [8]. The technique is based on the difference in vapour pressure above a curved surface and a flat surface. Frequently nitrogen is used as condensable gas at its boiling point. In this method the volume of gas adsorbed at various vapour pressures is measured both for an adsorption and desorption step. An adsorption-isotherm (amount of adsorbed gas versus relative pressure (pressure/saturation vapour pressure of the adsorbent)) is drawn and the data is analysed by assuming capillary condensation [8].

#### *Application of Nitrogen adsorption (BET area) to membranes prepared throughout this work*

Nitrogen adsorption has been used in this work for the characterization of the ultrafiltration support membranes. However, a disadvantage is that this technique determines the porosity of the whole membrane and not only the porosity of the top layer and that measurements are done dry so the pores of the polymeric membranes may collapse.

#### Mercury porosimetry

Mercury intrusion porosimetry is used extensively for the characterization of porous materials, including membranes. It consists of measuring the volume of mercury which is forced into the pores of an evacuated porous sample. The pressure at which mercury enters a pore is inversely proportional to the size of the opening to the void. As mercury is forced to enter pores within the sample material, it is depleted from a capillary stem reservoir connected to the sample cup [8]. The incremental volume depleted after each pressure change is determined by measuring the change in capacitance of the stem [8]. This intrusion volume is recorded with the corresponding pressure or pore size. By this technique, both pore size and pore size distribution can be determined [8].



### *Application of mercury porosimetry to membranes prepared throughout this work*

Some disadvantages of this technique is that it requires high pressure which could damage the surface, and that it measures all the pores present in the structure, including dead end pores. The method requires high pressures which may damage the porous structure of polymeric membranes

Mercury porosimetry has been used to estimate the tortuosity in the UF support membranes prepared in this work. In order to diffuse through a polymeric membrane the solute must follow a tortuous path of length greater than the membrane thickness. The ratio of the average path length to the geometrical membrane thickness is the tortuosity factor  $k$ . Tortuosity is defined as the ratio between the effective path length and the straight distance in the direction of motion through the porous medium.

#### **2.6.2.7 Positron annihilation spectroscopy (PAS)**

PAS coupled with a slow positron beam has been previously used to characterize *in situ* the layer structure and depth profile of the cavity size in ISA and TFC nanofiltration membranes [140, 141]. Using this technique, Tung *et al.* [140] were able to measure the thickness of the top layer of two different PA TFC membranes (ESNA1-K1 and DETA-NF); the thicknesses of the top layers were 57nm and 500nm respectively. The thickness of the top layer of the TFC membranes prepared in Chapter 4 have been measured using a novel nanoprobeing imaging technique [139] and compared to published results using PAS [41].

**Table 2.** Summary on membrane characterization

<b>Membrane property</b>	<b>Studied object</b>	<b>Characterization technique</b>
Membrane structure and morphology	Membrane cross section	SEM [129], AFM [130], TEM [131]
	Surface roughness	SEM [129], AFM [130]
	Thickness of top layer	SEM [129], PAS [140]
Chemical properties	Surface chemistry	FT-IR [124], XPS [8]
Physical properties	Surface polarity	Contact angle [125]
	Membrane swelling	Swelling test [142]
	Membrane porosity	Mercury porosimetry [8], N <sub>2</sub> adsorption [8]

## 2.7 Transport models

The driving force for the transport of species through a membrane is the gradient in their chemical potential, which is a result of pressure, temperature and concentration differences. In order to mathematically describe the mechanism of permeation two main mass transfer models are used: the pore flow model developed by Sourirajan and Matsura [143] and the solution diffusion model proposed by Lonsdale [144], modified later by Wijmans and Baker [145].

### 2.7.1 Pore-flow model

In the pore flow model, the permeants are transported by pressure driven convective flow through tiny pores. Separation occurs because one of the permeants is excluded from some of the pores in the membrane through which other permeants move [6].

The pore-flow model is based on the pressure-driven convective flow described by the Darcy's law:

$$J_{v,j} = K'c_j \frac{dP}{dx} \quad (6)$$

where  $dP/dx$  is the pressure gradient through a porous membrane,  $c_j$  is the concentration of compound  $j$  and  $K'$  is a coefficient related to the nature of the medium. The pore-flow model assumes that a membrane contains cylindrical fixed pores.

### 2.7.2 Solution-diffusion model

In the solution diffusion model, the permeants dissolve in the membrane material and then diffuse through the membrane down a concentration gradient. The permeants are separated because of the differences in their solubilities in the membrane and the differences in the rates at which the permeants diffuse through the membrane [6].

The solution-diffusion model is based on the Fick's law of diffusion

$$J_{v,j} = -D_j \frac{dc_j}{dx} \quad (7)$$

where  $J_{v,j}$  is the flux of compound  $j$ ,  $D_j$  is the diffusion coefficient is the measure of the mobility of the individual molecules, and  $dc_j/dx$  is the compound  $j$  concentration gradient. The minus sign indicated that the direction of diffusion is down the concentration gradient.

Both models differ in how the chemical potential gradient across the membrane is expressed (see Figure 7) [145]:

- the pore flow model assumes that the concentrations of the solute and solvent within the membrane are uniform and that the chemical potential gradient across the membrane is expressed only as a pressure gradient.
- the solution diffusion model assumes that the pressure within the membrane is uniform and that the chemical potential gradient across the membrane is expressed only as a concentration gradient.

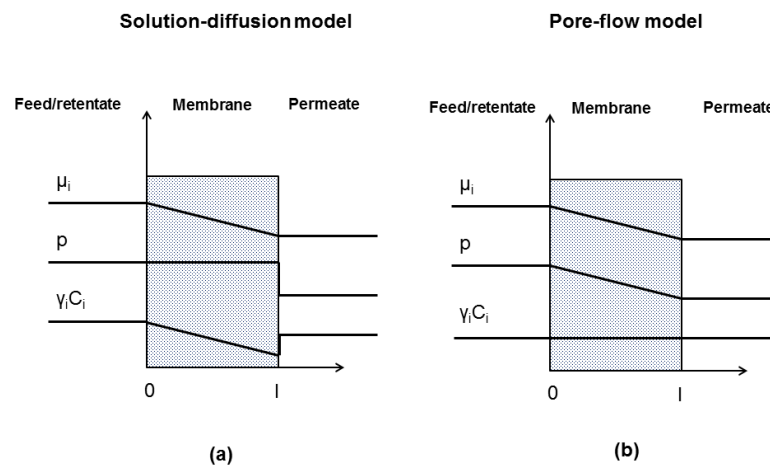


**Figure 7.** Chemical potential ( $\mu_i$ ), pressure ( $p$ ), and solvent activity ( $\gamma_i c_i$ ) profiles for pressure-driven permeation through a membrane according to (a) solution-diffusion and (b) pore-flow transport models [adapted from 145].

Another difference between the solution diffusion and pore flow mechanisms lies in the relative size and permanence of the pores. For membranes in which transport is best described by the solution-diffusion model and Fick's law, the free-volume elements (pores) in the membrane are tiny spaces between polymer chains caused by thermal motion of the polymer molecules. These volume elements appear and disappear on about the same timescale as the motions of the permeants traversing the membrane. On the other hand, for a membrane in which transport is best described by a pore-flow model and Darcy's law, the free-volume elements (pores) are relatively large and fixed, do not fluctuate in position or volume on the timescale of permeants motion, and are connected to one another. The larger the individual free volume elements (pores), the more likely they are to be present long enough to produce pore-flow characteristics in the membrane. The transition between transient (solution diffusion) and permanent (pore flow) pores is in the range 5–10 Å diameter [6].

# Chapter 3

## Project objectives

### Objective 1

#### **Development of high flux TFC OSN membranes for applications in polar solvents via IP**

The downside of integrally skinned asymmetric membranes is the difficulty in imposing control of the structure of their top layer, which controls selectivity, flux and separation. Furthermore, their formation process is limited to linear soluble polymers, whereas in TFC membranes the thin top layer can be formed of a large variety of chemical compositions, including both linear and crosslinked polymers. This makes tuning the polarity of TFC membranes possible, and gives them higher chemical stability for OSN applications compared to membranes prepared from linear polymers. It is well known that TFC membranes characteristically show a trade-off between permeability and solute rejection, which can be overcome by carefully choosing reaction and post-treatment parameters.

This work will focus on studying, elucidating and developing a new generation of OSN membranes: High flux Thin Film Composite membranes via interfacial polymerization with different MWCO, for polar solvents. The membrane performance will be studied in terms of flux and rejection and will be compared to conventional OSN integrally skinned asymmetric membranes. The structure, morphology, surface chemistry and surface polarity of these novel TFC membranes will also be studied. This work will be discussed in Chapter 4.

## Objective 2

### **Development of high flux TFC OSN membranes for applications in non-polar solvents via IP**

During the manufacture of Active Pharmaceutical Ingredients (APIs), non polar solvents are also used. To make OSN a viable process, there is a need for tight hydrophobic solvent stable membranes. Low MWCO integrally skinned asymmetric OSN membranes have poor fluxes in nonpolar solvents, including toluene. This limitation might be overcome by developing hydrophobic TFC membranes for OSN applications by IP.

Rubber coated TFC membranes are commercially available and have higher fluxes than ISA membranes. However, PDMS tends to swell excessively in nonpolar solvents, compromising selectivity. Currently, the tightest commercial OSN rubber coated TFC membrane (Puramem® S380 from Evonik MET Ltd, UK) has a molecular weight cut off (MWCO) of 600 Da in toluene according to the supplier's specifications, limiting its application in several purification processes.

Tight TFC OSN membranes prepared by IP have the potential to achieve higher fluxes than ISA OSN membranes, without sacrificing selectivity. However, to date there are no reported hydrophobic TFC OSN membranes prepared via IP. In this work, to increase permeabilities of nonpolar solvents, the external surface properties of the TFC membranes developed in objective 1 will be modified to decrease their hydrophilicity. The free acyl chloride groups on the TFC membrane surface will be capped with different monomers containing hydrophobic groups.

This thesis will focus on studying, elucidating and developing a new generation of OSN membranes: High flux hydrophobic Thin Film Composite membranes via interfacial polymerization with tuned MWCO for non polar solvents. A comparative study of TFC membranes formed with and without capping will be carried out to study the effects of surface chemistry on solvent permeation. The membrane performance will be studied in terms of flux and rejection and will be compared to commercial OSN ISA and TFC rubber-coated membranes. The structure, morphology, surface chemistry and surface polarity of these novel TFC membranes will also be studied. This work will be discussed in Chapter 5.

### **Objective 3**

#### **Study the influence of support membranes on formation and performance of novel TFC OSN membranes by IP**

The selection of the support layer is as important as the choice of the separation layer. The UF support membrane has to be resistant to solvents, it must be finely porous to stand the high pressures applied but should also have a high surface porosity so it is not obstructing solvent flow. The surface roughness, porosity and hydrophilicity of the support influence the adhesion and formation of the top-layer. Thereafter all these parameters must be carefully understood to select an appropriate support membrane.

This thesis will focus on studying and elucidating the optimum characteristics that the support should have to achieve the formation of a defect-free, high flux top layer. Two different solvent stable supports (crosslinked polyimide P84 and poly(ether ether ketone) (PEEK)) will be developed and characterized for a better understanding of the effects of the support on overall TFC membrane performance. The MWCO of the supports, their morphology, porosity, surface chemistry and polarity will be studied. Hydrophilic and hydrophobic TFC membranes will be formed via IP on each of the UF supports. The impacts of each support on overall membrane performance in polar and non-polar solvents will be studied in terms of flux and rejection and their structure, morphology, surface chemistry and surface polarity will also be studied. This work will be discussed in Chapter 6.

### **Objective 4**

#### **Develop new high free volume TFC OSN membranes via IP**

To achieve very high permeabilities in liquid applications, high free volume and microporosity are sought after. Advanced polymers, whose structure can be controlled at nano and molecular levels have promising applications for OSN and could result in highly porous membranes with narrower pore size distributions, and higher permeabilities than conventional OSN membranes. Recent studies showed polymers of intrinsic microporosity (PIMs) to be promising as membrane materials, exhibiting not only high fluxes, but also high selectivities [92]. To date, reported research on TFC-PIMs membranes has only used coating as the technique to fabricate the PIM top layer. However, TFC membranes might also be fabricated via interfacial polymerization, which has been demonstrated to be the method to obtain membranes with the highest flux in nanofiltration and RO [35]. To date, no TFC-PIMs membranes have been obtained by IP.

The aim of this work is to understand, elucidate and develop a new generation of OSN membranes: high flux TFC membranes with intrinsic microporosity prepared via interfacial polymerization on two different solvent stable support membranes (crosslinked PI, and PEEK). In order to increase free volume and provide higher solvent flux, a monomer with a contorted structure will be incorporated during the IP reaction. The contorted structure provides concavity, which in combination with the polymeric network could provide intrinsic microporosity to the top layer. This work will be discussed in Chapter 7.

## **Objective 5**

### **High flux TFC OSN membranes for the purification of Active Pharmaceutical Ingredients**

Conventional purification technologies include crystallisation, chromatography, liquid-liquid extraction and adsorption onto activated carbon or silica. These techniques are widely used and commercially available, but have limitations in cost, scale up or selectivity [1]. This work focuses on the application of high flux TFC membranes in the pharmaceutical industry.

To date, there is no research evidence on the use of TFC OSN membranes to purify Active Pharmaceutical Ingredients (APIs). However, such an OSN process, in principle, could be employed. Both polar and non-polar solvents are employed in the synthesis of APIs, and can have damaging effects on polymeric membranes and their ability to achieve molecular discrimination. Thus, the solvent stability of OSN membranes must be improved without compromising separation performance and flux. This will be accomplished by developing novel high flux TFC OSN membranes with different chemistries (hydrophilic and hydrophobic) to achieve good separation and high flux in both polar and non-polar solvents. Successful membranes prepared throughout this project will be selected for proof-of concept at a small scale. In collaboration with GlaxoSmithKline (GSK), rejection experiments will be carried out to demonstrate the membranes ability to purify APIs. Finally, the data obtained will be used to evaluate and confirm the viability of the process in terms of yield and productivity. This work will be discussed in the Appendix.

# Chapter 4

## High Flux Membranes for Organic Solvent Nanofiltration–Interfacial Polymerization with Solvent Activation

### Abstract

This chapter describes the formation of a new generation of organic solvent nanofiltration membranes: high flux thin film composite membranes prepared via interfacial polymerization and solvent activation. These are the first reported TFC membranes which are stable in DMF. They exhibit significantly higher permeabilities for polar aprotic solvents, including DMF, acetone and THF, than commercial integrally skinned asymmetric OSN membranes; and yet have comparable rejections. Solvent stable crosslinked polyimide ultrafiltration membranes were used as supports for the formation of these TFC membranes. To increase solvent flux two different approaches were employed. In the first approach, the UF support was impregnated with polyethylene glycol (PEG). Comparison of membranes formed using UF supports with and without PEG suggests that PEG impregnated in the support plays an important role in thin film formation and, consequently, in solvent permeation, resulting in increased fluxes. The second approach was to treat the TFC membranes with an “activating solvent” after the IP reaction. This resulted in dramatically improved solvent fluxes without compromising rejection; for some solvents, there was a flux only after activation.

### 4.1 Introduction

To date there are no reported TFC OSN membranes which are stable in strongly swelling solvents, such as polar aprotic solvents. In aqueous applications, the thin top layer prepared by IP mostly consists of crosslinked polyamide. This polymer is stable in a wide range of solvents, including polar aprotic solvents such as DMF [29, 30, 146]. Therefore, polyamide remains a promising material as the top layer for TFC OSN membranes. Conventional TFC membranes used for aqueous applications are not suited for performing filtrations in harsh solvents [1] because the support membranes have limited stability and tend to swell or dissolve, drastically affecting the membrane separation performance. Thus, other polymeric materials must be used as supports for developing TFC OSN membranes.



The use of polyamide TFC membranes in organic solvents has been reported previously. TFC membranes comprising a thin film synthesized from piperazine/m-phenylenediamine and trimesoyl chloride on a PAN support membrane performed well in methanol, ethanol and acetone, less well in iso-propanol and MEK, and gave no flux in hexane [84]. Polypropylene has also been used as a solvent stable support for polyamide hollow fibres and flat sheet TFC membranes [81, 82, 89, 90]. These membranes performed well in water, ethanol and methanol. However, TFC membranes prepared by IP which have been shown to withstand harsh solvents, such as DMF and THF, have not yet been reported.

Polyimides have been used as polymers for solvent resistant nanofiltration [56, 68] and UF [147] membranes. These polymers, when crosslinked, present high stability in a wide range of organic solvents, high temperature durability, and good mechanical properties which make them one of the most suitable polymers for the development of OSN membranes. Thus, in this work solvent stable crosslinked PI UF membranes were prepared and used as supports for the formation of TFC membranes.

The properties of the UF support have a major effect on the formation of the top layer. For membranes made by coating rubbery separating layers onto a support membrane, it has been shown that excessive penetration of the top layer into the support may reduce membrane flux considerably [78, 148]. In the formation of TFC membranes by IP, it seems reasonable to speculate that such additives might not only keep the UF support pores open, but also prevent intrusion of the aqueous solution into the support, and prevent pore collapse.

Polyethylene glycol (PEG) has been used previously to improve the formation of the top layer in TFC membranes [31]. Due to the poor hydrophilicity of polysulfone UF support membranes, Chen et al. added PEG to the aqueous solution as a wetting agent. Additives in the aqueous phase that can influence the diffusion of the amine into the organic phase have also been used [149].

Here, the solvent stable UF support membrane was impregnated with PEG400 prior to the interfacial polymerization reaction. This chapter reports on the effect that impregnating the UF supports with PEG has on TFC membrane performance in terms of flux and rejection.

The surface of TFC membranes is often modified to further enhance their performance. The most common modifications are plasma treatment, classical organic reactions and polymer grafting [150]. It has been reported that soaking freshly prepared TFC membranes in solutions containing various organic species, including glycerol, sodium lauryl sulfate, and the salt of triethylamine with

camphor sulfonic acid can increase the water flux in RO applications by 30-70 % [45]. Previous work shows that treating the membrane with some solvents can modify the surface permanently.

When aromatic polyamide (PA) membranes were immersed in ethanol, the subsequent water flux increased. Ethanol, being a good solvent for PA, made the membranes swell, and washing away the ethanol removed small molecular fragments, thus generating a more open structure [21]. The salt rejection was also increased, ascribed to elimination of defects in the top layer after swelling. According to their solubility parameters, ethanol and IPA are not the best swelling solvents for polyamide fragments. However, other stronger swelling solvents could not be used due to the instability of the UF supports used in conventional RO membranes. In the present work, it has been possible to use aggressive, polar aprotic solvents which are better solvents for the polyamide top layer, thanks to the solvent stability of the crosslinked polyimide UF supports. It has been described previously [151, 152] that the physical properties (abrasion resistance), and flux stability of TFC membranes can also be improved by applying an aqueous solution composed of poly(vinyl alcohol) (PVA) in a buffer solution as a post formation step during membrane preparation. As noted above, the supports used for conventional TFC membranes for water applications are not resistant to strong organic solvents, limiting the range of post-treatment solutions that can be used, and also the potential for employing additives in either the aqueous or the organic phases – use of solvent stable supports might create further opportunities in coating treatments. In this work, crosslinked P84 polyimide has been used for the first time as the support for the formation of TFC membranes via interfacial polymerization. As both the support and the top layer are stable in strongly swelling solvents, post-treatment of these novel TFC membranes with strong solvents to enhance flux has been possible. The effects of post-treatment with different solvents on the performance of TFC membranes, including the use of both DMF and DMSO are discussed in this chapter.

## 4.2 Experimental

### 4.2.1 Materials

Polyimide polymer (P84) was purchased from HP Polymer GmbH (Austria). All solvents used were HPLC grade. Isopropanol, acetone, toluene, methanol, ethyl acetate, tetrahydrofuran, hexane and polyethylene glycol hydroxyl terminated for synthesis (MW 400) were purchased from VWR international. Dimethylsulfoxide (DMSO), and DMF were purchased from Rathburn Chemicals, UK. Trimesoyl chloride (TMC) 98 %, m-phenylenediamine (MPD) flakes >99 %, piperazine (PIP) Reagent Plus 99 %, and 1,6 hexanediamine (HDA) 99.5 % were purchased from Sigma Aldrich, UK. Polystyrene oligomers for MWCO evaluation were purchased from Varian Ltd,

UK. Amines (MPD and PIP) and acyl chloride (TMC) were used as monomers for the formation of the polyamide active layer. Distilled water and hexane were used as aqueous and organic solvents, respectively.

#### 4.2.2 Preparation of crosslinked PI UF support membranes

A polymer dope solution was prepared by dissolving 24 % (w/w) polyimide (P84) in DMSO and stirring overnight until complete dissolution. A viscous solution (26,880 cP at 25°C) was formed, and allowed to stand for 10 hours to remove air bubbles. The dope solution was then cast on either a polyester or polypropylene (Viledon, Germany) non-woven backing material taped to a glass plate using a casting knife (Elcometer 3700) set at a thickness of 250  $\mu\text{m}$ . To make the UF support repeatable and uniform in performance, the non-woven was coated with dope at a casting speed of 0.035  $\text{ms}^{-1}$  using a continuous casting machine located in a room held at constant temperature (21°C). Immediately after casting, the membrane was immersed in a water bath (also at 21°C) where phase inversion occurred. After 15 minutes, lengths of membrane were transferred to a fresh water bath and left for an hour. The wet membrane was then immersed in a solvent exchange bath (isopropanol) to remove any residual water and preparation solvents. The support membranes were crosslinked as described elsewhere [68], by immersing the membrane in a solution of hexanediamine in isopropanol for 16 hours at room temperature. The membranes were then removed from the crosslinking bath and washed with isopropanol for 3 h to remove any residual HDA several times, until the Kaiser test was negative for the presence of amine. The Kaiser test kit (purchased from Sigma Aldrich) contains 50mL of each of the following solutions: (a) phenol, 80% in ethanol; (b) KCN in H<sub>2</sub>O/pyridine; (c) Ninhydrin, 6% in ethanol. The membrane was soaked in isopropanol for a few minutes. Two mL of the soaking solution were mixed with 3 drops of each of the Kaiser test solutions and heated at 120 °C for 5 minutes. The solution turns dark blue when free primary amine is present and remains transparent when no free primary amine is present (expected result after successful removal of excess HDA). Several membranes were prepared in order to evaluate repeatability. Some of these membranes were stored in IPA to avoid pore collapse and used for TFC membrane formation, and some other support membranes were conditioned with PEG before the interfacial polymerization reaction.

##### *Conditioning step*

The conditioning step involved immersing the support membrane overnight in a conditioning agent bath comprising polyethylene glycol 400/isopropanol at a volume ratio of 3:2. The membranes were then wiped with tissue paper and dried.

### 4.2.3 Preparation of polyamide thin film composite membranes

TFC membranes were hand-cast on UF support membranes through interfacial polymerization. TFC membranes were fabricated using both conditioned and non-conditioned support membranes to study the effect of the presence of PEG in the pores of the support on the performance of TFC membranes. The non-conditioned support membranes stored in IPA solution were rinsed with water and kept wet prior to interfacial polymerization to avoid pore collapse. Several TFC membranes were prepared in order to evaluate repeatability.

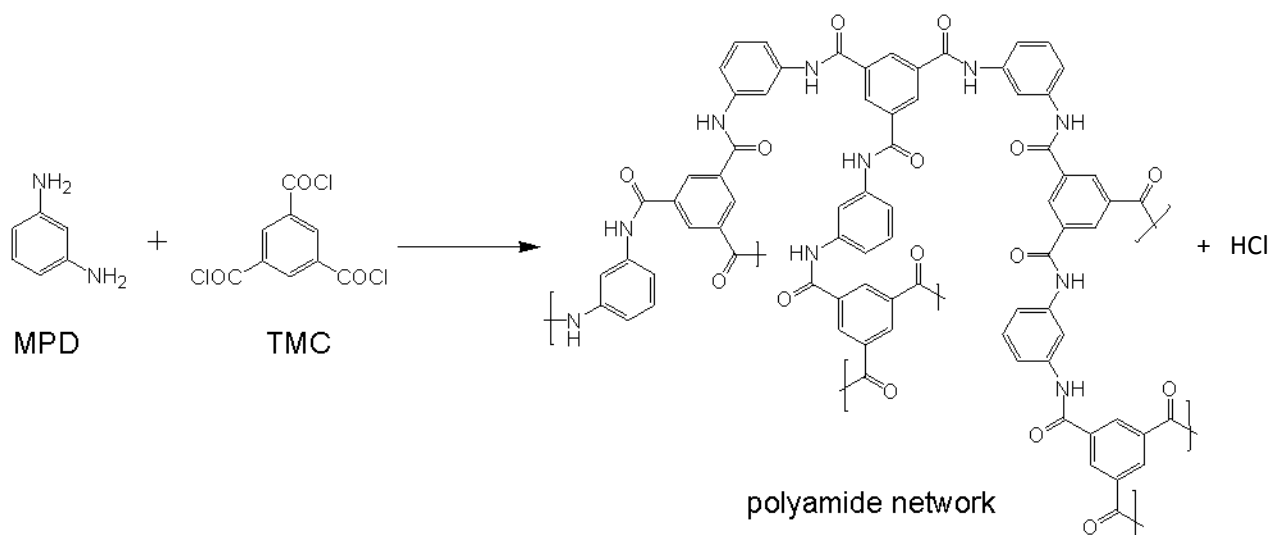
The UF support membrane, with skin layer facing upwards, was taped to a glass plate and placed in an aqueous solution of 2 % (w/v) m-phenylenediamine (MPD, >99 %, Sigma–Aldrich), piperazine or hexanediamine for 2 min. The amine loaded support membranes were then pressed with a roller and wiped to remove excess solution, and subsequently immersed in a solution of 0.1 % (w/v) trimesoyl chloride (TMC, 98 %, Sigma–Aldrich) in hexane. After 1 min reaction time, the resulting membranes were withdrawn from the hexane solution and rinsed with water. The TFC membranes were stored in water at 4°C. The chemical structures of the monomers used for the interfacial polymerization reaction, using MPD as the amine, are shown in Scheme 1.

In order to compare the morphology of RO membranes formed on the traditional polyethersulfone support with the ones formed in this work on crosslinked polyimide, a TFC-MPD membrane was prepared on a pre-formed polyethersulfone (PESf) UF support membrane impregnated with PEG. The PESf support was cast from a 25 %w/w (PESf:DMF) solution. Membrane identification codes for the TFC membranes prepared are shown in Table 3.

The performance of TFC membranes prepared on supports with and without PEG was evaluated by filtrations with both methanol and DMF as solvents.

**Table 3.** Membrane codes for the TFC membranes

Entry No.	Membrane	Membrane code
1	TFC membrane prepared on crosslinked PI support without PEG using MPD in the aqueous phase	TFC-MPD-NP
2	TFC membrane prepared on crosslinked PI support with PEG using MPD in the aqueous phase	TFC-MPD
3	TFC membrane prepared on crosslinked PI support with PEG using PIP in the aqueous phase	TFC-PIP
4	TFC membrane prepared on crosslinked PI support with PEG using HDA in the aqueous phase	TFC-HDA
5	TFC membrane prepared on PESf support with PEG using MPD in the aqueous phase	PESf-TFC-MPD



**Scheme 1.** Interfacial polymerization reaction (repeated from Figure 5).

#### 4.2.4 Treatment of TFC membranes with activating solvent

A post-formation treatment step was carried out on some of the composite membranes in order to further enhance solvent flux. The TFC membranes were contacted with a solvent (“activating solvent”) with a similar Hildebrand solubility parameter to the polyamide top layer ( $23 \text{ (MPa)}^{1/2}$ ). Hildebrand solubility parameters indicate the ability of solvents to act as swelling agents for membranes, and in this work the activating solvents used were DMF ( $24.8 \text{ (MPa)}^{1/2}$ ) or DMSO ( $26.6 \text{ (MPa)}^{1/2}$ ). The contact time was 10 minutes via filtration unless specified otherwise. This post-treatment step was not performed for all of the TFC membranes. After contacting with an activating solvent by filtration, the membranes were washed by filtering the selected solvent for the membrane performance test. The performance of TFC membranes with and without contacting with DMF was evaluated through filtrations using different solvents, including acetone, THF, methanol, ethyl acetate and toluene. In order to evaluate repeatability several TFC membranes were treated with activating solvent.

#### 4.2.5 Membrane Characterization

##### *FTIR*

The formation of the polyamide top layer was confirmed by Fourier transform-Infrared spectroscopy. Infrared spectra were recorded on a Perkin-Elmer Spectrometer 100, with samples mounted on a zinc-selenium/diamond plate. The membranes were washed in isopropanol to remove any contamination and dried before the analysis. Spectra of the crosslinked PI membrane and TFC membrane were compared.

### *Scanning electron microscopy (SEM)*

The surfaces of different TFC membranes were characterized by Scanning Electron Microscopy. For the analysis of a membrane's surface, samples were prepared by cutting a small square of 0.9 mm<sup>2</sup> and mounting these onto SEM stubs. The samples were then sputtered with chromium under an argon atmosphere (in an Emitech K575X peltier) to achieve the necessary conductivity. The microscopic analyses were performed at 5 KV in a Scanning Electron Microscope of high resolution (LEO 1525 from Karl Zeiss). At least three images of each membrane were scanned and membranes prepared from different batches were analysed in repeats of two to ensure there was no variation between samples of the same membrane type.

### *Contact angle*

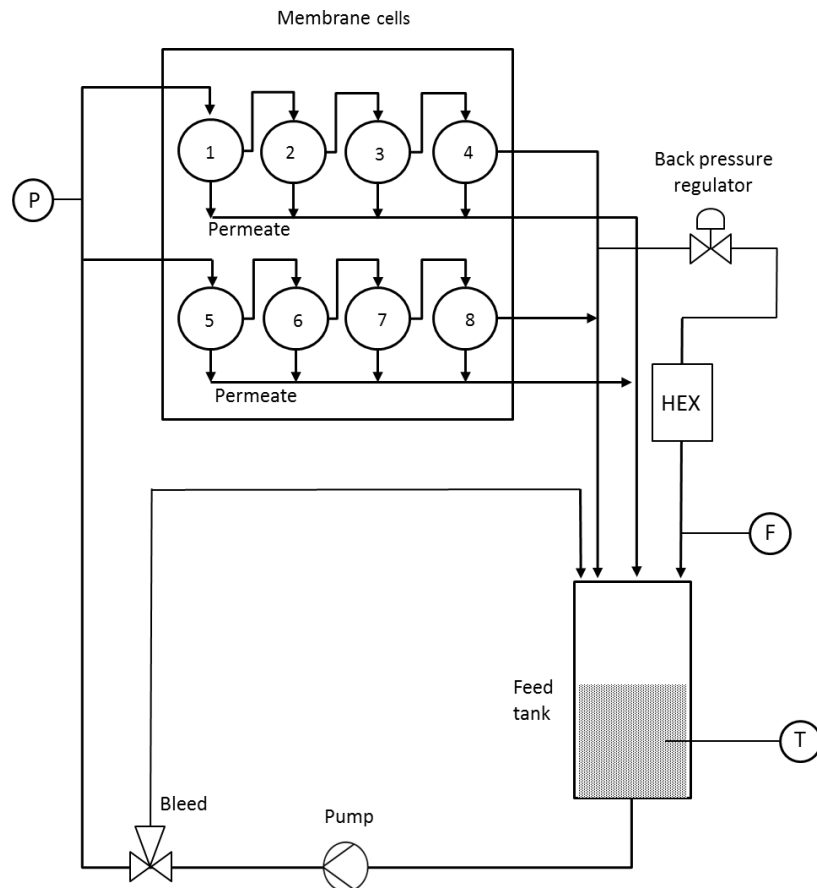
Contact angle measurements were performed with an EasyDrop Instrument (manufactured by Kruss) at room temperature using the drop method, in which a drop of water was deposited onto the surface of a piece of membrane using a micropipette. The contact angle was measured automatically by a video camera in the instrument using drop shape analysis software. Five measurements on different membrane pieces were performed. All membranes were dried prior to measurement of their contact angle. Five measurements on different membrane pieces were performed. In order to evaluate repeatability, contact angle measurements were performed on several membranes.

### *Nanoparticle contrast agents characterization technique*

This work was done in collaboration with Joanna Stawikowska (JS) and will be briefly described and discussed in this chapter. Maria F. Jimenez Solomon (MFJS) provided the TFC OSN membranes and, as part of her PhD thesis, JS performed a thorough structural characterization using her previously published novel nanoprobe technique [139]. In the JS technique, pores in the membranes identified by OsO<sub>2</sub> nanoprobe (NP) are considered to be permeation pathways participating in transport. The pore size, estimated using the nanoprobe imaging technique is assumed equal to the diameter of the particle lodging in the transport-active channel. This technique was performed to elucidate the structure of the TFC-MPD membranes prepared in this chapter. The preparation and filtration of OsO<sub>2</sub> NP in toluene, as well as the sample preparation for TEM is described elsewhere [153]. TEM cross-sectional images of the TFC OSN membranes were made to provide information on the nanostructure of the composite separation layer and pore size. Particularly, low magnification images were used to measure the thickness of the composite layer, and to characterize the morphology and the interface between the top layer and the ultrafiltration support. These TEM images can be found in a recently published paper by J. Stawikowska et al. [153] and are shown in the supplementary information at the end of this chapter; only the main findings of this collaboration will be discussed.

#### 4.2.6 Membrane performance

Membrane performance was evaluated according to flux profiles and MWCO curves. All nanofiltration experiments were carried out at 30 bar in repeats of 8 (two disks per membrane of four different membranes prepared the same way were tested to evaluate repeatability) using an 8 cells cross-flow filtration system consisting of two sets of 4 cells in series connected in parallel (see Scheme 2). The effective membrane area was 14 cm<sup>2</sup>, membrane discs were placed into 8 cross flow cells connected in series, and with a feed flow of 100 L h<sup>-1</sup>. Permeate samples for flux measurements were collected at intervals of 1 h, and samples for rejection evaluations were taken after steady permeate flux was achieved. The MWCO was determined by interpolating from the plot of rejection against molecular weight of marker compounds, and corresponds to the molecular weight for which rejection is 90 %. Before solute rejection tests, the selected pure solvent was filtered through the membrane for an hour in order to remove any leachables, including PEG400. The solute rejection test was carried out using two standard solutions. The first was a standard feed solution comprised of a homologous series of styrene oligomers (PS) dissolved in the selected solvent. The solvents used were MeOH, acetone, THF, DMF, toluene and ethyl acetate. The styrene oligomer mixture contained 2 g L<sup>-1</sup> each of PS 580 and PS 1090 (Polymer Labs, UK), and 0.01 g L<sup>-1</sup> of  $\alpha$ -methylstyrene dimer (Sigma-Aldrich, UK) [123]. Analysis of the styrene oligomers was undertaken using an Agilent HPLC system with UV/Vis detector set at a wavelength of 264nm. Separation was achieved using a reverse phase column (C18-300, 250x 4.6 mm). The mobile phase consisted of 35 vol % analytical grade water and 65 vol % tetrahydrofuran with 0.1 vol % trifluoroacetic acid. The second standard marker solution consisted of a solution of alkanes in THF containing 0.1 % (w/v) of each alkane. The alkanes used were: decane, n-hexadecane, n-tetradecane, eicosan, tetracosane, hexacosane. Their MWs are 142.3, 198.4, 226.4, 280.5, 338.7, and 366.7 Dalton respectively. Analysis of the alkanes was via gas chromatography. TFC membranes were compared with commercial Duramem® membrane (DM150). Two discs of the commercial membrane were tested to evaluate repeatability.



**Scheme 2.** Cross flow filtration system.

## 4.3 Results and discussion

### 4.3.1 Characterisation of TFC OSN membranes

#### SEM

Typical RO TFC membranes are prepared on polyethersulfone or polysulfone supports. To compare the surface morphology of TFC-MPD OSN membranes with RO membranes made with conventional support materials, a PESf-TFC-MPD membrane was prepared using the same methodology as described above and the PESf support was impregnated with PEG400 prior to the IP reaction. The surface morphology of the TFC-MPD and TFC-PIP membranes prepared in this work were also compared with each other, and the observations are explained in terms of the observations and conceptual model hypothesis of TFC membranes introduced by Ghosh and Hoek (2009) [148]. SEM photographs of the surface of TFC membranes are shown in Figure 8, where (a) is an SEM image of the surface of a PESf-TFC-MPD membrane prepared on polyethersulfone support. The surface exhibits the typical “ridge and valley” structure of polyamide RO membranes, where the white parts are the peaks and the black parts are the valleys; (b) is an

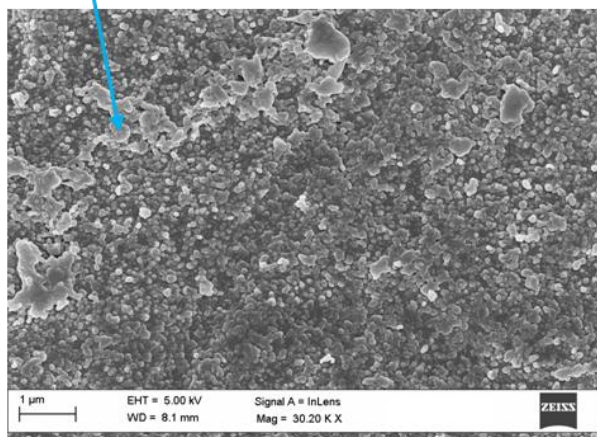


SEM image of the surface of a TFC-MPD membrane prepared on the crosslinked polyimide support, which has a “nodular” morphology and does not present a “ridge and valley type” structure; and (c) is an SEM image of the surface of a TFC-PIP membrane which has a rougher morphology and smaller closely packed nodules than (b) and was also prepared on a crosslinked polyimide support.

The reason for the difference in the surface morphology between the TFC membrane shown in 8(a) and the one shown in 8(b) is likely to be related to the influence that the chemistry and polarity of the support have on the rate and extent of polymerization by controlling the amount of MPD reaching the reaction zone, and the extent to which polyamide forms in the pores [148]. When using crosslinked polyimide support membranes, MPD likely diffuses more slowly out of the pores due to favourable hydrogen bond interactions with the hydrophilic support, limiting the size of initial polyamide tufts, and giving “nodular” structures instead of the typical “ridge and valley” morphology of TFC membranes. As suggested by Ghosh and Hoek, due to better wetting, the aqueous MPD solution meniscus is concave in hydrophilic pores of modified PSf supports [148]. It is believed the same happens with crosslinked polyimide, where the better wetting makes the meniscus drop below the PI interface, giving smaller tufts as compared to TFC’s prepared on PESf, where the MPD solution meniscus is convex in the hydrophobic pores, potentially protruding above the PESF interface and giving rise to bigger polyamide tufts.

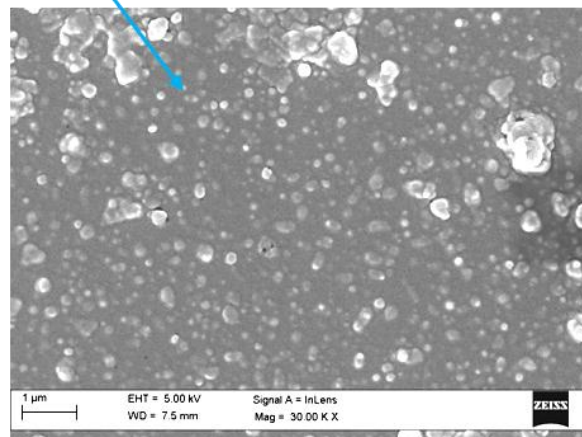
As shown in Figure 8 (b) and (c), the surfaces of TFC membranes having the same support (crosslinked polyimide) but prepared with different amines in the aqueous phase show a certain difference in their surface morphology. The partition coefficient of MPD into the organic phase is higher than that of PIP [84]; this means that PIP diffuses into the organic phase more slowly than MPD, and the “tufts” don’t have as much time to grow, giving smaller nodular structures than for the case of MPD as can be seen in Figure 8.

"Ridge and valley" structure



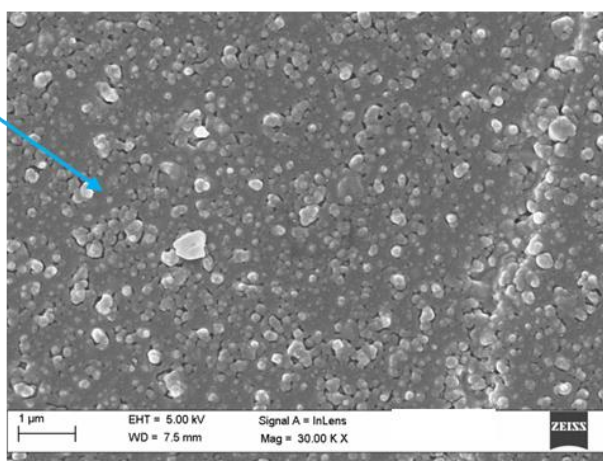
(a)

"Nodular" structure



(b)

"Nodular" structure



(c)

**Figure 8.** SEM images of surface of TFC membranes. (a) Shows the surface of a PESf- TFC-MPD membrane; (b) Shows the surface of a TFC-MPD membrane prepared on crosslinked polyimide support; (c) Shows the surface of a TFC-PIP membrane prepared on crosslinked polyimide support.

#### *ATR-FTIR of UF Support and TFC Membranes*

Figure 9 shows the Attenuated Total Reflectance (ATR)-FTIR spectra of the surface of the crosslinked polyimide support and of the TFC-MPD membrane. Both the support and the polyamide top layer present amide peaks. The polyimide peaks ( $1380$ ,  $1713$  and  $1780\text{ cm}^{-1}$ ) on the support's spectrum disappear on the TFC spectrum, suggesting that the polyamide top layer was properly formed on top of the UF support without defects. For the polyamide top layer, the most important bands of amide linkages formed by the interfacial polymerization are the  $1637\text{ cm}^{-1}$  and  $1601\text{ cm}^{-1}$  amide I band, associated with the C=O stretching vibration. The characteristic absorption band of amide II can be seen at  $1533\text{ cm}^{-1}$  and is attributed to (C-N stretching). The

peaks at 1465 and at 1440  $\text{cm}^{-1}$  correspond to aromatic ring breathing, which is evidence of the formation of the functional  $-\text{NHCO}-$  bond.

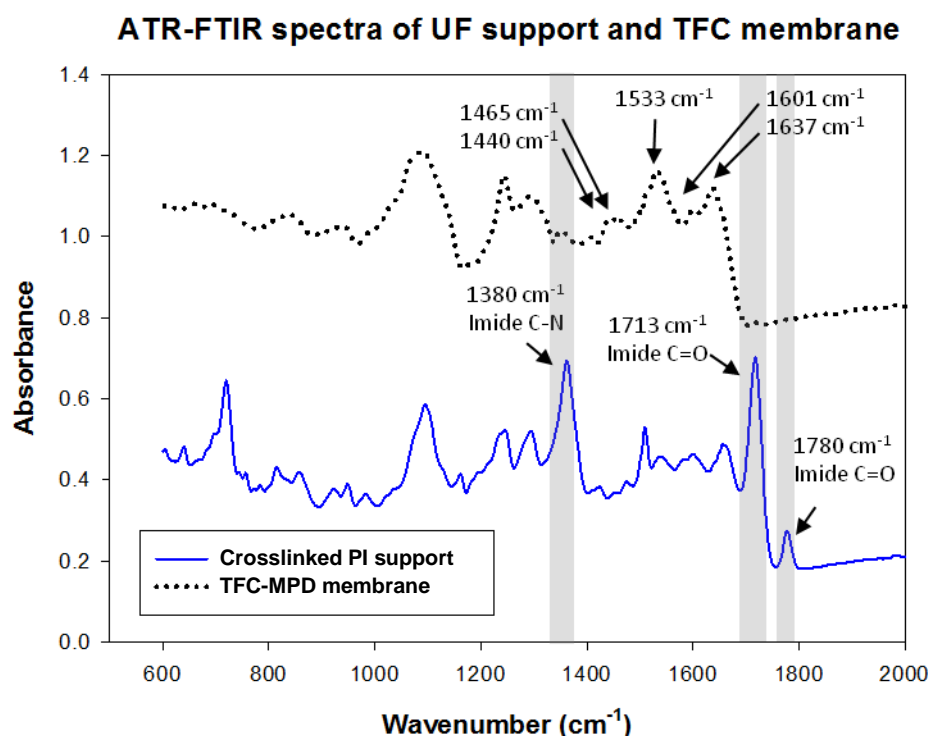


**Figure 9.** ATR-FTIR spectra of crosslinked polyimide support and TFC-MPD membrane.

#### *TFC membrane characterization using the nanoparticle contrast agents technique*

In the collaboration with J. Stawikowska, good contrast between the polyamide layer and the P84 support was achieved due to the difference in accumulation of the nanoprobe. Thus, relatively high magnification images could be acquired thanks to variations in content of the NP lodged into the polyamide film and the support (due to changes in the pore size and porosity) [153]. This effect allowed measurement of the separation layer thickness, which is equal to  $53 \pm 6$  nm and  $55 \pm 8$  nm for the membrane subjected to correspondingly tight- and open-side filtration. TEM cross-sectional images (see Figure S1 in the supplementary information at the end of this chapter) of the TFC OSN membranes were made to provide information on the nanostructure of the composite separation layer and pore size. Particularly, low magnification images were used to measure the thickness of the composite layer, and to characterize the morphology and the interface between the top layer and the ultrafiltration support.

It is well known that in the polyamide top layer there are two types of pores: free volume elements present between segments of chains building the polymeric network and larger voids formed between macromolecular aggregates [41]. In the present collaboration, the polyamide dense film

rejected the majority of the NP which accumulated below the composite film during open-side filtration or above the composite film during tight-side filtration. The mean pore size for the TFC membrane was estimated from TEM cross-sectional images of the PA dense layer (Figure S2) and found to be  $0.56 \pm 0.10$  nm. To compare the pore size estimated using the nanoprobe imaging technique with other experimental methods, we reviewed the literature to find the void size data in glassy polymeric membranes composed of polyamide. Their results of PAS indicated that the distribution of free volume elements had a bimodal profile. Their estimated pore size ranges for the polyamide film were 0.42 nm – 0.48 nm and 0.70 nm – 0.9 nm [41]. A comparison of the PAS with our nanoprobe imaging data suggests that the mean pore size determined in our study belongs to the lower range of the diameters estimated by PAS. The reason for this may be associated with the assumption that a pore is circular in the positronium lifetime formula, which uses this to calculate the pore radius [154, 155]. However, free volume elements present in a polymeric matrix are more likely to be irregular in shape, and so the pore size estimated from the nanoprobe imaging would be indeed smaller than a diameter estimated from the positronium lifetime formula.

The solute permeation mechanism through the PA composite membranes is still under discussion [156]. However, in recent work published by Singh et al. [157], transport through polyamide composite membranes was analysed to conclude that the pores are not well interconnected and the transport happens via both the solution–diffusion and pore–flow mechanisms. The pore size distributions in our work were measured and correlated with the membranes' functional performance, implying that the selectivity of the OSN TFC membranes was strongly related to the pore size. This correlation has suggested that the pore–flow model presumably governs the transport through these polyamide OSN TFC membranes.

#### **4.3.2 Effect of impregnating UF supports with PEG**

PEG was impregnated into the pores of the UF support membrane. PEG acts as a pore protector, avoiding pore collapse in polyimide membranes, and also has the effect of avoiding the formation of polyamide inside the support. Furthermore, it acts as a wetting agent for the polyimide support and as an additive that can influence the diffusion of the amine into the organic phase.

##### *Contact angle of UF supports*

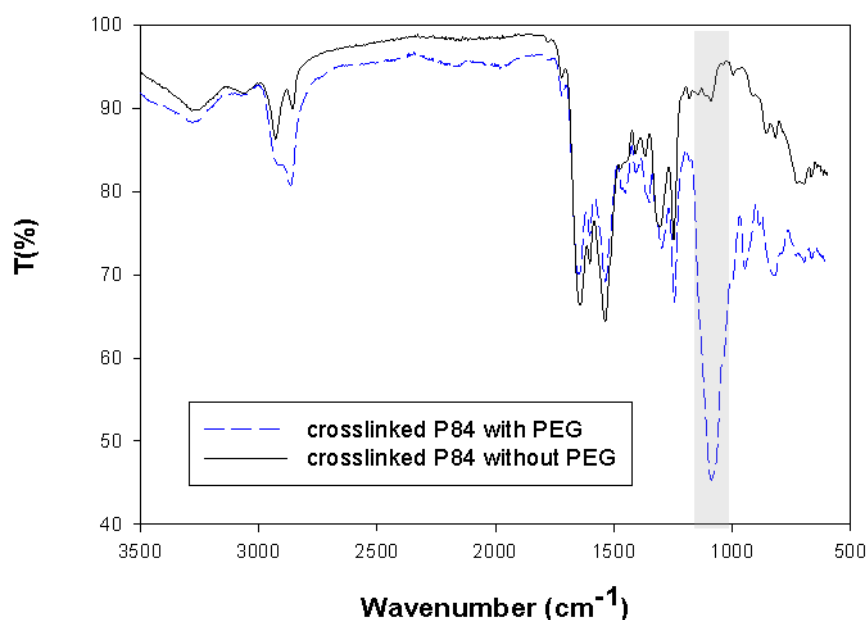
In order to better understand the effect of PEG in the UF support, the changes in contact angle with and without PEG for the crosslinked P84 UF support were measured and the average values are recorded in Table 4. The UF support impregnated with PEG has a lower contact angle, suggesting that PEG is making the UF support more hydrophilic, which will enhance wetting of the support with the aqueous amine solution.

**Table 4.** Contact angle of supports with and without PEG

Entry No.	Crosslinked P84 UF support without PEG	Crosslinked P84 UF support with PEG
6	53±4	31±3

*FT-IR of UF Supports with and without PEG*

This study was carried out to confirm the presence of PEG in the UF support. The peak at 1078  $\text{cm}^{-1}$  corresponds to the ether group (symmetric stretch of  $-\text{C}-\text{O}-$ ) of PEG, confirming that the membrane contains PEG (see Figure 10).

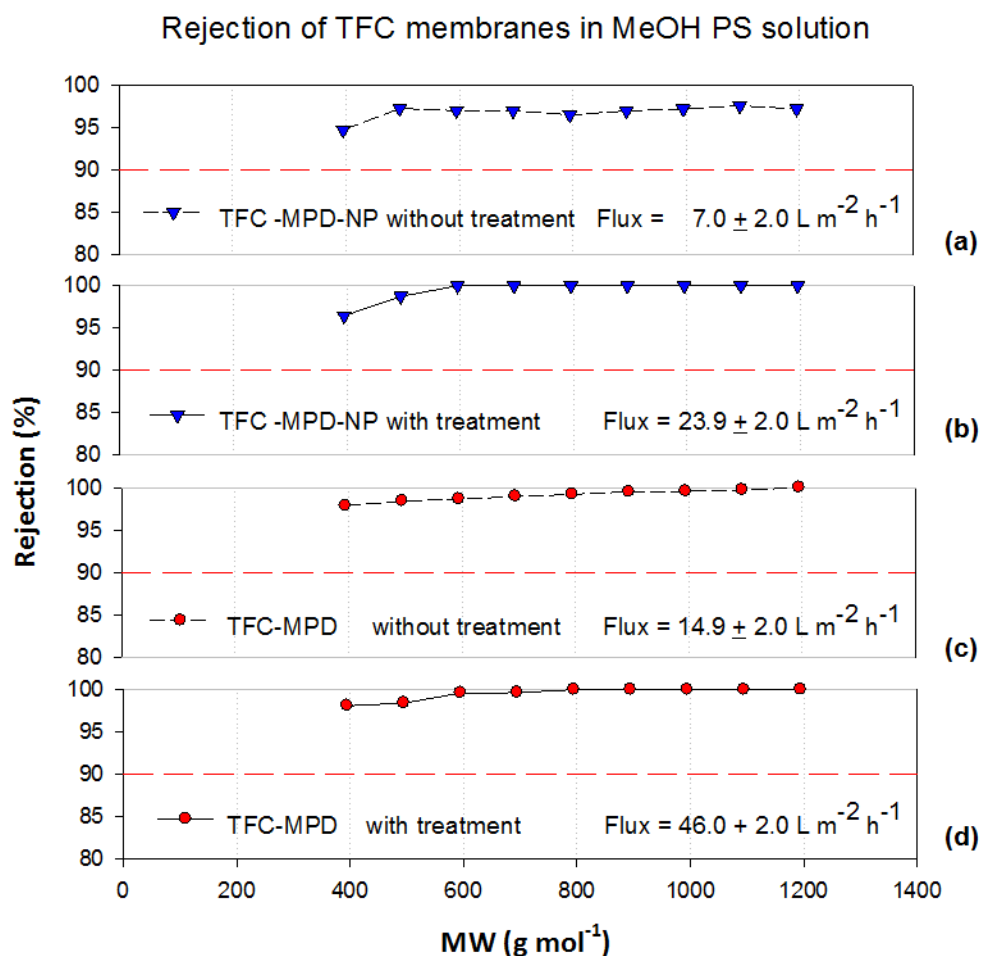
**ATR-FTIR spectra of crosslinked P84 support membranes****Figure 10.** ATR-FTIR spectra of crosslinked P84 UF supports with and without PEG.*Membrane performance*

The crosslinked PI UF support gave no rejection of styrene oligomers in acetone at 30 bar and, as expected, a high acetone flux ( $580 \text{ Lm}^{-2} \text{ h}^{-1}$ ), confirming its ultrafiltration nature. The performance of TFC membranes prepared with crosslinked polyimide UF supports with and without PEG in the pores, using methanol (MeOH) as a solvent, is compared in Figure 11 (a) and (c). Impregnating the UF support with PEG prior to the interfacial polymerization reaction results in an increase in MeOH flux without compromising rejection for these styrene oligomers. As seen in Table 4, as well as protecting the pores of the support PEG also makes it more hydrophilic, evidenced by the lower contact angle. The thickness of the top layer depends on diverse factors including reaction time, concentration of the monomers, the chemistry and pore size of the support and the diffusion of amine to the organic phase. It is known that the diffusion rate of MPD from inside the pore

structure to the membrane interface is certainly affected by the presence of PEG [148] and some of the MPD inside the pores may interact with PEG through hydrogen bonding.

### 4.3.3 Treatment with activating solvent

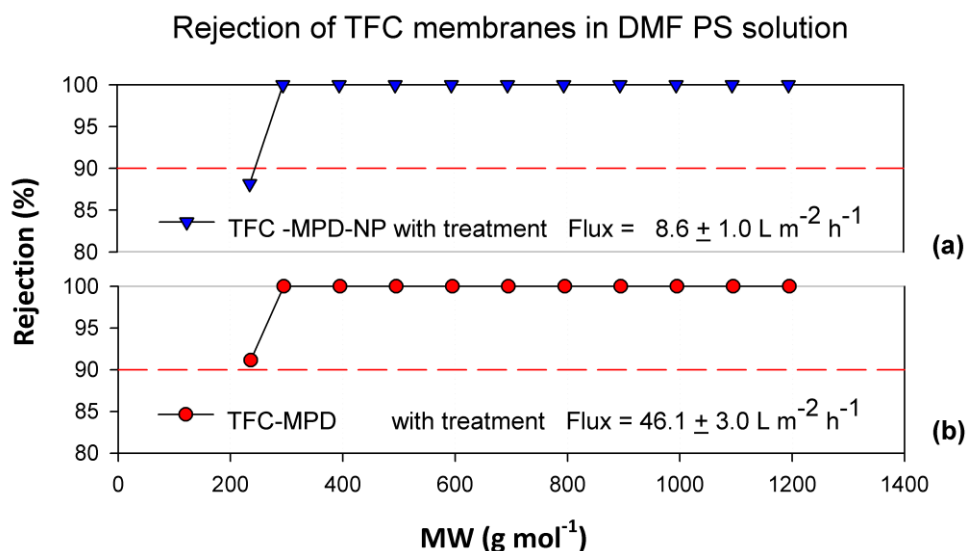
TFC membranes were post-treated with DMF or DMSO, and the performance of membranes prepared on UF supports with and without PEG was compared in different solvents before and after post-treatment with these solvents.



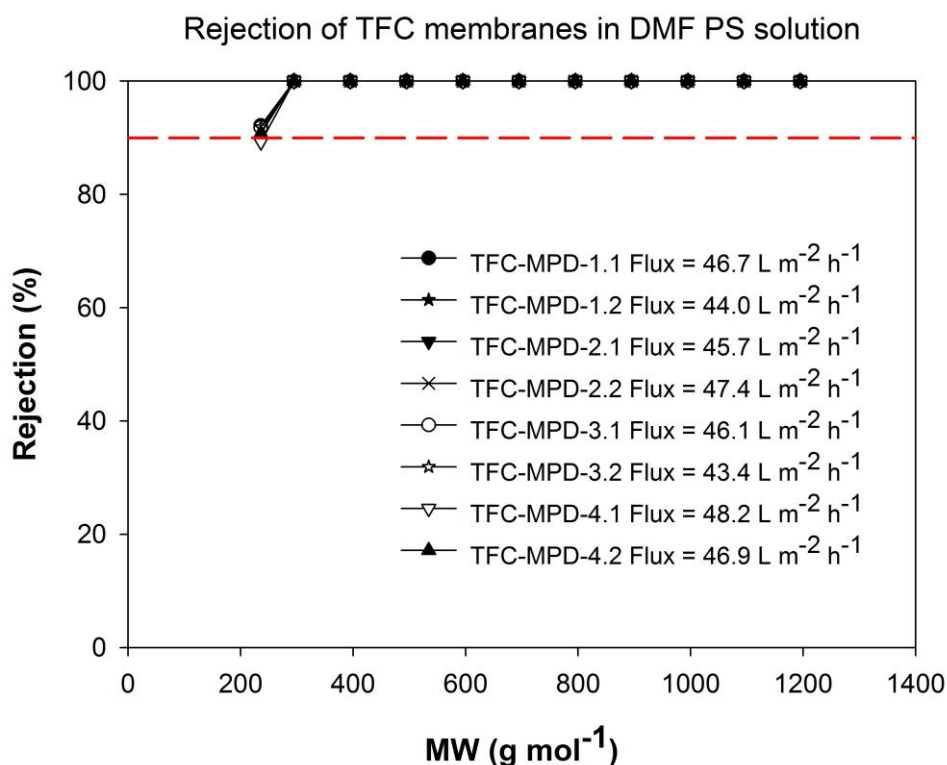
**Figure 11.** MWCO curves and fluxes of TFC membranes prepared on a crosslinked polyimide support membrane with and without PEG as conditioning agent, and with and without post-treatment with DMF as an activating solvent. Nanofiltration of a feed solution comprising polystyrene oligomers dissolved in methanol has been performed at 30 bar and 30°C. (a) No PEG, no activating solvent treatment; (b) No PEG, with activating solvent treatment; (c) With PEG, no activating solvent treatment; (d) With PEG, with activating solvent treatment.

Figure 11 (a) – (d) shows that for membranes with and without PEG impregnated supports, methanol flux after post-treatment with DMF is approximately three times higher than without solvent treatment. For TFC membranes formed on supports without PEG, flux increased from 7 to 23.9 L m<sup>-2</sup> h<sup>-1</sup>, while for TFC membranes formed on PEG impregnated supports, flux increases

from 14.9 to 46 L m<sup>-2</sup> h<sup>-1</sup>. All of the membranes show high rejection of these styrene oligomers and for all cases both rejection and flux are higher after treatment with DMF. The rejection curves show that these TFC membranes are among the tightest OSN membranes reported to date, with all markers being rejected >95 %. It appears that combining both approaches, i.e. impregnating the UF support with PEG as well as post-treating the membrane with DMF, gives the TFC membrane with the highest flux. Figure 12 shows the performance of the TFC membranes with DMF as a solvent. In this dissertation, all rejection figures where an error bar is not shown means that the rejection of the tested membranes was reproducible and overlaps (see Figure 13 for reproducibility data). In Figure 12, there is a remarkable increase in solvent flux between the TFC membranes, with the membrane formed on the PEG impregnated UF support (10(b)) showing a flux five times higher than the membrane formed on the non-impregnated support (10(a)). Given this data for PEG impregnation, subsequent membrane performance studies (Figures 14 to 16) comparing the performance of TFC membranes in different solvents, with and without activating solvent treatment, have all used TFC membranes prepared on PEG-impregnated UF supports. A filtration test in DMF was performed for 200h to see if there was an effect in performance over exposure time. Rejection of styrene oligomers in DMF remained constant over the 200h filtration period at 30bar, suggesting that exposure time in DMF has no effect on rejection of styrene oligomers.



**Figure 12.** MWCO curve and flux of TFC membranes prepared on a crosslinked polyimide support membrane without (a) and with (b) PEG as conditioning agent. Nanofiltration of a feed solution comprising polystyrene oligomers dissolved in DMF has been performed at 30 bar and 30°C.



**Figure 13.** Repeatability of MWCO curves and fluxes of TFC membranes prepared on a crosslinked polyimide support membrane with PEG as conditioning agent. Nanofiltration of a feed solution comprising polystyrene oligomers dissolved in DMF has been performed at 30 bar and 30°C.

The increase in flux observed after treatment with DMF may be attributed to its solvent characteristics with respect to polyamides. The values of Hildebrand solubility parameters for DMF and polyamide (MPD-TMC) are  $24.8 \text{ MPa}^{1/2}$  and  $23 \text{ MPa}^{1/2}$  respectively [158], which suggests that DMF is a swelling agent for the polyamide - DMF is among the top 3 swelling solvents for aromatic polyamides including NMP and DMAc [158]. Thus, it is speculated that on exposure to DMF the polyamide layer swells, and lower weight polyamide molecular fragments may dissolve. Washing away the DMF removes these small molecular fragments, unblocking many of the membrane pores as has been previously reported when treating membranes with ethanol and IPA [21]. The effect in this study is more marked than has been previously reported, due to the excellent solvent power of DMF for these polyamide fragments.

These results suggest that a permanent change occurs in the TFC top layer after treating with activating solvent. Based on the Brown theory of latex formation it is also suggested that imperfections or defects in the membrane are removed because of compression effects created by swelling, resulting in an increased rejection [21] as can be observed in Figure 11, where both non-impregnated and PEG impregnated membranes show an increase in rejection when treated with the activating solvent. The limited dissolution of polyamide caused by treatment with DMF should cause an increase in flux with a decrease in rejection. However as reported previously [159], the process of surface defect healing by surface tension driven pore collapse can actually increase



both flux and rejection, due to the lowering of the polymer matrix modulus. This previous work reported modest increases in flux of a TFC membrane upon treatment with IPA, and in this thesis it is speculated that similar but stronger effects are present upon treatment with DMF, i.e. that removal of small molecular fragments due to partial dissolution in DMF along with the elimination of surface discontinuities results in a thinner and smoother top layer.

Clearly, it would be desirable to actually see this dissolution effect on the top layer directly. According to Freger, the selective barrier in RO membranes constitutes only a fraction of the polyamide skin. *“The polymer density across the film is not uniform and shows a dense core (the actual selective barrier) hidden inside a looser polymer structure”*. The top layer is actually a “sandwich”; it is the central fraction of the top layer cross section that has the highest density and is significantly thinner than the superficial thickness of the polyamide [160]. It has been reported in previous work that in order to determine the thickness, interfacial morphology and swelling of polyamide films using AFM, the polysulfone support was dissolved using DMF [161]. Freger selected DMF as a good swelling agent for the skin layer, where swelling and softening (without dissolution, due to the cross-linking) helped the polyamide accommodate irregular stresses that occur during rapid deformation of polysulfone upon dissolution [161]. Freger claims that it is possible that some fraction of the polyamide could be dissolved in DMF, although, their data indicates that most of the polyamide did not dissolve. Furthermore, even if some dissolution had occurred, they suggest that it would have affected only the loosest and very lightly cross-linked parts of the polyamide that do not contribute to separation. Thus, it is believed that treating the TFC membranes prepared in this chapter with DMF removes some of the polyamide loose polymer structure, allowing access to the selective layer more rapidly and without affecting the UF support, resulting in significantly enhanced fluxes without compromising rejection. These results corroborate Freger’s “sandwich like” proposed structure for the polyamide layer and suggest that the loose polymer structure is undesired and does not contribute to separation. Therefore, this work seeks to directly observe changes in these gel-like layers on either side of the dense core.

Figure 14 shows the cross-section of a TFC-MPD membrane before (14(a)) and after (14(b)) treatment with DMF as an activating solvent, the top layer can hardly be seen and no substantial change in its cross-section is apparent after DMF treatment. This may be due to the resolution of the SEM failing to pick up molecular level changes which take place in the less cross-linked layer; the visually observed layer being lightly crosslinked material, sufficiently stable to resist DMF dissolution. On the other hand, surface morphological changes were successfully observed after DMF treatment and are shown in Figure 14, where (c) is an SEM image of the surface of a TFC-MPD membrane without DMF treatment. The surface exhibits a “nodular” structure with big “tufts”; (d) is an SEM image of the surface of a TFC-MPD membrane after immersing it in DMF for 10

minutes. The density of the surface packing of the membrane is decreased. This may be due to partial surface etching caused by DMF, thinning the polymeric network. As stated above, it is believed that part of the loose polyamide structure is dissolved and that oligomers of smaller molecular weights are removed from the surface and the pores of the TFC membrane due to swelling of the skin layer in DMF [158]. To corroborate this, the surface of a TFC membrane was treated with pure DMF (1mL), the solution was then recovered and analysed using GPC. Results showed peaks at around 13-18 minutes and at minute 20. The GPC had a Gilson 132 Refractive Index detector and NMP as the mobile phase at a flow rate of  $0.5\text{ mL min}^{-1}$ . It was run at a temperature of  $90^\circ\text{C}$  with a Waters HT3 column. With this method, PEG400 eluted at minute 20, suggesting that the peak in the recovered DMF solution corresponds to PEG400 and the peaks between 13-18 minutes do not correspond to PEG. After doing a calibration using PEGs of different MW from 400-20,000 Da, it was estimated that the oligomers present in the DMF correspond to polyamide oligomers ranging from around 1,700 to 11,700 Da.

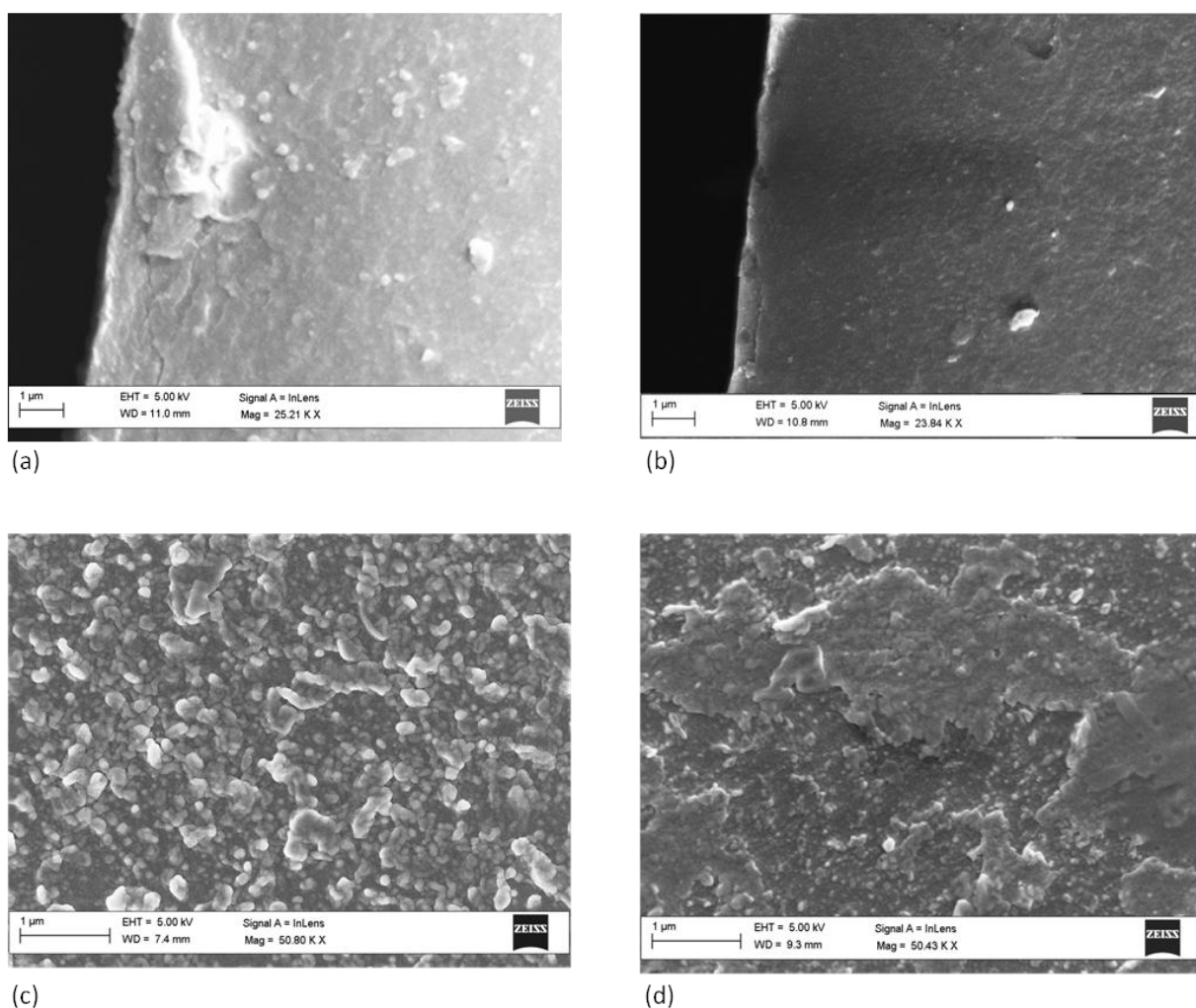


**Figure 14.** SEM images of TFC OSN membranes. (a) Shows the cross-section of TFC-MPD before DMF treatment; (b) Shows the cross-section of TFC-MPD after treating with DMF; (c) Shows the surface of TFC-MPD membrane before treating with DMF; (d) is the surface of TFC-MPD after treating with DMF.

As suggested by Freger [161], the loosest and very lightly cross-linked parts of the polyamide do not contribute to separation and are actually undesirable. It is proposed that this loose polyamide decreases flux in organic solvents and ideally should not be on the top layer. In this work, an aggressive activating solvent such as DMF is used to remove the loose polyamide and reduce the resistance that these loose polyamide structures give to solvent permeation.

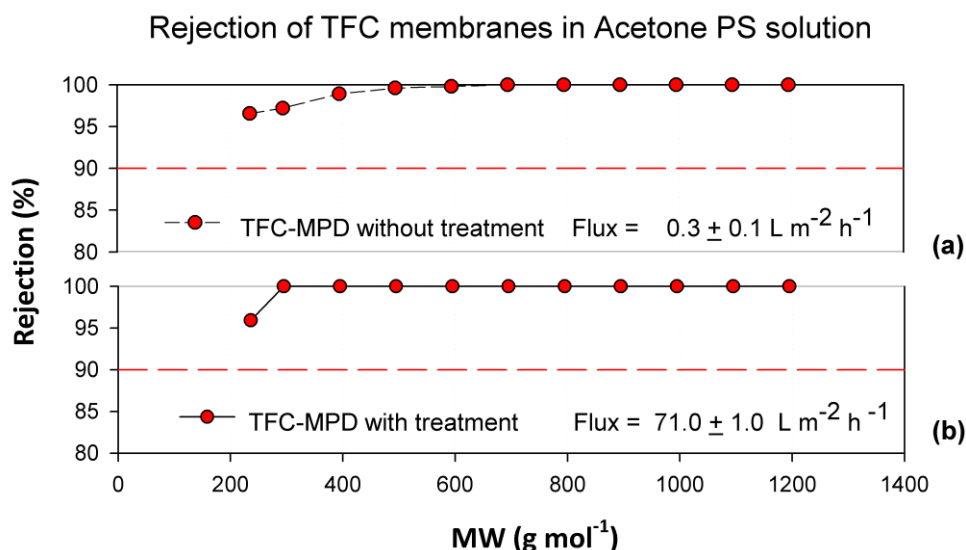


**Figure 15.** MWCO curves and fluxes of TFC-MPD membranes without (a) and with (b) treatment with DMF as an activating solvent. Nanofiltration of a feed solution comprising polystyrene oligomers dissolved in acetone has been performed at 30 bar and 30°C.

Further data on flux and rejection in a range of solvents has been obtained to study the effect of treatment with an activating solvent. TFC membranes had very little flux in acetone. However, after post-treatment acetone flux increased by two orders of magnitude, shown in Figure 15. TFC membranes showed no flux in toluene, ethyl acetate and THF before solvent treatment, presumably due to the hydrophilic nature of polyamide. After treating the membranes with DMF, flux was activated even for toluene, the most hydrophobic of these solvents, and Figure 16 shows flux and rejection of the TFC membranes in ethyl acetate (16(a)) and toluene (16(b)). Flux in THF after solvent treatment was also greatly increased, as shown in Figure 17. One of the drawbacks of tight integrally skinned asymmetric OSN membranes is their poor fluxes in acetone and THF. Figure 17 shows a comparison between the tightest available OSN integrally skinned commercial membrane (Duramem® DM150 from Evonik MET Ltd, UK) and the TFC membranes after treatment with activating solvent. For THF (Figure 17(a)), TFC membrane flux is fifteen times higher than that of DM150, and the MWCO shows the membrane is slightly tighter. For acetone (Figure 17 (b)) the TFC membrane flux is seven times higher than that of DM150 with comparable rejection. THF has been chosen as one of the solvents for a collaboration study with GSK as it presents a challenge in terms of permeability for current commercial ISA membranes. This collaboration study consists of a proof-of concept at a medium scale using TFC-MPD membranes

and commercial ISA membranes to purify active pharmaceutical ingredients. This study is described in the Appendix.

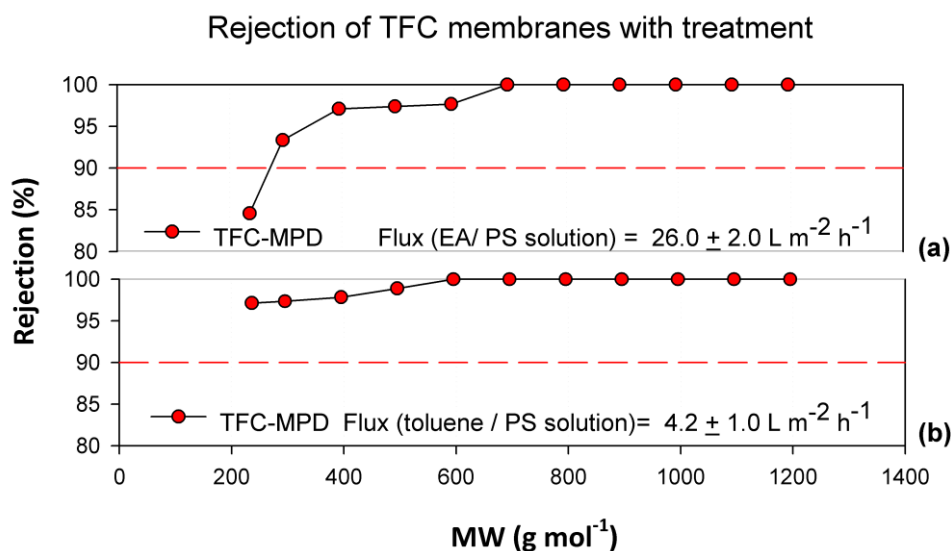


**Figure 16.** MWCO curves and fluxes of TFC-MPD membranes after treatment with DMF as an activating solvent. Nanofiltration of a feed solution comprising polystyrene oligomers dissolved in ethyl acetate or toluene has been performed at 30 bar and 30°C. (a) ethyl acetate (EA) as solvent; (b) toluene as solvent.

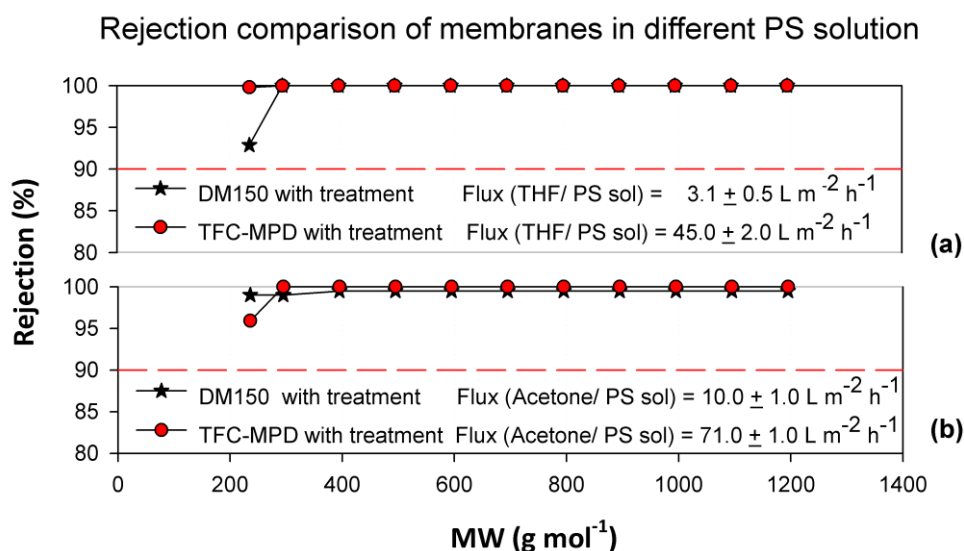


**Figure 17.** MWCO curves and fluxes of membranes after treatment with DMF as an activating solvent. Comparative study between TFC-MPD membranes and commercial integrally skinned asymmetric OSN membranes (DM150). Nanofiltration of a feed solution comprising polystyrene oligomers dissolved in THF or acetone has been performed at 30 bar and 30°C. (a) THF as solvent; (b) acetone as solvent.

The MW of the solvents used for the filtration tests decreases in the order toluene > THF > ethyl acetate > acetone > MeOH, while the polarity increases as toluene < ethyl acetate < THF < acetone < MeOH (dielectric constant = 33.6). The polyamide top layer of the TFC membrane is hydrophilic. Thus, considering both MW and polarity it is expected that the highest flux will be for MeOH and that toluene will give the lowest flux or no flux. The viscosities of the solvents decrease as follows:

MeOH>toluene>ethyl acetate>THF> acetone. Methanol and toluene present the highest viscosity; however, MeOH has good flux on TFC-MPD membranes without treatment with DMF, while toluene has no flux on the same membranes, suggesting that before treatment with DMF the solvent polarity is controlling the flux, and not the solvent MW or solvent viscosity.

After post-treatment with DMF, TFC membranes show fluxes for ethyl acetate and toluene (see Figure 16). However due to the hydrophilic nature of the top layer, these fluxes are not as high as for the other solvents, and the TFC cannot compete with commercial integrally skinned asymmetric OSN membranes in hydrophobic solvents. Further work to modify the chemistry of the top layer of the TFC OSN membranes to render them more hydrophobic in order to improve fluxes for non polar solvents will be described in the next chapter.

#### 4.3.4 Controlling permeation pathway dimensions of TFC OSN membranes

It has been widely reported that changing the chemistry of the monomers participating in the interfacial polymerization reaction has an effect on the MWCO of TFC membranes [29, 30, 84]. To investigate whether this is also the case for the TFC OSN membranes prepared in this work, membranes were fabricated using three different amines in the aqueous phase. It has been previously reported for aqueous systems that TFC membranes prepared with aromatic diamines show better rejections, but lower fluxes compared to those prepared with aliphatic diamines [84] because aliphatic diamines, such as piperazine, provide higher free volumes and larger pore sizes to the thin active layer.

##### *Solvent treatment by immersion*

In order to make the solvent treatment procedure more practical as part of a membrane formation process, instead of post-treating the TFC membranes by flushing DMF through them under pressure, they were immersed in DMF for 10 minutes. After immersion, the membranes were washed with IPA and water and stored in water at 4°C.

Figure 18 shows the results for membranes formed with MPD and PIP and filtrations with alkanes in THF as a solvent. TFC-PIP is looser than TFC-MPD with a MWCO of 370 Da as compared to 230 Da for TFC-MPD. In acetone/PS solution, the loosest membrane is TFC-HDA (Figure 19(c)) with a MWCO of 285 Da, followed by TFC-PIP (Figure 19(b)) with a MWCO of lower than 236 Da, and TFC-MPD (Figure 19(a)) is the tightest with a MWCO lower than 236 Da. These results indicate that, as for previously reported polyamide TFC nanofiltration membranes [84], the MWCO of these new TFC OSN membranes can be adjusted by using different amines in the aqueous solution.

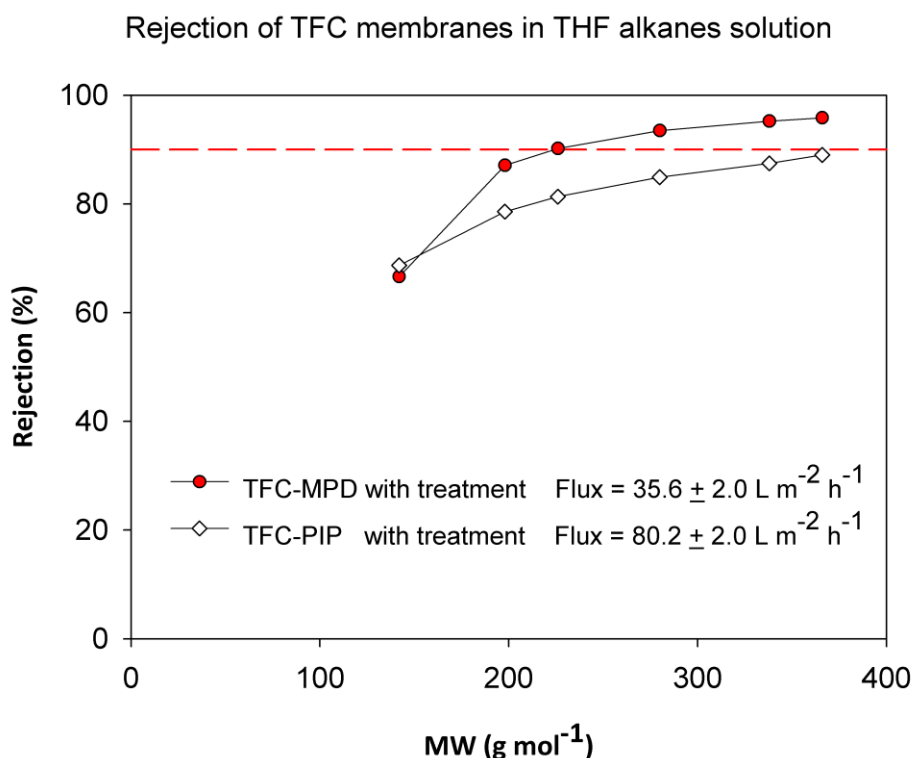


**Figure 18.** MWCO curves and flux of TFC membranes prepared with different amines after immersion in DMF as an activating solvent. Nanofiltration of a feed solution comprising alkanes dissolved in THF has been performed at 30 bar and 30°C.

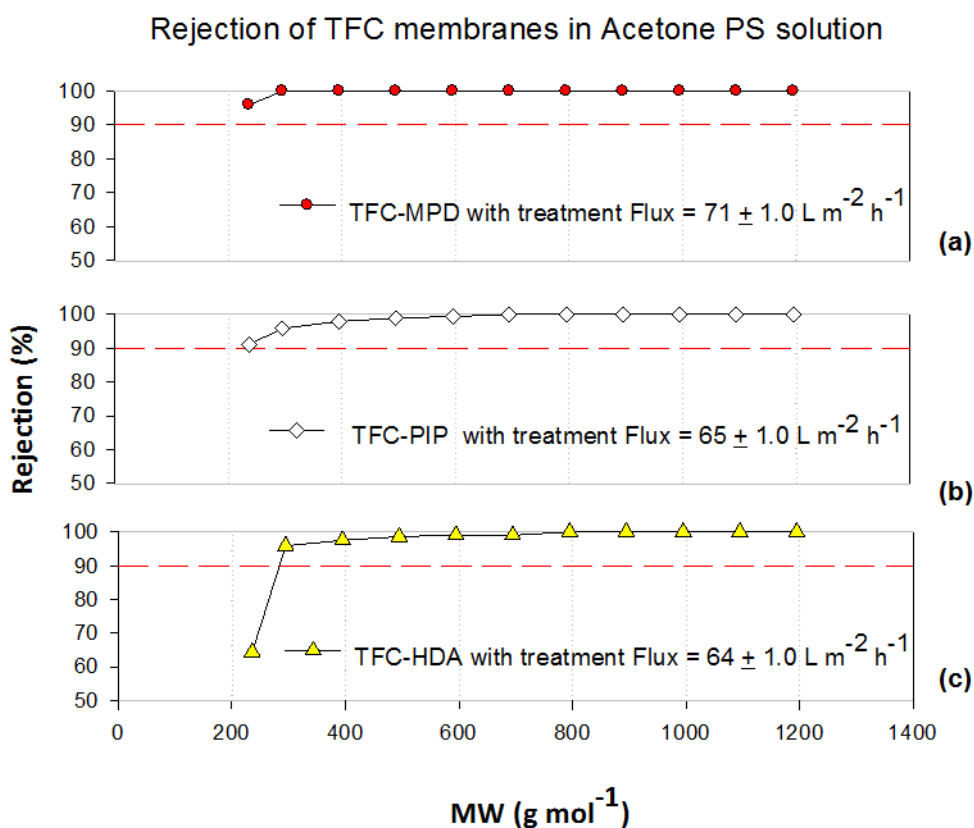


**Figure 19.** MWCO curves and flux of TFC membranes prepared with different amines after immersion in DMF as an activating solvent. Nanofiltration of a feed solution comprising polystyrene oligomers dissolved in acetone has been performed at 30 bar and 30°C. (a) amine is MPD; (b) amine is PIP; (c) amine is HDA.

### 4.3.5 DMSO as an alternative to DMF as activating solvent

DMSO is the fifth best swelling solvent for aromatic polyamide, based on the Hildebrand solubility parameter [158]. Importantly, it is relatively harmless, and relative to DMF can be considered a green solvent [162]. It is much less toxic than the other swelling solvents for aromatic polyamide such as DMF, DMAc and NMP. Here it is shown that DMSO has the same flux enhancing effect as DMF on TFC-MPD membranes. The selected solvent for testing permeability was THF, as TFC-MPD membranes have no flux in THF prior to treatment with activating solvent.

Four TFC-MPD membranes were tested for flux in THF/PS solution using dead-end filtration set-ups. After 2 hours of getting no flux, two of the TFC-MPD membranes were immersed in DMF and the other two in DMSO, all for 10 minutes. After immersion, the TFC-MPD membrane performance was tested in THF/PS solution at 30bar and 30 °C. All of the membranes showed the same rejection as in Figure 17. Flux results can be seen in Table 5. TFC membranes immersed in DMF and in DMSO exhibited the same flux, indicating that both solvents can be used as activating solvents. Since DMSO is non-toxic, it would appear to be an ideal choice for the activating solvent.

**Table 5.** TFC-MPD membranes flux after post-treatment in different solvents

Entry No.	Membrane	Solvent post-treatment	Flux (Lm <sup>-2</sup> h <sup>-1</sup> )
7	TFC-MPD	DMSO	49
8	TFC-MPD	DMSO	49
9	TFC-MPD	DMF	50
10	TFC-MPD	DMF	50

## 4.4 Conclusion

The formation of novel TFC OSN membranes prepared by interfacial polymerization has been demonstrated. These membranes exhibited significantly improved solvent permeabilities when compared to conventional integrally skinned asymmetric OSN membranes, without sacrificing rejection. These new membranes have been created by impregnating the UF support with PEG before the IP reaction, which enhances membrane flux without affecting selectivity.

Crosslinked polyimide has been used as a UF support, allowing the post-treatment of TFC membranes with some of the best solvents for aromatic polyamide (e.g. DMF and DMSO). It is asserted that these dissolve part of the loose polyamide structures on either side of the highly crosslinked core in the top layer, without affecting the core. This results in greatly enhanced fluxes without compromising rejection. The crosslinked polyimide supports introduce new degrees of

freedom in membrane fabrication due to their remarkable solvent stability, and it is believed TFC OSN membranes prepared via interfacial polymerization on these supports could lead to the next generation of high performance OSN membranes.

In collaboration with J. Stawikowska, it has been demonstrated that the nanoprobe imaging technique, based on filtering high contrast nanoparticles, can be used to characterise TFC OSN membranes prepared by IP. The pore size distributions were measured and correlated with the membranes' functional performance, implying that the selectivity of the TFC OSN membranes was highly related to the pore size. This correlation suggests that the pore-flow model presumably governs the transport through these membranes. Furthermore, the membranes' cross sectional images enabled detailed estimations of the thickness of the polyamide top layer.

One of the current challenges for OSN membranes is to improve permeability in non-polar solvents. TFC membranes prepared via IP could accomplish this. However, to be competitive with integrally skinned and rubber coated TFC membranes, the properties of polyamide membranes need to be modified to decrease their surface hydrophilicity. Thus, the next challenge is to develop hydrophobic TFC OSN membranes by interfacial polymerization. The work carried out in order to achieve this challenge and enhance flux in non-polar solvents is discussed in the next chapter.

#### 4.5 Supplementary information

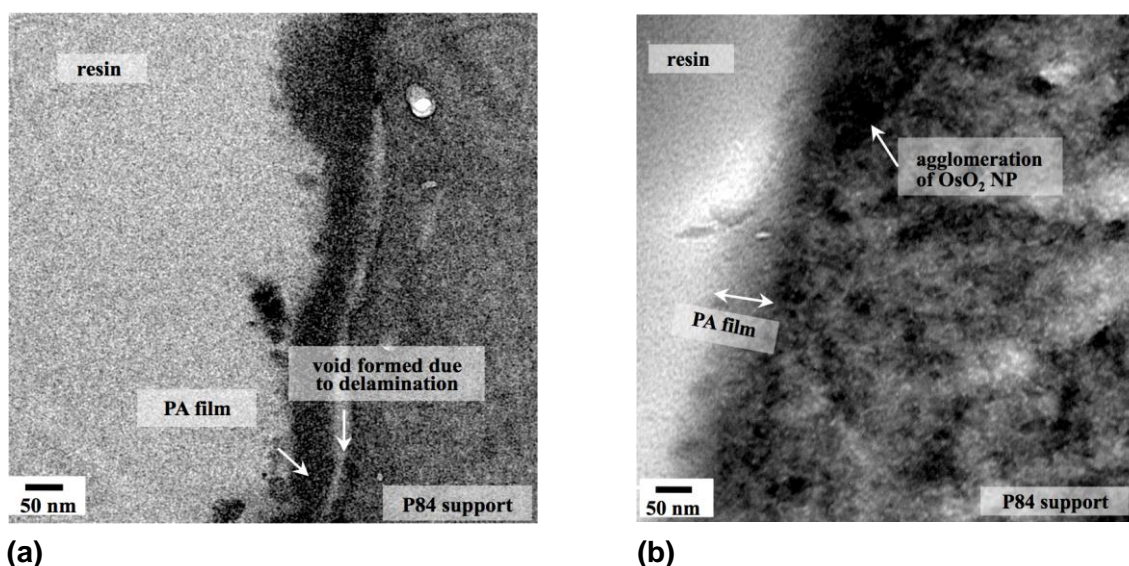


**Figure S1.** Electromicrographs of PA/XP84 TFC membrane (courtesy of J. Stawikowska). (a) TEM cross sectional image of the PA/P84 membrane after filtration from the surface side, (b) and the open side.



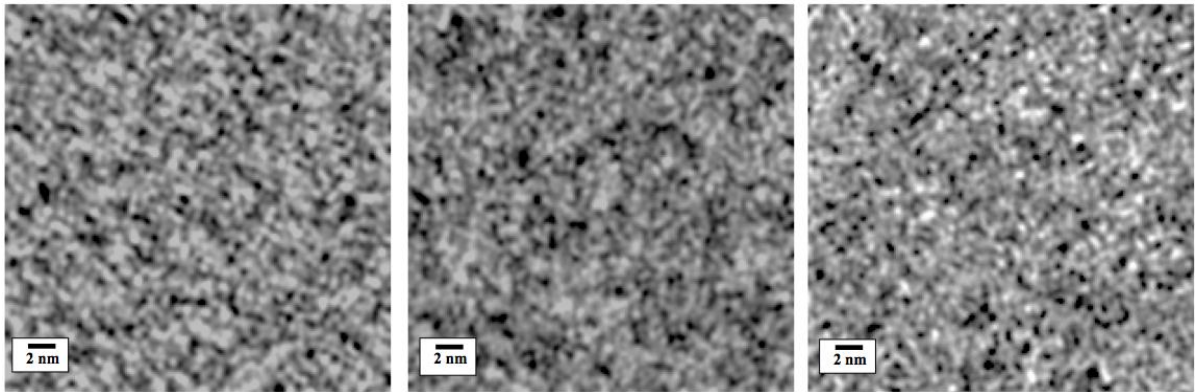


**Figure S2.** High magnification TEM cross-sectional images of the PA composite separation layer. Three images acquired from different regions (courtesy of J. Stawikowska).

# Chapter 5

## High Flux Hydrophobic Membranes for Organic Solvent Nanofiltration-Interfacial Polymerization, Surface Modification and Solvent Activation

### Abstract

This chapter describes the formation of a new generation of hydrophobic organic solvent nanofiltration membranes: high flux hydrophobic thin film composite membranes via interfacial polymerization. These are the first reported hydrophobic TFC membranes which are stable in DMF. They exhibit significantly higher permeabilities for nonpolar solvents, including toluene and ethyl acetate, than commercial OSN hydrophobic integrally skinned asymmetric and rubber coated membranes; and yet have comparable or better selectivity. Solvent stable crosslinked polyimide ultrafiltration membranes were used as supports for the formation of these TFC membranes. For some membranes, a mixture of acyl chlorides (trimesoyl chloride blended with a monoacyl chloride containing fluorine) was used during the interfacial polymerization to manipulate molecular weight cut off and to make the membranes more hydrophobic. Measured by the rejection curves, the loosest membrane was prepared when the mixture of acyl chlorides was used, and the tightest when trimesoyl chloride was used alone. To increase nonpolar solvent flux the free acyl chloride groups on the TFC membrane surface were capped with different monomers containing hydrophobic groups. Comparison of TFC membranes formed with and without capping suggests that the chemistry of the membrane surfaces plays an important role in solvent permeation. As reported previously in Chapter 4, in order to “activate” solvent flux the TFC membranes were post-treated with DMF. Incorporation of F and Si in the polyamide top layer resulted in dramatically improved permeabilities for non-polar solvents. Such hydrophobic TFC membranes prepared via interfacial polymerization and treated with an activating solvent may lead to the next generation of high performance hydrophobic OSN membranes.

## 5.1 Introduction

Integrally skinned asymmetric OSN membranes suffer from flux limitations for some organic solvents; and “tight” membranes have poor fluxes in nonpolar solvents, including toluene. This limitation might be overcome by carefully controlling the formation of the separation layer. Another possibility is to adopt a more sophisticated strategy: develop hydrophobic TFC membranes for OSN applications. Rubber coated thin film composite membranes are commercially available and have higher fluxes than integrally skinned asymmetric membranes. However, PDMS tends to swell excessively in nonpolar solvents, compromising selectivity. Currently, the tightest commercial OSN rubber coated TFC membrane (Puramem S380 from Evonik MET Ltd, UK) has a molecular weight cut off (MWCO) of 600 Da in toluene according to the supplier’s specifications, limiting its application in several purification processes. As demonstrated in Chapter 4, tight TFC OSN membranes prepared by interfacial polymerization have the potential to achieve higher fluxes than integrally skinned asymmetric OSN membranes, without sacrificing selectivity. However, to increase permeabilities of nonpolar solvents, the external surface properties of these polyamide TFC membranes still need to be modified to decrease their hydrophilicity. To date there are no reported hydrophobic TFC OSN membranes prepared via IP.

The surface of TFC membranes used for aqueous applications is often modified to further enhance their performance. The most common modifications are plasma treatment, classical organic reactions and polymer grafting [150]. Several efforts to modify the surface chemistry of TFC membranes have been reported for different purposes (e.g. antifouling properties, antimicrobial activity, and increased hydrophilicity) [150]. Thus, improving the performance of previously developed TFC OSN membranes by IP in hydrophobic solvents might be possible by modifying their surface chemistry.

Because the two monomers approach the interface from opposite directions, films from interfacial polymerization are asymmetric [163]. Gilbert et al. have demonstrated the surface asymmetry by contact angle titrations [163]. Freger has also provided evidence of nanoscale heterogeneity in polyamide membranes formed by IP [160], where the fixed charge is not uniform and the skin is actually a “sandwich” comprising two oppositely charged layers separated by a sharp boundary located inside the densest part of the skin. According to his results, the surface side loose polyamide contains more carboxylic groups, giving a negative fixed charge, while the loose polyamide on the polysulfone side has more amine groups, giving a fixed positive charge.

However, after characterizing isolated polyamide films with novel TEM techniques, Pacheco et al. [164] could only see the loose negatively charged polyamide on the surface of the membrane and their results do not support the existence of regions of loose polyamide on the polysulfone side of the film. They propose that this discrepancy between their results and Freger's may be because the model proposed by Freger does not consider the physical obstruction to film growth due to the polysulfone support, suggesting that the semicircular features described as "carboxyl-free polyamide" by Freger are artefacts created during the sample preparation process [164].

However, both groups suggest that the loose polyamide on the surface side is negatively charged, containing unreacted acyl chloride groups that eventually turn into carboxylic acid groups.

It is known that during IP, the reaction occurs in the organic phase. Once the polyamide layer precipitates, it limits the further diffusion of amine groups into the organic phase. With fewer and fewer amine groups in the organic phase, there are more unreacted acyl chloride groups on the membrane's surface. These groups would eventually hydrolyze to carboxylic acid groups. Since the hydrolysis reaction is slow [165], it is possible to modify the polyamide top layer's surface by chemical coupling with amines before the acyl chloride groups hydrolyze. As a result, Kang et al. developed a method of surface modification by grafting hydrophilic poly(ethylene glycol) chains onto the surface of a TFC polyamide RO membrane [165]. They used PEG containing an amino group (MPEG-NH<sub>2</sub>) as the grafting monomer, which capped the unreacted acyl chloride groups present on the surface of the thin active layer, resulting in improved membrane antifouling properties.

Here, the membrane's surface has been chemically modified to increase permeability in non-polar solvents by incorporating hydrophobic groups (i.e. F and Si) on the surface of the polyamide layer. This was achieved by capping the unreacted acyl chloride groups with hydrophobic monomers containing amino groups. The effect of using different hydrophobic capping-monomers on TFC membrane performance in terms of flux and rejection are discussed in this chapter.

Another possible way to make the surface of these TFC OSN membranes more hydrophobic is by capping with hydrophobic monomers containing acyl chloride groups. In order to achieve this, free amines must be present on the membrane's surface. Zou et al. [166] developed a novel interfacial polymerization approach, where they introduced an extra step in the IP reaction. They further reacted the free acyl chloride groups with a polyfunctional amine, MPD, leaving a large amount of amino groups on the top surface of the active skin layer, resulting in improved membrane antifouling properties. Using their approach [166], TFC membranes were prepared with free

unreacted amino groups on their surface, which were further capped with hydrophobic monomers containing acyl chloride groups.

The top layer chemistry can also be modified by introducing new monomers in the IP reaction, which could simultaneously help control MWCO. Monomers with different chemical structures; i.e., whether they are aromatic or aliphatic, mono-, di- or poly-functional and the position of the active group, give different nanostructures [32]. There is a broad range of mono-, bi- and tri-acyl chlorides to select from. Here, in order to prepare a looser TFC membrane the TMC was blended with a monoacyl chloride. The approach is to achieve both a looser membrane, and at the same time make it hydrophobic. The effects on membrane performance when further capping the free acyl chloride groups on the polyamide surface with hydrophobic monomers containing amino groups have also been studied.

In Chapter 4 it is shown that treating TFC polyamide membranes with an activating solvent (i.e. DMF or DMSO) increases flux significantly without compromising rejection. When TFC polyamide membranes were immersed in DMF, flux was greatly increased; for some solvents, there was a flux only after activation. Thus, in order to activate solvent flux the hydrophobic TFC membranes prepared in this work were post-treated with DMF as the activating solvent. Polyimides, when crosslinked, present high stability in a wide range of organic solvents, making them one of the most suitable polymers for the development of OSN membranes [56, 68, 147]. Thus, in this work solvent stable crosslinked PI UF membranes were prepared and used as supports for the formation of TFC membranes.

## 5.2 Experimental

### 5.2.1 Materials

Polyimide (PI) polymer (P84), all organic solvents, polyethylene glycol (MW 400), trimesoyl chloride (TMC), m-phenylenediamine (MPD), 1,6 hexanediamine (HDA) and polystyrene oligomers had the same purity and were purchased from the same companies described in *section 4.2.1*. Poly[dimethylsiloxane-co-(3-aminopropyl)methylsiloxane] was purchased from Sigma Aldrich, UK. Pentafluorooctanoyl chloride and 2,2,3,3,3-pentafluoropropylamine were purchased from Fluorochem. Amine MPD and acyl chlorides TMC and pentafluorooctanoyl chloride were used as monomers for the formation of the polyamide active layer. Poly[dimethylsiloxane-co-(3-aminopropyl)methylsiloxane], pentafluorooctanoyl chloride and 2,2,3,3,3-pentafluoropropylamine were used for the modification of the membrane surface by capping. Distilled water and hexane were used as aqueous and organic phases, respectively.

Commercial membranes Starmem™ 122 and Puramem® S380 were purchased from Evonik-MET.

### 5.2.2 Preparation of crosslinked PI UF support membrane

Crosslinked PI UF support membranes were prepared and conditioned following the same methodology explained in *section 4.2.2*.

### 5.2.3 Preparation of polyamide TFC membranes

TFC OSN membranes were hand-cast on the preformed crosslinked PEG-impregnated polyimide UF support membranes through interfacial polymerization. It was shown in Chapter 4 that adding PEG into the crosslinked UF support enhances permeability of TFC membranes. Two generations of hydrophobic membranes have been prepared; the first generation comprises tighter membranes and the second generation looser membranes. For comparison, control membranes that do not contain hydrophobic groups were prepared (the standard TFC OSN membrane described in Chapter 4 and the 3-step IP membrane, which involves an extra step of further reacting the membrane surface with an aqueous solution of MPD [166]). All TFC membranes were stored in water at 4° C.

#### *Preparation of TFC membranes (via interfacial polymerization)*

These TFC membranes were prepared following the same procedure described in *section 4.2.3*.

#### *Preparation of first generation hydrophobic TFC membranes (via interfacial polymerization)*

Crosslinked PI UF support membranes, with skin layer facing upwards, were taped to a glass plate and placed in Solution 1 for 2 min (see Table 6). The amine loaded support was then pressed with a roller and wiped to remove excess solution, and then immersed in Solution 2a for 1 minute (see Table 6), where the interfacial polymerization took place. After the reaction, the resulting membrane was withdrawn from the hexane solution and allowed to dry for 10 seconds. The TFC membranes were then immersed for 1 minute in one of the following solutions: 1, 3a, 3b or 3c (see Table 6, Scheme 3). Membranes reacted with Solution 1 (3-steps IP) were capped a second time with solution 3c under the same conditions (see Scheme 4). The resulting membranes were withdrawn from the capping solution and rinsed with hexane, let dry and rinsed with distilled water and stored in water at 4°C. The chemical structures of the monomers used for the capping step are shown in Scheme 3b.

*Preparation of second generation hydrophobic TFC membranes (via interfacial polymerization)*

These membranes were prepared following the same procedure described in 2.3.2 but using solution 2b (see Table 6) instead of solution 2a during the interfacial polymerization reaction. Capping was carried out using solutions 3a or 3b. The chemical structures of the monomers used for the interfacial polymerization reaction are shown in Scheme 3c.

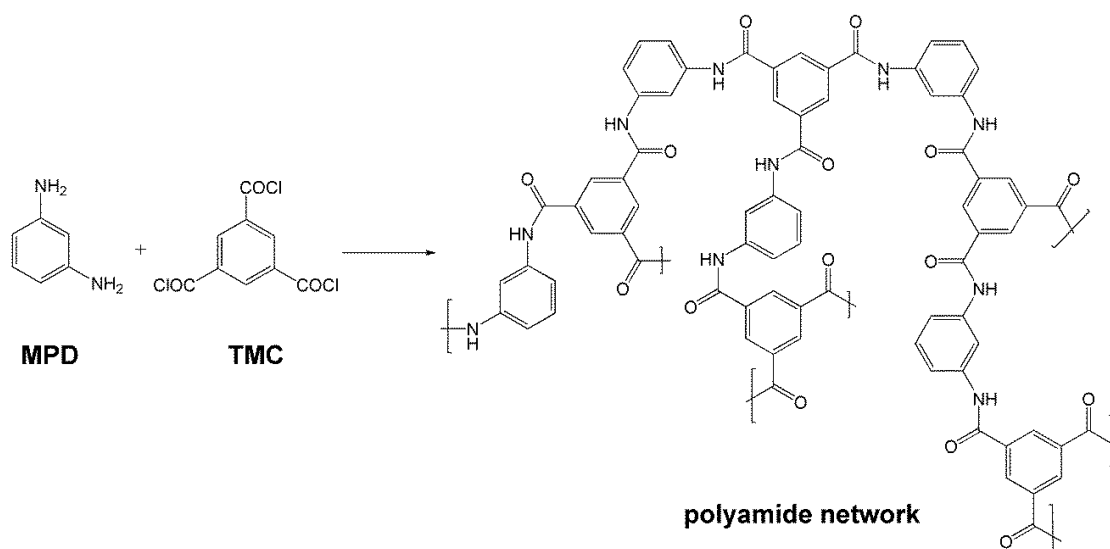
**Table 6.** Solutions used for the preparation of TFC membranes

Entry No.	Solution		Composition % (w/v)
11	aqueous (water)	<b>1</b>	2.0 % m-phenylenediamine (MPD)
12	organic (hexane)	<b>2a</b>	0.1 % trimesoyl chloride (TMC)
13		<b>2b</b>	0.1 % TMC and pentafluorooctanoyl chloride (7:1)
14		<b>3a</b>	0.1 % poly[dimethylsiloxane-co-(3-aminopropyl)methylsiloxane]
15		<b>3b</b>	0.1 % 2,2,3,3,3-pentafluoropropylamine
16		<b>3c</b>	0.1 % pentafluorooctanoyl chloride

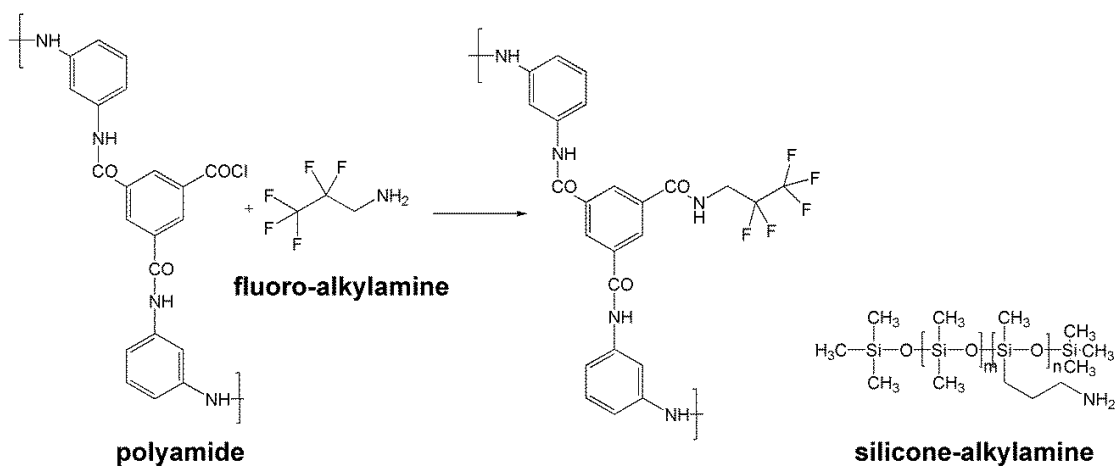
Membrane identification codes for the TFC membranes prepared in this work are shown in Table 7. First generation hydrophobic TFC membranes have been compared with the commercial membrane Starmem™122 and the second generation hydrophobic TFC membranes with the commercial rubber coated TFC membrane Puramem® S380.

**Table 7.** Membrane codes

Entry No	Membrane		Membrane code
17	<b>Control</b>	TFC membrane	<b>TFC</b>
18		TFC membrane-3 steps IP (capped with MPD)	<b>TFC-3steps</b>
19	<b>First generation hydrophobic TFC membranes</b>	TFC membrane capped with fluoro-alkylamine	<b>Hyphob(I)-TFC-F<sub>a</sub> (R<sub>F</sub>-NH<sub>2</sub>)</b>
20		TFC membrane capped with silicone-alkylamine	<b>Hyphob(I)-TFC-Si (R<sub>Si</sub>-NH<sub>2</sub>)</b>
21		TFC membrane capped with fluoro-alkylacylchloride	<b>Hyphob(I)-TFC-F<sub>b</sub> (R<sub>F</sub>-COCl)</b>
22		TFC membrane 3steps capped with fluoro-alkylacylchloride	<b>Hyphob(I)-TFC-3steps-F (R<sub>F</sub>-COCl)</b>
23	<b>Second generation hydrophobic TFC membranes</b>	TFC membrane (TMC blended with FCl)	<b>Hyphob(II)-TFC</b>
24		TFC membrane (TMC blended with FCl) capped with fluoro-alkylamine	<b>Hyphob(II)-TFC-F (R<sub>F</sub>-NH<sub>2</sub>)</b>
25		TFC membrane (TMC blended with FCl) capped with silicone-alkylamine	<b>Hyphob(II)-TFC-Si (R<sub>Si</sub>-NH<sub>2</sub>)</b>
26	<b>OSN IS asymmetric commercial membrane</b>	Starmem™ 122	<b>SM122</b>
27	<b>Rubber coated TFC commercial membrane</b>	Puramem® S380	<b>S380</b>

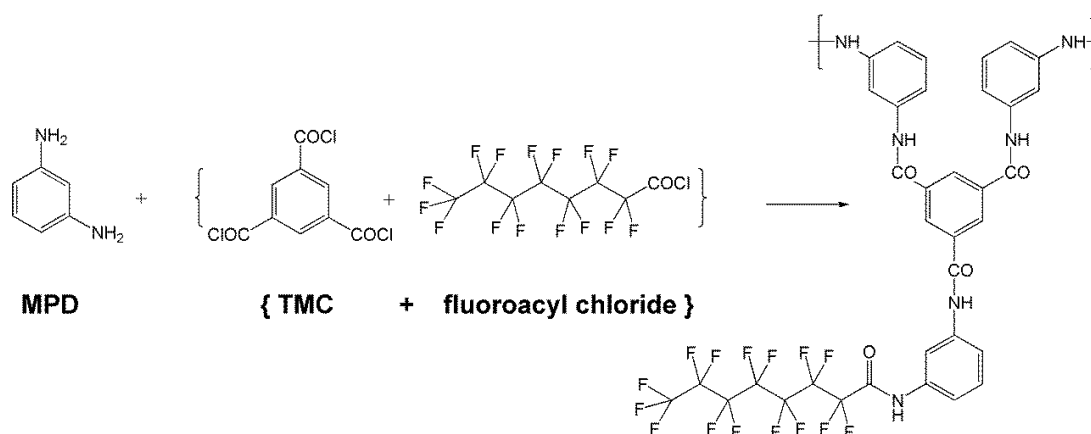


a)



b)

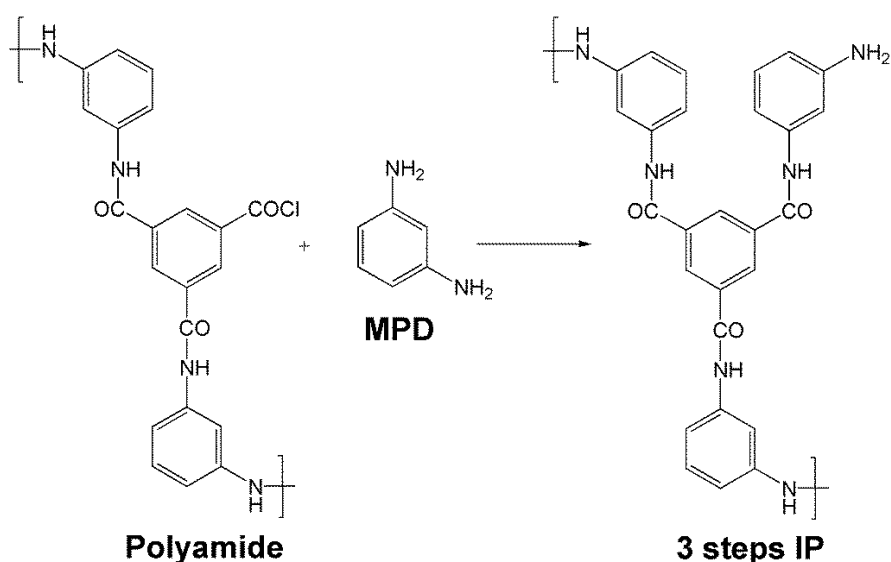
c)



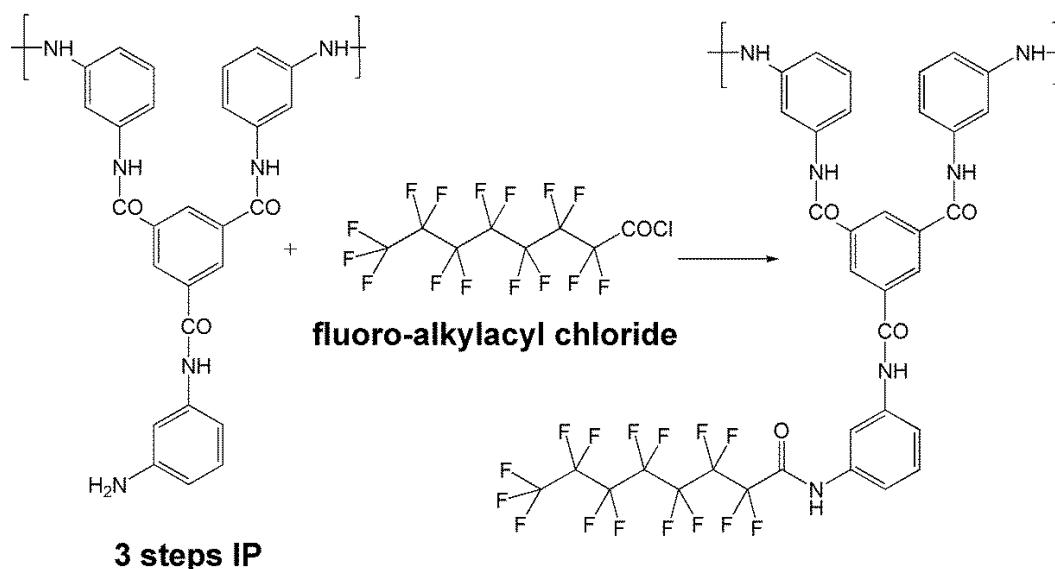
d)

**Scheme 3.** Chemistry of TFC membranes: standard polyamide TFC and 1<sup>st</sup> and 2<sup>nd</sup> generation Hydrophobic TFC membranes. **a)** Interfacial polymerization reaction; **b)** Polyamide with fluorinated backbone through capping with fluoro-alkylamine (1<sup>st</sup> generation hydrophobic membrane); **c)** Structure of one of the hydrophobic monomers used for capping (silicone-alkylamine); **d)** Interfacial polymerization reaction leading to a polyamide with fluorinated backbone through blending fluoro-alkylacylchloride and TMC in the organic phase (2<sup>nd</sup> generation hydrophobic membrane).





a)



b)

**Scheme 4.** Formation of TFC membranes. a) 3-steps Interfacial polymerization reaction through further reacting with MPD; b) Polyamide with fluorinated backbone through capping a 3-steps IP TFC membrane with fluoro-alkyl acyl chloride (1st generation Hydrophobic membranes).

Figure 20 is a flowchart of the strategies used for the preparation of TFC membranes (numbered from 1 to 9; these numbers in the flowchart correspond to the entries in the flowchart table). It is believed membrane 5 will not present hydrophobic groups on its surface, because after the standard 2-steps interfacial polymerization reaction, free acyl chloride groups are present on the surface and capping with pentafluorooctanoyl chloride is unlikely to work. To overcome this problem, membrane 2 (by 3-steps IP reaction) was prepared, which presents free amino groups on the surface and it is believed that further capping with the hydrophobic monoacyl chloride

should work. Second generation hydrophobic membranes have only been capped with hydrophobic monomers containing amino groups. As a control three membranes were prepared without capping: standard TFC membrane (by 2-steps interfacial polymerization), the 3-steps interfacial polymerization TFC membrane (TFC-3steps), and the second generation hydrophobic membrane Hyphob(II)-TFC.

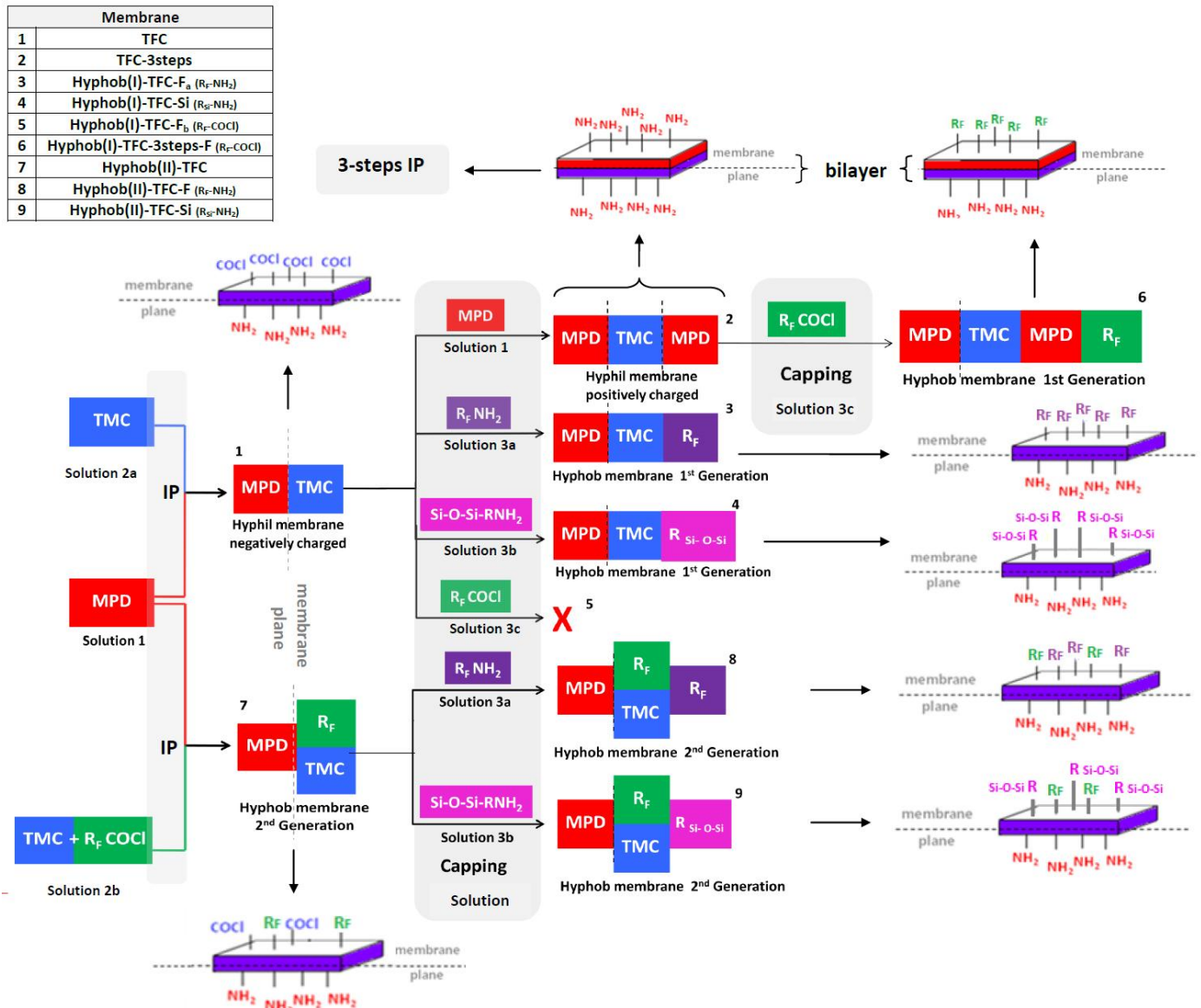


**Figure 20.** Strategies for Hydrophobic TFC membrane formation.

#### 5.2.4 Treatment of TFC membranes with activating solvent

As previously reported in Chapter 4, in order to further enhance or to activate solvent flux, the TFC membranes were post-treated with an activating solvent with similar Hildebrand solubility parameter than that of the polyamide top layer ( $23 \text{ (MPa)}^{1/2}$ ) [158]. DMF was the selected solvent and the contact time was 10 minutes via immersion.

### 5.2.5 Membrane Characterization

#### *Contact angle*

Contact angle measurements and sample preparation were performed following the same procedure described in *section 4.2.5*. Five measurements on different membrane pieces were performed.

#### *XPS analysis*

XPS analysis was performed by Begbroke Nano. Samples supported on carbon pads on stubs were introduced into the instrument via a turbo molecular pumped entry lock. The entry lock was pumped for 15 minutes before the sample was introduced into the analysis chamber. XPS was performed in an ion pumped VG Microtech CLAM 4MCD analysis system. 200 Watt unmonochromated Mg X-ray excitation was used. The analyser was operated at constant pass energy of 100eV for wide scans and 20eV for detailed scans setting the C1s peak at BE 284.8 eV to overcome any sample charging. Data was obtained using SPECTRA 8 operating system. Data processing was performed using CASAXPS. Peak areas were measured after satellite subtraction and background subtraction either a linear background or following methods of Shirley [167].

The area under the principal peak of each element in the spectrum, divided by an empirically derived sensitivity factor [168], is proportional to the concentration of that element on the surface (approximately the top 10 nm).

### 5.2.6 Membrane performance

Membrane performance was evaluated according to flux profiles and MWCO curves following the procedure described in *section 4.2.6* in repeats of 8 (two disks per membrane of four different membranes prepared the same way were tested to evaluate repeatability). The solute rejection test was carried out using the homologous standard feed solution comprised of a mixture of styrene oligomers described in *section 4.2.6*; analysis of styrene oligomers was carried out as previously described. The performance of TFC membranes prepared with and without capping was evaluated by filtrations with toluene and THF as solvents. The performance of second generation hydrophobic TFC membranes was evaluated by filtrations with toluene and ethyl acetate. TFC membranes were compared with commercial Starmem® and Puramem® membranes (SM122, S380). Two discs of each commercial membrane were tested to evaluate repeatability. In all rejection figures where an error bar is not shown, the rejection of the tested membranes was reproducible and overlaps.

### 5.3 Results and discussion

#### 5.3.1 TFC OSN membranes characterization

To study the effect of capping, the changes in contact angle with and without capping (control TFC) before DMF treatment were measured using two different monomers in the capping solution. The average values are recorded in Table 8. To corroborate the incorporation of hydrophobic groups on the membrane surface the surface chemistry was analysed using XPS (see Table 9), which is a highly sensitive technique for surface analysis, with the ability to measure elemental composition for the top 10 nm.

**Table 8.** Contact angle of TFC membranes

Entry No.	Membrane	Contact Angle
28	Hyphob(I)-TFC-3steps-F ( $R_F$ -COCl)	94+3
29	Hyphob(I)-TFC-F <sub>a</sub> ( $R_F$ -NH <sub>2</sub> )	92+3
30	Hyphob(I)-TFC-Si ( $R_{Si}$ -NH <sub>2</sub> )	90 +2
31	Hyphob(I)-TFC-F <sub>b</sub> ( $R_F$ -COCl)	64+2
32	TFC-3steps	62+3
33	TFC (control)	48+2

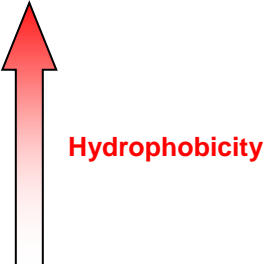


**Table 9.** Surface Elemental Composition

Entry No.	Membrane		Element (normalized At %)				
			O	C	N	F	Si
34	Control	TFC	14.7	74.3	8.0	0.6	1.9
35	First generation hydrophobic TFC membranes	Hyphob(I)-TFC-F <sub>a</sub> ( $R_F$ -NH <sub>2</sub> )	10.4	59.1	8.0	21.5	0.8
36		Hyphob(I)-TFC-F <sub>b</sub> ( $R_F$ -COCl)	16.4	67.2	11.6	3.8	0.7
37		Hyphob(I)-TFC-3steps-F ( $R_F$ -COCl)	9.8	53.7	7.7	28.0	0.9
38		Hyphob(I)-TFC-Si ( $R_{Si}$ -NH <sub>2</sub> )	19.9	57.8	5.0	0.9	16.3
39	Second generation hydrophobic TFC membranes	Hyphob(II)-TFC	14.7	66.4	8.4	8.7	1.6
40		Hyphob(II)-TFC-F ( $R_F$ -NH <sub>2</sub> )	11.2	63.1	8.0	16.9	0.9
41		Hyphob(II)-TFC-Si ( $R_{Si}$ -NH <sub>2</sub> )	13.8	59.3	6.6	15.7	4.4

Hyphob(I)-TFC-F<sub>a</sub> and Hyphob(I)-TFC-Si membranes have higher contact angles (CA=92° and 90°, respectively) than the control TFC membrane (CA=48), suggesting that incorporation of hydrophobic groups on the membrane surface took place successfully when capping with the hydrophobic alkylamines. This was further proven in Table 9 where the percentage of F is 21.5 % and of Si is around 16 % for Hyphob(I)-TFC-F<sub>a</sub> (entry 35) and Hyphob(I)-TFC-Si (entry 38) membranes respectively. As mentioned previously, very few amine groups are present on the surface of the TFC membrane. Thus, capping with fluoro-alkylchloride was not very successful;

the contact angle of Hyphob(I)-TFC-F<sub>b</sub> (CA=64) could not be as enhanced as those capped with hydrophobic alkylamines, and only about 4 % of F (entry 36) was detected on the surface using XPS. A successful incorporation of fluorine by capping with fluoro-alkylchloride was only achieved when more free amine groups were present on the membrane surface. This was only possible after the 3 steps IP reaction [166], where the free amines on the membrane surface were further capped with the fluoro-alkylchloride to give the Hyphob(I)-TFC-3steps-F membrane (entry 37), which showed a high F content (28 %) and gave the highest contact angle (CA= 94).

In the second generation hydrophobic membranes, XPS results for Hyphob(II)-TFC (entry 39) show a 9 % F content, suggesting that F was successfully incorporated in the top layer during the IP reaction. These results also show that further capping the Hyphob(II)-TFC membrane with fluoro- and silicone- alkylamines was successfully achieved, giving 4.4 % of Si for Hyphob(II)-TFC-Si (entry 41) and 16.9 % of F for Hyphob(II)TFC-F (entry 40).

Both the presence of hydrophobic groups shown in the XPS results and the increase in contact angle suggest that the membrane surface is more hydrophobic, which could potentially enhance permeability in non-polar solvents.

### 5.3.2 Membrane performance

#### *Effect of solvent treatment*

In this work, all TFC membranes prepared by IP showed no flux in toluene, THF and ethyl acetate. Thus, as reported in Chapter 4, to activate solvent flux, membranes were post-treated with DMF as the activating solvent. Treating TFC OSN membranes with DMF removes some of the polyamide loose polymer structure, allowing access to the selective layer more rapidly. These results are consistent with Freger's [161] "sandwich like" proposed structure for the polyamide layer, which suggests that the loose polymer structure is undesired and does not contribute to separation. After treating the TFC membranes prepared in this work with DMF, flux was activated for toluene, THF and ethyl acetate.

### First generation hydrophobic membranes

#### *Capping after standard IP reaction*

One of the drawbacks of the TFC OSN membrane prepared by IP in Chapter 4 is their poor flux in non-polar solvents. Due to the hydrophilic nature of their top layer, fluxes for toluene and ethyl acetate (see Figures 21a and 24) were not as enhanced as for THF (see Figure 22a) and cannot compete with the tightest commercial OSN integrally skinned asymmetric membrane (Starmem™ 122) in toluene. However, after solvent post-treatment, first generation hydrophobic TFC

membranes (see Figure 21b and 21c) showed greatly increased toluene fluxes, with five times higher toluene flux than the standard TFC OSN membrane (Figure 21a), and with higher selectivity and three times higher toluene flux than the tightest commercial integrally skinned hydrophobic membrane (Starmem™ 122).

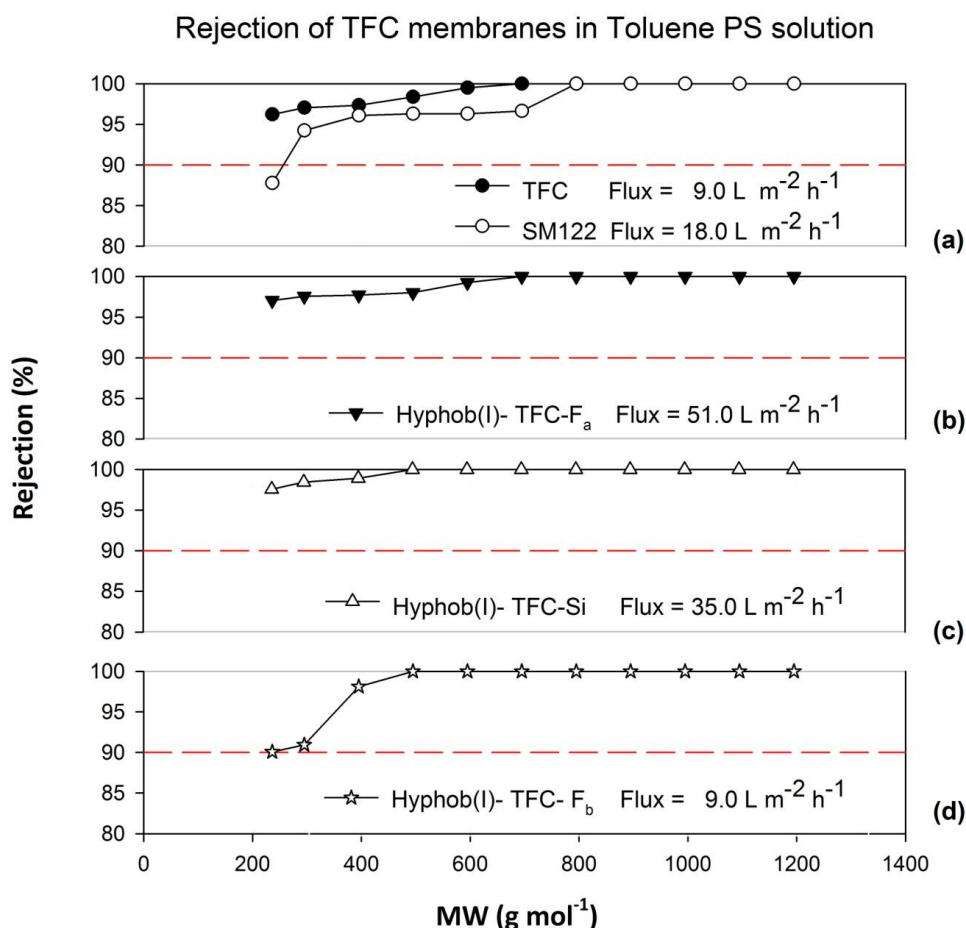


**Figure 21.** MWCO curves and fluxes of TFC membranes after treatment with DMF as an activating solvent. Nanofiltration of a feed solution comprising polystyrene oligomers dissolved in toluene has been performed at 30 bar and 30°C. (a) Comparison study between control TFC membrane and commercial integrally skinned asymmetric OSN membrane (SM 122); (b) TFC membrane capped with fluoro-alkylamine; (c) TFC membrane capped with silicone-alkylamine; (d) TFC membrane capped with fluoro-alkylacylchloride.

As shown in Figure 21b and 21c, capping the surface of TFC OSN membranes with hydrophobic monomers containing amino groups, results in significantly increased toluene fluxes, suggesting that the surface chemistry plays an important role in solvent permeation. Contact angle results show an increased hydrophobicity upon capping with hydrophobic monomers containing amino groups, suggesting that the amino groups in these monomers reacted with the free acyl chlorides that were present on the surface of the polyamide layer. The presence of F and Si on the surface of these TFC membranes was confirmed by XPS analysis. As expected, due to the heterogeneity of the polyamide layer [160], membranes capped with pentafluorooctanoyl chloride (Figure 21d) showed no increase in toluene flux, suggesting that there are not a lot of free amine groups

present on the surface of the TFC membrane that could be capped. This was further confirmed by XPS data, showing a very low percentage of F on the surface of TFC membranes capped with pentafluorooctanoyl chloride. Thus, the optimal method to render the membrane hydrophobic after the IP reaction is to cap the free acyl chloride groups with the alkylamines containing hydrophobic groups, poly[dimethylsiloxane-co-(3-aminopropyl)methylsiloxane] and (2,2,3,3,3-pentafluoropropylamine).

Figure 21 shows the performance for the first generation hydrophobic membranes in toluene. Hyphob(I)-TFC-F<sub>a</sub> shows the highest flux in toluene (50 Lm<sup>-2</sup>h<sup>-1</sup>), followed by Hyphob(I)-TFC-Si (35 Lm<sup>-2</sup>h<sup>-1</sup>), TFC and Hyphob(I)-TFC-F<sub>b</sub> have both the lowest flux (9 Lm<sup>-2</sup>h<sup>-1</sup>). Hyphob(I)-TFC-Si is tighter than the other membranes, and even with a similar contact angle than Hyphob(I)-TFC-F<sub>a</sub>, presents a lower toluene flux. This may be due to the fact that the silicone-alkylamine used for capping is bulkier than the fluoro-alkylamine, making the membrane tighter, resulting in an increase in rejection and a lower toluene flux when compared to Hyphob(I)-TFC-F<sub>a</sub>.

As expected, in Figure 22 the control TFC membrane (Figure 22a) had the highest THF flux, due to the solvent's polar aprotic nature. Hyphob(I)-TFC-Si gave the lowest flux, which is attributed to its high contact angle and also to the bulkiness of the silicone-alkylamines used for capping. Hyphob(I)-TFC-F<sub>b</sub> shows a lower THF flux than the control TFC. As confirmed by XPS, a small amount (4 %) of F was incorporated on the membrane surface, giving a higher contact angle than for the control TFC. MWCO curves show higher rejections for Hyphob(I)-TFC-F<sub>b</sub> than the control TFC, suggesting that THF flux decreased not only due to an increase in hydrophobicity, but also because the nature of the fluoro-alkylacylchloride monomer used for capping made the membrane tighter.

The MW of the solvents used for the filtration tests decreases in the order toluene>THF, while the polarity increases as follows: toluene<THF. Based on polarity, the control TFC membrane is expected to have a higher flux than the hydrophobic TFC membranes in THF, and Figure 22 confirms this prediction. Conversely, for the hydrophobic TFC OSN membranes it is expected based on polarity that toluene will have the highest flux, while due to MW the highest flux should be for THF. The viscosities of the solvents decrease as follows: toluene >THF. Toluene presents the highest viscosity and MW; however, it presents the highest flux, suggesting that in this case the solvent polarity is controlling the flux, and not the solvent MW or solvent viscosity.

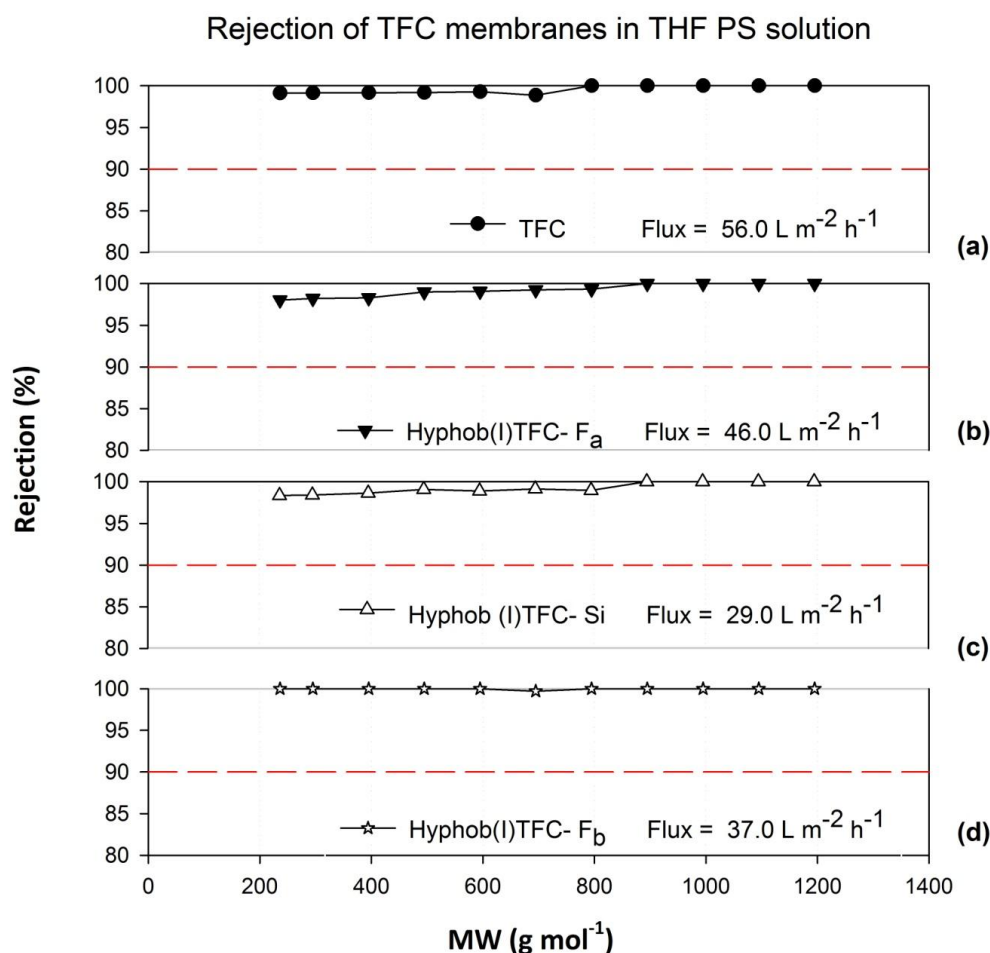


**Figure 22.** MWCO curves and fluxes of TFC membranes after treatment with DMF as an activating solvent. Nanofiltration of a feed solution comprising polystyrene oligomers dissolved in THF has been performed at 30 bar and 30°C. (a) Control TFC membrane; (b) TFC membrane capped with fluoro-alkylamine; (c) TFC membrane capped with silicone-alkylamine; (d) TFC membrane capped with fluoro-alkylacetylchloride.

#### *Capping after 3-steps IP reaction*

In order to effectively cap the surface of TFC membranes with an acyl chloride containing fluorine, due to the lack of free amines on the membrane surface, a 3-steps IP was performed first, which involves further reacting the membrane in an aqueous solution of MPD, resulting in free amine groups on the membrane surface [166]. It is also known that this 3-steps interfacial polymerization forms a thicker film composed of a “bilayer” (see Figure 20) because the third step involves again a reaction at the interface. It is believed that this increase in thickness could be a drawback in terms of permeability. The 3-steps TFC membrane was further capped with the selected fluoro-alkylacetylchloride.

Figure 23 shows the results in toluene for the control membranes (TFC and 3-steps TFC) before and after capping with fluoro-alkylacetylchlorides. As expected, Hyphob(I)-TFC-Fb shows no increase in toluene flux compared to the control TFC membrane due to the poor incorporation of F



on the membrane's surface, as confirmed by XPS. The poor capping is attributed to the lack of free amine groups on the membrane surface. Even though it shows a higher contact angle than the control TFC membrane, the control TFC-3 steps membrane shows the lowest flux, possibly due to an increase on the top layer thickness. Capping with fluoro-alkylacetylchloride after the 3steps IP reaction was successful, having the highest contact angle and the highest F content. However, for Hyphob(l)-TFC-3steps-F (Figure 23(b)) toluene flux was not as enhanced as for Hyphob(i)-TFC-Fa and Hyphob(l)-TFC-Si (Figure 21(b) and 21(c)) possibly due to an increased top layer thickness after the extra step in the IP reaction. Thus, the optimal method to render the membrane hydrophobic and increase flux was achieved by capping the free acyl chlorides after the standard IP reaction with F- and Si- alkylamines.

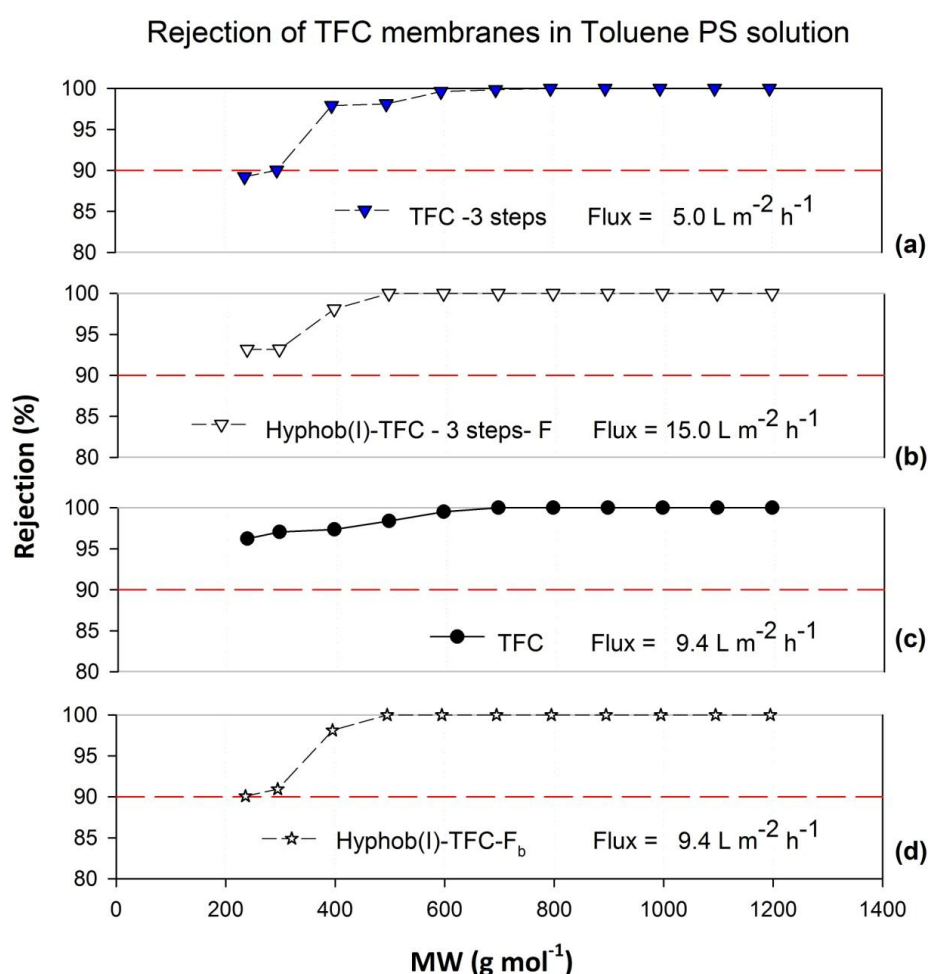


**Figure 23.** MWCO curves and fluxes of TFC membranes after treatment with DMF as an activating solvent. Nanofiltration of a feed solution comprising polystyrene oligomers dissolved in toluene has been performed at 30 bar and 30°C. (a) Control TFC membrane prepared by 3 steps IP; (b) 3-steps IP TFC membrane capped with fluoro-alkylacetylchloride; (c) Control TFC membrane; (d) TFC membrane capped with fluoro-alkylacetylchloride.

## Second generation hydrophobic membranes

It has been widely reported that changing the chemistry of the monomers participating in the interfacial polymerization reaction has an effect on the MWCO of TFC membranes [29, 30, 32, 84]. As reported in Chapter 4, it was possible to control MWCO of TFC OSN membranes by changing the type of amine. All those TFC OSN membranes (i.e. prepared with piperazine or other aliphatic amines such as hexanediamine) could, in principle, be capped in the same way as the TFC membranes in this work, creating a range of different MWCOs for hydrophobic membranes. However, instead of following the same approach, looser hydrophobic TFC membranes were developed by incorporating hydrophobic monomers during the IP reaction.

As previously reported for aqueous systems [32], TFC membranes prepared with aromatic acyl chlorides show better rejections, but lower fluxes compared to those prepared with aliphatic acyl chlorides because the latter provide higher free volumes and larger pore sizes to the thin active layer. Here, hydrophobic TFC OSN membranes with different MWCOs were developed by incorporating a hydrophobic monomer during the IP reaction, blending the TMC with a fluoro-monoacyl chloride in the organic phase, which hinders crosslinking, resulting in a more open polymer network. The effect of further capping these 2<sup>nd</sup> generation hydrophobic membranes with alkylamines containing F or Si has also been studied. It was decided to cap with alkylamines as it proved to be the most effective way to enhance solvent flux for the 1<sup>st</sup> generation hydrophobic membranes.

Figures 24 and 25 show results for the second generation hydrophobic membranes in ethyl acetate and toluene respectively. A comparison study of these membranes with the tightest commercial rubber coated membrane (S380) was performed in toluene and is shown in Figure 25. The MWCO of the commercial rubber coated membrane lies between that of Hyphob(II)-TFC and Hyphob(II)-TFC-F and shows a higher toluene flux than the aforementioned membranes, suggesting that these second generation hydrophobic membranes can compete with commercial rubber coated membranes but do not have a higher permeability than S380. The second generation hydrophobic membranes show higher MWCOs and higher fluxes than both the control TFC membrane and the first generation hydrophobic membranes. These results indicate that, as for previously reported polyamide TFC nanofiltration membranes [32], the MWCO of these new TFC OSN membranes can be adjusted by blending different acyl chlorides in the organic solution.

In both solvents, rejection increases as follows: Hyphob(II)-TFC-Si < Hyphob(II)-TFC-F < Hyphob(II)-TFC < TFC; flux increases as follows: TFC < Hyphob(II)-TFC < Hyphob(II)-TFC-F < Hyphob(II)-TFC-Si. These membranes are more open than the first generation hydrophobic

membranes, allowing the passage of polystyrene oligomers through the membrane more easily through solution diffusion. Hyphob(II)-TFC-F and -Si are more hydrophobic than Hyphob(II)-TFC and due to its hydrophobic nature, polystyrene has a higher affinity with the former membranes than with the latter, resulting in a higher solute flux that gives a lower rejection than the uncapped second generation hydrophobic membrane.

For the first generation hydrophobic membranes, the rejection remains the same. Thus, it is believed that the effect of concentration polarization at these fluxes and at this PS concentration is not significant. However, for the second generation hydrophobic membranes fluxes are higher and at this PS concentration the drop in rejection when flux increases after capping could also be due to an increase in concentration polarization. Concentration polarization could be another reason why, for the second generation membranes, the increase in flux upon capping is accompanied by a decrease in rejection.

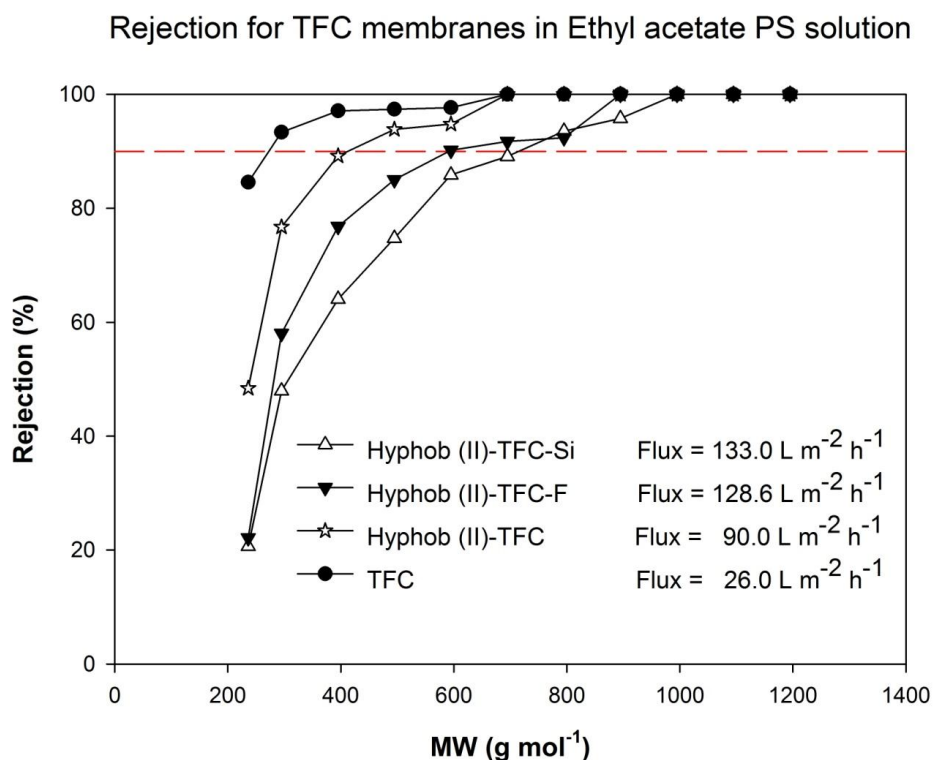


**Figure 24.** MWCO curves and fluxes of TFC membranes after treatment with DMF as an activating solvent. Nanofiltration of a feed solution comprising polystyrene oligomers dissolved in ethyl acetate has been performed at 30 bar and 30°C.

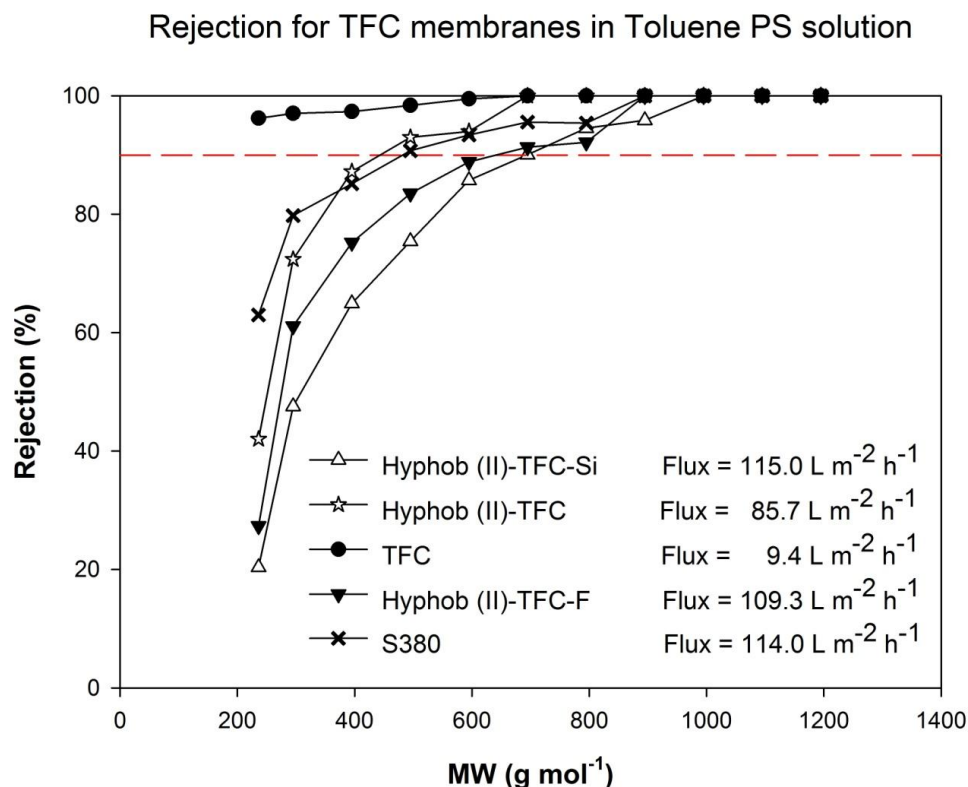


**Figure 25.** MWCO curves and fluxes of TFC membranes after treatment with DMF as an activating solvent. Nanofiltration of a feed solution comprising polystyrene oligomers dissolved in toluene has been performed at 30 bar and 30°C. Comparison study between TFC membranes and commercial rubber coated TFC OSN membranes (S380).

The MW of the solvents used for the filtration tests decreases in the order toluene > ethyl acetate, while the polarity decreases as follows: toluene > ethyl acetate (they have very similar polarity). The viscosities of the solvents decrease as follows: toluene > ethyl acetate. The top layer of the 2<sup>nd</sup> generation hydrophobic TFC membranes is hydrophobic. Thus, due to MW and viscosity it is expected that ethyl acetate will give the highest flux, and due to polarity, the highest flux will be for toluene. The polarity of these two solvents is very similar, so it is expected that MW and viscosity will be governing permeability. Ethyl acetate presents the highest flux, suggesting that in this case the MW and viscosity are controlling the flux and not the solvent polarity.

## 5.4 Conclusion

The formation of novel hydrophobic TFC OSN membranes prepared by interfacial polymerization has been demonstrated. These membranes exhibited significantly improved solvent permeabilities without sacrificing solute rejection, when compared to commercial rubber coated and hydrophobic OSN integrally skinned asymmetric membranes, and to the tight TFC OSN membrane previously developed in Chapter 4. These new membranes have been created modifying the membrane chemistry by grafting hydrophobic species on the membrane surface, or by incorporating

monomers with hydrophobic groups during the IP reaction, which greatly enhances flux for non-polar solvents.

This report is the first in which TFC membranes prepared by interfacial polymerization have been modified incorporating F and Si in the polyamide top layer to improve permeabilities in non-polar solvents. As previously reported in Chapter 4, UF supports were impregnated with PEG before the IP reaction in order to enhance solvent flux and post-treatment with an activating solvent (DMF) was necessary to activate solvent flux. This was only possible thanks to the crosslinked PI UF support.

As expected, it was not possible to change the polyamide surface properties by capping with hydrophobic acyl chlorides due to the skin layer's asymmetric nature [165]. This was only achieved after incorporating free amines on the membrane's surface. However, after successfully capping the free amines with acyl chlorides containing hydrophobic groups, flux was still not enhanced possibly due to an increased top layer thickness after the extra step in the IP reaction. Thus, the optimal method to render the membrane surface hydrophobic and increase flux was achieved by capping the free acyl chlorides after the standard IP reaction with amines containing hydrophobic groups.

Introducing hydrophobic species on the polyamide layer and solvent post-treatment enables the optimization of flux in non-polar solvents without sacrificing selectivity.

After successfully obtaining high flux hydrophilic and hydrophobic TFC OSN membranes by interfacial polymerization in chapters 4 and 5, it is intended to explore another solvent stable polymeric support with different chemical and physical properties to crosslinked PI. In the next chapter PI and PEEK supports are proposed as promising support membranes for the development of high flux hydrophilic and hydrophobic TFC OSN membranes based on porosity, pore size, chemistry, tortuosity and hydrophilicity. The next challenge is to understand and elucidate the influence of these different solvent stable supports on the overall TFC membrane performance. For this study, the tightest hydrophilic TFC membrane (prepared in chapter 4, TFC-MPD) and the tightest hydrophobic membrane with the highest flux (prepared in this chapter, Hyphob(I)-TFC-F<sub>a</sub>) will be prepared on each of the different solvent stable supports. The effects of impregnating each support with PEG before the interfacial polymerization reaction and of treating the TFC membranes with DMF as an "activating solvent" on the overall TFC membrane performance will also be studied in the following chapter.

# Chapter 6

## **Beneath the surface: Influence of supports on thin film composite membranes by interfacial polymerization for organic solvent nanofiltration**

### **Abstract**

For the development of thin film composite OSN membranes the choice of the UF support is as important as the selection of the separating layer. The support should be as smooth as possible (crucial to the formation of a defect free separating layer), and be stable in organic solvents. Other important support parameters that influence the mass transfer through the TFC membrane are porosity, tortuosity, pore size and hydrophilicity. Here, the impact of the physical-chemical properties of the support membranes on the performance of TFC membranes for OSN applications has been studied. Two different polymers; crosslinked PI and poly(ether ether ketone) (PEEK), were selected to prepare UF support membranes for the formation of TFC OSN membranes by interfacial polymerization. UF support membranes were characterized by pure water permeabilities, dextran rejections, water contact angles, mercury porosimetry, N<sub>2</sub> adsorption, and AFM. These results confirm that each support has a different skin layer pore morphology and chemistry. In this thesis, a comparison study of the effects of post-treating with an “activating solvent” and impregnating the supports with PEG on the performance of TFC membranes formed on two different supports was carried out. Polyamide and modified hydrophobic polyamide TFC membranes were formed on each of the UF supports. The impacts of each support on overall membrane performance in polar and non-polar solvents were studied and suggest that their hydrophilicity plays an important role in solvent permeation.

## 6.1 Introduction

The support membrane should give mechanical stability and should also allow the formation of a defect-free thin top layer. The properties of the support membrane are crucial for TFC membrane performance; its surface roughness and polarity determine the adhesion between both layers under filtration conditions. The thinner the top-layer, the higher the chance for the support to become rate limiting. Thus, permeability of TFC membranes can be further enhanced by decreasing the resistance of the support.

There is little information in the literature about the impact that physical-chemical properties of the support membrane have on the formation of composite membranes and resulting performance for RO and NF. Recently, Ramon et al. [169] suggested that such potential impacts may be separated into two categories: "(i) the support membrane surface chemistry and pore structure may influence the thickness, roughness, and crosslinked structure of films (especially those formed by interfacial polymerization) and (ii) for a given coating film structure, the pore size and porosity of the underlying support may contribute significantly to diffusive transport through the composite structure".

Interpenetration of the separating layer polymer into the pores of the support membrane should be avoided to prevent a decrease in flux. Top-layer intrusion can be reduced by using a support membrane with a uniform pore diameter which is small enough to avoid penetration, or by using a solvent or a non-volatile additive (e.g. glycerol) to fill the pores of the support prior to separating layer formation [27].

It has been previously proposed [148] that support membrane pore structure and chemistry (e.g. pore size, pore length, hydrophobicity, and reactivity with MPD or TMC) could influence the rate and extent of polymerization by controlling the amount of MPD reaching the reaction zone, the width of the reaction zone, and the extent to which polyamide material forms in the pores.

Singh et al. [170] studied the influence of support membrane pore size on top layer thickness for interfacially polymerized TFC membranes. Combined results of SEM surface analysis and ATR-IR surface structural analysis revealed that the surface porosity of polysulfone is an important parameter for the formation of different types of TFC membranes. Their ATR-IR studies show a two-fold thicker polyamide layer is formed when using a polysulfone support with smaller pores. They suggested that this is due to a reduced penetration of polyamide into the pores, and proposed that a polysulfone support with bigger pores, favours the penetration of diamine monomer into the pores. This in turn leads to formation of polyamide inside the pores, resulting in a

thinner top layer with higher permeability. Their conclusion for an increase in flux when using polysulfone with bigger pores only considers film thickness but does not explain why penetration of polyamide into the pores in this particular case does not have a negative effect on flux. Pore penetration is usually considered negative and is known to reduce flux.

Ghosh et al. [148] studied the properties of polyamide thin films formed by identical interfacial polymerization conditions over porous polysulfone supports with different physical and chemical properties using AFM, SEM and TEM. Hydrophilic supports produced low permeability TFC membranes, whereas relatively hydrophobic supports produced more permeable composite membranes. Their results show that a polysulfone support with pores twice as large and equally hydrophobic produced a thicker but yet more permeable polyamide top layer. They suggest that the film is thicker when using supports with bigger pores because less polyamide forms within the pores, producing an overall shorter path length for water. Their TEM observations and proposed model contradicts Singh et al.'s [170] conclusion and suggests that smaller pores make the initial MPD "eruption" less violent, allowing TMC to diffuse inside the pores, forming polyamide in the pores-creating a higher effective film thickness for water permeation.

It has been previously reported that as the top layer gets thinner, the permeability becomes more dependent on the support pore size and porosity [171]. Ramon et al. [169] explored the impacts of support membrane pore size and porosity along with coating film thickness on the apparent permeability of composite membranes, the observed flux, and the local distribution of flux through composite membranes using a model. Their results suggest that the choice of support is increasingly important as the thin film permeability increases (i.e., the film becomes less dense or thinner). They conclude that local permeate water flux through composite membranes is dictated by support membrane pore morphology, creating localized high flux "hot spots" with potentially high propensity for fouling and scaling. They propose that it is possible to fine-tune rejection and flux properties of a TFC membrane by varying support membrane skin layer porosity and pore size independently of the properties of the coating film.

A second model developed by Ramon et al. [172] suggests that transport through composite membranes is also influenced by the permeability and selectivity of the coating film; increasing coating film roughness can produce higher permeability provided that the mass of the coating film is redistributed to produce both thinner and thicker cross-sections. Making a film rougher will increase its permeability if proportional cross-sections of the film decrease in thickness to enable other cross-sections to increase in thickness. They suggest that the most promising strategy for tailoring composite membrane transport is the fabrication of support membranes with highly porous skin layers with small pores, ideally made from a material whose transport properties are



comparable to those of the thin film. However, according to their previous results [169], this might compromise rejection (in order to maximize rejection, large pores and low porosity are desirable).

Chapters 4 and 5 showed the potential for using TFC membranes prepared by IP over integrally skinned asymmetric membranes for OSN applications. In OSN, TFC membranes must be solvent stable and preserve their separation performance when in contact with organic solvents; that includes both separating layer and support membrane. Solvent stability is related to the chemical structure of the polymers and the presence of certain structural elements, such as aromatic groups, imide bonds or F-atoms. In general, copolymerization induces rigid segments which give solvent resistance [1]. In Chapter 4, it was possible to greatly increase permeability without compromising selectivity using two approaches: (a) impregnating the UF support with PEG; (b) treating the TFC membrane with an “activating solvent”, which is hypothesised to remove polyamide fragments (from the top layer) that do not contribute to separation.

In this chapter, solvent stable supports have been prepared from two polymer systems, crosslinked PI, and PEEK. The effects of these supports on the performance of TFC membranes in organic solvents is studied using approaches (a) + (b) to improve permeability. Hydrophilic and hydrophobic TFC membranes have been prepared on each support as described in Chapter 4 and Chapter 5. Hydrophilic TFC membranes were formed by IP, resulting in a polyamide top layer. To improve flux for non-polar solvents, the surface of the polyamide top layer was modified by capping the free acyl chloride groups with a fluoro-alkylamine, successfully enhancing toluene flux. The effect of using PEEK or crosslinked PI UF support membranes on the overall TFC membrane performance in polar and non-polar solvents is discussed in this chapter.

## 6.2 Experimental

### 6.2.1 Materials

Polyimide (PI) polymer (P84), all organic solvents, polyethylene glycol (MW 400), polystyrene oligomers, trimesoyl chloride (TMC), m-phenylenediamine (MPD), 1,6 hexanediamine (HDA), and 2,2,3,3,3-pentafluoropropylamine had the same purity and were purchased from the same companies described in *section 4.2.1*. Polyether ether ketone (PEEK) polymer Vicote® 704 in powder form was purchased from Victrex (Lancashire, UK), UK. Dextrans for MWCO evaluation were purchased from Sigma Aldrich. Amine MPD and acyl chloride TMC were used as monomers for the formation of the polyamide active layer. 2,2,3,3,3-pentafluoropropylamine was used for the modification of the membrane surface by capping. Distilled water and hexane were used as aqueous and organic phases, respectively.

### 6.2.2 Preparation of crosslinked PI UF support membranes

A polymer dope solution was prepared by dissolving 24 % (w/w) polyimide (P84) in DMSO or DMF. Crosslinked PI UF support membranes were prepared and conditioned following the same methodology explained in *section 4.2.2*. Some of these membranes were stored in IPA to avoid pore collapse and used for TFC membrane formation, and some other support membranes were conditioned with PEG before the interfacial polymerization reaction. Membrane identification codes for PI UF support membranes are shown in Table 10. Several membrane batches were prepared in order to evaluate repeatability (see Table 11 for repeatability analysis).

### 6.2.3 Preparation of PEEK UF support membranes

A polymer dope solution was prepared by dissolving 12.3 % (w/w) PEEK in 79.4 % methane sulfonic acid (MSA) and 8.3 % sulfuric acid ( $H_2SO_4$ ) and stirring overnight until complete dissolution. A viscous solution was formed, and allowed to stand for 10 hours to remove air bubbles. The dope solution was then cast on polyester non-woven backing using a continuous casting machine with a casting knife set at a thickness of 250  $\mu m$  located in a room held at constant temperature (21°C). Immediately after casting, the membrane was immersed in a water bath (also at 21°C) where phase inversion occurred. After 15 minutes, lengths of membrane were transferred to a fresh water bath and left for an hour. The wet membrane was then immersed in a water bath containing  $Na_2CO_3$  to avoid sulfonation and neutralize the pH. The membranes were then washed with water for 3 h and further immersed in a solvent exchange bath (isopropanol) to remove any residual water and preparation solvents. Some of these membranes were stored in water to avoid pore collapse and used for TFC membrane formation, and some other support membranes were conditioned with PEG before the interfacial polymerization reaction. Membrane identification codes for PEEK UF support membranes are shown in Table 10. Several membrane batches were prepared in order to evaluate repeatability (see Table 11 for repeatability analysis).

### 6.2.4 Preparation of polyamide thin film composite membranes

TFC membranes were hand-cast on UF support membranes (crosslinked PI and PEEK) through interfacial polymerization. TFC membranes were fabricated using both conditioned and non-conditioned support membranes to study the effect of the presence of PEG in the pores of the support on the performance of TFC membranes. The non-conditioned support membranes stored in IPA solution were rinsed with water and kept wet prior to the interfacial polymerization to avoid pore collapse. Membrane identification codes for TFC membranes are shown in Table 10. Several TFC membrane batches were prepared in order to evaluate repeatability (see Table 11 for repeatability analysis).

*Hydrophilic membranes*

These TFC membranes were prepared following the same procedure described in *section 4.2.3*. The chemical structures of the monomers used for the interfacial polymerization are shown in Scheme 3a.

*Hydrophobic membranes*

Hydrophobic TFC membranes were prepared as reported in Chapter 5. They were prepared following the same procedure described in *section 4.2.3* on both crosslinked PI and PEEK UF support membranes but with one extra capping step at the end of the process. After removing the membranes from the TMC solution, they were let dry for 10 seconds. The TFC membranes were then immersed for 1 minute in a 0.1% (w/v) 2,2,3,3,3-pentafluoropropylamine solution in hexane. The resulting membranes were withdrawn from the capping solution and rinsed with hexane, let dry and rinsed with distilled water and then stored in water at 4°C. The chemical structures of the monomers used for the capping step are shown in Scheme 3b.

**Table 10.** Membrane codes

Entry No.	Membrane	Membrane code
42	Crosslinked PI support prepared using DMSO	XP84 <sub>(DMSO)</sub>
43	Crosslinked PI support prepared using DMF	XP84 <sub>(DMF)</sub>
44	Poly(ether ether ketone) support	PEEK
45	TFC membrane prepared on crosslinked PI support without PEG	TFC-XP84
46	TFC membrane prepared on crosslinked PI support with PEG	TFC-XP84 <sub>(DMSO)</sub> -PEG
47	TFC membrane prepared on PEEK support without PEG	TFC-PEEK
48	TFC membrane prepared on PEEK support with PEG	TFC-PEEK-PEG
49	TFC membrane prepared on crosslinked PI support with PEG capped with fluoro-alkylamine	Hyphob-TFC-XP84 <sub>(DMSO)</sub> -PEG
50	TFC membrane prepared on PEEK support with PEG capped with fluoro-alkylamine	Hyphob-TFC-PEEK-PEG

**6.2.5 Treatment of TFC membranes with activating solvent**

As previously discussed in *section 5.2.4*, a treatment step was carried out on some of the composite membranes in order to further enhance solvent flux. The performance of TFC membranes with and without contacting with DMF was evaluated through filtrations using methanol, THF, and toluene. In order to evaluate repeatability several TFC membranes of each type were treated with activating solvent (see Table 11 for repeatability analysis).

## 6.2.6 Membrane Characterization

### *Contact angle*

Contact angle measurements and sample preparation were performed following the same procedure described in *section 4.2.5*. Five measurements on different membrane pieces were performed. In order to evaluate repeatability, contact angle measurements were performed on several membranes of each type (see Table 11 for repeatability analysis).

### *PEG uptake*

Five membranes of each polymer material (crosslinked PI and PEEK) were selected and two samples of each support membrane were cut into discs of equal sizes ( $19.63 \text{ cm}^2$ ); one of each was dipped into an isopropanol: PEG 2:3 solution for 16 hours, and the others were dried in the oven. The uptake of PEG was measured by weight difference per unit volume (see Table 11 for repeatability analysis).

### *Mercury Porosimetry*

As a fluid flows through the interconnected pore path in a porous material such as a UF support membrane, the flow path is tortuous in nature. Tortuosity is usually defined as the square of the ratio of actual distance travelled between two points to the minimum distance between the same two points. Mercury porosimetry measurements were performed in order to obtain the porosity and tortuosity of the UF support membranes using a Micromeritics Autopore IV Mercury Porosimeter based on the penetration of mercury into the pores under low and high pressure. The support membranes that were kept in IPA were cut into small pieces (without peeling off the non-woven backing) and dried in an oven at  $40^\circ\text{C}$  overnight before the analysis. A porosimeter penetrometer of 3mL volume was used and the characterization was carried out at room temperature. In order to evaluate repeatability, mercury porosimetry measurements were performed on two membranes of each type (see Table 11 for repeatability analysis).

### *N<sub>2</sub> adsorption analysis*

Cryogenic nitrogen adsorption experiments were used to determine the BET surface area of the support membranes using a TriStar surface area analyser (Micromeritics). Samples were dried at  $60^\circ\text{C}$  under vacuum for 2h before the analysis. In order to evaluate repeatability, N<sub>2</sub> adsorption analyses were performed on two membranes of each type (see Table 11).

### *AFM-surface roughness analysis*

AFM was performed on a Veeco AFM Dimension 3100 equipped with a DAFMLN Dimension AFM Scan Head and a Nanoscope VI controller. Samples were attached to glass slides using a double sided tape. The scans were performed in an air medium. The images were scanned in TM using silicone cantilevers having a nominal diameter of less than 10 nm. Scanning was performed at a speed of 1.3 Hz, and a scan size of 1  $\mu\text{m}$  was used for standard images. A sampling resolution of 512 points per line was selected.

Surface roughness can be presented as root-mean-square (RMS) roughness ( $R_q$ ), average roughness ( $R_a$ ), or peak-to-valley height ( $R_z$ ). In order to evaluate repeatability, the above listed roughness parameters have been estimated from at least three images of the same membrane scanned over an area of 1000 nm by 1000 nm from each sample (see Table 11 for repeatability analysis).

### *Scanning electron microscopy (SEM)*

SEM analysis of membrane surface and sample preparation were carried out as described in *section 4.3.5*.

## **6.2.7 UF support membranes performance**

UF support membrane performance was evaluated according to flux profiles and MWCO curves. All nanofiltration experiments were carried out at 2 bar using a dead-end filtration system under constant stirring in repeats of 3 (one disk of three membranes prepared the same way was tested to evaluate repeatability as shown in Table 11). The effective membrane area was 14  $\text{cm}^2$ . Permeate samples for flux measurements were collected at intervals of 1 h, and samples for rejection evaluations were taken after steady permeate flux was achieved. The MWCO was determined by interpolating from the plot of rejection against molecular weight of marker compounds, and corresponds to the molecular weight for which rejection is 90 %. Before solute rejection tests, distilled water was filtered through the membrane for an hour in order to remove any leachables. The solute rejection test was carried out using aqueous solutions of dextran with different MW (6,000, 40,000, 100,000, 200,000, and 500,000  $\text{g mol}^{-1}$ ). Dextran rejection tests were made separately for each solution of 1000 ppm (0.1 %) dextran in water, starting from the one with the highest MW. Concentrations of dextran in retentate and permeate were determined by total organic carbon (TOC) analysis. In all rejection figures where an error bar is not shown, the rejection of the tested membranes was reproducible and overlaps.

### 6.2.8 TFC membranes performance

Membrane performance was evaluated according to flux profiles and molecular weight cut off (MWCO) curves following the procedure described in *section 4.2.6*. The solute rejection test was carried out using the homologous standard feed solution comprised of a mixture of styrene oligomers described in *section 4.2.6*; analysis of styrene oligomers was carried out as previously described. The solvents used were THF, toluene and ethyl acetate.

TFC membrane performance was evaluated according to flux profiles and MWCO curves. All nanofiltration experiments were carried out at 30 bar using a cross-flow filtration system in repeats of 8 (two disks per membrane of four different membranes prepared the same way were tested to evaluate repeatability as shown in Table 11). TFC membranes were compared with commercial Duramem® and Starmem® membranes (DM150, SM122). Two discs of each commercial membrane were tested to evaluate repeatability. In all rejection figures where an error bar is not shown, the rejection of the tested membranes was reproducible and overlaps.

**Table 11.** Repeatability analysis

Test	Membrane	Number of membrane batches	Number of samples of each batch tested
Contact Angle	XP84 <sub>(DMSO)</sub> without PEG	2	5
	XP84 <sub>(DMSO)</sub> with PEG	2	5
	PEEK without PEG	2	5
	PEEK with PEG	2	5
Mercury porosimetry	XP84 <sub>(DMSO)</sub>	2	1
	XP84 <sub>(DMF)</sub>	2	1
	PEEK	2	1
N <sub>2</sub> adsorption	XP84 <sub>(DMSO)</sub>	2	1
	XP84 <sub>(DMF)</sub>	2	1
	PEEK	2	1
PEG uptake	XP84 <sub>(DMSO)</sub>	5	2
	PEEK	5	2
SEM	XP84 <sub>(DMSO)</sub> [cross-section]	2	2
	XP84 <sub>(DMF)</sub> [cross-section]	2	2
	PEEK [cross-section]	2	2
	TFC	2	2
	TFC	2	2
	TFC	2	2
AFM	XP84 <sub>(DMSO)</sub> without PEG	2	3
	XP84 <sub>(DMSO)</sub> with PEG	2	3
	PEEK without PEG	2	3
	PEEK with PEG	2	3
UF support membranes performance	XP84 <sub>(DMSO)</sub>	3	1
	PEEK	3	1
TFC membranes performance	TFC-XP84	4	2
	TFC-XP84-PEG	4	2
	TFC-PEEK	4	2
	TFC-PEEK-PEG	4	2
	Hyphob-TFC-XP84-PEG	4	2
	Hyphob-TFC-PEEK-PEG	4	2

## 6.3 Results and discussion

### UF support membranes

#### 6.3.1 PEG uptake, mercury porosimetry and BET analyses

As shown in Table 12, PEEK has a higher PEG uptake than XP84, suggesting that PEEK possesses a higher porosity. However, Table 13 shows a higher porosity for XP84 membranes prepared from both DMSO and DMF. For mercury porosimetry and BET surface area analysis, samples need to be dried for 2 h at 60°C without PEG, which collapses the pores of the support. This technique is good when comparing the same polymer material as it is expected to collapse in a similar way. For the PEG uptake studies, the membranes are impregnated wet and the pores of the support do not collapse. Thus, PEG uptake data is more reliable for porosity measurements, suggesting that the PEEK support membrane possesses the highest porosity.

XP84 support membranes prepared using DMSO or DMF as solvents are made from the same polymer. Thus, BET and Hg porosimetry can be used as reliable methods to compare their morphology. In Table 13 the XP84<sub>(DMF)</sub> UF membrane, prepared using DMF as a solvent, has a lower BET surface area, lower porosity and almost three times higher tortuosity than the XP84<sub>(DMSO)</sub> UF membrane, prepared using DMSO as the solvent. It has been previously reported that PI UF membranes prepared with DMSO as the solvent present a sponge-like structure [173]. The gelation point for the PI/DMSO/water system is very close to the binodal curve. Thus, the phase separation process stops almost instantaneously and the membrane morphology is determined at the gelation line. As a result, the polymer-lean phase does not have enough time to grow macrovoids, resulting in a macrovoid-free, sponge-like membrane, which gives higher porosity and a less tortuous path for a given solvent to permeate through. These results corroborate a higher porosity and lower tortuosity for the XP84 membrane prepared using DMSO. Thus, DMSO has been selected as the solvent to prepare XP84 UF support membranes for the preparation of TFC membranes. PEEK seems also a promising UF OSN support for the formation of TFC OSN membranes, as it presents a low tortuosity and is highly porous.

**Table 12.** PEG uptake

Entry No.	Support	Area (cm <sup>2</sup> )	Thickness (µm)	Volume (cm <sup>3</sup> )	Weight without PEG (g)	Weight with PEG (g)	PEG uptake (g.m <sup>-3</sup> )
51	XP84 <sub>(DMSO)-1</sub>	19.63	288	0.565	0.288 ± 0.0041	0.513 ± 0.0066	3.971 × 10 <sup>5</sup>
	XP84 <sub>(DMSO)-2</sub>	19.63	288	0.565	0.288 ± 0.0036	0.511 ± 0.0029	3.943 × 10 <sup>5</sup>
	XP84 <sub>(DMSO) Av.*</sub>	19.63	288	0.565	0.287 ± 0.0033	0.512 ± 0.0049	3.972 × 10 <sup>5</sup>
	PEEK <sub>1</sub>	19.63	341	0.679	0.252 ± 0.0003	0.632 ± 0.0114	5.604 × 10 <sup>5</sup>
	PEEK <sub>2</sub>	19.63	341	0.679	0.249 ± 0.0043	0.625 ± 0.0135	5.540 × 10 <sup>5</sup>
	PEEK <sub>Av.*</sub>	19.63	341	0.679	0.250 ± 0.0036	0.623 ± 0.0176	5.501 × 10 <sup>5</sup>

Av.\* is the average of five membrane batches.

**Table 13.** Mercury porosimetry <sup>a</sup> and N<sub>2</sub> adsorption <sup>b</sup> results

Entry No.	Support	BET surface area <sup>b</sup> (m <sup>2</sup> /g)	% Porosity <sup>a</sup> (Hg)	Tortuosity <sup>a</sup>
53	XP84 <sub>(DMF)</sub>	11.26 ± 0.76	45.77 ± 0.28	72.10 ± 0.53
54	XP84 <sub>(DMSO)</sub>	16.97 ± 0.60	56.20 ± 0.48	27.60 ± 0.42
55	PEEK	11.51 ± 0.34	42.57 ± 0.23	25.26 ± 0.39

### 6.3.2 UF membranes performance

The performance of PEEK support membranes and XP84 support membranes prepared using DMSO as a solvent have been compared. As shown in Figure 26, PEEK exhibits the lowest MWCO (25,000 g mol<sup>-1</sup>) and XP84<sub>(DMSO)</sub> the highest (500,000 g mol<sup>-1</sup>). PEEK has a higher contact angle than XP84<sub>(DMSO)</sub> (see Table 14). Thus, considering MWCO and polarity it is expected that the highest water flux will be for the XP84<sub>(DMSO)</sub> support. However, in Figure 27 flux for PEEK is only slightly lower than for XP84<sub>(DMSO)</sub>, suggesting that porosity of the support also has an impact on flux. PEG uptake studies (see Table 12) show that PEEK is more porous than XP84<sub>(DMSO)</sub>, which explains why PEEK, having a lower MWCO and a higher contact angle than XP84<sub>(DMSO)</sub>, has only slightly lower flux than XP84<sub>(DMSO)</sub>.

**Table 14.** Contact angle of UF supports with and without PEG

Entry No.	Support	Contact Angle (°)
56	XP84 <sub>(DMSO)</sub> without PEG	39 ± 2
57	XP84 <sub>(DMSO)</sub> with PEG	31 ± 3
58	PEEK without PEG	74 ± 2
59	PEEK with PEG	39 ± 3



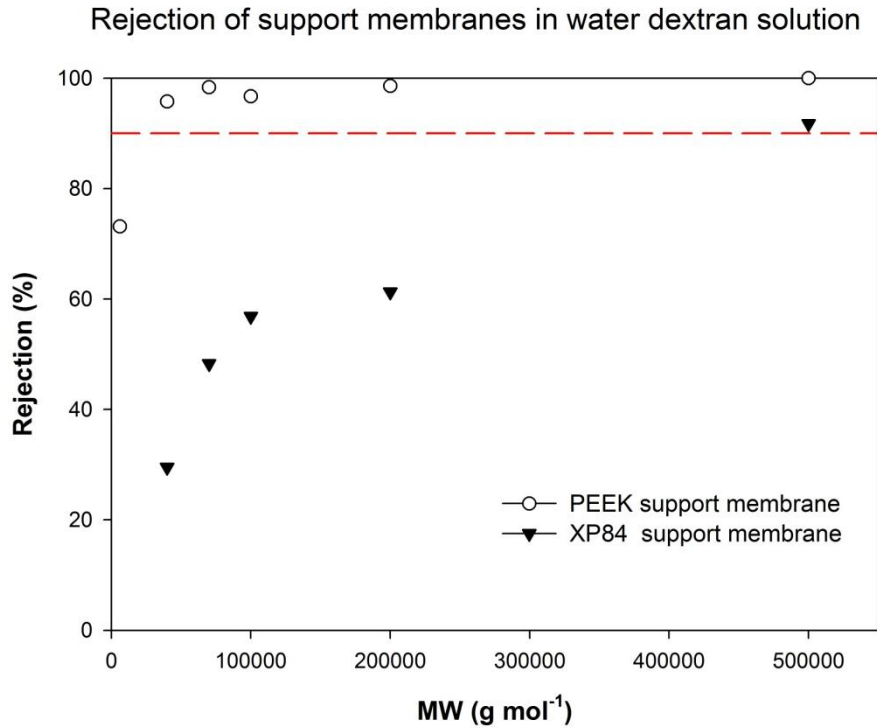


**Figure 26.** MWCO curves of crosslinked polyimide (XP84<sub>(DMSO)</sub>) and poly(ether ether ketone) (PEEK) UF support membranes. Filtration of feed solutions comprising dextran dissolved in water has been performed at 2 bar and 25°C.

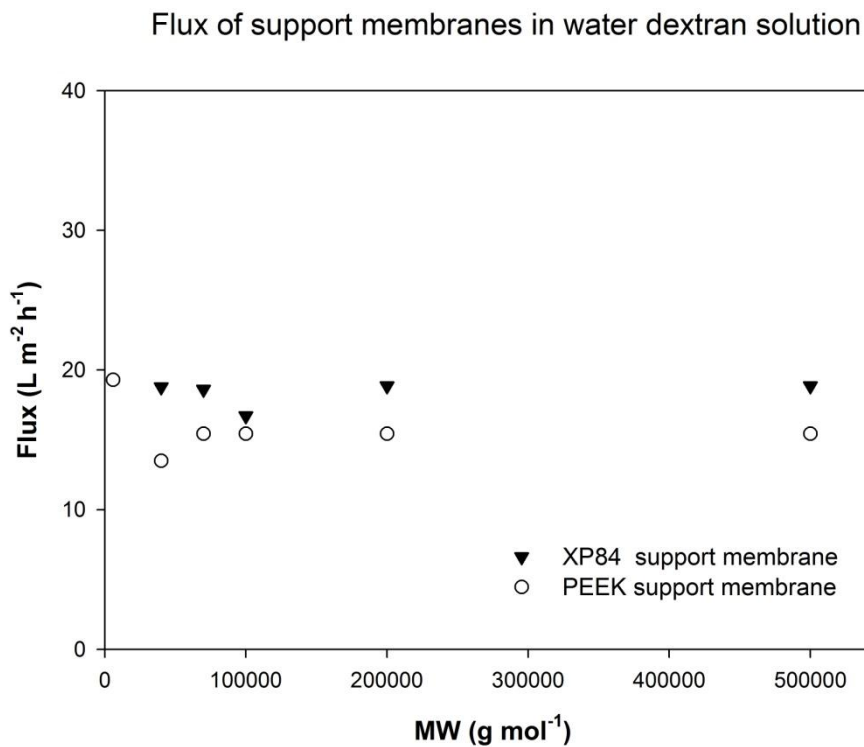


**Figure 27.** Flux curves of crosslinked polyimide (XP84<sub>(DMSO)</sub>) and poly(ether ether ketone) (PEEK) UF support membranes. Filtration of feed solutions comprising dextran dissolved in water has been performed at 2 bar and 25°C.

## 6.3.3 AFM-surface roughness analysis

Table 15. A quantitative summary of surface roughness

Entry No.	Support	RMS roughness $R_q$ (nm)	Average roughness $R_a$ (nm)	Peak-to-valley height $R_z$ (nm)
60	XP84 without PEG	$4.5 \pm 0.5$	$3.3 \pm 0.3$	$39.8 \pm 6.1$
61	XP84 with PEG	$3.0 \pm 0.2$	$2.4 \pm 0.1$	$26.0 \pm 5.8$
62	PEEK without PEG	$3.2 \pm 0.7$	$2.5 \pm 0.5$	$34.9 \pm 2.1$
63	PEEK with PEG	$1.2 \pm 0.1$	$0.9 \pm 0.0$	$12.0 \pm 1.0$

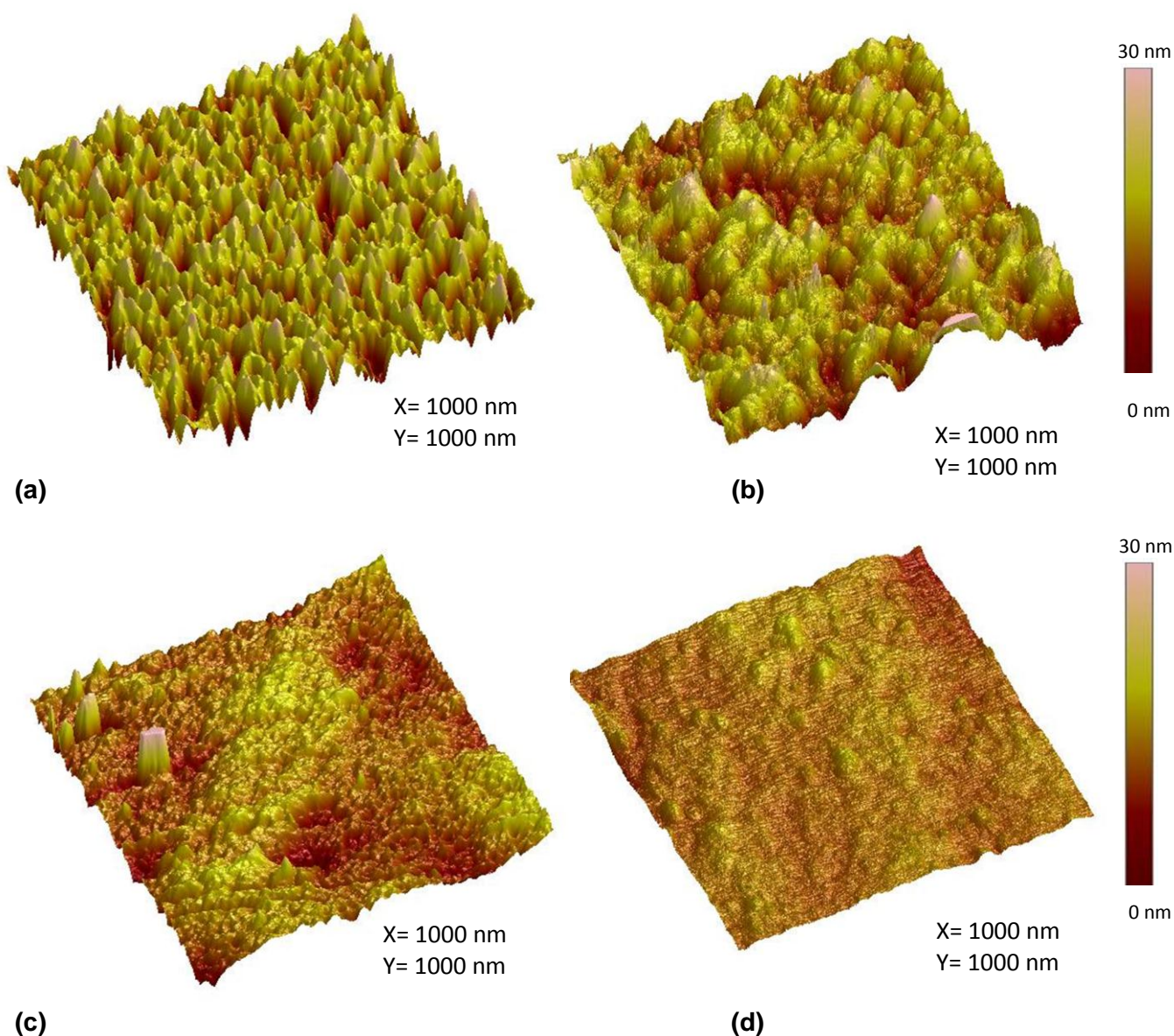


**Figure 28.** AFM topographical images of UF support membranes revealing changes in surface roughness: (a) XP84<sub>(DMSO)</sub> membrane without PEG, (b) XP84<sub>(DMSO)</sub> membrane with PEG, (c) PEEK membrane without PEG, (d) PEEK membrane with PEG.

The properties of the support membrane are crucial for the performance of TFC membranes; low surface roughness is crucial to allow the formation of the top layer without defects. The surface roughness and polarity of the support determine the adhesion between both layers under filtration conditions. Roughness parameters from at least three images of the same membrane were determined for each UF support. As shown in Table 15, adding PEG into the pores of the support makes the surface of both UF support membranes smoother (lower surface roughness), decreasing the likelihood of defects during the formation of the top layer. In this chapter, the effect that impregnating both UF supports with PEG has on the performance of TFC membranes in terms of flux and rejection has been further studied.

## TFC membranes

### 6.3.4 Contact angle

In Chapter 4, it has been observed that adding PEG into the pores of the support (XP84 in particular) prior to interfacial polymerisation results in an increase in flux without compromising rejection. It is believed that MPD diffuses more slowly to the organic interface due to interactions with PEG, resulting in a thinner separation layer. In order to understand this further, the changes in contact angle with and without PEG were measured for the two different supports (UF XP84<sub>(DMSO)</sub> and PEEK), and the average values recorded in Table 14. The UF support membranes impregnated with PEG have a lower contact angle, suggesting that PEG is making the membranes more hydrophilic, which will enhance wetting of the support with the aqueous amine solution.

### 6.3.5 TFC membranes performance and characterization

#### *Treatment with DMF as “activating solvent”*

The impacts of post-treating the TFC membranes with a solvent with similar Hildebrand solubility parameter to the polyamide top layer ( $23 \text{ (MPa)}^{1/2}$ ) were studied.

Figure 29 (a) and (b) shows that for TFC-XP84 membranes with non-PEG impregnated supports, methanol flux after post-treatment with DMF is approximately three times higher than without solvent treatment. These membranes show similar rejection curves for polystyrene markers. The values of Hildebrand solubility parameters for DMF and polyamide (MPD-TMC) are  $24.8 \text{ MPa}^{1/2}$  and  $23 \text{ MPa}^{1/2}$  respectively [158], which suggests that DMF is a swelling agent for the polyamide. Thus, as discussed in Chapter 4, it is believed that treating TFC-XP84 membranes with DMF removes some of the loose polyamide polymer fragments, allowing access to the selective layer more rapidly without affecting the UF support, resulting in dramatically enhanced fluxes without

compromising rejection. As explained in Chapter 4, due to the hydrophilic nature of the XP84 support, the surface of the TFC-XP84 membrane presents a nodular structure. The surface morphologies of TFC-XP84 membranes before and after exposure to DMF are different (see SEM images in Figures 30(a) and 31(a)). The density of the polymer on the surface decreases after DMF treatment; there are fewer nodules per unit area, suggesting that there has been a significant amount of loose polyamide fragments removed from the surface.

Figure 32 (a) and (b) shows that TFC-PEEK membranes without PEG impregnated supports show THF flux even without solvent treatment. After DMF treatment, THF flux is not enhanced. These membranes show similar rejection curves for polystyrene markers. The degree of crosslinking of the polyamide film depends on diverse factors including the chemistry and pore size of the support, which have an impact on the diffusion of amine to the organic phase. It is possible that due to the different polarity, chemistry, porosity and pore size of PEEK support membranes, there are fewer loose polyamide fragments on the surface of the TFC membrane and THF flux is not enhanced upon treating with DMF as an “activating solvent”. According to Ghosh et al. [148], large skin layer pores produce thicker, more permeable top layers because less polyamide forms within the pores. PEEK has smaller pores than XP84<sub>(DMSO)</sub>, suggesting that PEEK produces thinner, less permeable polyamide top layers because more polyamide forms within the pores. PEEK is also hydrophobic, which makes the diffusion of the MPD faster as there is no interaction between the amine and the support, forming the typical ridge and valley structure for the polyamide layer as shown in Figure 30(c). In supports with smaller pores, the amine comes out of the pores slower, making the film formation process slower. However, for the PEEK support, once the amine has come out of the pores, it will diffuse readily as it does not interact with PEEK. This could result in smaller amounts of loose polyamide fragments precipitating on the membrane surface, which may suggest why there is flux without solvent activation and no change in flux after treating the TFC-PEEK membrane with DMF. The surface morphologies of TFC-PEEK membranes before and after exposure to DMF are very similar (see SEM images in Figures 30(c) and 31(c)). The density of polymer on the surface remains the same in both images, suggesting that treatment with DMF was unnecessary as no loose polyamide fragments were present in the membrane surface.

#### *Impregnating with PEG*

The performance of TFC membranes prepared with XP84 supports with and without PEG in the pores, using MeOH as a solvent, is compared in Figure 29 (a) and (c). As discussed in Chapter 4, the results show that impregnating the XP84 support with PEG prior to the interfacial polymerization reaction results in an increase in MeOH flux without compromising rejection. As seen in Table 14, as well as protecting the pores of the support PEG also makes it more hydrophilic, evidenced by the lower contact angle. The thickness of the top layer depends on

diverse factors including reaction time, concentration of the monomers, the chemistry and pore size of the support and the diffusion of amine to the organic phase. It is known that the diffusion rate of MPD from inside the pore structure to the membrane interface is certainly affected by the presence of PEG [148], and some of the MPD inside the pores may interact with PEG through hydrogen bonding. It has been suggested in Chapter 4 that MPD diffuses more slowly to the organic phase when PEG is present in the pores of the XP84 support, resulting in a thinner top layer. The SEM image of the TFC membrane surface in Figure 30(b) shows that the presence of PEG in the pores of XP84 support results in a higher density of nodules with similar size compared to the surface of the TFC membrane prepared on XP84 without PEG in the pores (see Figure 30(a)).

Figure 32 (a) and (c) shows that impregnating the PEEK support with PEG prior to the interfacial polymerization reaction results in a slight decrease in flux. It is believed that the PEG in the pores interacts with MPD through hydrogen bonding, affecting the diffusion of the amine into the organic phase, and resulting in a thinner top layer, which should enhance permeability. However, flux remains almost the same with than without impregnating with PEG and is not enhanced as for the case of XP84.

To explain the discrepancy on the effect of PEG impregnation on TFC membrane performance, the following is suggested. For XP84, the TFC membrane presents loose polyamide fragments when it is formed on both PEG impregnated and non-impregnated supports. PEG interacts with MPD, affecting the diffusion of the amine to the organic phase, resulting in a thinner top layer, and therefore, a higher flux. On the other hand, for the case of PEEK, it is believed that the TFC-PEEK membrane does not present loose polyamide fragments when it is formed on non-impregnated support. When PEG is in the pores of the PEEK support, the MPD diffuses more slowly to the organic phase due to hydrogen bond interactions with PEG, resulting in a thinner top layer. Due to the slow diffusion of the amine and small pore size of the support, it is proposed that the thinner film that is formed is accompanied by precipitation of loose polyamide fragments. Thus, flux remains almost the same and is not enhanced.

#### *Combining PEG impregnation + DMF post-treatment*

Results in Figures 29 and 32 show that combining both approaches, i.e. impregnating the UF support with PEG as well as post-treating the TFC membranes with DMF, gives the TFC-XP84 and TFC-PEEK membranes with the highest flux. These results support the theory proposed in this work and suggest that when the supports are impregnated with PEG, thinner films are formed accompanied by precipitation of loose polyamide fragments. Upon DMF treatment, these fragments are dissolved, which possibly makes the film thinner, resulting in a dramatically

increased permeability for both TFC-XP84 and TFC-PEEK membranes. Given this data for PEG impregnation + DMF treatment, subsequent membrane performance studies comparing the performance of hydrophilic and hydrophobic TFC membranes in different solvents, with PEEK or XP84 as support membranes, have all used PEG-impregnated UF supports and have all been post-treated with DMF as an activating solvent.

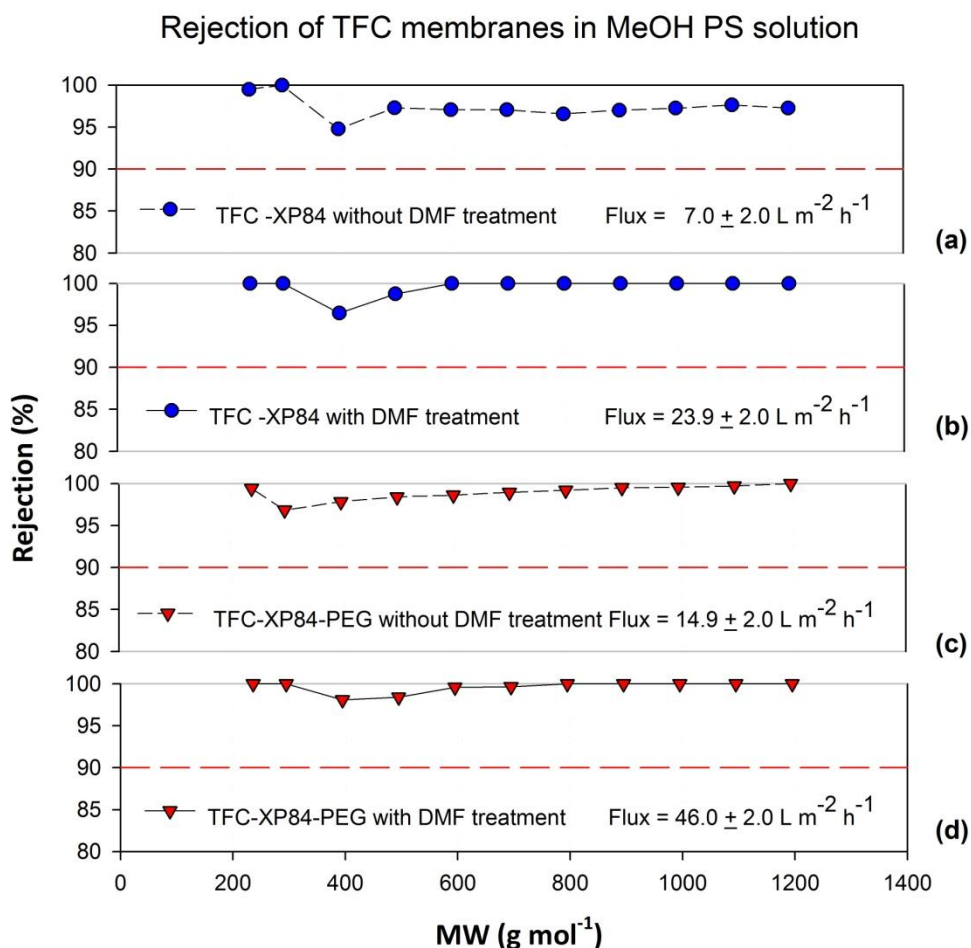
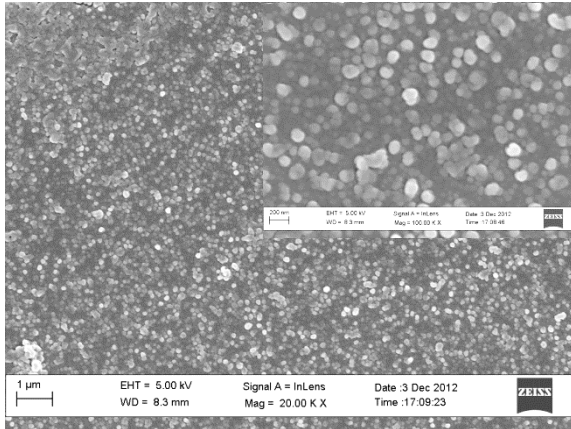
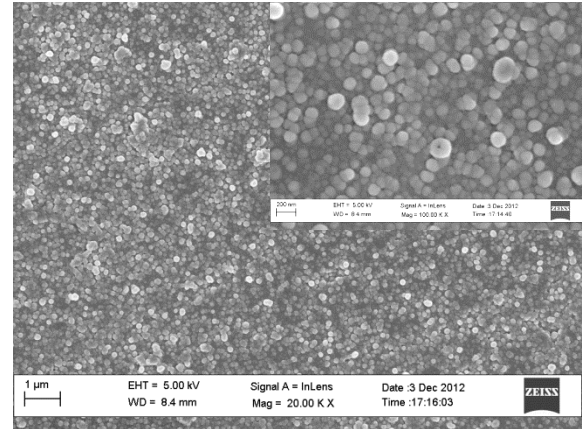


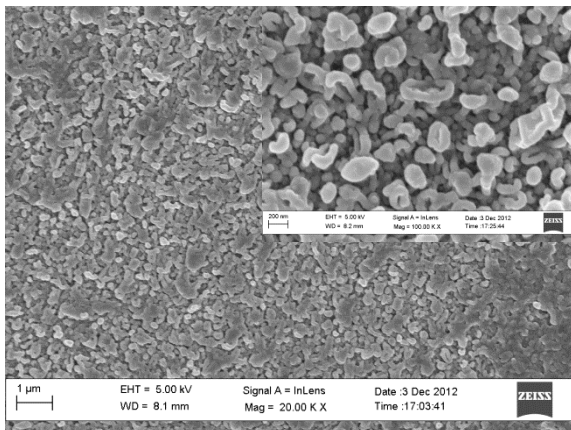
**Figure 29.** The data shown here has been reproduced from Figure 11 for convenience of comparison. MWCO curves and fluxes of TFC membranes prepared on a crosslinked polyimide support membrane with and without PEG as conditioning agent, and with and without post-treatment with DMF as an activating solvent. Nanofiltration of a feed solution comprising polystyrene oligomers dissolved in methanol has been performed at 30 bar and 30°C. (a) No PEG, no activating solvent treatment; (b) No PEG, with activating solvent treatment; (c) With PEG, no activating solvent treatment; (d) With PEG, with activating solvent treatment.



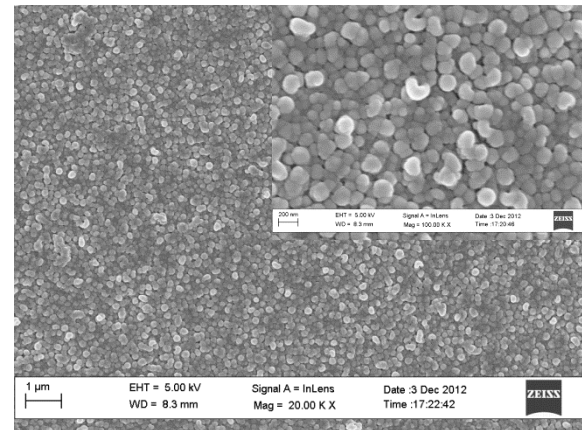
(a)



(b)

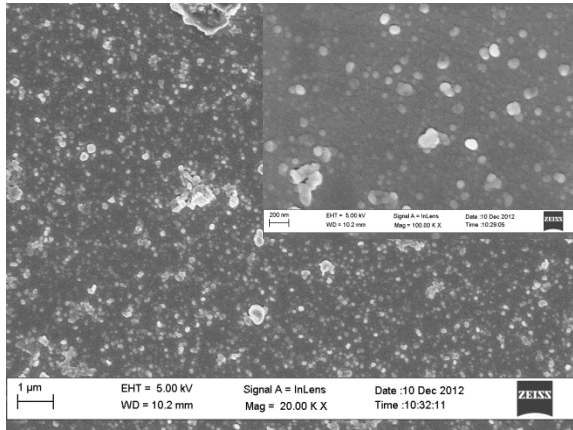


(c)

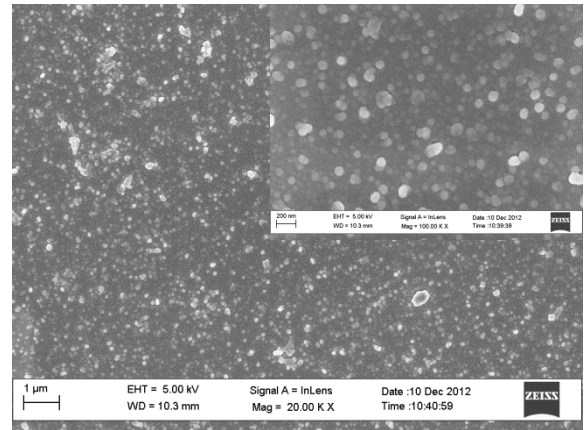


(d)

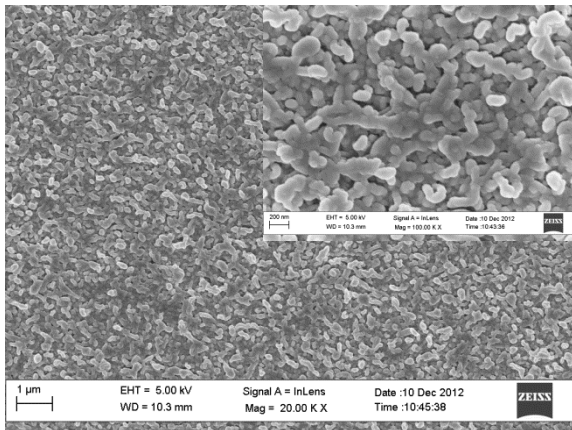
**Figure 30.** SEM images of TFC membranes revealing changes in surface morphology: (a) TFC membrane prepared on XP84<sub>(DMSO)</sub> without PEG, (b) TFC membrane prepared on XP84<sub>(DMSO)</sub> with PEG, (c) TFC membrane prepared on PEEK without PEG, (d) TFC membrane prepared on PEEK with PEG.



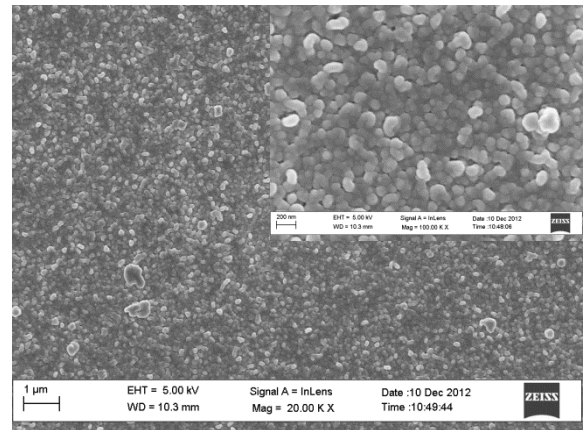
(a)



(b)



(c)



(d)

**Figure 31.** SEM images of TFC membranes revealing changes in surface morphology: (a) TFC membrane prepared on XP84<sub>(DMSO)</sub> without PEG post-treated with DMF, (b) TFC membrane prepared on XP84<sub>(DMSO)</sub> with PEG post-treated with DMF, (c) TFC membrane prepared on PEEK without PEG post-treated with DMF, (d) TFC membrane prepared on PEEK with PEG post-treated with DMF. Post-treatment was done by immersion in DMF for 10 min.



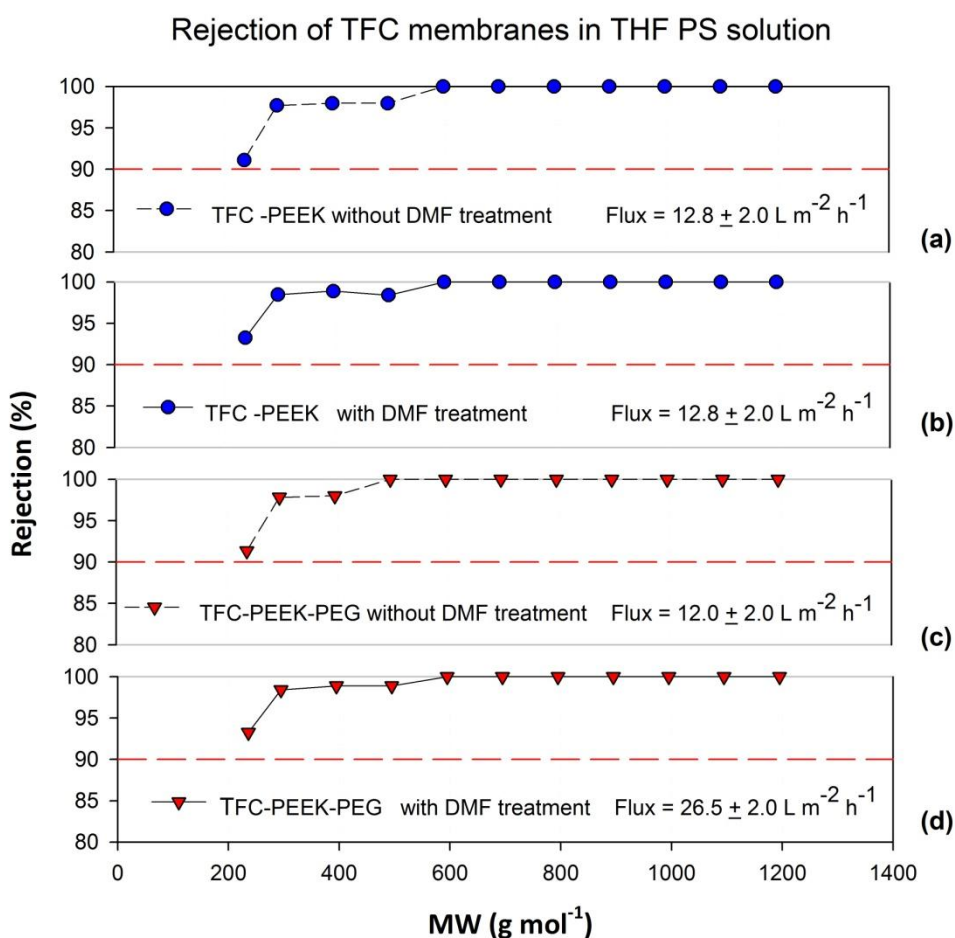


**Figure 32.** MWCO curves and fluxes of TFC membranes prepared on a poly (ether ether ketone) (PEEK) support membrane with and without PEG as conditioning agent, and with and without post-treatment with DMF as an activating solvent. Nanofiltration of a feed solution comprising polystyrene oligomers dissolved in methanol has been performed at 30 bar and 30°C. (a) No PEG, no activating solvent treatment; (b) No PEG, with activating solvent treatment; (c) With PEG, no activating solvent treatment; (d) With PEG, with activating solvent treatment.

### 6.3.6 Impacts of support on permeability for hydrophilic and hydrophobic TFC membranes

One of the drawbacks of the TFC OSN membranes prepared by IP in Chapter 4 is their poor flux in non-polar solvents. Due to the hydrophilic nature of their polyamide top layer, THF flux (see Figure 33(a)) is much more enhanced than toluene flux (see Figure 34a) and hydrophilic TFC membranes cannot compete with the tightest commercial OSN integrally skinned asymmetric membrane (Starmem™ 122) in toluene (see Figure 34(a)). However, Chapter 5 shows that capping the surface of TFC OSN membranes with a fluoro alkylamine, results in significantly increased toluene fluxes, suggesting that the surface chemistry plays an important role in solvent permeation. As well as the chemistry of the top layer, the chemistry of what lies beneath the surface should have an impact on solvent flux. This work seeks to study whether the chemistry of the support membrane plays an important role in the permeation of polar and non-polar solvents in TFC membranes. Both hydrophilic and hydrophobic TFC membranes were prepared on each UF

support membrane (PEEK and XP84) to compare their performance in a polar and a non-polar solvent (THF and toluene, respectively).

The performance of hydrophilic TFC membranes prepared with XP84 or PEEK supports, using THF as a solvent, is compared in Figure 33(a). These hydrophilic TFC membranes have much higher THF flux than the tightest commercial integrally skinned hydrophilic membrane (Duramem® 150, see Figure 33(b)). These results show that TFC-XP84 has a higher THF flux than TFC-PEEK. PEEK has a higher contact angle than XP84, making it more hydrophobic (see Table 14). As THF is a polar aprotic solvent, hydrophilic supports are expected to have higher THF flux than more hydrophobic supports. Thus, the optimal support membrane for the formation of hydrophilic TFC membranes to achieve the best permeability for polar solvents, such as THF, is XP84 support.

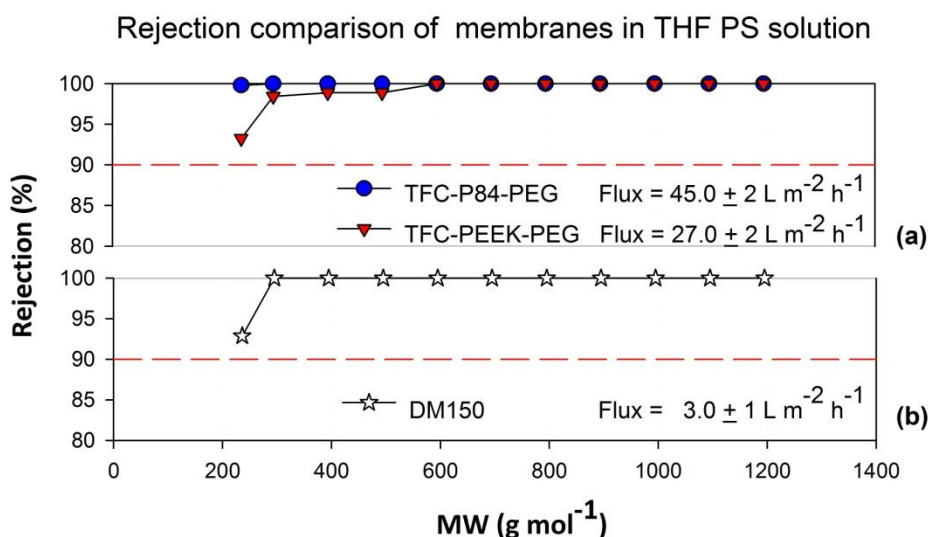


**Figure 33.** Comparison MWCO curves and fluxes of commercial membrane Duramem® 150 and TFC membranes prepared on either a poly (ether ether ketone) (PEEK) or a crosslinked polyimide support membrane impregnated with PEG as conditioning agent, and with post-treatment using DMF as an activating solvent. Nanofiltration of a feed solution comprising polystyrene oligomers dissolved in THF has been performed at 30 bar and 30°C.

Figure 34 (b) and (c) shows a comparison of the performance of hydrophobic TFC membranes prepared with XP84 or PEEK supports, using toluene as a solvent. These hydrophobic TFC membranes have three times higher toluene flux than the tightest commercial integrally skinned hydrophobic membrane (Starmem™ 122, see Figure 34(a) and more than six times higher toluene flux than the hydrophilic TFC-XP84 membrane (see Figure 34(a)). These results show that TFC-PEEK has a higher toluene flux than TFC-XP84. PEEK has a higher contact angle than XP84, making it more hydrophobic (see Table 14). As toluene is a non-polar solvent, hydrophobic supports are expected to have higher toluene flux than more hydrophilic supports. Thus, the

optimal support membrane for the formation of hydrophobic TFC membranes to achieve the best permeability for non-polar solvents, such as toluene, is a PEEK support. The hydrophilicity of the UF support membrane plays an important role on solvent permeation, enabling the optimization of flux in polar and non-polar solvents without sacrificing selectivity.

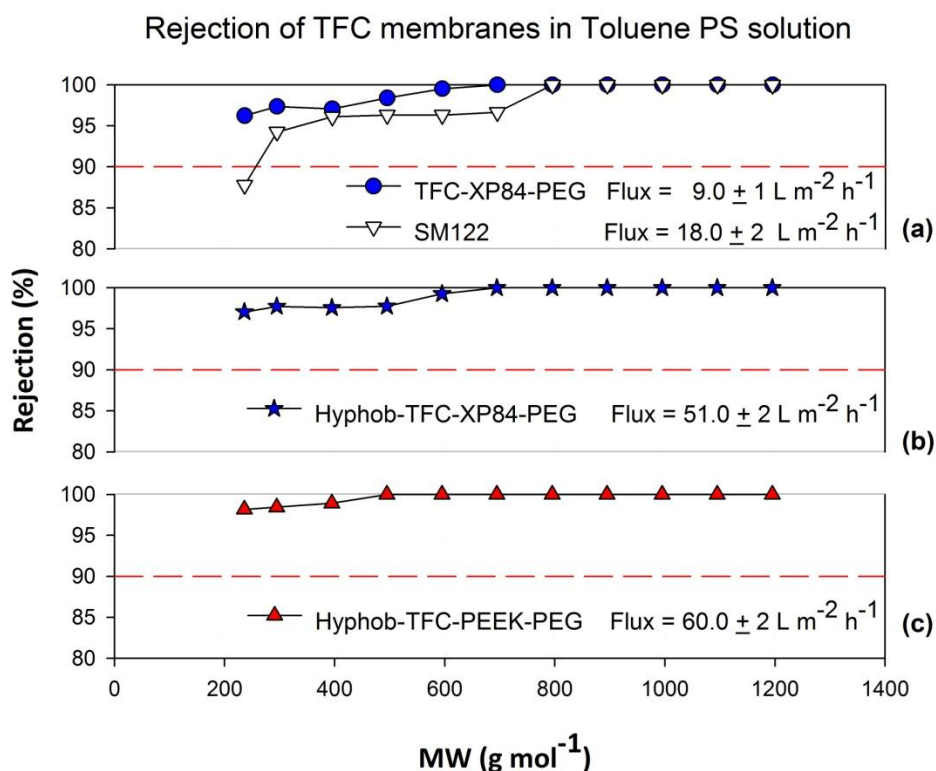


**Figure 34.** Comparison MWCO curves and fluxes of commercial membrane Starmem™ 122 and hydrophobic TFC membranes prepared on either a poly (ether ether ketone) (PEEK) or a crosslinked polyimide support membrane impregnated with PEG as conditioning agent, and with post-treatment using DMF as an activating solvent. Nanofiltration of a feed solution comprising polystyrene oligomers dissolved in toluene has been performed at 30 bar and 30°C.

## 6.4. Conclusion

The formation of TFC OSN membranes prepared by interfacial polymerization on both XP84 and PEEK solvent stable support membranes has been demonstrated. This report is the first in which PEEK has been used as a UF support for the formation of TFC membranes by IP.

For each support, two different effects were studied: (i) adding PEG into the pores of the support, and (ii) treating the TFC membranes with DMF, on the overall membrane performance. It was not possible to enhance solvent flux for TFC-PEEK membranes using each of the aforementioned techniques individually. Flux enhancement for TFC-PEEK membranes was only achieved after combining both techniques, i.e. impregnating the UF support with PEG as well as post-treating the membrane with DMF. For TFC-XP84 membranes each strategy resulted in an increased

permeability without compromising rejection. The results show that combining both approaches gives the TFC-XP84 membrane with the highest flux. Thus, the optimal method to increase permeability without compromising rejection using these two UF support membranes was achieved by combining both strategies.

One of the current challenges for OSN membranes is to improve permeability in non-polar solvents (e.g. hexane, heptane). Hydrophobic TFC OSN membranes via IP were prepared following the method described in Chapter 5. Hydrophilic and hydrophobic TFC membranes were formed on two chemically different solvent stable supports (PEEK and XP84<sub>(DMSO)</sub>). These membranes exhibited significantly improved solvent permeabilities without sacrificing solute rejection, when compared to commercial OSN integrally skinned asymmetric membranes. TFC-XP84-PEG had higher selectivity and 15 times higher THF flux than DM150 and Hyphob-TFC-PEEK-PEG had higher selectivity and 3 times higher toluene flux than SM122. The impacts of each support on the overall TFC membrane performance in polar and non-polar solvents were studied and suggest that their hydrophilicity plays an important role on solvent permeation. Introducing hydrophilic or hydrophobic solvent stable polymeric materials as support membranes enables the optimization of flux in polar and non-polar solvents without sacrificing selectivity. Thus, understanding and carefully selecting the support membrane for developing TFC membranes for a specific solvent system will improve the overall membrane performance in OSN. PEEK and XP84 supports introduce new degrees of freedom in membrane fabrication due to their remarkable solvent stability.

Once the formation of these high flux hydrophobic and hydrophilic TFC OSN membranes on two different solvent stable supports has been optimized, the next challenge is to use these supports for the formation of ultra high flux TFC membranes for OSN applications. This will also avoid the use of an activating solvent, which will make the membrane fabrication process more viable. A solution would be to make the top layer using advanced polymers possessing high nanoporosity. As mentioned in chapter 2, TFC OSN membranes composed of a top layer made of a linear polymer with intrinsic microporosity (PIMs) by dip-coating showed extremely high permeability in organic solvents without loss in porosity. The drawback is that these membranes have to be chemically crosslinked to ensure solvent stability and with the dip-coating technique very thin films cannot be obtained. The aim of this work is to understand, elucidate and develop TFC-PIMs membranes by interfacial polymerization to achieve a very thin top layer and form a crosslinked network PIM polymer *in situ* on two different solvent stable supports. This work will be discussed in the following chapter.

# Chapter 7

## High Flux TFC membranes with intrinsic microporosity by interfacial polymerization for Organic Solvent Nanofiltration

### Abstract

This chapter describes the formation of a new generation of organic solvent nanofiltration membranes: high flux thin film composite membranes with intrinsic microporosity prepared via interfacial polymerization. These are the first reported network PIM TFC membranes prepared by IP. They exhibit significantly higher permeabilities for organic solvents, including methanol, acetone, THF, DMF and toluene than commercial integrally skinned asymmetric OSN membranes; and yet have comparable rejections. Solvent stable UF membranes (crosslinked PI, and PEEK) were used as supports for the formation of these TFC membranes, which were prepared by the reaction of an aqueous basic solution containing the sodium salt of 5,5',6,6'-Tetrahydroxy-3,3,3',3'-tetramethyl-1,1'-spirobisindane (TTS) loaded into the UF support with an organic phase containing trimesoyl chloride (TMC). Comparison of TFC membranes with and without temperature treatment suggests that curing plays an important role in further crosslinking their top layer without compromising permeability. Using the sodium salt of TTS as one of the monomers resulted in dramatically improved solvent fluxes and similar selectivity when compared to previously prepared polyamide TFC membranes and commercial ISA membranes. It is believed that its contorted structure provides concavity, which in combination with the polymeric network provides intrinsic microporosity to the top layer. Such network TFC-PIMs membranes prepared by interfacial polymerization may lead to the next generation of high performance OSN membranes.

## 7.1 Introduction

Another challenge for NF and RO is the ability of controlling porosity and hence increase permeability. Advanced polymers, whose structure can be controlled at nano and molecular levels have promising applications for OSN and could result in highly porous membranes with narrower pore size distributions, and higher permeabilities than conventional OSN membranes.

In liquid applications to achieve very high permeabilities, high free volume and microporosity are sought after. Polymers presenting these properties are so-called high free volume polymers. These highly permeable polymers have been applied mostly to gas separations. Recent studies showed polymers of intrinsic microporosity (PIMs) to be promising as membrane materials, exhibiting not only high fluxes, but also high selectivities [92]. In these polymers, molecular linkers containing points of contortion are held in non-coplanar orientation by rigid molecules, which do not allow the resulting polymers to pack closely and ensure high microporosity. The PIMs concept has been reported for polyimides [174].

There are two different types of PIMs, i) non-network (linear) polymers which may be soluble in organic solvents, and ii) network polymers which are generally insoluble, depending on the monomer choice. While the intrinsic microporosity in linear PIMs lies in the impenetrable concavities given by their contorted and rigid structures, in network PIMs, microporosity is also given by the concavities associated with macrocycles. In non-network PIMs, rotation of single bonds has to be avoided, whereas the branching and crosslinking in network PIMs is thought to avoid structural rearrangement that may result in the loss of microporosity [92], so that single bonds can be present without loss of microporosity. In general, it has been observed that network PIMs possess greater microporosity than non-network PIMs due to their macrocyclization [92]. Non-network PIMs may be soluble, and so suitable for casting a membrane by phase inversion, or used for coating a support membrane to make a thin film composite. However, their solubility in a range of solvents restricts their applications in organic solvent nanofiltration [175]. Since network PIMs are not soluble, they can only be incorporated into a membrane if mixed as fillers with microporous soluble materials, which include soluble PIMs or other soluble polymers. Liu et al. patented a method to make polymer/polymer mixed matrix membranes incorporating network PIMs as microporous fillers, resulting in improved performance for gas separations [176].

To date, little research has been done on OSN using PIMs membranes; rather research has pursued pervaporation of mixtures of aliphatic alcohols and water, and gas separations [177, 178]. S. V. Adymkanov et al. [94] studied PIM-1 membranes for pervaporation of binary mixtures of

lower aliphatic alcohols and water, resulting in high flux ( $0.47 \text{ kg m}^{-2} \text{ h}^{-1}$ ) and high permeability ( $14.6 \text{ kg } \mu\text{m m}^{-2} \text{ h}^{-1}$ ) without decreasing over time.

A method of preparing TFC-PIM-1 membranes has been patented [179]. These TFC membranes are formed by coating a solution of PIMs in organic solvent onto a support membrane, and then optionally crosslinking the PIM film to enhance its stability in organic solvents. In another patent [180], high performance UV-crosslinked membranes made with PIMs are prepared and used in both gas separations, and liquid separations involving organic solvents such as olefin/paraffin, deep desulfurization of gasoline and diesel fuels, and ethanol/water separations.

Recently, Fritsch et al. [96] developed TFC membranes of PIM-1 and PIM copolymers on a PAN porous support for OSN applications. In order to make the membranes solvent stable and control swelling, they blended PIM-1 with polyethyleneimine (PEI) as the coating layer, and the TFC membranes were then crosslinked thermally (at  $120^\circ\text{C}$  for 16h) or chemically. As a result the blended TFC- PIM-1/PEI membranes were stable in acetone, THF, chloroform, toluene and heptane, showing better retentions and much higher fluxes than industrial Starmem™ 240 membranes.

To date, reported research on TFC- PIMs membranes has used coating as the technique to fabricate the PIM top layer. However, TFC membranes may be fabricated by coating or via IP [35]. Interfacial polymerization has been demonstrated to be the method to obtain membranes with the highest flux in nanofiltration and RO as it can produce the thinnest layers [35]. To date, no TFC- PIMs membranes have been obtained by interfacial polymerization. In this work IP is used to obtain a thin top layer formed of a network polymer of intrinsic microporosity, resulting in a solvent stable TFC-PIMs membrane with a very thin top layer, which could result in enhanced permeabilities.

In Chapters 4 and 5 TFC membranes for OSN made by interfacial polymerization with much higher permeabilities and comparable selectivities than commercial integrally skinned asymmetric membranes were developed. In this chapter, in order to increase flux even further and without the need of treating TFC membranes with an activating solvent, a monomer with a contorted structure has been incorporated during the IP reaction, forming a network PIM as the top layer. In this particular case single bonds can be present without loss of microporosity as the branching and crosslinking in network PIMs is thought to avoid structural rearrangement [92].

PIMs are promising advanced polymers for membrane applications. So far several efforts to make TFC-PIMs membranes solvent resistant have been reported, including photo-crosslinking,

blending with other thermally reactive polymers and chemical crosslinking. An ideal solution would be the ability to form a network PIM in-situ as the top layer, because network PIMs are solvent stable. Here, the formation of network PIMs *in situ* by interfacial polymerization to develop TFC-PIMs membranes for OSN applications is reported for the first time. When compared with TFC-PIMs membranes prepared by dip coating, one would expect solvent fluxes to be higher for TFC-PIMs membranes prepared by interfacial polymerization, as their top layer is much thinner. Another advantage of TFC-PIMs made by IP is that a network PIM is formed *in situ*, whereas for the conventional TFC-PIMs prepared by coating, further photo-crosslinking is necessary to make the membranes solvent stable. Furthermore, it is known that network PIMs possess greater microporosity than non-network PIMs (used in dip coating) due to their macrocyclization [92]. It is believed that TFC-PIMs membranes made by interfacial polymerization will possess greater microporosity than conventional TFC membranes prepared by IP, due to the contorted structures of the monomers used, resulting in enhanced permeabilities.

## 7.2 Experimental

### 7.2.1 Materials

Polyimide (PI) polymer (P84), all organic solvents, polyethylene glycol (MW 400), polystyrene oligomers, trimesoyl chloride (TMC), and 1,6 hexanediamine (HDA) had the same purity and were purchased from the same companies described in *section 4.2.1*. Polyether ether ketone (PEEK) polymer is the same as that described in *section 6.2.1*. NaOH was purchased from Sigma Aldrich and (5-5,6'6'-tetrahydroxy-3,3,3',3'-tetramethyl-1,1'-spirobisindane, 98 %) (TTS) was purchased from ABCR GmbH. The sodium salt of TTS and acyl chloride TMC were used as monomers for the formation of the polyester active layer. Distilled water and hexane were used as aqueous and organic phases, respectively. Integrally skinned asymmetric commercial membranes Duramem®300, Duramem®500 and Duramem®900 were purchased from Evonik-MET Ltd, UK.

### 7.2.2 Preparation of crosslinked polyimide (PI) UF support membranes

Crosslinked PI UF support membranes were prepared and conditioned following the same methodology explained in *section 4.2.2*. Several membranes were prepared in order to evaluate repeatability. All membranes were conditioned with PEG before the interfacial polymerization reaction.



### 7.2.3 Preparation of polyether ether ketone (PEEK) UF support membranes

PEEK UF support membranes were prepared and conditioned following the same methodology explained in *section 6.2.2*. Several membranes were prepared in order to evaluate repeatability. For the nanofiltration experiments all membranes were conditioned with PEG before the interfacial polymerization. For the gas permeation experiments, PEEK support membranes were not conditioned with PEG before the interfacial polymerization reaction.

### 7.2.4 Preparation of network PIMs-like thin film composite membranes by IP

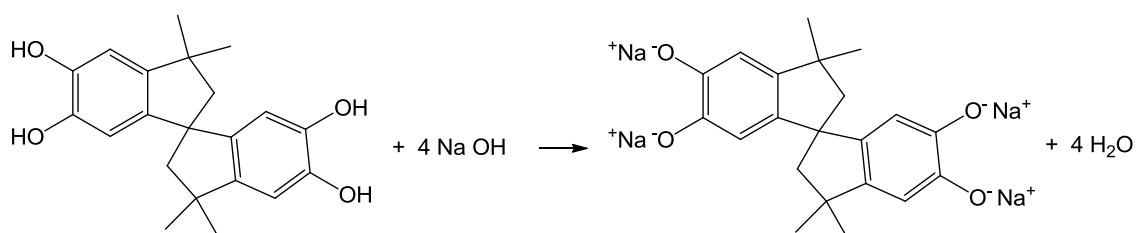
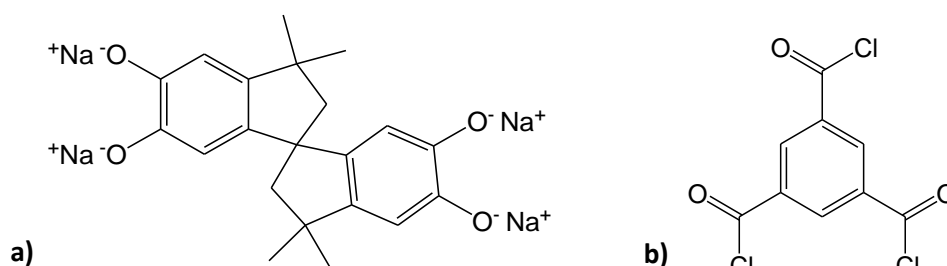
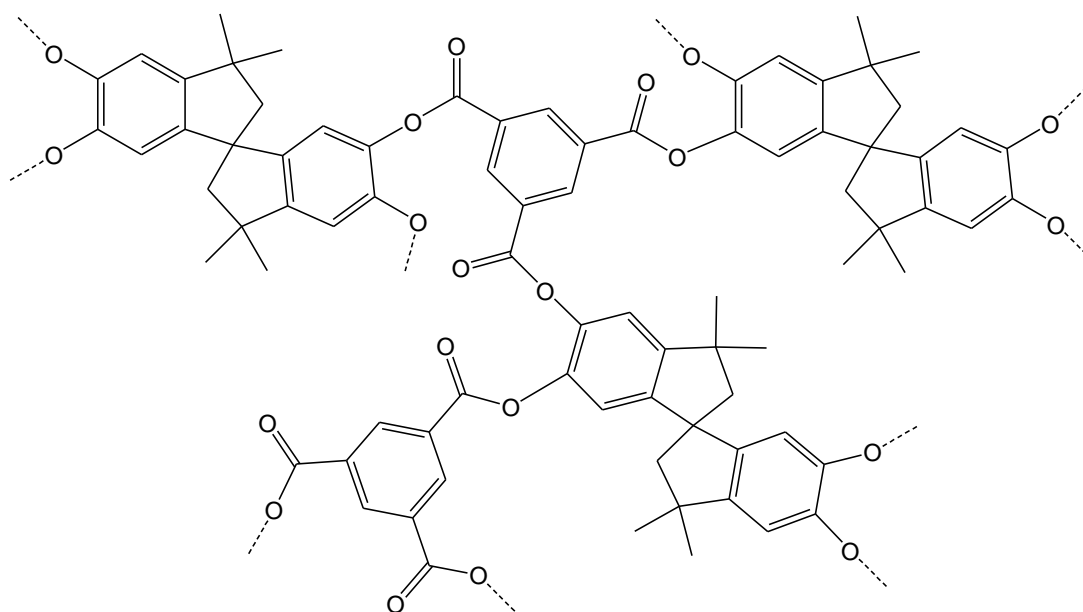
TFC membranes were hand-cast on conditioned UF support membranes through interfacial polymerization. A molecule with contorted and rigid structure was selected as one of the monomers for the IP reaction to provide intrinsic microporosity to the polymer network. The selected molecule (TTS) is one of the monomers used in the synthesis of PIM-1 [92]. As TTS is insoluble in water, 1 % (w/v) TTS was dissolved in an aqueous basic NaOH solution (pH=13) with a ratio of 4:1 Molar (NaOH:TTS). TTS reacts with NaOH to form the sodium salt of TTS (Scheme 5 shows the reaction of TTS with NaOH), which is soluble in water. The UF support membrane, with skin layer upwards was taped to a glass plate and placed in the aqueous basic solution of TTS sodium aryloxide for 2 min. The phenoxide loaded support membranes were then pressed with a roller and wiped to remove excess solution, and subsequently immersed in a solution of 0.1 % (w/v) trimesoyl chloride (TMC, 98 %, Sigma–Aldrich) in hexane. After 2 min reaction time, the resulting membranes were withdrawn from the hexane solution, let dry and either cured with temperature or rinsed three times with distilled water. After preparation, the membranes were stored in distilled water at 4°C. The chemical structures of the monomers used for the interfacial polymerization reaction are shown in Scheme 6; the resulting network polymer is a polyester (see Scheme 7).

#### *Curing TFC-PIMs membranes with temperature*

A post-formation treatment step was carried out on some of the TFC membranes prepared and involved curing with temperature in a ventilated oven at 85°C for 10 minutes to complete the crosslinking reaction in the polymer network. This curing temperature and time were previously optimized in collaboration with MSci student Marta Munoz [181]. The membranes were then rinsed three times with distilled water and stored in distilled water at 4°C. Membrane identification codes for TFC-PIMs prepared with and without temperature curing are shown in Table 16.

**Table 16.** Membrane codes for TFC-PIMs and commercial membranes

Entry No.	Membrane	Membrane code
64	TFC-PIMs membrane prepared on crosslinked PI support	TFC-PIMs-PI
65	TFC-PIMs membrane prepared on crosslinked PI support cured in the oven at 85°C for 10 min	TFC-PIMs-PI-oven
66	TFC-PIMs membrane prepared on PEEK support cured in the oven at 85°C for 10 min	TFC-PIMs-PEEK
67	TFC membrane prepared on PEEK support cured in the oven at 85°C for 10 min	TFC-PIMs-PEEK-oven
68	Duramem® 300 integrally skinned asymmetric membrane	DM300
69	Duramem® 500 integrally skinned asymmetric membrane	DM500
70	Duramem® 900 integrally skinned asymmetric membrane	DM900

**Scheme 5.** Reaction of TTS with sodium hydroxide to form the sodium salt of TTS.**Scheme 6.** Monomers involved in the IP reaction. a) Sodium salt of 5-5',6,6'-tetrahydroxy-3,3,3',3'-tetramethyl-1,1'-spirobisindane, b) 1,3,5-trimesoyl chloride.**Scheme 7.** Polyester network PIM-like polymer obtained by interfacial polymerization.

### 7.2.5 Membrane performance

#### *Nanofiltration performance*

Membrane performance was evaluated according to flux profiles and MWCO curves following the procedure described in *section 4.2.6* in repeats of 8 (two disks per membrane of four different membranes prepared the same way were tested to evaluate repeatability). The solute rejection test was carried out using the homologous standard feed solution comprised of a mixture of styrene oligomers described in *section 4.2.6*; analysis of styrene oligomers was carried out as previously described. The solvents used were MeOH, acetone, THF, DMF, toluene. A comparison study on membrane performance with and without curing with temperature was carried out for the membranes prepared on crosslinked P84 support, the membranes prepared on PEEK support were all cured in the oven and their performance was compared to those prepared on crosslinked P84 supports. The TFC-PIMs membranes with the highest performance were selected and compared with commercial Duramem® membranes (DM300, DM500 and DM900). Two discs of each commercial membrane were tested to evaluate repeatability. In all rejection figures where an error bar is not shown, the rejection of the tested membranes was reproducible and overlaps.

#### *Gas separation performance (see Appendix for results)*

Gas separation performance of oven cured TFC membranes prepared on non-conditioned PEEK supports was evaluated according to pure gas permeation measurements with CH<sub>4</sub>, N<sub>2</sub> and CO<sub>2</sub>. PEEK was selected as the support for TFC membranes for gas permeation performance studies because it does not suffer from plasticization as compared to crosslinked polyimide. Before the gas permeation tests the TFC membranes were immersed in MeOH, followed by hexane and left dry overnight. The gas selectivities were measured for CO<sub>2</sub>/N<sub>2</sub> and CO<sub>2</sub>/CH<sub>4</sub>. The reason for choosing these pairs of gases was because their permeability values differ more than for other gases, giving higher selectivity values and making characterization more sensitive. The gas permeabilities were measured with a soap-bubble meter at feed pressures of 40, 50 and 60 psig. The gas selectivity of the prepared TFC membranes was calculated by equation 8:

$$\alpha_{CO_2/N_2} = \frac{(P_g/l)CO_2}{(P_g/l)N_2} \quad (8)$$

, where  $\alpha$  is the selectivity and  $P_g$  is the gas permeability.

## 7.3 Results and discussion

### 7.3.1 TFC-PIMs-PI membrane performance

#### *Membrane performance with and without temperature curing*

The performance of TFC-PIMs-PI membranes in different solvents with and without curing in the oven at 85°C for 10 min is compared in Figures 35-39. Figure 35 shows the performance of these membranes in acetone, TFC-PIMs-PI-oven membranes show a much lower MWCO (250 Da) as compared to TFC-PIMs-PI (MWCO 600 Da), without significantly compromising solvent flux as only a 10 % decrease is observed upon curing. TFC PIMs-PI-oven membranes had an increase in flux of 55 % when compared with Duramem®300. However, Duramem®300 is tighter than TFC-PIMs-PI-oven membranes; thus, a comparison with looser commercial membranes is discussed later in this chapter. Figure 36 shows that in methanol, the MWCO of TFC-PIMs-PI-oven membranes is much lower (MWCO 300Da) than that of TFC-PIMs-PI membranes (MWCO 700Da), while flux is reduced by only 11 % (from 163 to 145 L m<sup>-2</sup> h<sup>-1</sup>).

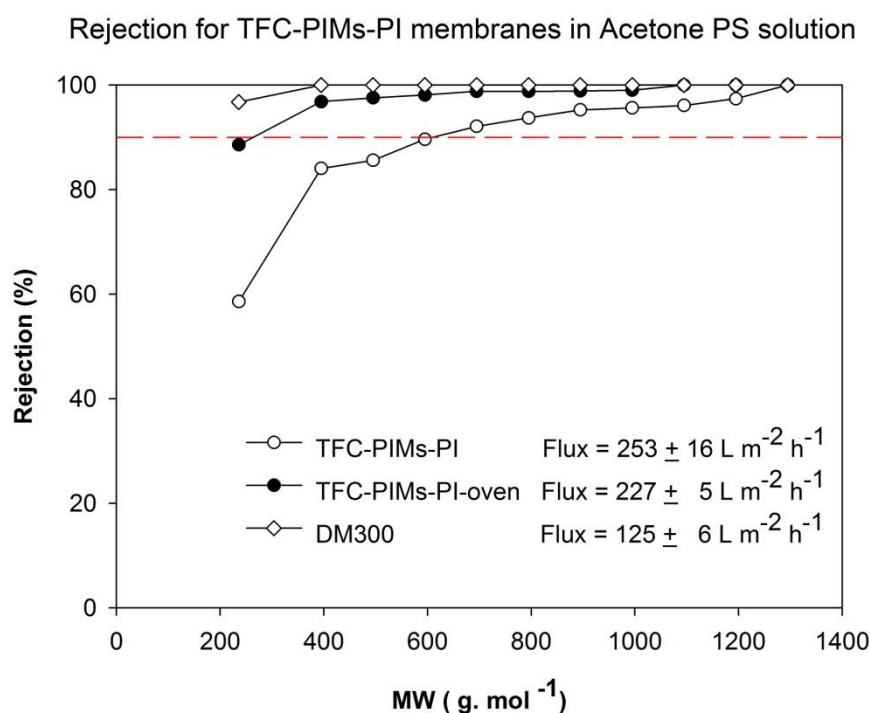


**Figure 35.** MWCO curves and flux of TFC-PIMs membranes prepared on a crosslinked polyimide (PI) support membrane with PEG as conditioning agent, and with and without post-treatment in the oven at 85°C for 10 minutes and commercial membrane DM300. Nanofiltration of a feed solution comprising polystyrene oligomers dissolved in acetone has been performed at 30 bar and 30°C.

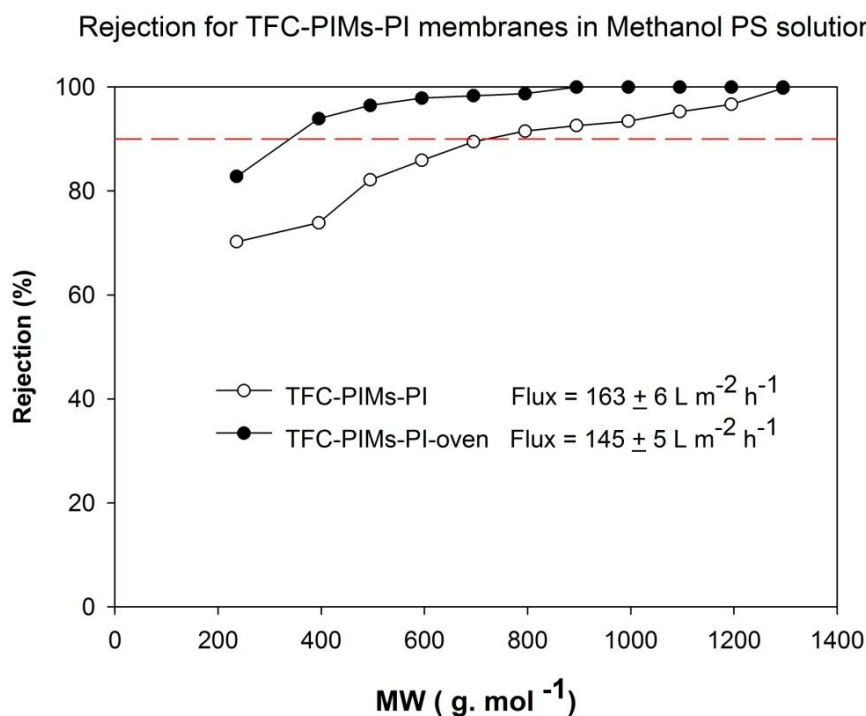


**Figure 36.** MWCO curves and flux of TFC-PIMs membranes prepared on a crosslinked polyimide (PI) support membrane with PEG as conditioning agent, and with and without post-treatment in the oven at 85°C for 10 minutes. Nanofiltration of a feed solution comprising polystyrene oligomers dissolved in methanol has been performed at 30 bar and 30°C.

In DMF (see Figure 37), after curing with temperature the MWCO is decreased from 800 Da to 300 Da, accompanied by a decrease in DMF flux of 32 %. The decrease in DMF flux is not optimum, however, the DMF flux of these TFC-PIMs-PI membranes is still very similar to that reported for the polyamide based TFC membranes prepared by IP in chapter 4, suggesting that the low flux caused by the hydrophobic nature of the polyester network is still counterbalanced by the top layer's high porosity.

As previously reported in Chapter 4, DM150 presents very poor flux in THF. Thus, more open commercial membranes (DM500 and DM900) were chosen for comparison studies in this solvent. Figure 38 shows the performance in THF of commercial membranes DM500 and DM900, and of TFC-PIMs-PI membranes with and without temperature curing. TFC-PIMs-PI-oven membranes have a MWCO of 300 Da, again much lower than TFC-PIMs-PI membranes (MWCO 800 Da), with only 9 % decrease in solvent flux. DM500, and DM900 membranes showed similar MWCO (500 Da). The average fluxes for TFC-PIMs-PI-oven, DM500, and DM900 were 175, 120 and 360 L m<sup>-2</sup> h<sup>-1</sup>, respectively. Network PIMs TFC membranes show much better performance, having higher flux and lower MWCO than DM500.

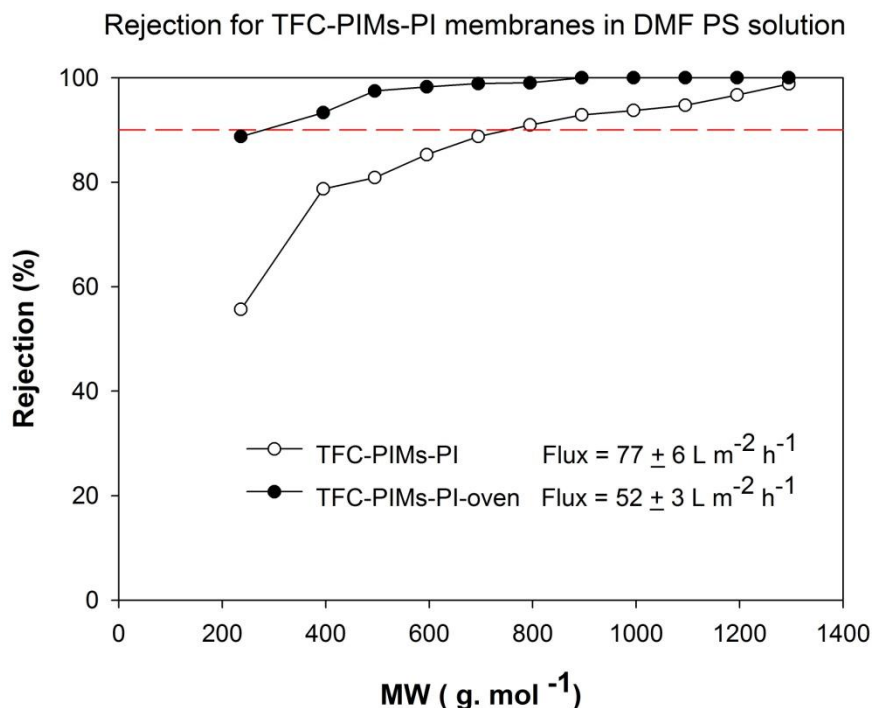


**Figure 37.** MWCO curves and flux of TFC-PIMs membranes prepared on a crosslinked polyimide (PI) support membrane with PEG as conditioning agent, and with and without post-treatment in the oven at 85°C for 10 minutes. Nanofiltration of a feed solution comprising polystyrene oligomers dissolved in DMF has been performed at 30 bar and 30°C.

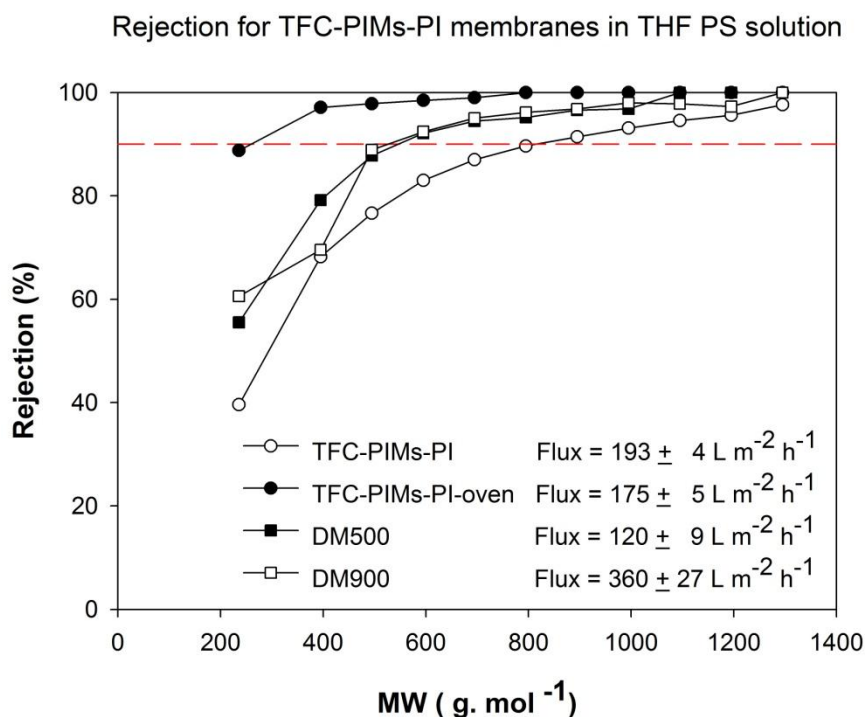


**Figure 38.** MWCO curves and flux of TFC-PIMs membranes prepared on a crosslinked polyimide (PI) support membrane with PEG as conditioning agent, and with and without post-treatment in the oven at 85°C for 10 minutes and commercial membranes DM500 and DM900. Nanofiltration of a feed solution comprising polystyrene oligomers dissolved in THF has been performed at 30 bar and 30°C.

Figure 39 shows that in toluene, the MWCO of TFC-PIMs-PI-oven membranes is much lower (MWCO 300Da) than TFC-PIMs-PI membranes (MWCO 900Da), but flux is significantly reduced 41 % (from 125 to 73 L m<sup>-2</sup> h<sup>-1</sup>). Similar to DMF, these novel TFC-PIMs-PI membranes show lower flux for toluene than for other solvents. However, they still show much higher toluene flux than previously developed high flux polyamide based TFC membranes by IP (see chapter 4) due to both the hydrophobic nature of the polyester top layer and its high porosity.

The MWCO of the solvents used for the filtration tests decreases in the order toluene>DMF>THF>acetone>MeOH, while the viscosities of the solvents decreases as follows: DMF>MEOH=toluene>THF>acetone. Considering both MW and viscosity it is expected that the highest flux will be for acetone and that the lowest will be for DMF. The polarity of the solvents increases as toluene<THF<acetone<MeOH<DMF. The polyester top layer of the TFC membrane is hydrophobic. Thus, considering polarity it is expected that the highest flux will be for toluene and that DMF will give the lowest flux. However, acetone shows the highest flux, followed by MeOH, and DMF shows the lowest flux, suggesting that the solvent MW and solvent viscosity are controlling flux, and not the solvent polarity. Nonetheless, DMF having a lower MW and higher viscosity than toluene shows a much lower flux, suggesting that solvent polarity in this particular case is decreasing DMF flux even further.

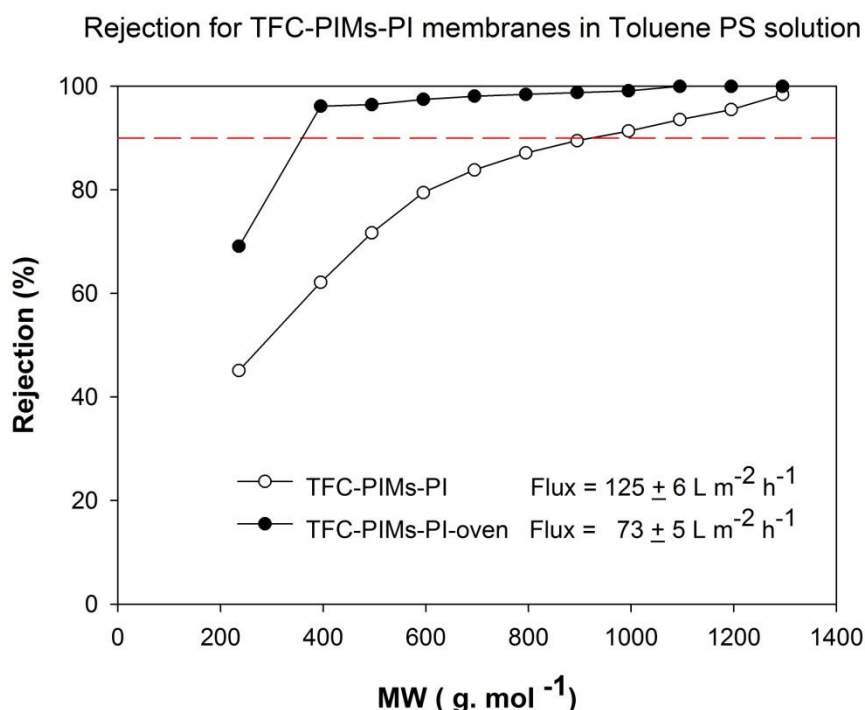


**Figure 39.** MWCO curves and flux of TFC-PIMs membranes prepared on a crosslinked polyimide (PI) support membrane with PEG as conditioning agent, and with and without post-treatment in the oven at 85°C for 10 minutes. Nanofiltration of a feed solution comprising polystyrene oligomers dissolved in toluene has been performed at 30 bar and 30°C.

TFC-PIMs-PI-oven membranes showed much lower MWCO than TFC-PIMs-PI without significantly compromising flux in different solvents. It is known that temperature curing is a necessary step after the IP reaction to promote additional crosslinking, which increases rejection without compromising permeability [51]. It is believed that curing TFC-PIMs-PI at 85°C promotes further crosslinking, resulting in tighter membranes without significant loss in flux.

After preparing these TFC-PIMs membranes on polyimide supports, another solvent stable support membrane will be studied in the next section (PEEK) to understand the effect of support membranes on the overall TFC-PIMs membrane performance.

Novel TFC-PIMs-PI-oven membranes show similar MWCO than the TFC OSN membranes made by IP on the same crosslinked PI support (see chapter 4) and much higher permeability without having to treat them with an “activating solvent”. TFC-PIMs-PI-oven show three to four times higher flux in acetone, methanol and THF than the TFC membranes prepared in chapter 4. Thus, it is believed that using the salt of TTS as one of the monomers for the IP reaction results in a polyester with network-PIM like properties due to its contorted structure and concavity, possibly providing much higher free volume than other monomers, such as MPD.

As previously mentioned, reported research on TFC-PIM membranes consist of TFCs with a coated layer of linear PIMs, which need to be further crosslinked to become solvent stable. To date network PIMs have only been used as fillers in membranes due to their insolubility in organic solvents. Here the formation of network PIMs *in situ* by interfacial polymerization to develop TFC-PIMs membranes for OSN applications is reported for the first time. It is speculated that incorporating a contorted monomer during the IP reaction gives TFC membranes with intrinsic microporosity, which can be confirmed with their extremely high permeability. It is known that in non-network PIMs, rotation of single bonds has to be avoided, whereas the branching and crosslinking in network PIMs is thought to avoid structural rearrangement that may result in the loss of microporosity [92], so that single bonds can be present without loss of microporosity as in the case of the polyester network PIM formed by IP in this chapter.

### 7.3.2 TFC-PIMs-PEEK membrane performance

#### *Nanofiltration membrane performance*

In the previous section, much tighter membranes were obtained after curing in the oven, without a significant loss in solvent flux. Tight membranes are more desirable than open membranes in the purification of active pharmaceutical ingredients. Given this data, subsequent membrane performance studies (Figure 40) comparing the performance of TFC-PIMs-PEEK membranes in different solvents, have all used TFC-PIMs-PEEK membranes cured in the oven.



Figure 40 shows flux and rejection of TFC-PIMs-PEEK membranes in different solvents with post-treatment in the oven at 85°C for 10 min. The solvents selected were acetone (40(b)), THF (40(b)) and toluene (40(c)). In acetone, their MWCO was slightly higher (300Da) than that of TFC-PIMs-PI-oven membranes (250Da). However, acetone flux of TFC-PIMs-PEEK-oven membranes was almost 6 times lower than that of TFC-PIMs-PI-oven membranes (see Figure 35). In THF, TFC-PIMs membranes prepared on PEEK are tighter than those prepared on crosslinked PI (see Figure 38), again their flux is about 6 times lower than that of TFC-PIMs-PI-oven membranes and about the same flux than the TFC-PEEK membranes discussed in *section 6.3.5*. In toluene, TFC-PIMs-PEEK-oven membranes have the same MWCO than TFC-PIMs-PI-oven membranes but 3 times lower flux (see Figure 39). Even though TFC-PIMs-PEEK-oven membranes show low permeabilities when compared to TFC-PIMs-PI-oven membranes, they have similar THF flux and 3 times higher toluene flux than the TFC-PEEK membranes prepared in chapter 6 without having to treat them with an activating solvent. It is believed that the top layer of these TFC-PIMs-PEEK-oven membranes possesses intrinsic microporosity but that the collapsing of the pores of the PEEK support upon heating in the oven restricts solvent flow. Thus, other solvent and temperature stable supports should be developed to understand the influence of different supports on the overall membrane performance, without restricting the top layer's flux.

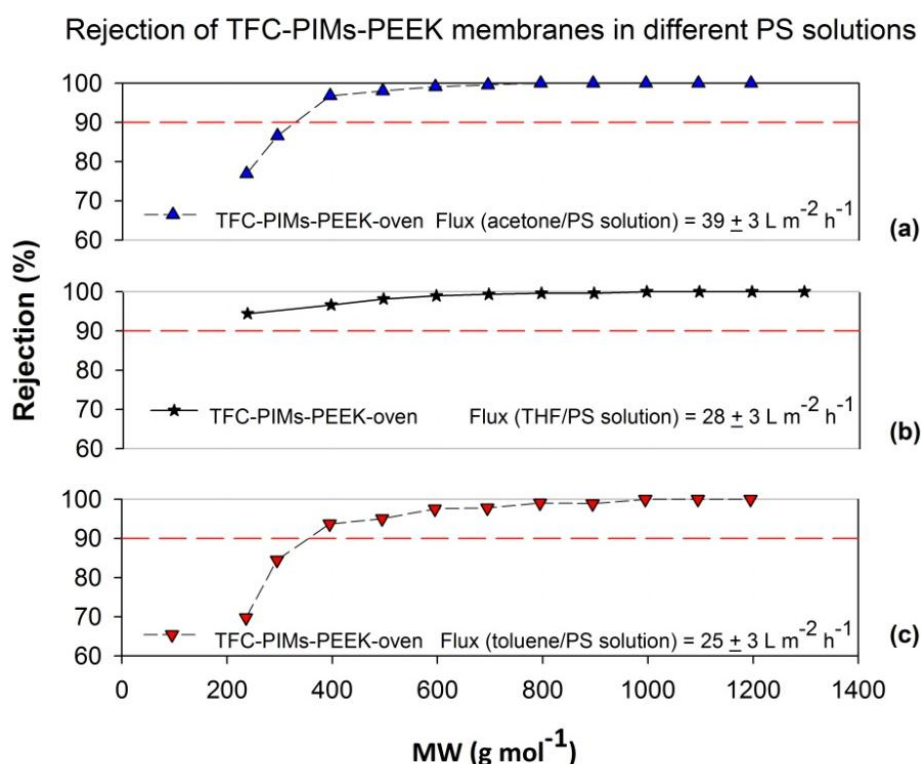


**Figure 40.** MWCO curves and flux of TFC-PIMs membranes prepared on a poly(ether ether ketone) (PEEK) support membrane with PEG as conditioning agent, and with post-treatment in the oven at 85°C for 10 minutes. Nanofiltration of a feed solution comprising polystyrene oligomers dissolved in acetone, THF or toluene has been performed at 30 bar and 30°C; (a) acetone as a solvent; (b) THF as a solvent; (c) toluene as a solvent.

The MWCO of the solvents used for the filtration tests decreases in the order toluene>THF>acetone, while the viscosities of the solvents decreases as follows: toluene>THF>acetone. Considering both MW and viscosity it is expected that the highest flux will be for acetone and that the lowest will be for toluene. The polarity of the solvents increases as toluene<THF<acetone. The polyester top layer of the TFC membrane is hydrophobic. Thus, considering polarity it is expected that the highest flux will be for toluene and that acetone will give the lowest flux. However, acetone shows the highest flux, followed by THF, and toluene shows the lowest flux, suggesting that the solvent MW and solvent viscosity are controlling flux, and not the solvent polarity.

## 7.4 Conclusion

The TFC-PIMs-PI OSN membranes prepared in this chapter showed a great improvement in permeability when compared to ISA OSN membranes and TFC OSN membranes developed in chapter 4 without the need of an “activating solvent”. A post-treatment curing step was necessary to promote additional crosslinking of the polyester network, which increased rejection without significantly compromising permeability. However, this curing step was counterproductive for the TFC-PIMs-PEEK membranes as it not only promoted additional crosslinking, but also collapsed the pores of the PEEK support, resulting in lower permeabilities. Other solvent stable temperature resistant supports should be explored to develop novel TFC-PIMs membranes by interfacial polymerization. TFC-PIMs membranes prepared by interfacial polymerizations still need to be optimized for gas separations.

This is the first time that a crosslinked network PIMs has been formed *in situ* by interfacial polymerization to develop TFC-PIMs membranes for OSN applications. This novel preparation technique represents an advantage compared to conventional TFC-PIMs membranes prepared by coating, where further photo-crosslinking is necessary to make the membranes solvent stable. Moreover, forming the top layer by interfacial polymerization has the advantage of producing thinner top layers than when prepared by dip-coating, which results in higher permeability.

It is speculated that incorporating a contorted monomer during the IP reaction gives TFC membranes with intrinsic microporosity, which can be confirmed with their extremely high permeability when compared to TFC OSN membranes prepared by IP with non-contorted monomers (chapter 4). Because the top layer of these novel interfacially prepared membranes is a network PIMs, single bonds can be present without loss of microporosity. Furthermore, it is known that network PIMs possess greater microporosity than non-network PIMs (use in dip coating) due to their macrocyclization [92].

PIMs are known to preserve their microporosity when curing at high temperatures for a long period of time. To corroborate these results and confirm that the TFC-PIMs membranes developed in this chapter possess intrinsic microporosity, they should be prepared on an inorganic temperature resistant support to avoid pore collapse and, in the future, temperature exposure experiments should be carried out to evaluate their microporosity.

Introducing a contorted monomer during the IP reaction enables a dramatic improvement of flux without sacrificing selectivity.

# Chapter 8

## High flux TFC OSN membranes for the purification of Active Pharmaceutical Ingredients

### 8.1 Introduction

Conventional purification technologies in the manufacture of active pharmaceutical ingredients (APIs) include crystallisation, chromatography, liquid-liquid extraction and adsorption onto activated carbon or silica. These techniques are widely used and commercially available, but have limitations in cost, scale up or selectivity [1]. The purity of APIs is crucial as small amounts of impurities can have detrimental effects on patients.

To date, there is no research evidence in the use of TFC OSN membranes to purify APIs. However, such an OSN process, in principle, could be employed. As a result, a cheaper, more selective and more efficient process for the removal of impurities during the manufacture of APIs could be developed. A great advantage of using OSN membranes will be a decrease in costs because OSN only uses a pressure gradient at room temperature. The aim of this work is to use TFC OSN membranes as an alternative for the purification of Active Pharmaceutical Ingredients.

Both polar and non polar solvents are employed in the synthesis of APIs, and can have damaging effects on polymeric membranes and their ability for molecular discrimination. Thus, in order to make this OSN process viable and versatile TFC OSN membranes with high selectivity and improved permeability (prepared in chapter 4) and commercial membrane Duramem®200 were selected for proof-of concept at a medium scale. In collaboration with GlaxoSmithKline (GSK) rejection experiments were carried out to demonstrate the potential of the membranes to separate an active pharmaceutical ingredient (molecule A) from impurity (molecule B). Mechanical failure has been observed for Duramem® (200 and 300) membranes in TFH/water mixture (75vol:25vol) used in previous tests. As a second objective, mechanical stability of TFC OSN and DM200 membranes was tested under process-relevant conditions (*i e.* by pressurisation/depressurisation

cycles). Finally, the data obtained was used to evaluate and confirm the viability of the process in terms of yield and productivity. It is expected that new OSN membranes tailored towards specific separation processes will yield high purity API rendering the process suitable for industrial applications.

## 8.2 Experimental

### 8.2.1 Materials

HPLC grade THF and de-ionised water were used as filtration studies throughout this study. Active pharmaceutical ingredient (molecule A) and impurity (molecule B) were supplied by GlaxoSmithKline (GSK). Duramem®200 membranes were purchased from Evonik-MET.

### 8.2.2 TFC membrane preparation

TFC membranes were prepared on crosslinked polyimide supports impregnated with PEG as described in *section 4.2.3* and post-treated with DMF as an “activating solvent” as described in *section 4.2.4*. TFC OSN membranes were compared to Duramem®200 membranes throughout this study. A summary of the membranes used is given in Table 17.

**Table 17.** Membranes identification codes

Membrane	Membrane Code	No. of discs tested
TFC membrane prepared on crosslinked polyimide with PEG	TFC-OSN	2
Duramem®200	DM200	2

### 8.2.3 Membrane performance

Membrane performance was evaluated according to flux and rejection. All nanofiltration experiments were carried out at 30 bar using the 8 cell cross-flow filtration system described in *section 4.2.6* in repeats of 2. The effective membrane area was 14 cm<sup>2</sup>, membrane discs were placed into 8 cross flow cells consisting of two sets of 4 cells in series connected in parallel, and with a feed flow of 100 L h<sup>-1</sup>. The system was run continuously under pressure for long periods of time, with permeate and retentate ports connected to valves enabling sampling or re-circulation as needed. All membranes were pre-conditioned using pure THF at 30bar and a temperature of 30°C. THF was re-circulated for 4.5h, until a constant flux was obtained, to ensure sufficient membrane compaction and remove any leachables. Following pre-conditioning pure THF was changed for the feed solution, which was re-circulated at the desired operating pressure for three

days without depressurisation. The feed solution consisted of 0.038M concentrations of molecule A and B respectively in a 75vol THF and 25vol water mixture. 0.038M corresponds to approximately 12.5g API per L solvent mixture. Approximate molecular weights for molecules A and B are 330Da and 110Da respectively. Flux was measured twice daily and samples of permeate and retentate were collected for rejection estimations once per day. On the fourth day a schedule of pressure cycles was started and 4x1.0h cycles were carried out where the membrane was depressurised, left for 30min, re-pressurised, left for 1.0h *etc.* During the fifth and sixth day further pressure cycles were carried out but the pressurised time was extended to 2.0h to enable monitoring of potential compaction effects. 3x2.0h pressure cycles were carried out during day five and six respectively. Concentrations of molecule A and molecule B were analysed in collaboration with Elin Rundquist by HPLC, using CDD open Access 8min generic gradient method ( $\lambda_d=220\text{nm}$ ). Molecule A has a retention time of approximately 5min versus ~2.6min for molecule B. Rejection was calculated based on relative concentrations of molecules A and B.

## 8.3 Results and discussion

### 8.3.1 Membrane Flux and Rejection

Flux measurements can be an indicator of membrane performance and stability over time. Measured fluxes for all tested membranes are presented in Figures 41 and 42. After initial compaction all membranes reached a steady-state flux which was maintained throughout operation. Flux was higher for TFC OSN membranes ( $30 \text{ Lm}^{-2}\text{h}^{-1}$  at 30bar) and lower for DM200 membranes ( $5\text{-}10 \text{ Lm}^{-2}\text{h}^{-1}$  at 30bar). In general flux remained stable for all membranes indicating reproducibility and steady-state operation. Samples for rejection calculations were taken daily. Rejection values were calculated for molecules A and B and are summarised in Table 18 and Table 19.

Data in Table 18 and Table 19 indicate that the rejection for all membranes remained similar throughout the experiment. For TFC OSN and DM200 membranes the rejection of API/molecule A is close to 100 %, indicating the possibility of a high API yield. Additionally rejection of the impurity/molecule B is significantly lower, indicating a feasible separation. Further study and diafiltration modelling data is presented in *section 0*.

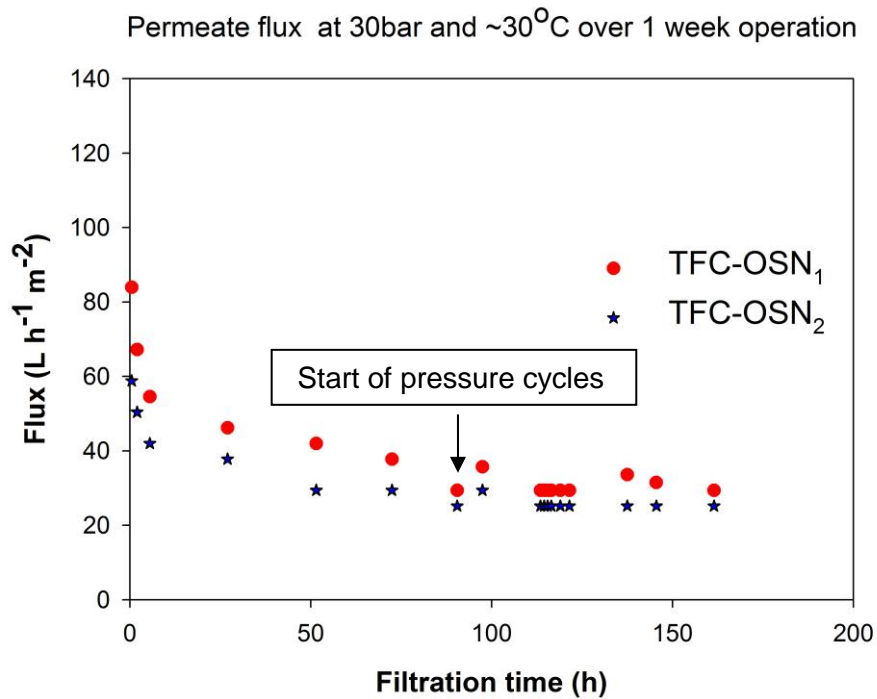


Figure 41. Permeate flux of TFC OSN membranes at 30bar and  $30^{\circ}\text{C}$  over 1 week operation.

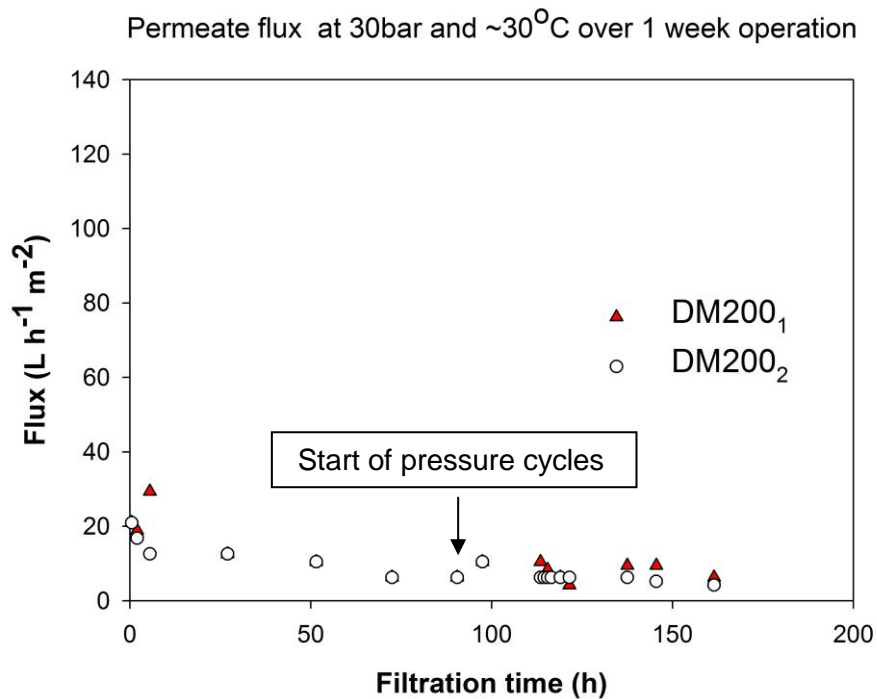


Figure 42. Permeate flux of DM200 membranes at 30bar and  $30^{\circ}\text{C}$  over 1 week operation.

**Table 18.** Rejection of Molecule A at 30bar and ~30°C over 1 week operation

Membrane	Rejection (%)			
	TFC-OSN <sub>1</sub>	TFC-OSN <sub>2</sub>	DM200 <sub>1</sub>	DM200 <sub>2</sub>
Day 1	98	96	97	97
Day 2	99	95	97	97
Day 3	98	97	97	97
Day 4	100	98	100	97
Day 5	100	98	98	98
Day 6	100	98	98	98
Day 7	100	98	98	98
Day 8	100	99	98	98

**Table 19.** Rejection of Molecule B at 30bar and ~30°C over 1 week operation

Membrane	Rejection (%)			
	TFC-OSN <sub>1</sub>	TFC-OSN <sub>2</sub>	DM200 <sub>1</sub>	DM200 <sub>2</sub>
Day 1	32	33	49	48
Day 2	27	28	48	47
Day 3	35	35	48	47
Day 4	34	34	45	44
Day 5	38	36	46	46
Day 6	40	38	48	47
Day 7	40	38	48	47
Day 8	41	39	45	46

### 8.3.2 Membrane Stability

After compaction membrane flux was expected to remain at steady-state. Large differences in flux can depend on a number of factors, but is commonly a result of insufficient membrane stability. Data in Figures 41 and 42 indicate steady-state performance for all membranes throughout operation. Stable fluxes were additionally obtained after 90h when membranes were exposed to pressure cycles. Pressure cycles increase the overall strain on the membrane, which could potentially lead to membrane failure. DM200 membranes showed small variations after the first day of pressure cycles however flux values returned to base-line for all subsequent measurements. Stable fluxes, even after pressure cycles, indicate high membrane stability for all membranes tested. Indication of high stability is further supported by consistent rejection data in Table 18 and Table 19.



### 8.3.3 Separation of API/impurity and process comparison

The technique currently in use for the separation of molecule A and B is a 3 stage liquid-liquid extraction (LLE). The maximal impurity level accepted is 5 mol% and to obtain this target the LLE requires 9mL of solvent per g API/molecule A purified, resulting in an overall yield loss of 5 mol% API. In collaboration with Elin Rundquist, a diafiltration process model developed by Bowen *et al.* [184] was used to predict diafiltration performance of the membranes (TFC-OSN and DM200). Model data is used as a process comparison base to the LLE. Individual membrane predictions are given in Figure 43 and Figure 44.

The TFC-OSN membranes show slight variations in rejection of molecule A. Process modelling was performed for the average rejection value of the two discs over the last 4 days of operation. Rejections used for molecules A and B are 99.9 and 39 % for TFC OSN membranes respectively. Modelling data for TFC-OSN membranes is illustrated in Figure 43.

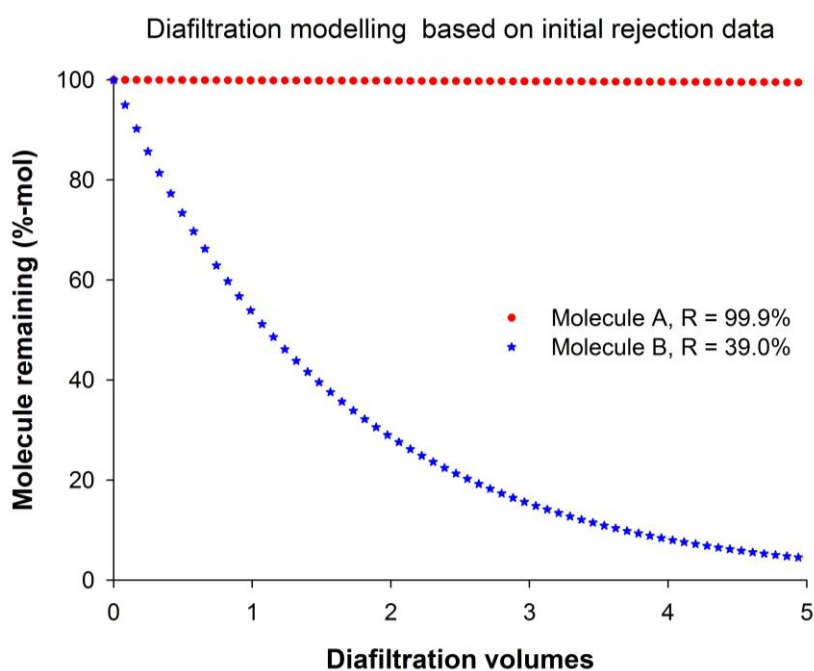


**Figure 43.** Diafiltration modelling of TFC-OSN membranes based on initial rejection data.

Data in Figure 43 indicate that an impurity level of 5 mol% is reached after 4.9 diafiltration volumes have permeated. This is equivalent to an overall solvent requirement of 19.4mL per g of purified API/molecule A, and a 0.5 mol% yield loss of API for a rejection of 99.9 and 99 % respectively.

Process modelling data for DM200 membranes are summarised in Figure 44. Rejection for molecules A and B are based on an average of the two discs over the last 4 days of operation. Rejections used for molecules A and B are 98 and 47 % for DM200 membranes respectively.

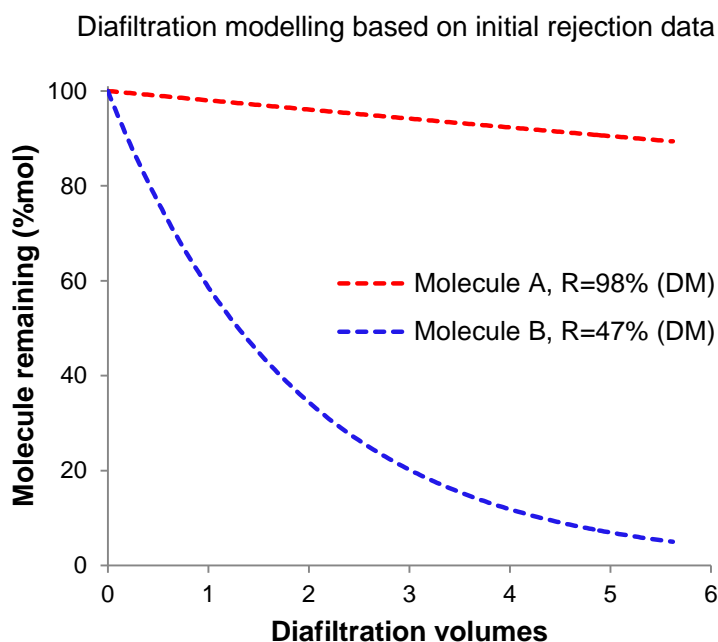


**Figure 44.** Diafiltration modelling of DM200 membranes based on initial rejection data.

For DM200 membranes a total of 5.62 diafiltration volumes must be permeated through the membrane to reach the maximum impurity concentration allowed. This is equivalent to a solvent requirement of 22.5mL per g API purified and results in an overall loss of 10.6 mol% API. Modelled process performance for TFC-OSN and DM200 are summarised in Table 20 along with comparative data for the LLE.

**Table 20.** Process comparison for TFC-OSN and DM200 membranes and 3 stage LLE

Comparison parameter	TFC-OSN	DM200	LLE
Impurity level (mol%)	5.0	5.0	5.0
API yield loss (mol%)	0.5	10.6	5.0
Solvent requirement (mL per g API)	19.4	22.5	9.0

Data in Table 20 indicate that all membrane processes require significantly more solvent to reach the same impurity level as the LLE. However, depending on the overall API yield loss the membrane processes might still offer significant advantages. TFC OSN membranes have a 99.9% rejection resulting in an overall API loss of only 0.5 mol%. This is significantly lower than the LLE making the membrane process more suitable or equivalent in comparison.

The estimated performance of the DM200 membranes indicates a significant API loss of 10.6 mol% throughout the separation. API losses in combination with the increased solvent requirement make DM200 membranes a less suitable option compared to the LLE.

## 8.4 Conclusion

All membranes showed stable performance throughout the experiment indicating sufficient stability under the given process conditions. Out of the membranes tested the TFC OSN membranes show the most promising results with a separation potential of ~60 % and an API rejection of 99-100 % at 30bar and ambient temperature. TFC OSN membranes indicate stable performance and feasible separation performance. Separation can be performed with smaller or equivalent losses of API compared to the LLE, however significantly larger amounts of solvent are predicted. These TFC OSN membranes could offer advantages compared to the LLE and potential gain should be evaluated based on economical and process considerations.

The separating potential of DM200 membranes is ~55 % at 30bar and ambient temperature with an API rejection of 97-98 %. The slight decrease in API rejection compared to the TFC OSN membranes, will result in additional API losses; another disadvantage is that they have much lower flux than TFC OSN membranes. DM200 membranes show significantly larger losses of API and require a larger amount of solvent compared to the LLE. Thus DM200 membranes are deemed unsuitable for further processing.

Potential continuation of this project with GSK using these TFC OSN membranes (prepared in Chapter 4) will be considered based on economic evaluation including but not limited to savings from increased API yield, additional cost of solvent, additional disposal cost, capital cost of equipment and additional costs from increased energy demands. Project future will be discussed with GSK project leader. Finally, the potential for including a second membrane stage for solvent recovery should be considered for future work. Solvent recovery would increase the overall mass-efficiency of the system but at the cost of reduced energy efficiency. Currently no membrane capable of fully rejecting the impurity and enabling solvent recovery is commercially available.

# Chapter 9

## 9.1 Final conclusions

In this research project, different aspects on novel hydrophilic and hydrophobic TFC OSN membranes by interfacial polymerization were investigated, including support membrane optimization, different parameters during and after the formation of the top layer were studied. Thanks to the knowledge gained during the work presented here, understanding of TFC OSN membrane formation and methods of influencing membrane performance have been substantially deepened. It was learnt how to significantly improve solvent permeability without compromising selectivity by impregnating the UF support with PEG before the IP reaction, and/or post-treating the membrane with some of the best solvents for aromatic polyamide (e.g. DMF and DMSO). This was only possible thanks to the use of solvent stable supports (crosslinked polyimide and PEEK). Moreover, introducing hydrophobic species on the polyamide layer followed by solvent post-treatment enabled the optimization of flux in non-polar solvents without sacrificing selectivity. This report is the first in which TFC membranes prepared by interfacial polymerization have been modified incorporating F and Si to the polyamide top layer to improve permeabilities in non-polar solvents. It is believed both hydrophilic and hydrophobic TFC OSN membranes prepared via interfacial polymerization on crosslinked PI and PEEK supports introduce new degrees of freedom in membrane design, which could lead to the next generation of high performance hydrophobic OSN membranes.

The study on the effect of support membrane on overall TFC membrane performance in polar and non-polar solvents has shown that their hydrophilicity plays an important role on solvent permeation. For each support, two different effects have been studied: (i) adding PEG into the pores of the support, and (ii) treating the TFC membranes with DMF. The study shows that combining both approaches gives the maximum improvement of permeability without sacrificing selectivity. Introducing hydrophilic or hydrophobic solvent stable polymeric materials as support membranes (e.g. XP84 and PEEK) enables the optimization of flux in polar and non-polar solvents without sacrificing selectivity. Thus, understanding and carefully selecting the support membrane

for developing TFC membranes for a specific solvent system can improve the overall membrane performance in OSN.

To improve flux even further, it was decided to interfacially make the top layer using advanced polymers possessing high porosity. The TFC-PIMs-PI membranes developed showed a great improvement in permeability when compared to ISA OSN commercial membranes and TFC OSN membranes developed in chapter 4 without the need of an “activating solvent”.

This is the first time that a crosslinked network PIMs has been formed *in situ* by interfacial polymerization to develop TFC-PIMs membranes for OSN applications. This novel preparation technique represents an advantage compared to conventional TFC-PIMs membranes prepared by coating, where further photo-crosslinking is necessary to make the membranes solvent stable. Moreover, forming the top layer by interfacial polymerization has the advantage of producing thinner top layers than when prepared by dip-coating, which results in a much higher permeability. Thus, introducing a contorted monomer during the IP reaction enabled a dramatic improvement of flux without sacrificing selectivity. Thus, it is believed ultra-high flux TFC-PIMs OSN membranes prepared via interfacial polymerization introduce new degrees of freedom in membrane design, which could lead to the next generation of high performance OSN membranes.

Finally, as a proof of concept at a medium scale in collaboration project with GSK, the TFC OSN membranes developed in chapter 4 were used for the purification of an active pharmaceutical ingredient and compared to commercial membranes. These TFC OSN membranes resulted promising for the purification of APIs. However, commercial membrane Duramem®200 was unsuitable for this specific separation. TFC OSN membranes showed a separation potential of ~60 % and an API rejection of 100 %. Thus, separation can be performed with smaller losses of API compared to the LLE, however significantly larger amounts of solvent are predicted. However, they could still offer advantages compared to the LLE and potential gain should be evaluated based on economical and process considerations, including savings from increased API yield. Currently, no membrane capable of fully rejecting the impurity and enabling solvent recovery is commercially available.

## 9.2 Future directions

Given the high complexity and interdependence of the parameters governing TFC OSN membrane performance, there are still numerous aspects of this work to be recommended for further investigation.

In this dissertation, in chapter 4, the potential of the use of PEG inside the pores of the support was shown. The advantage of incorporation of PEG inside the pores of the support could be further investigated with respect to how it affects diffusion of the amine into the organic phase, by using PEGs of different MW to see if what slows down diffusion of the amine is a change in viscosity caused by the PEG leaching out of the support into the aqueous phase or if it is due to hydrogen bonding interactions between the amine and PEG. Additionally, the encouraging results for controlling MWCO by using different amines in the organic phase could be compared with TFC membranes prepared with alternative di-functional or tri-functional acyl chlorides, for instance, sebacoyl chloride (SC), isophthaloyl chloride (IPC), and terephthaloyl chloride (TPC). A more thorough TEM study of the TFC membranes formed on PEG impregnated and non-impregnated supports, and DMF treated and non-treated TFC membranes will help in the understanding of the effects that PEG and DMF have on TFC membrane morphology. It may be possible to avoid the use of an activating solvent by carefully controlling the monodispersity of the polyamide top layer during the interfacial polymerization reaction to avoid the formation of low MW polyamide, while controlling the reaction parameters to achieve high selectivity.

In chapter 5 a new and simple approach to render TFC membranes more hydrophobic was shown. Moreover, as it was shown that the surface chemistry of the top layer greatly influences flux, fine-tuning the top layer chemical structure is very recommendable. Performance experiments were all carried out at the same pressure, to better understand whether concentration polarization influences rejection in the second generation hydrophobic membranes, future studies could be carried out at the same flux, using different pressures. To better understand the effects of capping on solute rejection, a future characterization of top layer thickness and pore size using TEM with the nanoprobeing technique developed by J. Stawikowska is strongly recommended [139].

In view of the findings in chapter 6, it is recommended to further investigate the impact of other solvent stable support membranes on the top layer formation and overall TFC membrane performance. PALS could be used to further explore the properties and porosity of the top layer on different solvent stable supports. Moreover, TEM images of the cross-section of TFC membrane could further enrich the characterization of their top layer.

Given the encouraging results in chapter 7, showing a dramatic improve in permeability by incorporating a contorted monomer during the IP reaction without the need of an activating solvent, further investigation on the use of other contorted monomers is of great interest. Different chemistries and structures of monomers possessing contorted structures, which result in a crosslinked network with extremely high free volume, should be explored to further tune the MWCO of these novel membranes. The exploration of pore-protecting agents or temperature

resistant support membranes that do not collapse upon temperature curing is further recommended. Additionally to better understand how different monomers affect membrane porosity, the use of PALS to characterize the top layer of the membranes is recommended. In chapter 7, it is speculated that incorporating a contorted monomer during the IP reaction gives TFC membranes with intrinsic microporosity, which can be confirmed with their extremely high permeability. It is known that in non-network PIMs, rotation of single bonds has to be avoided, whereas the branching and crosslinking in network PIMs is thought to avoid structural rearrangement that may result in the loss of microporosity [92], so that single bonds can be present without loss of microporosity as in the case of the polyester network PIM formed by IP in this chapter. Moreover, PIMs are known to preserve their microporosity and their permeability upon heating at high temperatures for several hours. Therefore, it is recommended to prepare these TFC membranes on temperature resistant supports to perform an in depth study of the effect of temperature on microporosity and prove whether they possess intrinsic microporosity.

In Chapter 8, the TFC membranes prepared in Chapter 4 were selected to demonstrate their applicability in the purification of APIs at a medium scale. The data obtained confirms the viability of using these novel TFC OSN membranes in terms of yield and productivity for the purification of APIs. Finally, the potential of the TFC OSN membranes formed via the implementation of the methods and ideas developed in this dissertation should be scaled up and demonstrated in real separation processes involving organic solvents such as pharmaceutical purification.

# Bibliography

- [1] P. Vandezande, L.E.M. Gevers, I.F.J. Vankelecom, Solvent resistant nanofiltration: separating on a molecular level, *Chem. Soc. Rev.* **37** (2008) 365-405.
- [2] L.S. White, A.R. Nitsch, Solvent recovery from lube oil permeates with a polyimide membrane, *J. Membr. Sci.* **179** (2000) 267-274.
- [3] R.J. Petersen, Composite reverse osmosis and nanofiltration membranes, *J. Membr. Sci.* **83** (1993) 81-150.
- [4] C. Fritzmann, J. Löwenberg, T. Wintgens, and T. Melin, State-of-the-art of reverse osmosis desalination. *Desalination.* **216**, (2007) 1-76.
- [5] R. Behrend, E. Meyer and F. Rusche, Über Condensationsprodukte aus Glycoluril und Formaldehyd, *Justus Liebigs Ann. Chem.*, **339**, (1905) 1-37.
- [6] Richard W. Baker, *Membrane Technology and Applications*, 2<sup>nd</sup> edition, John Wiley and Sons, Ltd, (2004).
- [7] M. Mulder, *Basic Principles of Membrane Technology*, ed. M. Mulder, Kluwer Academic Publishers, Dordrecht, 2<sup>nd</sup> edn., 3, 71, 2004.
- [8] A. I. Schaefer, A. G. Fane and T. D. Waite, *Nanofiltration, Principles and Applications*, 1st edition, Elsevier, UK (2005).
- [9] A. S. Jonsson, and G. Tragardh, Fundamental principles of ultrafiltration. *Chem. Eng. Process.* **27** (1990) 67-81.
- [10] R.L. Riley, R. W. Baker, E. L. Cussler, W. Eykamp, W.J. Koros, and H. Strathmann (eds), *Reverse Osmosis in Membrane Separation Systems*, Noyes Data Corp., Park Ridge, NJ, 276-328 (1991).
- [11] J.E. Cadotte, Interfacially synthesized reverse osmosis membrane, US Pat., 4277344, 1981.
- [12] J.E. Cadotte, Evaluation of Composite Reverse Osmosis Membrane Cell, in *Materials Science of Synthetic Membranes*, D.R. Lloyd, ACS Symposium Series Number 269, American Chemical Society, Washington, DC (1985).
- [13] R.E. Larson, J.E. Cadotte, and R.J. Petersen, The FT-30 seawater reverse osmosis membrane-element test results. *Desalination.* **38** (1981) 473-483.
- [14] S. Loeb and S. Sourirajan, Sea Water Demineralization by Means of an Osmotic Membrane, in *saline Water Conversion-II, Advances in Chemistry Series Number 28*, American Chemical Society, Washington, DC, 117-132 (1963).
- [15] J.S. Park, S.K. Kim, K.H. Lee, Effect of ZnCl<sub>2</sub> on formation of asymmetric PEI. Membrane by phase inversion process, *J. Ind. Eng. Chem.*, **6** (2000) 93-99.
- [16] J.E. Cadotte, R.J. Petersen, *Synthetic Membranes, Vol. I, Desalination*, ACS Symp. Ser. No. 153, American Chemical Society, Washington, DC (1981) 305.



- [17] L.E.M. Gevers, S. Aldea, I. F. J. Vankelecom, P.A. Jacobs, Optimisation of a lab-scale method for preparation of composite membranes with a filled dense top-layer, *J. Membr. Sci.* **281** (2006) 741-746.
- [18] K.A. Ghosh, B.H. Jeong, X. Huang, E.M.V. Hoek, Impacts of reaction and curing conditions on polyamide composite reverse osmosis membrane, *J. Membr. Sci.* **311** (2008) 34-45.
- [19] M.L. Lind, D.E. Suk, T.V. Nguyen, E.M. V. Hoek, Tailoring the Structure of Thin Film Nanocomposite Membranes to Achieve Seawater RO Membrane Performance, *Environ. Sci. Technol.* **44** (2010) 8230-8235.
- [20] D. Mukherjee, A. Kulkarni, W.N. Gill, Flux enhancement of reverse osmosis membranes by chemical surface modification, *J. Membr. Sci.* **97** (1994) 231-249.
- [21] A. Kulkarni, D. Mukherjee, W.N. Gill, Flux enhancement by hydrophilization of thin film composite reverse osmosis membranes, *J. Membr. Sci.* **114** (1994) 39-50.
- [22] S. Verissimo, K.-V. Peinemann, J. Bordado, Thin-film composite hollow fibre membranes: An optimized manufacturing method, *J. Membr. Sci.* **264** (2005) 48-55.
- [23] V. Ramachandhran, A.K. Ghosh, S. Prabhakar, P.K. Tewari, Separation Behaviour of Composite Polyamide Membranes from Mixed Amines: Effects of Interfacial Reaction Condition and Chemical Post-Treatment, *Sep. Science and Technology*, **44** (2009) 599-614.
- [24] Sanchuan Yua, Meihong Liu, Xuesong Liu, Congjie Gao, Performance enhancement in interfacially synthesized thin-film composite polyamide-urethane reverse osmosis membrane for seawater desalination, *J. Membr. Sci.* **342** (2009) 313-320.
- [25] S.P. Nunes K. and Peinemann, *Membrane Technology in the Chemical Industry*, ed. S. P. Nunes and K. Peinemann, Wiley-VCH, Weinheim, **part I** (2006) 1-85.
- [26] H.I. Shaban, Reverse-osmosis membranes for seawater desalination state-of-the-art. *Sep. Purif. Methods.* **19** (1990) 121-131.
- [27] S.K. Karode, S.S. Kulkarni, A.K. Suresh, and R.A. Mashelkar, Molecular weight distribution in interfacial polymerization--model development and verification. *Chemical Engineering Science.* **52** (1997) 3243-3255.
- [28] V.V. Yashin, and A.C. Balazs, Theoretical model of interfacial polymerization. *J. Chem. Phys.* **121** (2004) 11440-11454.
- [29] C.K. Kim, J.H. Kim, I.J. Roh, and J.J. Kim, The changes of membrane performance with polyamide molecular structure in the reverse osmosis process. *J. Membr. Sci.* **165** (2000) 189-199.
- [30] I.J. Roh, S.Y. Park, J.J. Kim, and C.K. Kim, Effects of the polyamide molecular structure on the performance of reverse osmosis membranes. *J. Polym. Sci. Pt. B-Polym. Phys.* **36** (1998) 1821-1830.
- [31] S.H. Chen, D.J. Chang, R.M. Liou, C.S. Hsu, and S.S. Lin, Preparation and separation properties of polyamide nanofiltration membrane. *J. Appl. Pol. Sci.* **83** (2002) 1112-1118.
- [32] I.J. Roh, Influence of rupture strength of interfacially polymerized thin-film structure on the performance of polyamide composite membranes. *J. Membr. Sci.* **198** (2002) 63-74.
- [33] D.M. Koenhen, A.H. A. Tinnemans, Semipermeable composite membrane, a process for the manufacture thereof, as well as application of such membranes for the separations of components in an organic liquid phase or in the vapour phase, US Pat. 5274047, 1993.
- [34] J. Jegal, S.G. Min, and K.H. Lee, Factors affecting the interfacial polymerization of polyamide active layers for the formation of polyamide composite membranes. *J. Appl. Pol. Sci.* **86** (2002) 2781-2787.

- [35] X. Lu, X. Bian, and L. Shi, Preparation and characterization of NF composite membrane. *J. Membr. Sci.* **210** (2002) 3-11.
- [36] G.Y. Chai, and W.B. Krantz, Formation and characterization of polyamide membranes via interfacial polymerization. *J. Membr. Sci.* **93** (1994) 175-192.
- [37] A.L. Ahmad, and B.S. Ooi, Properties-performance of thin film composites membrane: study on trimesoyl chloride content and polymerization time. *J. Membr. Sci.* **255** (2005) 67-77.
- [38] S. Zhang, X. Jian, and Y. Dai, Preparation of sulfonated poly(phthalazinone ether sulfone ketone) composite nanofiltration membrane. *J. Membr. Sci.* **246** (2005) 121-126.
- [39] P. W. Morgan, and S.L. Kwolek, Interfacial polycondensation .2. Fundamentals of polymer formation at liquid interfaces. *J. Polym. Sci. Pol. Chem.* **34** (1996) 531-559.
- [40] E.L. Wittbecker, and P.W. Morgan, Interfacial polycondensation .1. *J. Polym. Sci. Pol. Chem.* **34** (1996) 521-529.
- [41] S.H. Kim, S.Y. Kwak, and T. Suzuki, Positron annihilation spectroscopic evidence to demonstrate the flux-enhancement mechanism in morphology-controlled thin-film-composite (TFC) membrane. *Environ. Sci. Technol.* **39** (2005) 1764-1770.
- [42] M. Hirose, H. Ito, and Y. Kamiyama, Effect of skin layer surface structures on the flux behaviour of RO membranes. *J. Membr. Sci.* **121** (1996) 209-215.
- [43] Z. Yong, Y. Sanchuan, L. Meihong, and G. Congjie, Polyamide thin film composite membrane prepared from m-phenylenediamine and m-phenylenediamine-5-sulfonic acid. *J. Membr. Sci.* **270** (2006) 162-168.
- [44] S.Y. Kwak, S.G. Jung, and S.H. Kim, Structure-motion-performance relationship of flux-enhanced reverse osmosis (RO) membranes composed of aromatic polyamide thin films. *Environ. Sci. Technol.* **35** (2001) 4334-4340.
- [45] M.A. Kuehne, R.Q. Song, N.N. Li, and R.J. Petersen, Flux enhancement in TFC RO membranes. *Environ. Prog.* **20** (2001) 23-26.
- [46] J.E. Tomaschke, Interfacially synthesized reverse osmosis membrane containing an amine salt and processes for preparing the same, US Pat. 4872984, 1989.
- [47] W.E. Mickols, Composite Membrane and Method for Making the Same, Patent Application No. 6878278 (2005).
- [48] W.E. Mickols, Composite Membrane and Method for Making the Same, Patent Application No. 6337018 (2002).
- [49] W.E. Mickols, Method of treating polyamide membranes to increase flux, US Pat, 5755964, 1998.
- [50] J.E. Cadotte, D.R. Walker, Polyamide membranes useful for water softening, US Pat. 4765897, 1988.
- [51] A. Prakash Rao, N.V. Desai, and R. Rangarajan, Interfacially synthesized thin film composite RO membranes for seawater desalination. *J. Membr. Sci.* **124** (1997) 263-272.
- [52] A. Prakash Rao, S.V. Joshi, J.J. Trivedi, C.V. Devmurari, and V.J. Shah. Structure-performance correlation of polyamide thin film composite membranes: effect of coating conditions on film formation. *J. Membr. Sci.* **211** (2003) 13-24.
- [53] W.E. Mickols, Composite membrane and method for making the same, US Pat. 6562266, 2003.
- [54] R.G. Gutman, Membrane Filtration. "The Technology of Pressure-driven Crossflow Processes", Adam Hilger, Bristol, Chapt. 1, 1987.

- [55] E. P. Cuperus and K. Ebert, in *Nanofiltration. Principles and Applications*, ed. A. I. Schaefer, A. G. Fane and T. D. Waite, Elsevier, Oxford, 2005, ch. 21, 521–536.
- [56] Y. H. See-Toh, F. C. Ferreira, A. G. Livingston, The influence of membrane formation parameters on the functional performance of organic solvent nanofiltration membranes, *J. Membr. Sci.* **299** (2007) 236-250.
- [57] K. Boussu, C. Vandecasteele, B. Van der Bruggen, Study of the characteristics and the performance of self-made nanoporous polyethersulfone membranes, *Polymer* **47** (2006) 3464-3476.
- [58] A.F. Ismail, P.Y. Lai, Effects of phase inversion and rheological factors on formation of defect-free and ultrathin-skinned asymmetric polysulfone membranes for gas separation, *Sep. Purif. Technol.* **33** (2003) 127-143.
- [59] Kim, H. Yoon, K. Lee, Formation of integrally skinned asymmetric polyetherimide nanofiltration membranes by phase inversion process, *J. Appl. Polym. Sci.* **84** (2002) 1300-1307.
- [60] H. Hicke, I. Lehmann, G. Malsch, M. Ulbricht, M. Becker, Preparation and characterization of a novel solvent-resistant and autoclavable polymer membrane, *J. Membr. Sci.* **198** (2002) 187-196.
- [61] Y. Dai, X. Jian, S. Zhang, M.D. Guiver, Thermostable ultrafiltration and nanofiltration membranes from sulfonated poly(phthalazine ether sulfone ketone), *J. Membr. Sci.* **188** (2001) 195-203.
- [62] F. J. Vankelecom and L. E. M. Gevers, *Fundamentals and Applications in Green Separation Processes*, ed. C. A. M. Alfonso and J. G. Crespo, Wiley-VCH, Weinheim (2005) ch. 3.6, 251–270.
- [63] M. Bulut, L.E.M. Gevers, J.S. Paul, I.F.J. Vankelecom, P. A. Jacobs, Directed Development of High-Performance Membranes via High-Throughput and Combinatorial Strategies, *J. Comb. Sci.* **8** (2006) 168-173.
- [64] N. Leblanc, D. Le Cerf, C. Chappay, D. Langevin, M. Metayer, G. Muller, Polyimide asymmetric membranes: Elaboration, morphology, and gas permeation performance, *J. Appl. Polym. Sci.*, **89** (2003) 1838-1848.
- [65] H. Ohya, I. Okazaki, M. Aihara, S. Tanisho, Y. Negishi, Study on molecular weight cut-off performance of asymmetric aromatic polyimide membrane, *J. Membr. Sci.*, **123** (1997) 143-147.
- [66] K.C. Gupta, Synthesis and evaluation of aromatic polyamide membranes for desalination in reverse-osmosis technique, *J. Appl. Polym. Sci.* **66** (1997) 643-653.
- [67] X. Jian, Y. Dai, G. He, G. Chen, Preparation of UF and NF poly (phthalazine ether sulfone ketone) membranes for high temperature application, *J. Membr. Sci.* **161** (1999) 185-191.
- [68] Y.H. See Toh, F.W. Lim, A.G. Livingston, Polymeric membranes for nanofiltration in polar aprotic solvents, *J. Membr. Sci.* **301** (2007) 3-10.
- [69] E.M. Tsui, M. Cheryan, Characteristics of nanofiltration membranes in aqueous ethanol, *J. Membr. Sci.* **237** (2004) 61-69.
- [70] C. Linder, M. Nemas, M. Perry, R. Katraró, Solvent-stable semipermeable composite membranes US Pat., 5032282, 1991.
- [71] C. Linder, M. Perry, M. Nemas, R. Katraró, Solvent stable membranes US Pat., 5039421, 1991.
- [72] X.X. Loh, M. Sairam, A. Bismarck, J.H.G. Steinke, A.G. Livingston and K. Li, Crosslinked integrally skinned asymmetric polyaniline membranes for use in organic solvents, *J. Membr. Sci.*, **326** (2009) 635-642.

- [73] Y.H. See-Toh, M. Silva, A. Livingston, Controlling molecular weight cut-off curves for highly solvent stable organic solvent nanofiltration (OSN) membranes, *J. Membr. Sci.* **324** (2008) 220–232.
- [74] I. Soroko, M.P. Lopes, A. Livingston, The effect of membrane formation parameters on performance of polyimide membranes for organic solvent nanofiltration (OSN). Part A. Effect of polymer/solvent/non-solvent system choice, *J. Membr. Sci.* **381** (2011) 152–162.
- [75] I. Soroko, M. Makowski, F. Spill, A. Livingston, The effect of membrane formation parameters on performance of polyimide membranes for organic solvent nanofiltration (OSN). Part B. Analysis of evaporation step and the role of a co-solvent, *J. Membr. Sci.* **381** (2011) 163-171.
- [76] I. Soroko, M. Sairam, A.G. Livingston, The effect of membrane formation parameters on performance of polyimide membranes for organic solvent nanofiltration (OSN). Part C. Effect of polyimide characteristics, *J. Membr. Sci.* **381** (2011) 172–182.
- [77] L.S. White, Polyimide membranes for hyperfiltration recovery of aromatic solvents, US Pat., 6180008, 2001.
- [78] I.F.J. Vankelecom, B. Moermans, G. Verschueren, and P.A. Jacobs, Intrusion of PDMS top layers in porous supports. *J. Membr. Sci.* **158** (1999) 289-297.
- [79] N.W. Oh, J. Jegal, and K.H. Lee, Preparation and characterization of nanofiltration composite membranes using polyacrylonitrile (PAN). II. Preparation and characterization of polyamide composite membranes. *J. Appl. Pol. Sci.* **80** (2001) 2729-2736.
- [80] H.I. Kim, and S.S. Kim, Plasma treatment of polypropylene and polysulfone supports for thin film composite reverse osmosis membrane. *J. Membr. Sci.* **286** (2006) 193-201.
- [81] A.P. Korikov, P.B. Kosaraju, and K.K. Sirkar, Interfacially polymerized hydrophilic microporous thin film composite membranes on porous polypropylene hollow fibres and flat films. *J. Membr. Sci.* **279** (2006) 588-600.
- [82] P.B. Kosaraju, and K.K. Sirkar, Interfacially polymerized thin film composite membranes on microporous polypropylene supports for solvent-resistant nanofiltration. *J. Membr. Sci.* **321** (2008) 155-161.
- [83] W.K. Miller, S.B. McCray, D.T. Friesen, Solvent-resistant microporous polyimide membranes, US Pat. , 5725769, 1998.
- [84] I.C. Kim, J. Jegal, K.H. Lee, Effect of aqueous and organic solutions on the performance of polyamide thin-film-composite nanofiltration membranes. *J. Polym. Sci., Part B: Polym. Phys.* **40** (2002) 2151-2163.
- [85] I.C. Kim, and K.H. Lee, Preparation of interfacially synthesized and silicone-coated composite polyamide nanofiltration membranes with high performance. *Ind. Eng. Chem. Res.* **41** (2002) 5523-5528.
- [86] K-H. Lee, I-C. Kim, H-G. Yun, Silicone-coated organic solvent resistant polyamide composite nanofiltration membrane, and method for preparing the same, US. Pat., 6887380, 2005.
- [87] L.E. Black, Interfacially polymerized membranes for the reverse osmotic separation of organic solvent solutions, US Pat. 5173191, 1992.
- [88] P.R. Buch, D.J. Mohan, and A.V. Reddy, Poly(amide imide)s and poly(amide imide) composite membranes by interfacial polymerization. *Polymer International* **55** (2006) 391-398.
- [89] P.B. Kosaraju, K.K. Sirkar, Novel solvent-resistant hydrophilic hollow fibre membranes for efficient membrane solvent back extraction, *J. Membr. Sci.* **288** (2007) 41-50.
- [90] US Pat. No. 0197070, 2008.

- [91] L.E.M. Gevers, I.F.J. Vankelecom, and P.A. Jacobs, Zeolite filled polydimethylsiloxane (PDMS) as an improved membrane for solvent-resistant nanofiltration (SRNF). *Chem. Commun.* (2005) 2500-2502.
- [92] N.B. McKeown and P.M. Budd, Exploitation of Intrinsic Microporosity in Polymer-based Materials. *Macromolecules* **43** (12) (2010) 5163-5176.
- [93] P.M. Budd, K.J. Msayib, C.E. Tattershall, B.S. Ghanem, K.J. Reynolds, N.B. McKeown, D. Fritsch, Gas separation membranes from polymers of intrinsic microporosity. *J. Membr. Sci.* **251**(2005) 263-269.
- [94] S. V. Adymkanov Y.P. Yampol'skii, A.M. Polyakov, P.M. Budd, K.J. Reynolds, N.B. McKeown, K.J. Msayib, Pervaporation of alcohols through highly permeable PIM-1 polymer films. *Polymer Science Series A.* **50** (2008) 444-450.
- [95] P.M. Budd, E.S. Elabas, B.S. Ghanem, S. Makhseed, N.B. McKeown, K.J. Msayib, C.E. Tattershall, D. Wang, Solution-processed organophilic membrane derived from a polymer of intrinsic microporosity. *Advanced Materials.* **16** (5) (2004) 456.
- [96] D. Fritsch, P. Merten, K. Heinrich, M. Lazar, M. Priske, High performance organic solvent nanofiltration membranes: Development and thorough testing of thin film composite membranes made of polymers of intrinsic microporosity (PIMs). *J. Membr. Sci.* **401** (2012) 222-231.
- [97] S. Tsarkov, V. Khotimskiy, P.M. Budd, V. Volkov, J. Kukushkina, A. Volkov, Solvent nanofiltration through high permeability glassy polymers: Effect of polymer and solute nature. *J. Membr. Sci.* **423** (2012) 65-72.
- [98] Li Xianfeng, C. A. Fustin, N. Lefevre, J.F. Gohy, S.D. Feyter, J.D. Baerdemaeker, W. Egger and I.F.J. Vankelecom, Ordered nanoporous membranes based on diblock copolymers with high chemical stability and tunable separation properties. *J. Mater. Chem.* **20** (2010) 4333-4339.
- [99] Y. Lu, T. Suzuki, W. Zhang, J.S. Moore, B.J. Marinas, Nanofiltration membranes based on rigid star amphiphiles, *Chem. Mater.* **19** (2007) 3194–3204.
- [100] T. Suzuki, Y. Lu, W. Zhang, J.S. Moore, B.J. Marinas, Performance characterization of nanofiltration membranes based on rigid star amphiphiles, *Environ. Sci. Technol.* **41** (2007) 6246–6252.
- [101] B.H. Jeong, E.M.V. Hoek, Y. Yan, A. Subramani, X. Huang, G. Hurwitz, A.K. Ghosh, A. Jawor, Interfacial polymerization of thin film nanocomposites: a new concept for reverse osmosis membranes, *J. Membr. Sci.* **294** (2007) 1–7.
- [102] M.L. Lind, A.K. Ghosh, A. Jawor, X. Huang, W. Hou, Y. Yang, E.M.V. Hoek, Influence of zeolite crystal size on zeolite-polyamide thin film nanocomposite membranes, *Langmuir.* **25** (2009) 10139–10145.
- [103] M. Majumder, N. Chopra, R. Andrews, B.J. Hinds, Nanoscale hydrodynamics: enhanced flow in carbon nanotubes, *Nature.* **438** (2005) 44.
- [104] J.K. Holt, H.G. Park, Y. Wang, M. Stadermann, A.B. Artyukhin, C.P. Grigoropoulos, A. Noy, O. Bakajin, Fast mass transport through Sub-2-nanometer carbon nanotubes, *Science.* **312** (2006) 1034–1037.
- [105] T.V. Ratto, J.K. Holt, A.W. Szmodis, Membranes with Embedded Nanotubes for Selective Permeability, Patent Application No. 20100025330 (2010).
- [106] K. Peng Lee, T.C. Arnot, D. Mattia, A review of reverse osmosis membrane materials for desalination-Development to date and future potential, *J. Membr. Sci.* **370** (2011) 1-22.
- [107] A. Noy, H.G. Park, F. Fornasiero, J.K. Holt, C.P. Grigoropoulos, O. Bakajin, Nanofluidics in carbon nanotubes, *Nano Today.* **2** (2007) 22–29.

- [108] M.S. Mauter, M. Elimelech, Environmental applications of carbon-based nanomaterials, *Environ. Sci. Technol.* **42** (2008) 5843–5859.
- [109] S. Karan, S. Samitsu, X. Peng, K. Kurashima, I. Ichinose, Ultrafast viscous permeation of organic solvents through diamond-like carbon nanosheets, *Science*. **335**, 6067(2012) 444-447.
- [110] [www.kochmembrane.com](http://www.kochmembrane.com) (accessed December 2012).
- [111] C. Linder, M. Nemas, M. Perry, R. Katraró, Silicone-derived solvent stable membranes, US Pat., 5205934, 1993.
- [112] C. Linder, M. Nemas, M. Perry, R. Katraró, Silicon-derived solvent stable membranes, US Pat., 5265734, 1993.
- [113] J. T. Scarpello, D. Nair, L.M. Freitas dos Santos, L.S. White, and A.G. Livingston, The separation of homogeneous organometallic catalysts using solvent resistant nanofiltration. *J. Membr. Sci.* **203** (2002) 71-85.
- [114] Solsep, <http://www.solsep.com> (accessed December 2012).
- [115] B. Van der Bruggen, J.C. Jansen, A. Figoli, J. Geens, K. Boussu, E.J. Drioli, Characteristics and Performance of a “Universal” Membrane Suitable for Gas Separation, Pervaporation, and Nanofiltration Applications, *J. Phys. Chem. B.* **110** (2006) 13799-13803.
- [116] F.P. Cuperus, Recovery of Organic Solvents and Valuable Components by Membrane Separation *Chem. Ing. Tech.* **77** (2005) 1000–1001.
- [117] J. Geens, B. Van der Bruggen, C. Vandecastleele, Transport model of solvent permeation through nanofiltration membranes, *Sep. Purif. Technol.* **48** (2006) 255–263.
- [118] G. Bargeman, J. Albers, J.B. Westerlink, C.F.H. Manahutu, A.T. Kate, Proceedings of the International Workshop on Membranes in Solvent Filtration, Leuven, Belgium, 2006.
- [119] Livingston, A. G., See Toh, Y. H. (Imperial Innovations Ltd.). Method of Separation. Great Britain Pat. 2437519, 31 October 2007.
- [120] Evonik- MET, <http://duramem.evonik.com> (accessed December 2012).
- [121] M. Schmidt, K.V. Peinemann, N. Scharnagl, K. Friese, R. Schubert, Strahlenchemisch modifizierte Silikonkompositmembran für die Ultrafiltration, DE Patent 19507584 A1.
- [122] F.P. Cuperus, C.A. Smolders, Characterization of UF membranes: Membrane characteristics and characterization techniques, *Adv. Colloid Interface Sci.* **34** (1991) 135–173.
- [123] Y.H. See Toh, X. X. Loh, K. Li, A. Bismarck, A.G. Livingston, In search of a standard method for the characterisation of organic solvent nanofiltration membranes, *J. Membr. Sci.* **291** (2007) 120–125.
- [124] Song, Y., Liu, F. & Sun, B. Preparation, characterization, and application of thin film composite nanofiltration membranes. *Journal of Applied Polymer Science.* **95** (2005) 1251-1261.
- [125] W. Zhang, and B. Hallström, Membrane characterization using the contact angle technique I. methodology of the captive bubble technique. *Desalination.* **79** (1990) 1-12.
- [126] D. Bhanushali, S. Kloos, C. Kurth, D. Bhattacharayya, Performance of solvent resistant membranes for non-aqueous systems: solvent permeation results and modelling, *J. Membr. Sci.* **189** (2001) 1–21.
- [127] D. Bhanushali, D. Bhattacharyya, *D. Ann. N.Y. Acad. Sci.* **984** (2003) 159–177.
- [128] D.R. Paul, M. Garcin, W.E. Garmon, Solute diffusion through swollen polymer membranes, *J. Appl. Poly. Sci.* **20** (1976) 609-625.

- [129] Q. Wu, and B. Wu, Study of membrane morphology by image analysis of electron micrographs. *J. Membr. Sci.* **105** (1995) 113-120.
- [130] J.M. Sheldon, The fine-structure of ultrafiltration membranes. I. Clean membranes. *J. Membr. Sci.* **62** (1991) 75-86.
- [131] A. Bottino, G. Capannelli, A. Grosso, O. Monticelli, O. Cavalleri, R. Rolandi, R. Soria, Surface characterization of ceramic membranes by atomic force microscopy. *J. Membr. Sci.* **95** (1994) 289-296.
- [132] J. Stawikowska, A.G. Livingston, Assessment of atomic force microscopy for characterisation of nanofiltration membranes, *J. Membr. Sci.* **425-426** (2013) 58-70.
- [133] L. Zeman, and L. Denault, Characterization of microfiltration membranes by image analysis of electron micrographs.: Part I. Method development, *J. Membr. Sci.* **71** (1992) 221-231.
- [134] J. A. Otero, O. Mazarrasa, J. Villasante, V. Silva, P. Pradanos, J. I. Calvo, A. Hernandez, Three independent ways to obtain information on pore size distributions of nanofiltration membranes, *J. Membr. Sci.* **309** (2008) 17-27.
- [135] N. Hilal, A.W. Mohammad, B. Atkin, N.A. Darwish, Using atomic force microscopy towards improvement in nanofiltration membranes properties for desalination pre-treatment: a review, *Desalination.* **157** (2003) 137-144.
- [136] K.C. Khulbe, C.Y. Feng, T. Matsuura, *Synthetic Polymeric Membranes Characterization by Atomic Force Microscopy*, Springer, 2008.
- [137] K. Boussu, B. Van der Bruggen, A. Volodin, J. Snauwaert, C. Van Haesendonck, C. Vandecasteele, Roughness and hydrophobicity studies of nanofiltration membranes using different modes of AFM, *J. Colloid Interface Sci.* **286** (2005) 632-638.
- [138] D. F. Stamatialis, C .R. Dias, M. Norberta de Pinho, Atomic force microscopy of dense and asymmetric cellulose-based membranes, *J. Membr. Sci.* **160** (1999)235-242.
- [139] J. Stawikowska and A.G. Livingston, Nanoprobe imaging molecular scale pores in polymeric membranes, *J. Membr. Sci.* **413-414** (2012) 1-16.
- [140] K.L. Tung, Y-C. Jean, D. Nanda, K-R. Lee, W-S. Hung, C-H. Lo, J-Y. Lai, Characterization of multilayer nanofiltration membranes using positron annihilation spectroscopy. *J. Membr. Sci.* **343** (2009) 147-156.
- [141] A. Cano-Odena, P. Vandezande, K. Hendrix, R. Zaman, K. Mostafa, W. Egger, P. Sperr, J. De Baerdemaeker, I.F. Vankelecom, Probing the Molecular Level of Polyimide-Based Solvent Resistant Nanofiltration Membranes with Positron Annihilation Spectroscopy. *Journal of Physical Chemistry B*, 113(30) (2009) 10170-10176.
- [142] Tarleton, E. S., Robinson, J. P. & Salman, M. Solvent-induced swelling of membranes - Measurements and influence in nanofiltration. *J. Membr. Sci.* **280** (2006) 442-451.
- [143] Nogami, N., Chowdhury, G. & Matsuura, T. Preparation and performance testing of sulfonated poly(phenylene oxide) based composite membranes for nanofiltration. *J. Appl. Pol. Sci.* 91 (2004) 2624-2628.
- [144] H.K. Lonsdale, U. Merten, and R.L. Riley, Transport properties of cellulose acetate osmotic membranes. *J. Appl. Pol. Sci.* 9 (1965) 1341-1362.
- [145] J.G. Wijmans, R.W. Baker, The solution-diffusion model: a review, *J. Membr. Sci.* **107** (1995) 1-21.
- [146] Shu-Hsien Huang, Chi-Lan Li, Chien-Chien Hu, H.A. Tsai, Kueir-Rarn Lee, Juin-Yih Lai, Polyamide thin-film composite membranes prepared by interfacial polymerization for pervaporation separation. *Desalination.* **200** (2006) 387-389.
- [147] H. Ohya, V.V. Kudryavtsev and S. I. Semenova, *Polyimide Membranes-Application, Fabrications, and Properties*, Gordon and Breach, Chapter 6.4, Tokyo, 1996.

- [148] A.K. Ghosh, E.M.V. Hoek, Impacts of support membrane structure and chemistry on polyamide–polysulfone interfacial composite membranes, *J. Membr. Sci.* **336** (2009) 140-148.
- [149] M. Duan, Z. Wang, J. Xu, J. Wang, S. Wang, Influence of hexamethyl phosphoramidate on polyamide composite reverse osmosis membrane performance, *Sep. Purif. Technol.* **75** (2010) 145-155.
- [150] I.F.J. Vankelecom, K. De Smet, L.E.M. Gevers, P.A. Jacobs in *Nanofiltration: principles and applications*, A.I. Schaefer, A.G. Fane, T.D. Waite, first edition, Elsevier, Chapter 3, (2005).
- [151] C.N. Tran, A.C. Maldonado, R. Somanathan, Thin-film composite membrane, U.S. Pat. No. 5234598, 1993.
- [152] C.N. Tran, A.C. Maldonado, R. Somanathan, Method of making thin-film composite membranes, U.S. Pat No. 5358745, 1994.
- [153] Joanna Stawikowska, PhD dissertation, Imperial College London, 2013.
- [154] M. Eldrup, D. Lightbody, J.N. Sherwood, The temperature dependence of positron lifetimes in solid pivalic acid, *Chem. Phys.*, **63** (1981) 51-58.
- [155] S.J. Tao, Positronium annihilation in molecular substances, *J. Chem. Phys.* **56** (1972) 5499-5510.
- [156] D. Bhanushali, S. Kloos, D. Bhattacharyya, Solute transport in solvent-resistant nanofiltration membranes for non-aqueous systems: experimental results and the role of solute-solvent coupling, *J. Membr. Sci.*, **208** (2002) 343-359.
- [157] P.S. Singh, A.P. Rao, P. Ray, A. Bhattacharya, K. Singh, N.K. Saha, A.V.R. Reddy, Techniques for characterization of polyamide thin film composite membranes, *Desalination*, **282** (2011) 78-86.
- [158] S.M. Aharoni, The solubility parameters of aromatic polyamides, *J. Appl. Polym. Sci.*, **45** (1992) 813-817.
- [159] D. Mukherjee, A. Kulkarni, W.N. Gill, Chemical treatment for improved performance of reverse osmosis membranes, *Desalination*. **104** (1996) 239-249.
- [160] V. Freger, Nanoscale Heterogeneity of Polyamide Membranes Formed by Interfacial Polymerization, *Langmuir*. **19** (2003) 4791-4797.
- [161] V. Freger, Swelling and Morphology of the Skin Layer of Polyamide Composite Membranes: An Atomic Force Microscopy Study, *Environ. Sci. Technol.* **38** (2004) 3168-3175.
- [162] I. Soroko, Y. Bhole, A.G. Livingston, Environmentally friendly route for the preparation of solvent resistant polyimide nanofiltration membranes, *Green Chem.* **13** (2011) 162-168.
- [163] C.C. Wamser, M.I. Gilbert, Detection of Surface Functional Group Asymmetry in Interfacially-Polymerized Films by Contact Angle Titrations, *Langmuir*. **8** (1992) 1608-1614.
- [164] F.A. Pacheco, I. Pinnau, M. Reinhard, J.O. Leckie, Characterization of isolated polyamide thin films of RO and NF membranes using novel TEM techniques, *J. Membr. Sci.* **358** (2010) 51-59.
- [165] G. Kang, M. Liu, B. Lin, Y. Cao, Q. Yuan, A novel method of surface modification on thin-film composite reverse osmosis membrane by grafting poly(ethylene glycol), *Polymer*. **48** (2007) 1165-1170.
- [166] H. Zou, Y. Jin, J. Yang, H. Dai, X. Yu, J. Xu, Synthesis and characterization of thin film composite reverse osmosis membranes via novel interfacial polymerization approach, *Sep. Purif. Technol.* **72** (2010) 256-262.
- [167] D. A. Shirley, High-Resolution X-Ray Photoemission Spectrum of the Valance Bands of Gold, *Phys. Rev. B.* **5** (1972) 4709-4714.



- [168] D. Briggs and M. P. Seah, Practical Surface Analysis, Vol. 1, second edition, Wiley, 1990.
- [169] G. Z. Ramon, M. C.Y. Wong, E. M. V. Hoek. Transport through composite membrane, part 1: Is there an optimal support membrane? , J. Membr. Sci. **415-416** (2012) 298-305.
- [170] P.S. Singh, S.V. Joshi, J.J. Trivedi, C.V. Devmurari, A. Prakash Rao, P.K Ghosh, Probing the structural variations of thin film composite RO membranes obtained by coating polyamide over polysulfone membranes of different pore dimensions, J. Membr. Sci. **278** (2006) 19-25.
- [171] H. K. Lonsdale, R. L. Riley, C. R. Lyons, D. P. Carosella, Transport in composite reverse osmosis membranes, in: M. Bier (Ed.), Membrane Processes in Industry and Biomedicine, Plenum Press, New York, 1971, 101.
- [172] G. Z. Ramon and E. M. V. Hoek, Transport through composite membranes, part 2: Impacts of roughness on permeability and fouling, J. Membr. Sci **425-426** (2013) 141-148.
- [173] Wang, L., Li, Z., Ren, J., Li, S.-G. & Jiang, C. Preliminary studies on the gelation time of poly(ether sulfones) membrane-forming system with an elongation method, J. Membr. Sci **275** (2006) 46-51.
- [174] P.M. Budd and N.B. McKewon, "Highly permeable polymers for gas separation membranes, Polymer Chemistry, 1 (2010) 63-68.
- [175] M. Ulbricht, Advanced functional polymer membranes. Single Chain Polymers, **47** (2006) 2217- 2262.
- [176] C. Liu, S.T. Wilson, Mixed matrix membranes incorporating microporous polymers as fillers, US Patent No. 7410525 B1.
- [177] Emmler, Free Volume Investigation of Polymers of Intrinsic Microporosity (PIMs): PIM-1 and PIM1 copolymers incorporating ethanoanthracene units. Macromolecules, **43** (2010) 6075-6084.
- [178] M. Carta, K.J. Msayib and N.N. McKeown, Novel polymers of intrinsic microporosity (PIMs) derived from 1,1-spiro-bis(1,2,3,4-tetrahydronaphthalene)-based monomers. Tetrahedron, **50** (2009), 5954-5947.
- [179] N.B. McKeown, P.M. Budd, D. Fritsch, Thin layer composite membrane, Patent Application No. WO 2005/113121 A1 (PCT/GB2005/002028).
- [180] C. Liu, S.T. Wilson, D.A. Lesch, UV-crosslinked membranes from polymers of intrinsic microporosity for liquid separations, US Patent No 7758751 B1.
- [181] M. Munoz-Ibanez, MSci Thesis, Novel advanced polymeric thin film composite membranes for organic solvent nanofiltration, Imperial College London, 2011.
- [182] L. M. Robeson, The upper bound revisited, J. Membr. Sci. **320** (2011) 390-400.
- [183] P.M. Budd, N.B. McKeown and D. Fritsch, Free volume and intrinsic microporosity in polymers, J. Mater. Chem. **15** (2005) 1977-1986.
- [184] R.W. Bowen, B. Cassey, P. Jones, D.L. Oatley, Modelling the performance of membrane nanofiltration – application to an industrially relevant separation, J. Membr. Sci. **242** (2004) 211-220.

# Appendix

## A1. Gas separation performance of TFC-PIMs-PEEK membranes

The gas separation performance of TFC-PIMs-PEEK membranes prepared in chapter 7 and treated in the oven at 85°C for 10 min was evaluated for two gas systems (N<sub>2</sub> and CO<sub>2</sub>) and (CO<sub>2</sub> and CH<sub>4</sub>). The permeabilities vs. selectivities at different pressures are shown in Figure 45.

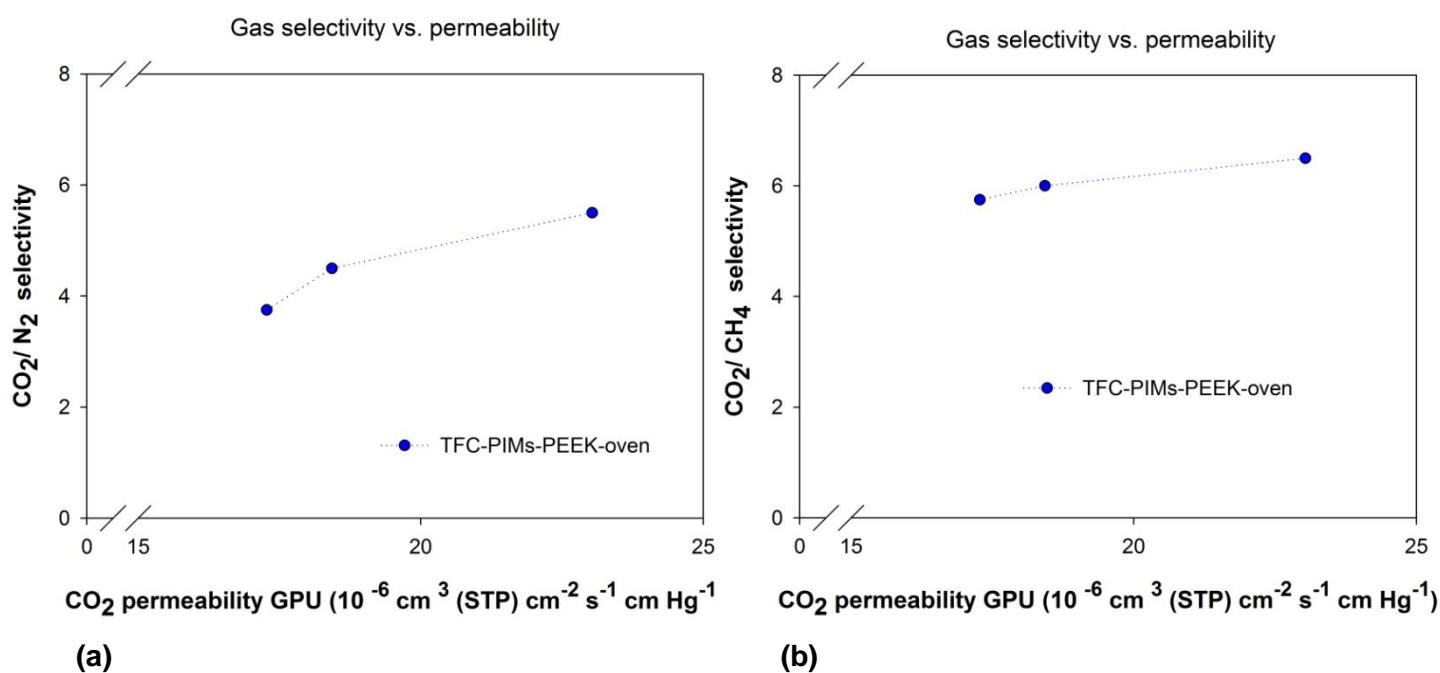


**Figure 45.** Gas separation performance of TFC-PIMs membrane prepared on a PEEK support membrane. The membrane has been post-treated in the oven at 85°C for 10 minutes. Gas permeation experiments were carried out at 40, 50 and 60 psig. (a) shows CO<sub>2</sub>/N<sub>2</sub> selectivity vs. CO<sub>2</sub> permeability; (b) shows CO<sub>2</sub>/CH<sub>4</sub> selectivity vs. CO<sub>2</sub> permeability.

Figure 45 shows that for both gas systems permeability increases with pressure, suggesting that the gas transport through the TFC membranes is a combination of viscous flow with Knudsen diffusion. Knudsen diffusion occurs when the mean free path of the diffusing gas molecules is much larger than the pore size. In this regime the gas molecules pass through the pores undergoing random collisions with the pore walls. Selectivity is higher at higher pressure, possibly

due to selective adsorption of CO<sub>2</sub> in the top layer. The selectivity results shown in Figure 45 are below Robeson upper bound [182], and is lower than that of PIM-1 (which has a selectivity of  $\alpha_{\text{CO}_2/\text{N}_2}$  of 25 [183]), suggesting that this particular PIM-like polyester does not have a good selectivity to separate CO<sub>2</sub> from N<sub>2</sub> and CH<sub>4</sub>.

## A2. Products Data sheets

### A2.1 Polymers

#### HP-POLYMER

EU-MATERIAL SAFETY DATA SHEET  
according rule 91/155/EWG

Version 7 08.11.2007  
page 1 of 6

#### 1.1 CHEMICAL PRODUCT/COMPANY IDENTIFICATION

##### Material identification

P84-Powder is a registered trademark of HP-Polymer GmbH

##### Tradenames and synonyms

P84 Powder VPD (325/+1200, 325, 425, 1200 mesh)  
P84 Powder HT VPD (325/+1200, 325, 425, 1200 mesh)  
P84 Powder STD (140/325, 200, 325, 425, 1200 mesh; 45/75 $\mu$ m;)  
P84 Powder HCM (40, 200, 325, 1200 mesh)  
P84 Powder HCM Blends (15G, 40G, 30P, 20CF, 30 CF, 15G/MB, 40G/MB, 50 Glass/5P, 15G/10P)  
P84 Powder HT HCM (40, 325, 1200 mesh)  
P84 Powder HP and HP/HT HCM (40 mesh)  
P84 Granulate (STD, SG)

#### 1.2 COMPANY IDENTIFICATION

**Manufacturer:** ENSINGER SINTIMID GmbH  
Werkstraße 3  
A-4860 Lenzing/Austria

**Distributor:** HP-Polymer GmbH  
Werkstraße 3  
A-4860 Lenzing/Austria

**Phone Numbers:** Product-information: 0043 7672 701-3572  
Transport-emergency: 0043 7672 701-2800  
Medical-emergency: 0043 7672 701-2222

#### 2.1. COMPOSITION/INFORMATION ON INGREDIENTS

Components Material	CAS No.	%
Aromatic Polyimide	TSCA 58698-66-1 TSCA 134119-41-8	60-100
Present in HCM Blend 15G, 40G, 15G10P, 15G/MB, 40G/MB: Graphite	TSCA 7782-42-5	15-40
Present in HCM Blend 30P, 15G/10P, 50 Glass/5P Polytetrafluorethylene	TSCA 9002-84-0	5-30
Present in HCM Blend 20CF, 30 CF: Carbon fibre	CAS 7440-44-0	20-30
Present in HCM Blend 50 Glass/5P Glass	CAS 65997-17-3	50



VICTREX® PEEK COATING TECHNOLOGY

## 700 SERIES ELECTROSTATIC POWDER COATINGS PRODUCT DATA SHEET

## VICOTE® 701, 702, 703, 704, 705, 706 and 707 Powder Coatings

VICOTE® is the brand name for VICTREX® PEEK polymer-based coatings. VICOTE Coatings are only available through Victrex or its preferred coater network. Contact Victrex for further details.

### PROPERTIES

VICOTE 701-707 grades are specially developed powder coatings. They are available in various average particle sizes from 10 - 50 microns. The powders are off-white in color and are available in various melt viscosities depending on the film thickness and level of melt flow required. Typical film thicknesses range from < 100 microns up to 500 microns. Film thicknesses above 1 mm are possible by building up the coating thickness by the hot flocking technique.

Like other non-coating grades of VICTREX PEEK polymer, VICOTE Coatings are thermoplastic in nature and exhibit flow above the melt temperature. When processed using the correct guidelines, the coatings will exhibit the excellent properties that VICTREX PEEK polymer is renowned for.

- High continuous use temperature of 260°C
- Excellent wear, abrasion and cut through resistance at these high temperatures
- Excellent chemical and radiation resistance
- Low level of extractables
- Hydrolysis resistant
- Inherently flame retardant

### Typical Properties of 701-707 Grade Powder Coatings

Property	Test Method	Units	Value
Density	ISO 1183	g cm <sup>3</sup>	1.32
Melt Temp.	DSC	°C	343
Glass Transition	DSC	°C	143
CUT (RTI)	UL746B	°C	260
Konig Hardness	BS EN ISO 1522	seconds	200

### FDA COMPLIANCE

Materials and articles manufactured from VICOTE grades 701, 702, 703, 704, 705, 706, 707 comply with

**Note:** The colour of the final coating when using VICOTE 700 series natural resins may depend on the substrate. For example, if a thin VICOTE Coating is applied, the processing temperatures will turn some steels blue and may impart a blue/grey colour to the final VICOTE Coating.

the compositional requirements of regulation 21 CFR 175.300 for resinous and polymeric coatings of the Food and Drug Administration (FDA) of the United States of America.

Regulation 21 CFR 175.300 further specifies that the finished coated part which is in contact with food is subject to extractive limitations. Compliance with any applicable extractive limits can only be demonstrated by testing carried out on the finished article.

### SUBSTRATES AND PREPARATION

VICOTE coatings can be applied to most ferrous and non-ferrous metals. A primer is not required.

- Cast metals need to be de-gassed in an oven to prevent pin holes in the coating surface. Aluminium may be coated. However, the mechanical properties of the Aluminium will be affected at VICOTE coatings processing temperatures.
- Substrates should be free from grease, oils and corrosion prior to coating. Solvent de-greasing and grit blasting with Aluminium Oxide with final solvent wash should ensure a suitable surface for coating.

**Note:** phosphate pre-treated substrates are not recommended for VICOTE coating grades as the high processing temperatures required for processing can result in de-lamination of the coating.

### PROCESSING

Conventional electrostatic spray equipment is suitable for VICOTE coating products. Ovens should be capable of attaining up to 450°C. For general processing information consult the VICOTE powder coating guide.

- By following the processing guide, smooth coatings should be achievable. VICOTE materials are semi-crystalline thermoplastics, and as with all these types of products, shrinkage will take place when the coating cools. Depending on the mass of the substrate, coating thickness and rate of cooling will determine the amount of shrinkage.
- Normally processed and cooled coatings should result in crystalline coatings, which should not require further post processing treatment. However, an increase in crystallinity may enhance certain properties such as wear and scratch resistance. To anneal the coating, the part should be placed in an air circulating oven and the temperature raised at 10°C per minute to 250°C and held at that temperature for 30 minutes to 1 hour.

## A2.2 Membranes

## Specifications

DuraMem®150; DuraMem®200; DuraMem®300; DuraMem®500; DuraMem®900

**General**

• Membrane Material	Modified Polyimide					
• Modules						
Spiral Wound	1812	2512	2540	4020	4040	8040*
Nominal Size (Dia x L)	1.8"×12"	2.5"×12"	2.5"×40"	4.0"×20"	4.0"×40"	8.0"×40"
Active Membrane Area (m <sup>2</sup> ) <sup>1</sup>	0.11	0.17	1.8	2.0	5.4	24.0
Typical Feed Flow (L.h <sup>-1</sup> ) <sup>2</sup>	150	500	500	1500	1500	7500
Standard Feed Spacer (all) <sup>1</sup>	31 mil (0.76 mm)					

\*Female type of permeate tube.

**Solvent stability**

- Type T1 DuraMem® Membranes
  - Stable in Solvents<sup>1</sup> Acetone, Tetrahydrofuran  
Methanol, Ethanol  
Methyl-*tert*-Butyl-Ether  
Methyl-Ethyl-Ketone, Methyl-*iso*-Butyl-Ketone  
Butyl Acetate, Ethyl Acetate
- Type T2 DuraMem® Membranes
  - Stable in Solvents<sup>1</sup> Dimethylformamide, Dimethylsulfoxide, N-Methylpyrrolidone
- Type T1 and T2 DuraMem® Membranes are generally stable in aqueous/organic solvent mixtures. Please contact us for more information.

**Use conditions**

• Membrane Code	DuraMem®				
• MWCO / Dalton <sup>2,3</sup>	150	200	300	500	900
• Maximum Pressure (bar)	60	60	60	20	20
• Maximum Temperature	50 °C (for all)				
• pH	7				
• Maximum pressure drop per element	0.5 bar				
• Maximum permeate pressure	0.2 bar				

<sup>1</sup> Data referring to pure solvents. If you intend to use a solvent not listed above please contact us for further advice.<sup>2</sup> Performance Data are approximate.<sup>3</sup> Based on rejection of styrene oligomers dissolved in acetone, MWCO = molecular weight cut-off, defined as MW at which 90% rejection is obtained from a curve of rejection versus molecular weight of styrene oligomers dissolved in acetone. See Journal of Membrane Science 291 (2007) 120-125.For further information please contact us at [emet@evonik.com](mailto:emet@evonik.com).

This information and all technical and other advice are based on Evonik's present knowledge and experience. However, Evonik assumes no liability for such information or advice, including the extent to which such information or advice may relate to third party intellectual property rights. Evonik reserves the right to make any changes to information or advice at any time, without prior or subsequent notice. Evonik disclaims all representations and warranties, whether express or implied, and shall have no liability for, merchantability of the product or its fitness for a particular purpose (even if Evonik is aware of such purpose), or otherwise. Evonik shall not be responsible for consequential, indirect or incidental damages (including loss of profits) of any kind. It is the customer's sole responsibility to arrange for inspection and tasting of all products by qualified experts. Reference to trade names used by other companies is neither a recommendation, nor an endorsement of the corresponding product, and does not imply that similar products could not be used.

February 2012

Evonik MET Ltd Unit 8 Wharfside Rosemont Road Wembley HA0 4PE, UK  
 Phone +44 (0) 208 902 0040 Fax +44 (0) 208 902 0001  
 E-mail: [emet@evonik.com](mailto:emet@evonik.com)  
[www.puramem.com](http://www.puramem.com)



# Specifications

## PuraMem® S600

### General

• Membrane Material	Silicone-coated polyimide					
• Flat Sheet	210 x 297 mm					
• Modules						
Spiral Wound	1812	2512	2540	4020	4040	8040*
Nominal Size (Dia x L)	1.8"×12"	2.5"×12"	2.5"×40"	4.0"×20"	4.0"×40"	8.0"×40"
Active Membrane Area (m <sup>2</sup> ) <sup>1</sup>	0.11	0.17	1.8	2.0	5.4	24.0
Typical Feed Flow (L.h <sup>-1</sup> ) <sup>2</sup>	150	500	500	1500	1500	7500
Standard Feed Spacer (all) <sup>1</sup>	31 mil (0.76 mm)					

\*Female type of permeate tube.

### Solvent stability

• Stable in Solvents <sup>1</sup>	Toluene, Xylene Hexane, Heptane Butanol, Ethanol, Isopropanol Methyl- <i>tert</i> -Butyl-Ether Methyl-Ethyl-Ketone, Methyl-iso-Butyl-Ketone Butyl Acetate, Ethyl Acetate
-----------------------------------	---

### Use conditions

• Membrane Code	PuraMem® S600
• MWCO / Dalton <sup>2,3</sup>	600
• Flux <sup>2</sup> / L m <sup>-2</sup> h <sup>-1</sup> toluene at 30 bar	160
• Maximum Pressure (bar)	60
• Maximum Temperature	50 °C
• pH	7

<sup>1</sup> Data referring to pure solvents. If you intend to use a solvent not listed above please contact us for further advice.

<sup>2</sup> Performance Data are approximate.

<sup>3</sup> Based on rejection of styrene oligomers dissolved in toluene, MWCO = molecular weight cut-off, defined as MW for 90% rejection.

For further information please contact us at [emet@evonik.com](mailto:emet@evonik.com).

This information and all technical and other advice are based on Evonik's present knowledge and experience. However, Evonik assumes no liability for such information or advice, including the extent to which such information or advice may relate to third party intellectual property rights. Evonik reserves the right to make any changes to information or advice at any time, without prior or subsequent notice. Evonik disclaims all representations and warranties, whether express or implied, and shall have no liability for, merchantability of the product or its fitness for a particular purpose (even if Evonik is aware of such purpose), or otherwise. Evonik shall not be responsible for consequential, indirect or incidental damages (including loss of profits) of any kind. It is the customer's sole responsibility to arrange for inspection and testing of all products by qualified experts. Reference to trade names used by other companies is neither a recommendation, nor an endorsement of the corresponding product, and does not imply that similar products could not be used.

August 2012

Evonik MET Ltd Unit 8 Wharfside Rosemont Road Wembley HA0 4PE, UK  
Phone +44 (0) 208 902 0040 Fax +44 (0) 208 902 0001  
E-mail: [emet@evonik.com](mailto:emet@evonik.com)  
[www.puramem.com](http://www.puramem.com)

